

The Receptor for Advanced Glycation End-products in Pulmonary Hypertension

David George Stephen Farmer
B.Sc. (Hons)

Submitted in fulfilment of the requirements for the
Degree of Doctor of Philosophy

Institute of Cardiovascular and Medical Sciences,
University of Glasgow



University
of Glasgow

November 2012

© David Farmer

Author Declaration

In declaration, the entire contents of this thesis were written solely by me. All experimental data were generated by me with the exception of images of histological sections which were kindly provided by Margaret Nilsen. No contents of this thesis have been previously submitted for a Higher Degree. All research was performed at the Institute of Cardiovascular and Medical Sciences, College of Medical, Veterinary and Life Sciences, University of Glasgow under the supervision of Dr. Simon Kennedy and Professor Margaret R. MacLean.

David Farmer

March 2012

Acknowledgements

There are a large number of people without whom this piece of work would not have reached completion.

First and foremost, I would like to thank Dr. Simon Kennedy and Prof. Mandy MacLean for their guidance and particularly for their patience whilst supervising my PhD. I would also like to acknowledge the Integrative Mammalian Biology Initiative Award funded by the Biotechnology and Biological Sciences Research Council, British Pharmacological Society, Knowledge Transfer Network, Medical Research Council and Scottish Funding Council for their financial support of this work.

Thanks to Ian, Yvonne, Lynne, Mags and everyone who came through the MacLean lab for their invaluable expertise, assistance and chat. Thanks are also due to Kev and all the staff at the Chart Room bar. A huge thanks to Marie-Ann, Fiona, Ian (Watt) and Kirsty for their constant banter and for keeping the office fully stocked with cakes and, when necessary, wine. Thanks to Stu, Flash and Lewis for lunch and to Hannah and Nick for the 'office space' (aka 'the sofa'). Thanks to Johnny for your help with drawing diagrams and with life. Thanks to Dad for getting it. Thanks to mum for the encouragement and the French toast.

Finally, thanks be to Karen, to whom I dedicate this work.

Table of Contents

Author Declaration.....	I
Acknowledgements.....	II
List of Figures.....	VI
List of Publications.....	VII
List of Tables.....	XI
List of Abbreviations.....	XII
Abstract.....	XVII

Chapter 1. Introduction	1
1.1 Introduction.....	2
1.2 The pulmonary circulation.....	2
1.2.1. Pulmonary vascular resistance.....	3
1.3 Pulmonary hypertension.....	6
1.3.1. Pathophysiology of PAH.....	7
1.3.2. Pulmonary vascular vasoconstriction.....	8
1.3.2.1. Mechanisms of smooth muscle contraction.....	8
1.3.2.2. Ca ²⁺ homeostasis in smooth muscle cells.....	10
1.3.2.3. Pulmonary vasoconstriction and its contribution to PAH	12
1.3.2.4. Hypoxic pulmonary vasoconstriction.....	14
1.3.3. Pulmonary vascular remodelling.....	15
1.3.4. Models of experimental pulmonary hypertension	17
1.4 The receptor for advanced glycation end-products.....	20
1.4.1. Characteristics of RAGE.....	21
1.4.2. Ligands for RAGE.....	24
1.4.2.1. Advanced glycation end-products.....	24
1.4.2.2. S100 Proteins.....	25
1.4.2.3. HMGB-1.....	27
1.4.2.4. Mac-1.....	28
1.4.3. Intervention in RAGE-ligand binding	30
1.4.4. The pathogenesis of pulmonary hypertension and RAGE.....	31
1.4.4.1. MTS1/S100A4 mice the serotonin hypothesis.....	33
1.5 Aims.....	35
Chapter 2. Materials and Methods	37
2.1 Materials.....	38
2.2 Animal studies.....	39
2.2.1. Transgenic mice.....	39
2.2.2. Induction of chronic hypoxia and establishment of PAH in mice.....	39
2.2.3. Assessment of haemodynamic properties <i>in vivo</i>	40
2.2.4. Tissue harvest.....	43
2.2.5. Assessment of right ventricular hypertrophy.....	44
2.2.6. Assessment of vascular reactivity and vascular elastance	44
2.2.7. Assessment of pulmonary vascular remodelling.....	50

2.3 Cell culture.....	52
2.4 Statistical Analysis.....	54
 Chapter 3. Chronic hypoxia-induced pulmonary hypertension in mice and the monocyte chemoattractant protein-1 synthesis inhibitor bindarit	55
3.1 Introduction.....	56
3.1.1. Aims.....	59
3.2 Methods.....	59
3.2.1. Induction and assessment of chronic hypoxia-induced pulmonary hypertension.....	59
3.2.2. Cell culture.....	60
3.2.3. Statistical Analysis.....	61
3.3 Results.....	62
3.3.1. <i>In vivo</i> effects of bindarit in normoxia and hypoxia.....	62
3.3.2. MCP-1 and proliferation of fibroblasts.....	66
3.3.3. Effects of conincubation of MCP-1 with 5HT.....	67
3.4 Discussion.....	68
3.5 Conclusions.....	71
 Chapter 4. Effects of RAGE ligand overexpression in a hypoxic mouse model of PAH	73
4.1 Introduction.....	73
4.1.1. Mice overexpressing the RAGE ligand MTS1/S100A4.....	74
4.1.2. RAGE blockade in PAH.....	76
4.1.3. Aims.....	79
4.2 Methods.....	79
4.2.1. Statistical analysis.....	81
4.3 Results.....	81
4.3.1. Effects of strain and hypoxia on haemodynamics and remodelling in C57BL/6 and MTS1/S100A4 mice.....	80
4.3.2. Effects of strain and hypoxia on haemodynamics and remodelling in C57BL/6 and MTS1/S100A4 mice.....	87
4.3.3. Vascular compliance.....	94
4.3.4. Responses of isolated intrapulmonary arteries to pharmacological agents.....	98
4.3.5. Responses to 5HT.....	100
4.3.5.1. Responses to U46619.....	104
4.3.5.2. Responses to SNP.....	108
4.4 Discussion.....	112
4.4.1. Further work.....	117
4.5 Conclusions.....	118
 Chapter 5. Treatment with recombinant soluble receptor for advanced glycation end-products in a hypoxic mouse model of PAH	121
5.1 Introduction.....	122
5.2 Aims.....	124

5.3 Methods.....	125
5.3.1. Statistical Analysis.....	125
5.4 Results.....	125
5.4.1. Effects of sRAGE dosing and hypoxia in C57BL/6 mice in vivo..	128
5.4.2. Vascular compliance.....	132
5.4.3. Responses to pharmacological agents.....	135
5.4.3.1. Responses to KCl.....	135
5.4.3.2. Responses to 5HT.....	138
5.4.3.3. Responses to U46619.....	143
5.4.3.4. Responses to SNP.....	149
5.4.3.5. Acute effects of sRAGE in isolated intrapulmonary arteries	
5.4.3.6. Responses to 5HT: effects of sRAGE treatment.....	155
5.4.4. Cellular Proliferation.....	157
5.4.4.1. 5HT-induced increases in cell number.....	157
5.4.4.2. Effects of sRAGE upon 5HT-induced increases in cell	
number.....	160
5.4.4.3. Effects of sRAGE upon hypoxia-induced increases in cell	
number.....	159
5.5 Discussion.....	162
5.5.1. Further work.....	168
5.6 Conclusions.....	172
	168
Chapter 6. General Discussion.....	176
6.1 General Discussion.....	176
6.2 Conclusions.....	180
Reference list.....	182

List of Publications

Farmer, D.G.S. & Kennedy, S., 2009. RAGE, vascular tone and vascular disease.
Pharmacology & Therapeutics, 124(2), pp.185-194.

List of figures

Figure 1.1	Mechanisms of smooth muscle contraction.....	9
Figure 1.2	Calcium homeostasis in smooth muscle cells.....	11
Figure 2.1	Placement of needle for right ventricular haemodynamic measurements in the mouse.....	42
Figure 2.2	Representative right ventricular pressure trace.....	43
Figure 2.3	Schematic diagram of wire myograph.....	45
Figure 2.4	Representative trace depicting the normalisation of intrapulmonary vessels mounted on a wire myograph.....	48
Figure 2.5	Assessment of vascular remodelling using sagital sections of formalin-fixed murine lung.....	51
Figure 3.1	Effects on sRVP, vascular remodelling and RVH in mice exposed to hypoxia and treated with bindarit.....	64
Figure 3.2	Images of representative small pulmonary arteries in C57BL/6 mice treated with bindarit or methylcellulose vehicle in normoxia and after chronic hypoxia.....	65
Figure 3.3	MCP-1 produces no significant effect on proliferation in response to MCP-1.....	66
Figure 3.4	No co-operative effects upon proliferation in FBs were observed in the presence of both MCP-1 and 5HT.....	67
Figure 4.1	Systemic arterial pressure and HR remain unaltered in all treatment groups studied.....	81
Figure 4.2	Pulmonary hypertension in C57BL/6 and MTS1/S100A4 mice in normoxic, hypoxia and after recovery.....	84
Figure 4.3	Mean RVP is significantly elevated after hypoxia in MTS1/S100A4 mice but not C57BL/6 mice.....	85
Figure 4.4	Images of representative small pulmonary arteries in C57BL/6 and MTS1/S100A4 mice in normoxia, after chronic hypoxia and after recovery from hypoxia.....	86
Figure 4.5	Mouse body mass and weight of left ventricle plus septum in normoxic C57BL/6 and MTS1/S100A4 mice.	88
Figure 4.6	Weight of LV+S appears to vary closely with mouse body weight.....	91
Figure 4.7	Normalisation of right ventricle weight to body weight and weight of left ventricle plus septum.....	93
Figure 4.8	Overexpression of MTS1/S100A4 produces no alteration in the compliance of intrapulmonary mouse vessels.....	94
Figure 4.9	Compliance is reduced by hypoxia in vessels from WT but not MTS1/S100A4 mice.....	96
Figure 4.10	Compliance returns to baseline values in WT mice allowed to recover from chronic hypoxia.....	97
Figure 4.11	Responses to 50mM KCl were unaltered between normoxia, hypoxia and recovery in WT and MTS1/S100A4 mice.....	98

Figure 4.12	Contractile responses to 5HT in intrapulmonary arteries of C57BL/6 and MTS1/S100A4 mice.....	102
Figure 4.13	Effect of chronic hypoxia and recovery on contractile responses to 5-HT in intrapulmonary arteries.....	103
Figure 4.14	Contractile responses to U46619 in intrapulmonary arteries of C57BL/6 and MTS1/S100A4 mice.....	106
Figure 4.15	Effect of chronic hypoxia and recovery on contractile responses to U46619 in intrapulmonary arteries.....	107
Figure 4.16	Effect of MTS1/S100A4 overexpression on the relaxatory response to sodium nitroprusside.....	110
Figure 4.17	Effect of chronic hypoxia and recovery on relaxatory responses to U46619 in intrapulmonary arteries.....	111
Figure 5.1	Mean systemic arterial pressure and heart rate - effects of sRAGE and hypoxia.....	127
Figure 5.2	Treatment with sRAGE blunts a hypoxia-induced increase in sRVP but does not prevent increases in PVR or RVH.....	130
Figure 5.3	Images of representative small pulmonary arteries in C57BL/6 mice treated with vehicle or sRAGE in normoxia and after 2 weeks hypoxia.....	131
Figure 5.4	Treatment with sRAGE produces no alteration in compliance in intrapulmonary vessels.....	133
Figure 5.5	Vascular compliance is reduced by exposure to chronic hypoxia in vehicle-treated but not sRAGE-treated mice....	134
Figure 5.6	Treatment with sRAGE results in an increased force of contraction in response to 50mM KCl in intrapulmonary arteries isolated from animals exposed to chronic hypoxia.....	137
Figure 5.7	Treatment with soluble RAGE has no effect on the response to 5HT in vessels isolated from normoxic mice compared to vehicle-dosed controls.....	140
Figure 5.8	Effects of sRAGE treatment on 5HT-induced contraction in normoxia and hypoxia.....	141
Figure 5.9	Effects of sRAGE treatment on the absolute force of contraction in response to 5HT in normoxia and hypoxia...	142
Figure 5.10	Concentration-response curves to U46619 are not altered by treatment with 20 μ g/day IP sRAGE.....	146
Figure 5.11	Chronic-hypoxia appears to increase sensitivity of intrapulmonary arteries to U46619 in vessels isolated from animals receiving 20 μ g/day sRAGE or vehicle.....	147
Figure 5.12	Effects of sRAGE treatment on the absolute force of contraction in response to U46619 in normoxia and hypoxia.....	148
Figure 5.13	Administration of 20 μ g/day sRAGE produced no alteration in the concentration-response to SNP.....	150
Figure 5.14	Responses to SNP is comparable in vessels isolated from mice treated with both 20 μ g/day sRAGE or vehicle.....	151
Figure 5.15	Representative myography traces displaying increased generation of force with time in response to sRAGE.....	
Figure 5.16	Treatment with sRAGE results in the generation of	153

	contractile force in isolated intrapulmonary arteries.....	
Figure 5.17	Preincubation with 10 μ g/ml sRAGE augments the contractile response to 5HT.....	154
Figure 5.18	5HT produces an increase in cell number in CCL39 Chinese hamster lung fibroblasts.....	156
Figure 5.19	Incubation with 2.5 μ g/ml sRAGE produces an increase in cell number and does not inhibit the 5HT-induced increase in cell number in CCL39 Chinese hamster lung fibroblasts.....	158
Figure 5.20	2.5 μ g/ml sRAGE enhances the hypoxia-induced increase in cell number in CCL39 Chinese hamster lung fibroblasts.....	146
		159
		161

List of Tables

Table 4.1	Emax and EC50 values for responses to pharmacological agents in C57BL/6 and MTS1/S100A4 in normoxia, after hypoxia and after recovery from hypoxia.....	89
Table 5.1	Normalised Emax and EC50 values for responses to pharmacological agents in vehicle-treated and sRAGE-treated mice in normoxia and hypoxia.....	123
Table 5.2	Absolute Emax and EC50 values for responses to pharmacological agents in vehicle-treated and sRAGE-treated mice in normoxia and hypoxia.....	123

List of Abbreviations

[Ca ²⁺] _{cyt}	Concentration of calcium in the cytoplasm
γHV68	Murine γ-herpesvirus
5HT	5-Hydroxytryptamine/Serotonin
ACh	Acetylcholine
AGE	Advanced glycation end-product
ANOVA	Analysis of variance
ApoE	Apolipoprotein E
ATIIR1	Angiotensin II receptor 1
BH4	Tetrahydrobiopterin
BMPRII	Bone morphogenetic protein receptor II
Ca ²⁺	Calcium
CaCl ₂	Calcium Chloride
CaM	Calmodulin
CCR2	Chemokine receptor 2
CO	Cardiac output
CO ₂	Carbon dioxide
COX-2	Cyclooxygenase-2
DAG	Diacylglycerol
dH2O	Distilled water
DMEM	Dulbecco's Modified Eagle Medium

DN-RAGE	Dominant negative receptor for advanced glycation end-products
EC	Endothelial cell
EDTA	Ethylene-diamine-tetracetic acid
Em	Membrane potential
ERK	Extracellular signal-related kinase
ET	Endothelin
FBS	Foetal bovine serum
FPAH	Familial pulmonary arterial hypertension
GPCR	G-protein coupled receptor
H ₂ O ₂	Hydrogen peroxide
Hb-AGE	Advanced glycation end-product bound haemoglobin
HMGB-1	High mobility group box-1 protein
HPV	Hypoxic pulmonary vasoconstriction
ICAM-1	Intercellular adhesion molecule 1
IF	Interferon
IP	Intraperitoneal
IP ₃	Inositol 1,4,5-trisphosphate
IPA	Intrapulmonary artery
JNK	c-Jun N-terminal kinase
KCl	Potassium chloride
KH ₂ PO ₄	Monopotassium phosphate
K _v	Voltage-dependent potassium channel

LSD	Least Significant Difference
LME	Linear mixed effects
LPS	Lipopolysacharide
LV+S	Left ventricle plus septum
MAPK	Mitogen-activated protein kinase
MCP-1	Monocyte chemoattractant protein 1
MgSO ₄	Magnesium sulphate
MLA	Mean lesion area
MLC	Myosin light-chain
MLCK	Myosin light-chain kinase
MLCP	Myosin light-chain phosphatase
MMP	Matrix metalloproteinase
mRVP	Mean right ventricular pressure
MTS1	Multiple tumour suppressing protein 1
N ₂	Nitrogen
Na ₂ HPO ₄	Disodium phosphate
NaCl	Sodium chloride
NaH ₂ PO ₄	Monosodium phosphate
NaHCO ₃	Soium bicarbonate
NF-κB	Nuclear Factor-κB
NO	Nitric oxide
O ²⁻	Superoxide

ONOO ⁻	Peroxynitrite
oxLDL	Oxidised low-density lipoprotein
PAH	Pulmonary arterial hypertension
PAP	pulmonary arterial pressure
PASMC	pulmonary arterial smooth muscle cell
PBS	Phosphate buffered saline
PH	Pulmonary hypertension
PPAR γ	Peripheral peroxisome activated receptor gamma
PRR	Pattern-recognition receptor
PVD	Pulmonary vascular disease
PVR	Pulmonary vascular resistance
RAGE	Receptor for advanced glycation end-products
RhoA	ras homologue gene family, member A
RhoK/ROCK	ras homologue gene family kinase
RNS	Reactive nitrogen species
ROCC	Receptor-operated Ca ₂₊ channels
ROS	Reactive oxygen species
RV	Right ventricle
RVH	Right ventricular hypertrophy
RVP	Right ventricular pressure
RyR	Ryanodine receptor
SAP	Systemic arterial pressure

SEM	Standard Error of the Mean
SERCA	Sarcoplasmic reticulum Ca_{2+} - Mg_{2+} ATPase
SERT	Serotonin Transporter
SMC	Smooth muscle cell
SNP	Sodium Nitroprusside
SR	Sarcoplasmic reticulum
sRAGE	Soluble receptor for advanced glycation end-products
sRVP	Systolic right ventricular pressure
TLR	Toll-like receptor
TNF	Tumour necrosis factor
TRPC	Transient receptor potential channels
U46619	9,11-Dideoxy-11 α ,9 α -epoxymethanoprostaglandin F2 α
VCAM-1	Vascular cell adhesion molecule 1
VDCC	Voltage-dependent Ca^{2+} channel
VEGF	Vascular endothelial growth factor
WT	Wildtype

Abstract

The receptor for advanced glycation endproducts (RAGE) is a 35-kDa polypeptide of the immunoglobulin superfamily that has been implicated as a mediator of both acute and chronic vascular inflammation. RAGE has also recently been implicated in the pathology of pulmonary hypertension (PH): a rare, progressive disease of the small pulmonary arteries characterised by pulmonary vascular remodelling, thrombosis, vasoconstriction and increased pulmonary vascular resistance. A ligand for RAGE, the calcium binding protein MTS1/S100A4, is expressed in occlusive vascular lesions of patients with advanced PH. MTS1/S100A4 is upregulated and secreted by pulmonary arterial smooth muscle cells (PASMCs) *in vitro* on activation of the 5HT_{1b} receptor and 5HT transporter (5HTT). Additionally, the proliferative effect of 5HT on these cells, which is mediated by 5HT_{1b} and 5HTT, may be inhibited by antagonism of RAGE or reduced bioavailability of MTS1/S100A4. These data suggest that MTS1/S100A4, through its action at RAGE, is a key mediator of 5HT-induced hPASMC proliferation. Transgenic mice overexpressing MTS1/S100A4 are observed to develop obliterative pulmonary vascular disease and possess increased right ventricular pressure at baseline and after hypoxia when compared to wildtype mice (WT). These increases occur in the absence of an increase in pulmonary vascular remodelling suggesting that MTS1/S100A4 overexpression is associated with some other structural or functional change in the pulmonary circulation.

We sought to further our understanding of the role of RAGE in pulmonary hypertension through treatment with a small molecule inhibitor of monocyte chemoattractant protein 1(MCP-1), a marker of downstream of RAGE rage activation; through further characterisation of the MTS1/S100A4 mouse in a

chronic hypoxic model of PAH; and through treatment with soluble RAGE (sRAGE) to reduce RAGE ligand bioavailability *in vivo*. In each case systolic right ventricular pressure (sRVP), right ventricular hypertrophy (RVH) and pulmonary vascular remodelling were measured in normoxic conditions or after a two week chronic hypoxia challenge to induce PH. These *in vivo* experiments were supplemented with functional studies in isolated intrapulmonary arteries to assess vascular reactivity and vascular elastance as well as studies of pulmonary fibroblast proliferation *in vitro*.

Treatment with the MCP-1 synthesis inhibitor Bindarit produced no detectable effects upon the pulmonary response of mice to chronic hypoxia, though this study may have been hampered by difficulties with the methylcellulose vehicle. MCP-1 produced no degree of proliferation in pulmonary fibroblasts and neither augmented nor inhibited proliferation induced by 5HT.

We found little evidence for the exacerbation of PH in MTS1/S100A4 mice in normoxia, hypoxia or after 4 weeks of normoxic recovery. Mean RVP was elevated above that in WT mice exposed to hypoxia. However, MTS1/S100A4 mice appeared protected against hypoxia-induced vascular remodelling and decreases in vascular elastance. No other significant differences in sRVP, RVH or remodelling were observed between strains. Vessels isolated from MTS1/S100A4 mice tended towards an enhanced contractile response to 5HT in normoxia compared with vessels in WT mice but were also more sensitive to the nitric oxide donor SNP. These differences in vasoreactivity were largely abolished by exposure to hypoxia. Treatment with soluble RAGE (sRAGE) to reduce RAGE ligand bioavailability produced a significant reduction in sRVP after hypoxia in comparison to vehicle-dosed mice -possibly associated with the prevention of a hypoxia-induced decrease in proximal vascular elastance. However, no benefit

upon the development of remodelling or the extent of RVH was observed. Vessels isolated from mice treated with sRAGE and challenged with hypoxia showed a marked increase in contractility. Further work demonstrated that sRAGE produces a small, slowly developing contraction in isolated vessels and that the maximal force of contraction to 5HT was markedly augmented in the presence of sRAGE. Finally, treatment with sRAGE did not inhibit fibroblast proliferation *in vitro* as induced by 5HT but was observed to cause a small degree of proliferation alone and to augment hypoxia-induced proliferation.

In summary, we have reported a number of seemingly contradictory findings associated with RAGE in pulmonary hypertension. Treatment with sRAGE produced a beneficial reduction in hypoxia-induced PH associated with protection against decreased proximal vascular elastance but produced no change in hypoxia-induced RVH or remodelling as well as greatly increasing vascular contractility. MTS1/S100A4 mice show some evidence of deleterious changes to the pulmonary circulation, but these may be offset by beneficial compensatory mechanisms such as increased sensitivity to nitric oxide and protection against vascular remodelling.

MTS1/S100A4 stimulates smooth muscle cell proliferation suggesting that it may involved pulmonary vascular remodelling. However, inhibition of RAGE was observed to enhance fibroblast proliferation in response to hypoxia here. Fibroblasts are important regulators of SMC proliferation *in vivo*. These findings therefore suggest a more complicated relationship between RAGE, its ligands and the remodelling process. Since both MTS1/S100A4 overexpression and sRAGE treatment *in vivo* produced findings which are difficult to reconcile using the currently employed techniques, it is clear that furthering our understanding of RAGE will require study with greater focus upon the interaction of different cell

types in the pulmonary vasculature and the manner in which the disturbance of this may lead to alterations in the physical and physiological properties of the pulmonary circulation.

Chapter 1. Introduction

1.1 Introduction

Pulmonary hypertension (PH) is a rare, progressive disease of the small pulmonary arteries characterised by chronically increased pulmonary vascular resistance, thrombosis and a sustained increase in pulmonary arterial pressure. This chronic rise in pulmonary arterial pressure (PAP) places a large strain upon the right side of the heart, which has only a limited capacity for adaptation to the increased afterload leading to right heart failure and death (Rubin, 1997; Jeffery and Morrell, 2002; Humbert, Morrell, et al., 2004).

Recent studies have suggested a novel role for the recently described receptor for advanced glycation end-products (RAGE) in the regulation of deleterious processes in the pulmonary circulation which are thought to contribute to the generation of PH (Ambartsumian et al., 2005; Lawrie et al., 2005; Merklinger et al., 2005; Spiekerkoetter et al., 2005). RAGE and its ligands have been widely implicated as key mediators of inflammatory processes leading to the generation of systemic vascular disease (Schmidt et al., 1994; Hudson et al., 2003; Ramasamy et al., 2005; Basta, 2008)

In the course of this introductory chapter, the pathogenesis of pulmonary hypertension will be described and discussed. The nature of RAGE and signalling events downstream of receptor binding will be also be discussed, with particular reference made to established roles of RAGE and RAGE ligands in vascular inflammation and cellular proliferation; and to recent evidence implicating RAGE in pathogenic processes leading to the generation of PH, particularly pulmonary vascular remodelling and pulmonary vascular vasoconstriction.

1.2 The pulmonary circulation

The pulmonary circulation is the branch of the circulatory system in which blood is brought into close proximity with the air via the pulmonary microvasculature for the purposes of reoxygenation and carbon dioxide (CO_2) elimination. Deoxygenated blood enters the right atrium through the superior and inferior vena cava and is then pumped into the right ventricle before being ejected at relatively low pressure (9-24mmHg) into the pulmonary artery. The main artery divides into the left and right pulmonary artery which proceed into the left and right lung respectively. Within the lung, these arteries repeatedly branch in an asymmetrical pattern and in association with the bifurcations of the airway, into arteries of progressively smaller arteries, arterioles and eventually capillaries.

At the capillary level, vessels are located within the alveolar wall and just adjacent to the alveolar spaces. This brings deoxygenated blood into close proximity with inspired air allowing for the transference of O_2 into, and CO_2 out of, the blood by passive diffusion (Comroe, 1966; Berne et al., 2008).

1.2.1 Pulmonary vascular resistance

In contrast to the systemic circulation, the pulmonary circulation is a low-pressure, high-flow system. The PAP may be considered to be the product of the cardiac output (CO) of the right ventricle and the total pulmonary vascular resistance as may be seen in *Equation 1*. Under normal conditions, a rise in CO (e.g. due to exercise) does not produce a large increase in PAP due to an accompanying fall in pulmonary vascular resistance (PVR). This fall in PVR occurs

primarily as the result of two features of the pulmonary circulation: first, distension of vessels comprising the pulmonary circulation which are highly compliant and elastic; second, the recruitment of previously unperfused vessels in the superior portion of the lung. These adaptations allow for the accommodation of large increases in blood flow without a substantial increase in PAP (Mandegar et al., 2004; Berne et al., 2008).

Equation 1: $PAP = CO [PVR_{art} + PVR_{cap} + PVR_{vein}]$

PAP = *pulmonary arterial pressure;*

CO = *cardiac output;*

PVR_{art} = *vascular resistance of the pulmonary arteries;*

PVR_{cap} = *vascular resistance of the pulmonary capillaries;*

PVR_{vein} = *vascular resistance of the pulmonary veins.*

From the Hagen-Poiseuille equation (*Equation 2*), it may be surmised that while many factors have influence over the total resistance to flow within a fluid filled tube, in this case a pulmonary blood vessel, by far the most important is the vessel's radius. PVR is inversely proportional to the fourth power of the radius. Therefore, relatively minor changes in radius may produce very large fluctuations in PVR.

$$\text{Equation 2: } PVR = \frac{8L\eta}{\pi r^4}$$

L = Length of vessel;

η = Viscosity coefficient;

r = radius

When the pulmonary circulation is considered as a network of tubes, the PVR may also be expressed by Kirchoff's equations describing resistance in an electric circuit (*Equation 3 and Equation 4*). From these two equations, we see that connections in series produce a total resistance which is the sum of all individual resistances in the circuit, while connections in parallel produce a total resistance which must be less than any one element in the circuit. Therefore, in the context of the pulmonary circulation, the larger the number of vessels connected in parallel, the lower the total PVR.

$$\text{Equation 3: } R_s = R_1 + R_2 + \dots + R_n$$

R_s = Total resistance of vessels in series.

$$\text{Equation 4: } \frac{1}{R_p} = \frac{1}{R_1} + \frac{1}{R_2} + \dots + \frac{1}{R_n}$$

R_p = Total resistance of vessels in parallel.

As was previously mentioned, the pulmonary circulation branches extensively on the main pulmonary arteries' entry into the lungs. Based upon the diameter-defined Strahler's system, the model which most accurately describes experimental observation of branching in the pulmonary circulation, it was

demonstrated that while vessel diameter and length decrease exponentially for each order of branching, the number of vessels which are connected in parallel increases exponentially (Singhal et al., 1973; Huang et al., 1996). An interesting consequence of this is that the relative ability to influence PVR and blood flow remain roughly similar throughout vessels of all size in the pulmonary circulation (Mandegar et al., 2004).

1.3 Pulmonary hypertension

Physiologically, pulmonary hypertension may be broadly classified as obliterative pulmonary hypertension, which is defined as a disorder of the pulmonary vasculature itself (*i.e.* pulmonary arteriopathy), or secondary pulmonary hypertension, where pulmonary hypertension arises as a secondary consequence of a pre-existing disorder. Obliterative PH is defined by a sustained and chronic elevation in PAP caused by impaired bloodflow through small pulmonary vessels. It is observed in idiopathic pulmonary arterial hypertension (PAH), as well as PAH occurring as a consequence of HIV infection, anorexigen use and persistent PAH of the newborn. Clinically, pulmonary hypertension arising as a consequence of pulmonary arteriopathy is referred to as idiopathic pulmonary arterial hypertension or familial pulmonary arterial hypertension (FPAH) where there is evidence of a genetic component to the disease. Secondary PAH may arise as a consequence of a wide variety of conditions such as pulmonary embolism, parenchymal lung disease, chronic hypoxia (*e.g.* at altitude) and atrial or ventricular septal defects leading to increased (hyperkinetic) bloodflow through the pulmonary circulation (Rubin, 1997; Mandegar et al., 2004).

It is interesting that even though the various causes of PH encompass a very wide variety of scenarios, the resulting alterations in pulmonary histology are very similar. As will be discussed in detail below, the various mechanisms by which PVR is increased and PAP raised serve to reinforce one another, leading to the maintenance and progression of PAH.

1.3.1 Pathophysiology of PAH

There are three classically defined elements of PAH: pulmonary vascular remodelling, vasoconstriction and thrombosis (Rubin, 1997). This remodelling process consists of smooth muscle migration and proliferation leading to the muscularisation of peripheral, typically non-muscular, pulmonary arteries and increased medial thickness in larger pulmonary arteries. These areas of increased muscularisation are associated with fibroelastosis, ablated responses to vasodilators and eventually the formation of obliterative plexiform lesions. Sustained elevation of pulmonary pressure due to vascular narrowing and increased vascular resistance increases afterload in the right ventricle, ultimately leading to right heart failure and death (Rubin, 1997; Jeffery and Morrell, 2002; Humbert, Morrell, et al., 2004).

Alterations in PVR can be fixed or reversible. Fixed changes in PVR characteristic of PAH refer to pathological alterations to the structure of the pulmonary circulation. That is to say, arterial occlusion or obliteration caused by vascular remodelling. Reversible changes refer to chronically increased vasomotor tone in the pulmonary circulation which can be reversed by the administration of agents which relax pulmonary vascular smooth muscle. While alterations in both parameters are hallmarks of disease, no causal relationships

have yet been established between the two, though it now seems likely that chronic activation of vasoconstrictive pathways on smooth muscle also contributes to smooth muscle proliferation and remodelling.

1.3.2 Pulmonary vascular vasoconstriction

Vasoconstriction refers to an increase in contractile force generated by the smooth muscle of a blood vessel. While the word can refer to the contraction of smooth muscle oriented either longitudinally or circumferentially around a vessel, the latter context will be taken as the definition in this thesis except where otherwise stated. If smooth muscle arranged circumferentially around a vessel is shortened, the result is a reduction in the diameter of the vessel. In the context of a circulatory system, this reduction in diameter will produce an increase in vascular resistance.

1.3.2.1 Mechanisms of smooth muscle contraction

The shortening of individual smooth muscle cells (SMCs) and the generation of contractile force is greatly dependent on the concentration of Ca^{2+} ions in the cytoplasm of these cells ($[\text{Ca}^{2+}]_{\text{cyt}}$) (Figure 1.1) (Mandegar et al., 2004; Murphy and Rembold, 2005). An increase in $[\text{Ca}^{2+}]_{\text{cyt}}$ leads to an interaction between Ca^{2+} and the protein calmodulin (CaM). This $\text{Ca}^{2+}/\text{CaM}$ complex associates with the catalytic subunit of myosin light-chain kinase (MLCK), activating its ability to phosphorylate the myosin light-chain (MLC). Phosphorylation of MLC permits hydrolysis of ATP by myosin ATPase when activated by actin filaments in the cell. Actin filaments are predominantly

oriented in parallel along the length of the cell, therefore the net result of activating the actin-myosin ATPase contractile machinery is a reduction in the length of the cell.

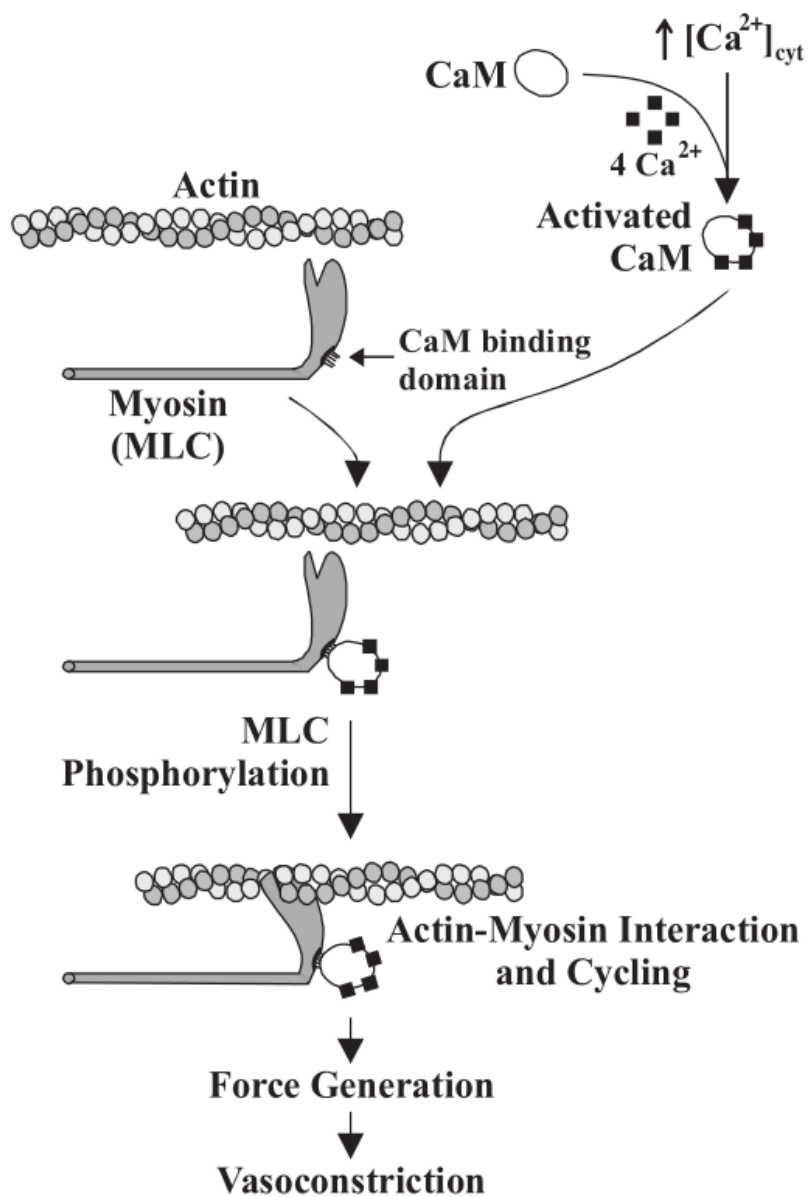


Figure 1.1 Mechanisms of smooth muscle contraction. Increases in $[Ca^{2+}]_{cyt}$ lead to formation of Ca^{2+}/CaM complexes which phosphorylate the MLC. This facilitates the interaction of the myosin ATPase with actin and leads to contraction of the smooth muscle. Figure adapted from (Mandegar et al., 2004)

1.3.2.2 Ca^{2+} homeostasis in smooth muscle cells

Calcium may enter the cytosol of smooth muscle cells via a variety of different Ca^{2+} channels on the cell's external membrane, as well as from internal Ca^{2+} stores in the sarcoplasmic reticulum (SR). Similarly, it may be removed from the cytosol via extrusion at the plasma membrane or reuptake by the SR. This occurs via the action of the plasmalemmal $\text{Ca}^{2+}\text{-Mg}^{2+}$ ATPase and the SR $\text{Ca}^{2+}\text{-Mg}^{2+}$ ATPase (SERCA) respectively. Important subtypes of ion channel on the extracellular membrane include voltage-dependent Ca^{2+} channels (VDCC) and receptor-operated Ca^{2+} channels (ROCC) and store-operated Ca^{2+} channels (Figure 1.2).

VDCCs are activated by the depolarisation of the cell's membrane potential (E_m) and inactivated by the hyperpolarisation of the cell (Mandegar et al., 2004). Calcium may be liberated from the sarcoplasmic reticulum through stimulation of ligand-binding Ca^{2+} channels which are blocked by ryanodine (RyR) or to inositol 1,4,5-trisphosphate (IP_3). IP_3 is a molecule generated by enzymatic cleavage of phosphatidylinositol 4,5-bisphosphate by phospholipase C (PLC), producing both IP_3 and diacylglycerol (DAG) (Berridge, 1993). PLC is activated by binding of G-protein coupled receptors (GPCR) activating the $\text{G}_{q/11}$ pathway including α_{1a} , α_{1b} and α_{1d} adrenoceptors, 5-Hydroxytryptamine (5HT)_{2A}, 5HT_{2b} and 5HT_{2c} receptors, ET_A and ET_B endothelin receptors, thromboxane A₂ receptors, angiotensin II receptor type-1 among many others (Alexander et al., 2011).

RyRs on the SR are endogenously activated by cytosolic $[\text{Ca}^{2+}]_i$ in what is termed 'calcium-induced calcium release'. In this manner, cytoplasmic Ca^{2+} itself may act as a second messenger to stimulate further elevation of $[\text{Ca}^{2+}]_{\text{cyt}}$.

Receptor-operated Ca^{2+} channels are activated by the binding of specific

receptors on the cell membrane by vasoconstrictive molecules such as norepinephrine and serotonin (Nelson et al., 1990; Mandegar et al., 2004). Calcium entry via ROCCs and store-operated Ca^{2+} channels is dependent on expression of transient receptor potential channels (TRPC) in smooth muscle cells. The expression and function of these channels has been demonstrated in both human (Golovina et al., 2001) and mouse pulmonary arterial smooth muscle cells (PASMC) (Ng et al., 2009). It is clear that regulation of $[\text{Ca}^{2+}]_i$ is a key determinant in regulating vasoconstriction in SMCs. Another factor which must be considered in determining the magnitude of contraction is the sensitivity of the contractile machinery to Ca^{2+} . The phosphorylation of MLC is reversed by myosin phosphatase, therefore an alteration in the relative activities of this enzyme and MLCK can alter the force generated by Ca^{2+} influx (Somlyo and Somlyo, 2003).

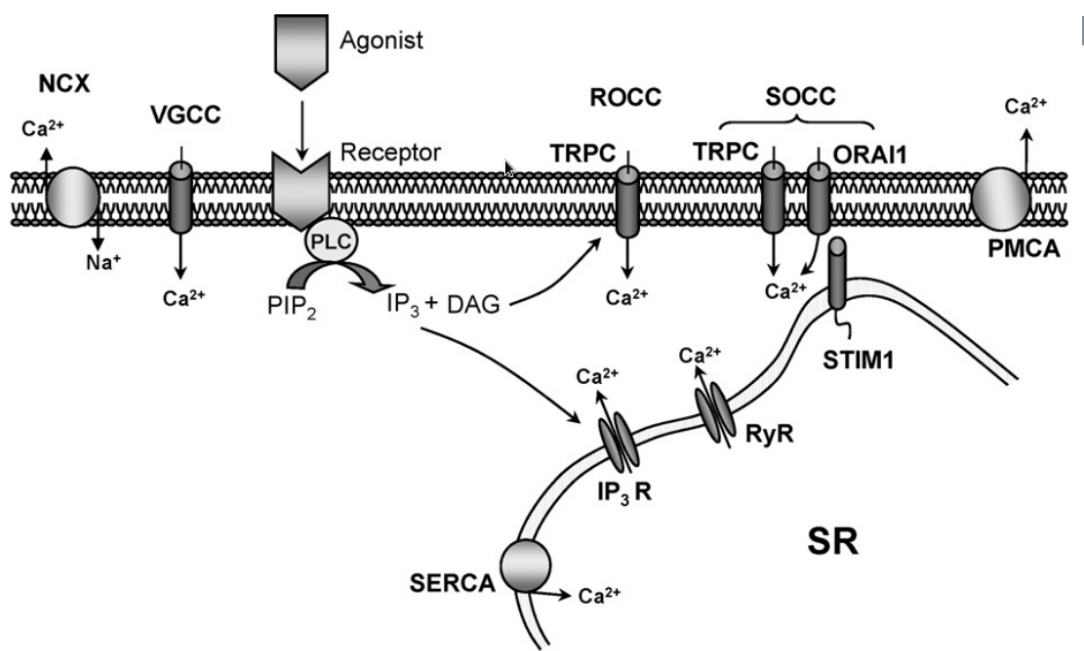


Figure 1.2 Calcium homeostasis in smooth muscle cells. Adapted from (Shimoda and Undem, 2010).

1.3.2.3. Pulmonary vasoconstriction and its contribution to PAH

The contribution of vasoconstriction to PAH was first suggested by Wood (1958) who observed that injection of acetylcholine into the pulmonary artery of PH patients produced a decrease in both PVR and PAP. The inference of this finding was that a component of the increased pulmonary pressure was due to reduced lumen diameter caused by the presence of a vasoconstrictive factor. Vasoconstriction in patients with PH was later correlated with medial hypertrophy of pulmonary vessels suggestive of smooth muscle cell proliferation (Wagenvoort, 1960). Despite this, initial attempts at treatment with vasodilators were only partially successful. Treatment with the β -adrenoceptor agonist isoprenaline resulted in reduced PVR and PAP in some patients but no change or even a worsening of these parameters in others (Person and Proctor, 1979; Lupi-Herrera et al., 1981). Generally, vasodilators as a therapy for pulmonary hypertension produce immediate haemodynamic benefits in only a subset of patients. In cases where treatment is successful in reducing PVR and/or PAP, it is not clear to what extent this is associated with decreased mortality. Furthermore, dilators such as β -adrenoceptor agonists, nitric oxide and calcium channel blockers do not have a selective action on the pulmonary circulation and can produce an undesirable hypotension through their action in the systemic circulation (Rubin, 1997, 2002).

Current therapeutics still target vasoconstrictive pathways. However, the development of these has been informed by a greater understanding of pathological changes in the pulmonary circulation leading to pulmonary hypertension. When a particular proportion of the vascular diameter was occupied by the vascular intima, this was predictive of which patients would

respond favourably to vasodilators and which would fair poorly in subsequent clinical assessments (Palevsky et al., 1989). It now appears that many of the currently targeted vasoconstrictive pathways are also associated with proliferative effects, the inhibition of which may produce long-term clinical benefits. Patients with pulmonary hypertension show decreased expression of nitric oxide synthase and prostacyclin in the endothelium of pulmonary vessels (Giaid and Saleh, 1995; Tuder et al., 1999). Each compound has both vasodilatory and anti-proliferative actions (Barst et al., 1996; Clapp et al., 2002; Wedgwood and Black, 2003; Barman, 2005). The observation that inhaled nitric oxide is efficacious in reducing PAP and PVR in some patients has led to the use of treatments which have targets downstream of NO (Pepkezaba, 1991; Sitbon et al., 1998). Two of these, sildenafil and tadalafil, inhibit the actions of phosphodiesterase-5; reducing the action of this enzyme on cyclic-guanosine monophosphate and facilitating vasodilatation. These have proven beneficial in clinical trials involving PH patients (Galiè et al., 2005, 2009; O'Callaghan et al., 2011). Treatment with stable analogues of prostacyclin have proven similarly effective in improving clinical outcomes despite producing only modest effects upon haemodynamic parameters (McLaughlin et al., 2002; Humbert, Sitbon, et al., 2004).

Similarly, PH patients show increased expression of the vasoactive peptide endothelin in the vascular endothelium (Giaid et al., 1993). Endothelin is both a vasoconstrictor and a mitogen for PASMCs (McCulloch et al., 1998). Endothelin receptor antagonism with bosentan has also produced some benefit on pulmonary haemodynamics in PH patients though the differential expression of two types of endothelin receptor (ET_A on PASMCs which mediates vasoconstriction and proliferation; and ET_B on endothelial cells which mediates a

beneficial release of NO and prostacyclin from the endothelium) has led to the generation of the selective ET_A antagonists ambrisentan and sitaxentan. The use of VDCC blockers has also shown long-term efficacy in a subset of patients (~10%) as predicted by a favourable effect of NO on haemodynamic parameters in these patients (Sitbon et al., 1998, 2005).

In recent years, there has been a tendency in studies of experimental PH towards a reduced emphasis on the contribution of vasoconstriction to the onset and maintenance of elevated pulmonary blood pressure. However, evidence continues to emerge from pre-clinical studies using models of both mild and severe occlusive PAH that the active maintenance of SMC tone contributes to elevated PVR and PAP (Oka, Fagan, et al., 2008; Oka, Homma, et al., 2008; McMurtry et al., 2010). The continued study of the mechanisms of vasoconstriction and its contribution to the disease state may therefore highlight potential sites of clinical intervention, increasing the likelihood of providing a tangible benefit to PAH patients.

1.3.2.4 Hypoxic pulmonary vasoconstriction

Hypoxia is an important stimulus in the pulmonary circulation. In contrast to the systemic circulation where hypoxia provokes dilatation of vessels (Madden et al., 1992), acute hypoxia results in vasoconstriction in the pulmonary circulation (Euler and Liljestrand, 1946). Physiologically, this is thought to aid in ventilation-perfusion matching in the lung; vascular resistance will be lowest in vessels which are well ventilated, facilitating blood flow through these vessels. Similarly, blood flow will be diverted away from poorly ventilated areas.

Hypoxia causes vasoconstriction in isolated pulmonary arteries and

isolated PASMCs (Murray et al., 1990; Yuan et al., 1990), suggesting that it is an intrinsic property of pulmonary smooth muscle cells. Hypoxic pulmonary vasoconstriction (HPV) is sustained for the duration of a hypoxic insult and even increases in magnitude over time. Indeed, the initial or transient phase of contraction (Phase 1) is thought to arise in a manner which is mechanistically separate to the second, sustained response (Phase II). This biphasic contractile response corresponds with a biphasic increase in $[Ca^{2+}]_{cyt}$.

Calcium entry via both the plasma membrane and the SR appear to be important for HPV (McMurtry et al., 1976; Robertson et al., 2000; Dipp et al., 2001; Mark Evans and Ward, 2009). Key to the maintenance of this vasoconstriction is sensitisation of the contractile machinery of Ca^{2+} , modulation of the expression and function of ion channels and the activation of pathways which lead to structural remodelling of the circulation.

The mechanisms by which this contractile response is generated remain controversial, however it appears to occur as a result of a hypoxia-dependent depolarisation via the inhibition of K_v channels (Post et al., 1992; Barman, 1998). The resulting change in E_m leads to the opening of L-Type VDCCs, Ca^{2+} entry and contraction.

1.3.3 Pulmonary vascular remodelling

The remodelling of the pulmonary vasculature is considered to be one of the hallmarks of PAH. Regardless of the stimulus responsible for the induction of pulmonary hypertension, structural alteration of the vasculature is considered as the means by which elevated pulmonary pressures which are not susceptible to reversal by vasodilatators are maintained. Vasconstriction and the proliferation

of PAMSCs in idiopathic disease are probably closely linked. Intracellular Ca^{2+} is a mediator of proliferation and many endogenous vasoactive compounds (including 5HT, ET-1, prostacyclin and NO) also have actions upon proliferation. Furthermore, the alteration of haemodynamic stresses upon vessels produced by vasoconstriction, in the initial stages of disease or as induced by hypoxia, may itself contribute to activation of pathways which promote proliferation and remodelling (Hishikawa et al., 1994; Hardingham et al., 1997; Rubin, 1997; Mandegar et al., 2004).

The remodelling process generally consists of the extension of smooth muscle into distal, previously non-muscular arteries and smooth muscle cell hypertrophy and hyperplasia in proximal muscular arteries. In each case the increased deposition of extracellular membrane proteins such as collagen and elastin are observed. (Rubin, 1997; Jeffery and Wanstall, 2001; Hopkins and McLoughlin, 2002; Humbert, Morrell, et al., 2004).

These changes can be observed in histological sections. Small, distal vessels develop a distinctive double elastic lamina with a muscular media which is not observed in the healthy lung. The overall extent of this remodelling can be assessed as the ratio of small, remodelled vessels to the total number of vessels (MacLean et al., 2004; Merklinger et al., 2005). Similarly, increased medial diameter in muscular vessels can be quantified as the ratio of the medial diameter to the total diameter (Morrell et al., 1995). This gives a proxy for the degree of luminal occlusion produced by formation of the media.

All three layers of pulmonary vessels, adventitia, media and intima are observed to increase in size in remodelling.

In addition to smooth muscle proliferation, proliferation of fibroblasts and adventitial hypertrophy is also observed. In experimental hypoxic PH, the

migration and proliferation of adventitial fibroblasts is one of the earliest observable changes in the pulmonary vasculature, preceding the formation of a double elastic lamina and smooth muscle cell proliferation. Fibroblasts are also observed to differentiate into so-called myofibroblasts: fibroblasts expressing smooth muscle actin (Meyrick and Reid, 1979; Jones, 1992). Indeed, fibroblasts have been implicated as important mediators of PASMC in response to stimuli such as hypoxia as they are also observed to secrete molecules which are mitogens for PASMC (Rose et al., 2002; Stenmark et al., 2006) and chemotactic for circulating inflammatory cells (Li et al., 2011).

PAH is a progressive disease and remodelled vessels in advanced disease are observed to display distinctive morphologies. These include neointimal lesions - a vascular layer comprised of migrated myofibroblasts and extracellular matrix which forms between the endothelium and internal elastic lamina in advanced PH and advanced plexiform lesions. A plexiform lesion is an obliterative plexus of proliferating cells including myofibroblasts and atypical endothelial cells separated by capillary-like channels (Jeffery and Wanstall, 2001). The proliferation of endothelial cells appears to be important in the generation of these lesions (Tuder et al., 1994; Cool et al., 1997).

1.3.4 Models of experimental pulmonary hypertension

The study of the pathology of PAH has been hampered by a lack of animal models in which advanced pathologies, similar to those observed in human PAH, are observed. Exposure of animals to chronic hypoxia or a single injection of monocrotaline, a toxic pyrolizidine alkaloid, are the most commonly used models.

Chronic hypoxia can be induced in either a normobaric manner, through reduction of the proportion of oxygen in respired air and replacement with nitrogen, or a hypobaric manner, through reduction of atmospheric pressure. In mice, chronic hypoxia produces increased right ventricular pressure (RVP), right ventricular hypertrophy (RVH) and vascular muscularisation, though relatively less vascular remodelling is observed in comparison to the rat (Stenmark et al., 2009). Of the rodents, fawn-hooded rats develop the most pronounced pulmonary vascular remodelling and the most severe elevation in PAP. Neonatal calves develop extremely high PAP associated with remodelling of both proximal and distal pulmonary vessels (Stenmark et al., 1987, 2006). The primary drawbacks of the chronic hypoxia model of PH is a lack of similarity to the human disease, particularly where idiopathic/primary PH is concerned. While increased PAPs associated with vascular remodelling is observed in these models, no plexiform-like lesions are observed. Also, any changes induced by exposure to hypoxia are reversed if the animal is returned to normoxic conditions and allowed to recover. This is in contrast to the progression observed in PH patients, except those with PH arising from exposure to hypoxia, e.g. as a result of living at altitude. In that sense, the hypoxic model has an advantage in that it directly reproduces a stimulus to which a direct causal link to PH has been established in humans. In addition, the ease with which the stimulus can be administered, the reproducibility of its effects and the large base of information on the technique in the literature which is available for consultation make this an attractive model for use in the study of PH.

The second 'classical' model of PH is produced using the toxic pyrrolizidine alkaloid monocrotaline. Ingestion or intraperitoneal (IP) Injection of this compound results in the progressive development of pulmonary vascular

remodelling associated with elevated PAPs (Kay et al., 1967). An interesting characteristic of this model, and possibly its greatest drawback as a model of human disease, is the relative ease with which it is cured (Stenmark et al., 2009).

These models have contributed to knowledge of the processes leading to the generation of PH. However, their primary failure is the lack of progression and advanced vasculopathy as observed in PAH patients. Such lesions have been produced to some extent using multimodal interventions for the generation of PH in mice. A combination of monocrotaline injection with either pneumonectomy or the generation of an anastomosis between the subclavian and pulmonary arteries produced extensive neointimal formation in the pulmonary vasculature of rats. These studies also highlight the potential role of haemodynamic flow in the generation of pulmonary hypertension (Okada et al., 1997; Kimura et al., 2001). Another study demonstrated that antagonism of the vascular endothelial growth factor (VEGF) receptor 2 in concert with hypoxia produced severe pulmonary hypertension in rats which persists and progresses even when these animals were returned to normoxia (Taraseviciene-Stewart et al., 2001).

Though mice show a relatively modest amount of vascular remodelling in response to chronic hypoxia, their experimental utility is increased by the generation of transgenic animals. These models are of particular interest due to the observation of familial and genetic predispositions to PH in humans. They include mice overexpressing the serotonin transporter (SERT+ mice) (MacLean et al., 2004), mice which are heterozygous for knockout of bone morphogenetic protein receptor 2 (BMPR2 +/- mice) (Song et al., 2005) and mice overexpressing the RAGE ligand MTS1/S100A4 (Greenway et al., 2004), the latter of which is discussed in detail below.

1.4 The receptor for advanced glycation end-products

The receptor for advanced glycation end-products is a 35-kDa polypeptide of the immunoglobulin superfamily (Nepper et al., 1992) that has recently been widely implicated as a mediator of both acute and chronic vascular inflammation in conditions such as atherosclerosis, in particular as a complication of diabetes (Schmidt et al., 1994; Hudson et al., 2003; Ramasamy et al., 2005; Basta, 2008). As shall be discussed, activation of RAGE may alter the response of vessels to mediators of tone by contributing to the phenotypical changes and remodelling associated with vascular disease.

An early study demonstrated that RAGE is basally expressed in both smooth muscle and endothelial cells of the bovine systemic vasculature and in neurones innervating them in both large vessels (*e.g.* aorta) and the microvasculature (Brett et al., 1993). In the human peripheral vasculature, endothelial expression of RAGE is typically diffuse and variable but is enhanced by risk factors for vascular disease such as hyperlipidaemia and in patients with symptomatic occlusive vascular disease. RAGE has also been found in early and end stage atherosclerotic lesions in the endothelium of human coronary artery (Ritthaler et al., 1995). Interestingly, this upregulation in disease states occurs in both the presence and the absence of hyperglycaemia associated with diabetes though both the severity of vascular perturbation and RAGE expression are enhanced by diabetes (Burke et al., 2004). These findings are corroborated by an observed upregulation of RAGE in the systemic vasculature of mice used as models of vascular inflammation in both euglycaemia and hyperglycaemia (Park et al., 1998; Kislinger et al., 2001; Bucciarelli et al., 2002; Harja et al., 2008).

1.3.1 Characteristics of RAGE

RAGE is able to bind a variety of structurally diverse ligands and sites of RAGE upregulation tend to show colocalisation with molecules thought to bind and activate the receptor. These include advanced glycation end-products (AGEs), S100/calgranulin proteins, high mobility group box 1(HMGB-1) protein and oxidised low density lipoprotein (oxLDL) and lipopolysaccharide (LPS) (Hofmann et al., 1999; Basta et al., 2002; Harja et al., 2008; Sun et al., 2009; Yamamoto et al., 2011). These sites also tend to display other markers of inflammation such as adhesion molecules for circulating inflammatory leukocytes (e.g. vascular cell adhesion molecule 1 (VCAM-1), intercellular adhesion molecule 1 (ICAM-1) and E-selectin), matrix metalloproteinases (MMPs) and cyclooxygenase-2 (COX-2,) (Palinski et al., 1995; Basta et al., 2002; Harja et al., 2008). In addition to causing upregulation of adhesion molecules, RAGE is a counter-receptor for integrins on the surface of circulating leukocytes, specifically the β2-integrin Mac-1 (Chavakis et al., 2003), and participates directly in firm adhesion of leukocytes to the endothelium.

The ability of RAGE to recognise such a varied selection of ligands has led to the hypothesis that it is a pattern-recognition receptor (PRR) (Li et al., 2006). PRRs, such as the toll-like receptors (TLRs), are involved in innate immunity and depend upon recognition of three-dimensional structures rather than peptide sequence (Medzhitov and Janeway, 1997).

One of the best documented consequences of RAGE activation is the generation of reactive oxygen species (ROS) (Mullarkey et al., 1990; Yan et al., 1994; Basta et al., 2002; Vincent et al., 2007). Increased ROS is also associated with formation of AGEs (Mullarkey et al., 1990). Thus, at sites of vascular

inflammation there would be an expectation of increased ROS formation which would be enhanced further by activation of RAGE. ROS such as superoxide (O_2^-) and hydrogen peroxide (H_2O_2) have direct effects on vascular tone (Rubanyi, 1988). In addition, O_2^- is able to react with NO to form peroxynitrite ($ONOO^-$); a reactive nitrogen species (RNS) and a vasodilator (Li et al., 2005; Szasz et al., 2007).

RAGE binding also results in the activation and translocation of proinflammatory kinases and transcription factors including p21 ras, extracellular signal-related (ERK) and c-Jun N-terminal (JNK) mitogen-activated protein (MAP) kinases, and the proinflammatory transcription factor Nuclear Factor- κ B (NF- κ B) (Lander et al., 1997; Hofmann et al., 1999). Experimentally, this activation is prevented by the presence of ROS scavengers or dismutases and enhanced by glutathione depletion, though there is some evidence of a ROS independent component (Lander et al., 1997; Basta et al., 2005). NF- κ B-DNA binding is associated with the expression of an altered cellular phenotype including the expression of adhesion molecules for circulating inflammatory cells such as VCAM-1 and ICAM-1 (Voraberger et al., 1991; Neish et al., 1992; Schmidt et al., 1995)(Voraberger et al., 1991; Neish et al., 1992; Schmidt et al., 1995). Increased NF- κ B activity has been observed in endothelial cells (EC), smooth muscle cells (SMC) and monocytes in atherosclerotic plaques (Brand et al., 1996). One potential source of inflammation is the presence of infectious agents such as viruses which can induce NF- κ B activation in these cells via activation of PRRs such as TLRs (Kol and Libby, 1998; Krakauer, 2008). There are a number of ligands which have been shown to act at both TLRs and RAGE.

Key to the implication of RAGE as a mediator of chronic vascular inflammation is the observation that NF- κ B possesses a binding site for the RAGE

gene (Li and Schmidt, 1997). NF- κ B is activated by a large number of stimuli including hyperglycaemia (Nobe et al., 2003), oxHDL (Matsunaga et al., 2003), oxLDL and reduced shear stress (Lan et al., 1994; Mohan, Hamuro, Koyoma, et al., 2003; Mohan, Hamuro, Sorescu, et al., 2003; Yang et al., 2005). Thus, even if RAGE-ligand interactions are not the trigger in inflammation, NF- κ B activation in response to other stimuli may sensitise the vessel to RAGE ligands, providing a means for the maintenance and amplification of the inflammatory response beyond an initial inflammatory insult. This observation is particularly important given that, as will be discussed in further detail below, ligands of RAGE possess characteristics beyond their RAGE binding affinity which are directly or indirectly proinflammatory.

While there are no RAGE receptor antagonists *per se*, RAGE antagonism in experimental models may be accomplished using either antibody against RAGE or using soluble RAGE (sRAGE). sRAGE possesses the ligand binding domain but lacks the cytoplasmic and transmembrane domains; sRAGE will therefore compete for ligands which bind to cell-bound RAGE. Endogenous sRAGE is present at low concentrations (~1nM) in the serum of healthy individuals (Park et al., 1998) and is generated as a splice variant of RAGE and by proteolytic cleavage (Galichet et al., 2008; Harja et al., 2008).

In addition to the use of sRAGE, prevention of RAGE signal transduction can also be studied using RAGE^{-/-} animals and transgenic animals expressing dominant negative RAGE (DN-RAGE) which lacks the cytoplasmic (*i.e.* signal transducing) domain of the receptor. This may be accomplished by inserting a stop codon into the cDNA sequence at the end of the region encoding the transmembrane domain (Harja et al., 2008). Studies using these models have provided an insight into the role of RAGE and will be discussed in more detail

below.

1.4.2 Ligands for RAGE

1.4.2.1 Advanced glycation end-products

Advanced glycation end-products are reactive derivatives of nonenzymatic glucose-protein reactions that form gradually and irreversibly in healthy individuals. This occurs at an increased rate with ageing, under conditions of hyperglycaemia and in areas of increased oxidant stress (Brownlee et al., 1984; Mullarkey et al., 1990; Yan et al., 1994; Bierhaus et al., 1998). AGEs represent the prototypical ligand for RAGE (Neeper et al., 1992; Schmidt et al., 1992) and, even prior to the cloning and expression of RAGE, they had been implicated in the pathogenesis of diabetic complications (Brownlee et al., 1984). They were later shown to bind to endothelial cells and to dose-dependently evoke changes in vascular properties such as permeability and the expression of molecules involved in thrombogenesis (Esposito et al., 1989). The ability of AGEs to bind RAGE was subsequently inferred by the fact that binding of radioactively labelled AGE protein to tissue known to express RAGE is inhibited by unlabelled AGE protein and by sRAGE (Schmidt et al., 1992).

AGEs are present in atherosclerotic plaques found in animals (Palinski et al., 1995) and diabetic patients (Nakamura et al., 1993). Blood concentration of AGE bound haemoglobin (Hb-AGE) in these patients is raised (Makita et al., 1992) and in animal models of both diabetes and atherosclerosis RAGE is upregulated in the systemic vasculature (Bucciarelli et al., 2002; Harja et al., 2008). The co-localisation of RAGE with ligands which are present at elevated levels in disease

suggests RAGE involvement in the pathogenesis of inflammatory cardiovascular diseases such as atherosclerosis and their exacerbation in diabetics. In addition to forming extracellularly and in the serum where they may bind RAGE, AGEs have been shown to form intracellularly in a ROS dependent manner. This can lead to deleterious effects including further ROS generation and lipid oxidation leading to the retention of oxLDL in the vessel wall (Giardino et al., 1996; Anderson and Heinecke, 2003).

1.4.2.2 S100 proteins

S100 proteins are low molecular weight (~11kDa) calcium binding proteins similar to calmodulin and possessing a characteristic loop-helix-loop structure termed the E-hand (Donato, 2003; Gifford et al., 2007). On interaction with calcium, a conformational change exposes a hydrophobic domain which can interact with and regulate the function of target proteins. Unlike the ubiquitous calmodulin, various S100 isoforms appear to show an association with particular tissues and, furthermore, to particular intracellular compartments within them (Donato, 2003). The nature of these tissues is widely varied and includes human aortic SMCs (Mandinova et al., 1998; Daub et al., 2003), endothelial cells (Burke et al., 2004; Harja et al., 2008), and post ganglionic sympathetic nerves (Sandelin et al., 2004). S100 proteins relocate within cells in a calcium-dependent manner (Mandinova et al., 1998) and carry out various intracellular roles in the regulation of cell function (for extensive reviews see (Donato, 1999, 2001, 2003; Heizmann et al., 2007)). In addition, S100 proteins are upregulated in response to inflammatory stimuli (Hofmann et al., 1999; Sandelin et al., 2004) including RAGE activation by AGEs or S100 itself (Hofmann et al., 1999; Harja et

al., 2008). As with RAGE, this upregulation is observed at sites of vascular inflammation and disease in both humans (Burke et al., 2004) and animals (Hofmann et al., 1999; Harja et al., 2008).

A potent source of S100 protein is activated monocytes (Rammes et al., 1997; Hofmann et al., 1999), and released S100 can act in a paracrine manner to induce monocyte chemotaxis (Yang et al., 2001). This may explain the accumulation of S100 proteins at sites of inflammation where recruited monocytes are activated by RAGE ligands and other inflammatory stimuli (*e.g.* cytokines), resulting in the generation of S100. These findings are strong arguments in favour of the involvement of S100-RAGE interactions in the onset, amplification and maintenance of vascular inflammation.

The S100 - RAGE interaction displays an interesting and complex pharmacology. Different S100 proteins are able to differentially activate downstream signalling pathways by binding to different domains of the RAGE protein, *i.e.* S100B binds to the V and C₁ domains, activating phosphatidylinositol 3-kinase and NF-κB, while S100A6 binds to the C₁ and C₂ domains, activating JNK (Leclerc et al., 2007). Many of the S100 proteins have been shown to produce their effects by interacting with RAGE (Heizmann et al., 2007), however, the consequences of ligand binding also appear dependent on the concentration of S100 present. In neuroblastoma cells, S100B produces trophic effects at nanomolar concentrations and inflammatory effects at micromolar concentrations (Huttunen et al., 1999, 2000). There is also evidence in the literature of S100 induced cellular effects which do not depend on RAGE signalling but require the receptor. For example, the consequences of S100B exposure in microglial cells include NF-κB activation and NO release. Transfection of these cells with DN-RAGE ablated NF-κB activation but not the

release of NO (Adami et al., 2004). Furthermore, the transfected cells, possessing a greater density of RAGE on the extracellular membrane showed even greater NO release than non-transfected cells.

1.4.2.3 HMGB-1

High mobility group box-1 protein, also known as amphotericin is a ubiquitous nuclear protein which is loosely bound to DNA where it stabilises nucleosome formation and is involved in the regulation of transcription. It consists of three domains: two DNA-binding elements (an A-box and a B-box) and a negatively charged C-terminal. It is basally expressed by vascular and inflammatory cells and is upregulated in cells of atherosclerotic plaques, particularly macrophages (Kalinina et al., 2004). It is upregulated and secreted by endothelial cells and monocytes stimulated by cytokines such as interferon (IF) γ , tumour necrosis factor (TNF) α or TNF β (Kalinina et al., 2004). It is also secreted by necrotic, though not apoptotic, cells (Li et al., 2006; van Beijnum et al., 2008). Areas adjacent to the necrotic core of vascular lesions show intense concentration of HMGB-1.

Once secreted, HMGB-1 may act at cellular receptors to cause further inflammation. HMGB-1 was identified as a ligand for RAGE by Hori et al., 1995. In addition, it is able to bind the TLR2 and TLR4 (Park et al., 2004) receptors which are expressed on both vascular and inflammatory cells (van Beijnum et al., 2008) and are responsible for the innate immune response to bacterial toxins such as LPS (Lin et al., 2009). In addition to the upregulation and secretion of HMGB-1, inflammatory cytokines cause upregulation of TLR2, TLR4 and RAGE on the cell surface of smooth muscle cells, which may sensitise them to HMGB-1

and/or other RAGE ligands such as AGEs or S100 protein (Jaulmes et al., 2006).

Indeed, administration of LPS in mice *in vivo* resulted in elevated plasma concentration of S100A12 (Hofmann et al., 1999).

HMGB-1 is somewhat unique in representing an endogenous ligand for TLRs. This is in contrast to its other cellular receptor RAGE, which is activated exclusively by endogenous ligands. As such, identifying which of these receptors is responsible for the induction of inflammatory responses by HMGB-1 is complicated and may explain why treatment with antibody for RAGE or sRAGE produces a dose dependent, though incomplete, inhibition of the effects of HMGB-1 in some instances (Hori et al., 1995; Treutiger et al., 2003). Indeed, a study by Park *et al* (2004) demonstrated little interaction between HMGB-1 and RAGE, and very little NF- κ B activation by RAGE on macrophages. Conversely, neutrophil migration in response to HMGB-1 is strongly dependent on the presence of RAGE on the cell surface of these cells (Orlova et al., 2007). This appears to occur due to an HMGB-1-induced *cis* dimerisation between RAGE and the Mac-1 integrin on the surface of these cells. This dimerisation increases the affinity of Mac-1 for ICAM-1; its counterreceptor on the endothelial cell surface. Cytokine production and adhesion molecule upregulation by endothelial cells is at least partially mediated by RAGE (Treutiger et al., 2003).

The implications of the ability of HMGB-1 to induce cytokine production/secretion, and *vice versa*, leading to adhesion molecule, TLR and RAGE expression are clear with respect to the amplification of inflammation.

1.4.2.4 Mac-1

The Mac-1 integrin (also known as α M β 2 and CD11b/CD19) is a member of

the β_2 -integrin family and is expressed on the cell surface of circulating leukocytes. This protein interacts with ICAM-1 on endothelial cells and is involved in firm adhesion of leukocytes to the endothelium. This event is part of a cascade of events which lead to leukocyte migration into the vessel wall, a key event in the pathogenesis of vascular disease (Carlos and Harlan, 1994). In addition to recognising ICAM-1, a direct interaction between Mac-1 and endothelial RAGE has been observed (Chavakis et al., 2003). In this study it was observed that neutrophil migration in a mouse model of peritonitis was reduced by antibody for ICAM-1 or sRAGE and was abolished by antibody for Mac-1. It is of note that mice which were rendered diabetic showed an increase in neutrophil migration which was affected by these treatments in a similar manner. Neutrophil migration was also reduced in RAGE^{-/-} mice. Importantly, this change was produced with no effect on expression levels of Mac-1 in neutrophils isolated from RAGE^{-/-} mice. These results were confirmed *in vitro*: both human neutrophils and cells transfected with Mac-1 adhered to immobilised RAGE or cells expressing RAGE in a manner which was prevented by sRAGE or antibody for Mac-1.

One of the most interesting and surprising observations of this study was that the RAGE ligand S100B enhanced RAGE and Mac-1 interaction by 250% (Chavakis et al., 2003). The enhancement of leukocyte migration by RAGE therefore appears to represent yet another mechanism by which inflammation may be augmented by RAGE and its ligands: the enhancement of the Mac-1-ICAM-1 interaction as a consequence of HMGB-1 activation of RAGE on leukocytes is another example of this (Orlova et al., 2007).

1.4.3 Intervention in RAGE-ligand binding

RAGE-ligand binding has been used to produce marked benefits in models of systemic vascular disease. In a model of diabetes-exacerbated atherosclerosis, treatment with sRAGE prevented increases in serum AGE, expression levels of RAGE, S100 protein, VCAM-1, Tissue Factor (TF), COX-2 and MMPs. This was associated with inhibition of monocyte infiltration, collagen deposition, smooth muscle cell proliferation and oxidative stress (Park et al., 1998; Kislinger et al., 2001). Soluble RAGE treatment also prevented disease progression in a model of established atherosclerosis (Bucciarelli et al., 2002).

Interference with the RAGE pathway has also been accomplished using transgenic animals. RAGE^{-/-} animals and animals expressing DN-RAGE have given an insight into the impact of RAGE activation in disease. Interestingly, *in vitro* studies on endothelial cells from atherosclerotic mice transfected with DN-RAGE appear to have even greater protection against vascular inflammation compared to cells from RAGE^{-/-} mice (Harja et al., 2008). This may be because RAGE^{-/-} mice do not possess the full length membrane bound RAGE receptor responsible for the activation of proinflammatory pathways and so they will also lack endogenous sRAGE protein due to splice variation and/or proteolytic cleaving. This latter process has recently been demonstrated to occur independently of RAGE activity and in a calcium-dependent, caveolin-1 mediated manner (Galichet et al., 2008).

It is possible that this improved protection in DN-RAGE mice may be due to the removal of AGEs via an sRAGE dependent pathway. Immunoprecipitation of compounds displaying both AGE and RAGE epitopes from serum of sRAGE treated atherosclerotic mice has been observed (Park et al., 1998). Since plasma

AGE concentration is lowered in these animals, this suggests that the sRAGE-AGE interaction is not transient but may be part of a clearance mechanism for AGEs. Transgenic mice expressing DN-RAGE will presumably retain this mechanism while RAGE^{-/-} mice will not.

These data highlight one of the difficulties in studying the role of RAGE. Treatment with sRAGE may overemphasise the role of RAGE in vascular inflammation in that it is not acting on the receptor itself, but its ligands. Therefore, treatment with sRAGE informs us of the consequences of reducing the bioavailability of RAGE ligands as opposed to the consequences of preventing RAGE signal transduction. In addition, compounds which may act at RAGE in addition to other receptors will also be bound by sRAGE, possibly preventing the production of inflammation *via* other ROS generation and NF-κB activating pathways. Examples of this include HMBG-1 protein which activates Toll Like Receptors 2 and 4 (Park et al., 2006; Heizmann et al., 2007) and oxLDL which, in addition to acting at oxLDL receptor 1, possesses AGE epitopes (Imanaga et al., 2000) and produces vascular inflammation *via* RAGE activation (Harja et al., 2008; Sun et al., 2009).

While this may reduce the usefulness of sRAGE in investigating the physiological and pathophysiological characteristics of RAGE, the possibility that it may act as both a decoy for RAGE ligands and as part of a clearance mechanism for harmful compounds make it an attractive target of study with the aim of developing therapeutics.

1.4.4 The pathogenesis of pulmonary hypertension and RAGE

In comparison to the systemic circulation, there are far fewer studies

published concerning pulmonary vascular disease (PWD) and, considering that RAGE was described relatively recently, it is perhaps not surprising that there is less information relating to the involvement of RAGE in the development of PWD. However, RAGE is basally expressed to a high degree in the lung (Neeper et al., 1992), particularly in the small arteries and arteriolar capillaries (Brett et al., 1993). Recent *in vivo* and *in vitro* studies have provided evidence which strongly suggests a role for RAGE in PWD and PAH. The observation by Ambartsumian et al. (2005) that overexpression of the RAGE ligand MTS1/S100A4 leads to the occasional, spontaneous development of obliterative plexiform-like lesions in mice was the first and perhaps the most important of these. Given the difficulty of replicating neointimal formation or formation of plexiform lesions in animal models, the occurrence of spontaneous and severe PWD in a subset of MTS1/S100A4 mice (~5%) by Ambartsumian et al. is of great interest.

The development of obliterative lesions in MTS1/S100A4 mice is associated with a marked upregulation of MTS1/S100A4, particularly in occluded vessels and particularly in the endothelial cells lining the obstructed lumen of the vessel. In addition, infiltration by circulating inflammatory cells is increased in these mice (Greenway et al., 2004). Neither of these features was observed in wild type mice or in MTS1/S100A4 mice which do not develop occlusive lesions. A comparison of the morphology of these lesions, as well as associated MTS1/S100A4 expression, with those observed in human tissue obtained from lung biopsy samples taken from PAH patients demonstrated that the cellular constituents and morphology of occlusive lesions in humans and MTS1/S100A4 mice are similar. MTS1/S100A4 expression is also increased in human PAH patients in a manner which correlates to the severity of disease observed (Greenway et al., 2004).

As pointed out by Merklinger et al., (2005), the development of occlusive PVD by a subset of MTS1/S100A4 mice certainly suggests an involvement of MTS1 in the pathogenesis of PVD though offers no explanation for why only a small number of these mice go on to develop it. In their follow up study, it was demonstrated that MTS1/S100A4 mice display mildly increased RVP and RVH in comparison to wild type mice. Exposure to hypoxia for 2 weeks resulted in increased RVP and RVH in both MTS1/S100A4 mice and wild type mice that were enhanced in MTS1/S100A4 mice. Hypoxia also caused increased muscularisation of small pulmonary arteries and decreased artery concentration (taken to be proxies of PVD). Interestingly, these were similar between MTS1/S100A4 mice and wild type mice. However, if returned to normoxia, wild type mice displayed significant or complete recovery to baseline values in each of the criteria measured. This recovery is blunted in the MTS1/S100A4 mouse. In concert with the observation that MTS1/S100A4 is only increased in the later stages of PH in humans, in particular, those involving SMC proliferation (Greenway et al., 2004), this suggests that MTS1/S100A4 may be involved in the maintenance of the inflammatory response as opposed to its induction.

1.4.4.1 MTS1/S100A4 and the serotonin hypothesis

Recent *in vitro* studies have provided evidence of a role for an interaction between MTS1/S100A4 (also known as Fibroblast Specific Protein-1) and RAGE in human PASMCs and suggested that MTS1/S100A4 may have an important role in the 'serotonin hypothesis' of pulmonary hypertension (for recent reviews see (Dempsie and MacLean, 2008; Maclean and Dempsie, 2010)).

Serotonin (5HT), both a vasoconstrictor and a mitogen, can stimulate

human PASMC migration and proliferation (MacLean et al., 2000). In PASMCs, 5HT produces dose dependent upregulation of MTS1/S100A4 (Lawrie et al., 2005). This upregulation appears to be dependent on both the 5-HT_{1b} receptor and the serotonin transporter in that pharmacological inhibition of either prevents its occurrence. This is supported by the observation that inhibition of pathways activated downstream of either molecule (ERK1/2 in the case of 5-HT_{1b} and monoamine oxidase in the case of SERT) inhibit the upregulation of MTS1/S100A4 by 5-HT while, conversely, SERT overexpression leads to its enhancement (Lawrie et al., 2005).

Phosphorylation and translocation of ERK to the nucleus leads to phosphorylation of the transcription factor GATA-4 (Suzuki et al., 2003) which possesses a binding site for the MTS1/S100A4 gene. Both 5-HT and MTS/S100A4 induce PASMC migration and proliferation in a manner that is inhibited by antibody for RAGE, sRAGE or antibody for MTS1/S100A4 (Spiekerkoetter et al., 2005). The upregulation of MTS1 by 5HT therefore represents a novel pathway by which 5-HT_{1b} receptor activation and SERT activity may be linked to increased proliferation and migration of SMCs through activation of RAGE. However, this has yet to be shown *in vivo* as no studies on the effects of RAGE blockade in this or any other animal model has been carried out.

Encouragingly, roles for both RAGE and sRAGE have recently been established in other lung pathologies such as acute lung injury (Calfee et al., 2008; Zhang et al., 2008). Further circumstantial evidence in favour of a role for extracellular MTS1/S100A4 in PVD comes from the observation that MTS1/S100A4 is expressed in different cell types in occlusive lesions in MTS1/S100A4 mice and humans (ECs and SMCs respectively) suggesting that MTS1/S100A4 may be acting in a paracrine or an autocrine fashion to cause SMC proliferation and migration

(Merklinger et al., 2005).

Based on the ability of MTS1 to induce SMC migration and proliferation by activating RAGE *in vitro* (Lawrie et al., 2005), as well as the ability of sRAGE to prevent SMC migration and proliferation in response to 5HT, it seems likely that RAGE is involved in the enhanced hypoxia-induced vascular remodelling observed in MTS1/S100A4 mice. Combined with the observation that MTS1/S100A4 is upregulated in lesions from PAH patients (Greenway et al., 2004) as well as the implication of 5HT in the development of the pulmonary hypertension, the role of the MTS1/S100A4-RAGE interaction represents an avenue of study which may yield worthwhile information regarding the pathogenesis of this disease.

ROS generation is thought to be important in the phenomenon of hypoxic pulmonary vasoconstriction (Ward, 2007) and possibly to the development of hypoxia-induced models of pulmonary hypertension (Hoshikawa et al., 2001) and, given the association between RAGE ligand binding and ROS generation, there is significant scope for modification of vascular tone by RAGE in the pulmonary vasculature.

1.5 Aims

RAGE appears centrally placed to modulate the development of inflammation in pulmonary hypertension and initial *in vitro* and *in vivo* studies have provided compelling evidence that RAGE and its ligands are important in the development of this disease

In the course of this thesis, we aim to further explore the role of RAGE in pulmonary hypertension, using a combination of disease models *in vivo*, isolated tissue preparations *ex vivo* and *in vitro* cell culture in an attempt to piece

together the mechanisms by which RAGE and its ligands may effect structural and functional change in the pulmonary circulation.

Chapter 2.

Materials and methods

2.1 Materials

Cambrex Bio Science, Berkshire, UK:

- Dulbecco's Modified Eagle Medium with 4.5g/l glucose (DMEM),
- Dulbecco's Phosphate Buffered Saline without Ca^{2+} and Mg^{2+} (PBS).

Sigma-Aldrich, Poole, UK:

- 5-hydroxytryptamine hydrochloride (5HT),
- Foetal bovine serum (FBS),
- L-glutamine (200mM),
- penicillin streptomycin solution (10,000 units penicillin and 10mg streptomycin per ml in 0.9% NaCl),
- trypsin-EDTA
- 9,11-Dideoxy-11 α ,9 α -epoxymethanoprostaglandin F2 α (U46619)
- Sodium Nitroprusside (SNP),
- Heparin Sodium Salt,
- Methylcellulose.

Calbiochem, UK

- Monocyte chemoattractant protein-1 (MCP-1), recombinant (ecoli).

Fisher Scientific

- BD micro-fine insulin syringes.

The soluble receptor for advanced glycation end-products was kindly

provided by Dr. Anne Marie Schmidt of Columbia University, New York, USA.

Bindarit was kindly supplied by Angelo Guglielmotti and Angelini

Pharmaceuticals, Rome, Italy. Frozen CCL39 Chinese hamster lung fibroblasts

were kindly provided by Prof. Andrew Baker of Glasgow University.

2.2 Animal studies

All animal studies were carried out in adherence with the Animals (Scientific Procedures) Act 1986, UK and under project license number 60/3773 held by Professor M.R. MacLean (University of Glasgow, Scotland).

2.2.1 Transgenic mice

Mice overexpressing the MTS1/S100A4 gene were generated and provided by Dr. Noonah Ambartsumian as described in the literature (Ambartsumian et al., 2005). The C57BL/6 mouse is the genetic background strain and these were used as controls in experimental studies.

2.2.2 Induction of chronic hypoxia and establishment of PAH in mice

Mice were placed in long 'shoebox' cages with *ad libitum* access to food and water. These cages were placed into a hypobaric chamber consisting of a sealed plastic box, an air pump and an inlet of variable resistance. By activating the pump and slowly increasing the resistance of the inlet, the atmospheric pressure inside the chamber can be made to fall. Mice were allowed to slowly acclimatise to hypoxia: 550mbar. This is equivalent to a reduction of oxygen

content to 10%. The pressure was reduced by 50mbar/hour over two days, after which they received a chronic-hypoxic challenge of 12 further days. For the purpose of dosing studies, the chamber was repressurised daily at a rate of 50mbar/15mins, dosed, and then restored to hypoxia at a similar rate. Dosing was by intraperitoneal (IP) injection in all cases. Hypoxic and normoxic mice were treated with either 300 μ l/day of 10mg/ml bindarit suspended in a solution of 0.5% methylcellulose solution; 300 μ l/day of 0.5% methylcellulose solution (vehicle); 100 μ l/day of 200 μ g/ml sRAGE in phosphobuffered saline (PBS); 100 μ l/day of PBS. BD micro-fine syringes were used to minimise dead space and waste.

2.2.3 Assessment of haemodynamic properties in vivo

Fourteen days after the induction of hypoxia, mice were re-pressurised slowly to atmospheric pressure. Mice were then placed in an anaesthetic box. Anaesthesia was induced by inhalation of 3% isoflurane supplemented with O₂. The criterion for assessment of successful anaesthesia was abolition of the hind limb flexor withdrawal reflex. This was routinely checked throughout the experiment. Mice were transferred to the bench-top and anaesthesia maintained using 1.5-2% isofluorane by means of a face mask.

Mice were secured supine and the right carotid artery exposed by blunt dissection. Measurement of the systemic mean arterial pressure was accomplished by cannulation of the carotid artery with an appropriately sized cannula primed with saline and heparin (50U/ml). Assessment of right ventricular pressure was achieved using a 25 gauge needle mounted on a micromanipulator and attached to a Elcomatic E751A pressure transducer. This

fed input to a BIOPAC Systems Inc MP100 interface which was linked to the BIOPAC data acquisition software.

A small area of skin at the base of the sternum was removed and the needle positioned just caudal to the xiphoid cartilage and approximately 1.5mm right of the midline. The needle was then advanced at an angle of approximately 25° through the skin and the diaphragm and ultimately into the right ventricle (Figure 2.1). Successful advancement of the needle into the right ventricle produced a pressure trace of characteristic form and magnitude, and could be further verified by the presence of a dicrotic notch (Figure 2.2) at the point of the waveform corresponding to diastole. Readings were collected for 10-15 minutes or for as long as the preparation remained viable. At the conclusion of the experiment, animals were euthanised by dislocation of the neck.

For the analysis of right ventricular pressure traces, 10 consecutive waves were highlighted. Biopac data acquisition software was configured to calculate the mean peak value of waves (corresponding to the mean sRVP) and the average overall pressure (corresponding to the mRVP) of waves in the selection as the length of time (Δt) in seconds of the selected section. Heart rate in beats/minute could then be calculated as $(60/\Delta t)$ multiplied by 10. For each experiment the mean sRVP, mean mRVP and mean heart rate were calculated as the mean of values obtained from three distinct representative regions of the pressure trace, *i.e.* where the reading appeared stable.

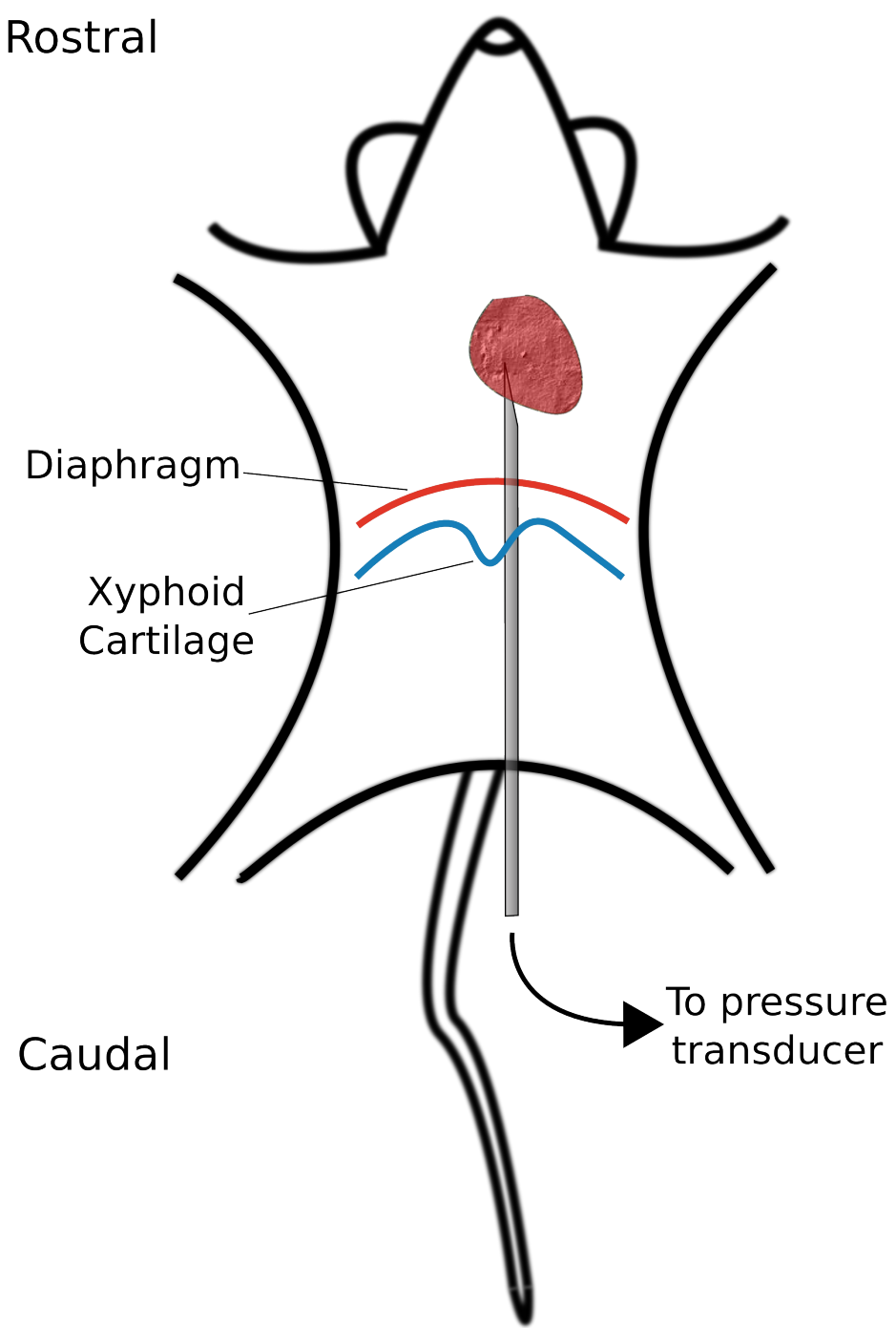


Figure 2.1 Placement of needle for right ventricular haemodynamic measurements in the mouse. After removing a small area of skin at the base of the sternum was removed and the needle positioned just caudal to the xiphoid cartilage and approximately 1.5mm right of the midline. The needle was then advanced at an angle of approximately 25° through the skin and the diaphragm and ultimately into the right ventricle

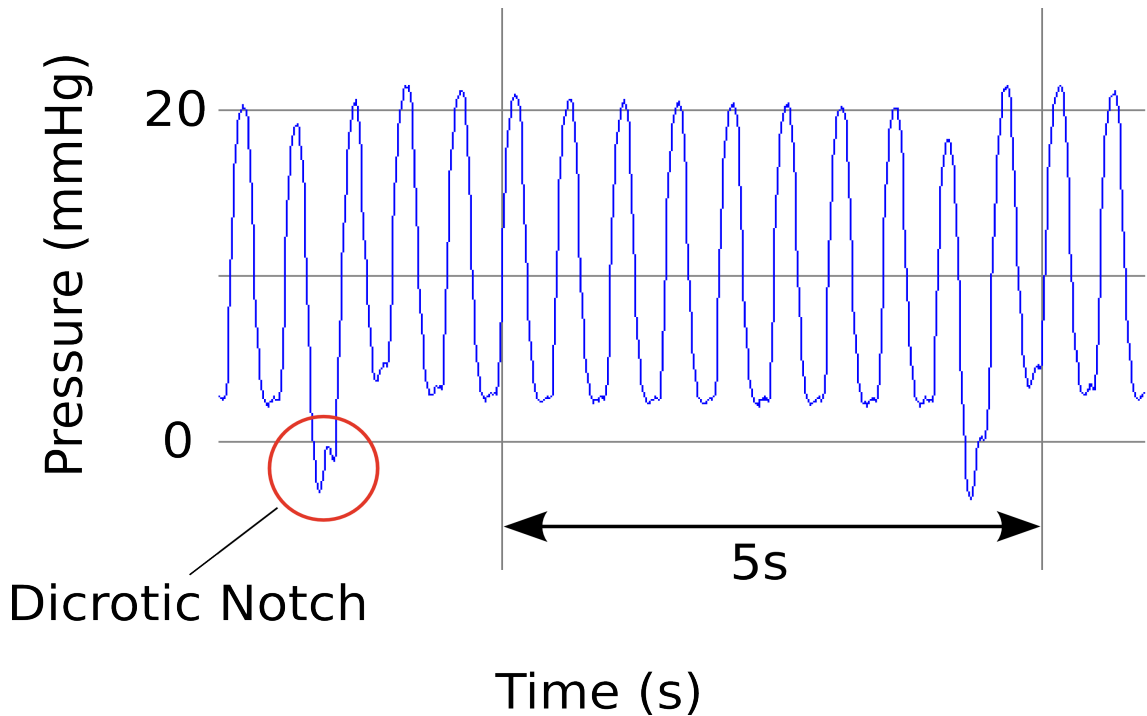


Figure 2.2 Representative right ventricular pressure trace. Successful advancement of the needle into the right ventricle produced a pressure trace of the form displayed above e.g. with a diastolic pressure approaching zero and a systolic pressure of approximately 20mmHg in untreated C57BL/6 mice. Successful positioning of the needle could be further verified by the presence of a dicrotic notch (circled) at the point of the waveform corresponding to diastole.

2.2.4 Tissue harvest

At the end of *in vivo* experiments, the heart and lungs were removed *en bloc*. The right lung was fixed in chilled 10% neutral buffer formalin (Composition: 90% dH₂O, 10% formalin, 33M NaH₂PO₄, 45M Na₂HPO₄) and kept agitated for a period of 3 days. All extraneous fat and vascular tissue were removed from the heart. It was frozen at -20°C for later assessment of right ventricular hypertrophy (RVH). The left lung was placed into chilled Krebs' buffer (composition: 118 mM NaCl, 4.7 mM KCl, 1.2 mM MgSO₄, 1.25 mM CaCl₂, 1.2 mM KH₂PO₄, 25 mM NaHCO₃, 11 mM glucose) solution for later dissection.

2.2.5 Assessment of right ventricular hypertrophy

Hearts were removed from the freezer and allowed to defrost. The atria were removed and the right ventricle separated from the left ventricle and the ventricular septum. The wet weight of the right ventricle (RV) as well as the mass of the left ventricle plus septum (LV+S) were assessed on an analytical balance. The ratio of RV:LV+S was taken as an index of the extent of right ventricular hypertrophy. This value was compared between treatment groups to give a comparative indication of the extent of right ventricular hypertrophy.

2.2.6 Assessment of vascular reactivity and vascular compliance

For studies in the pulmonary vasculature, the intralobar pulmonary artery was located by orienting the lung such that the visceral side is accessible and cutting along the primary bronchus allowing the identification and careful dissection of the intralobar pulmonary artery (diameter 200-250 μ M).

After the removal of excess connective tissue and peri-vascular fat, the vessel was divided into two 2mm segments. Vessel segments were mounted on a heated wire myograph (Danish Myotechnology, Aarhus, Denmark) and allowed to equilibrate for 30 minutes. A schematic of the wire myograph may be seen in Figure 2.3.

Gas of composition 16% O₂, 5% CO₂, 79% N₂ was bubbled through buffer in the organ baths throughout the experiment. This results in an O₂ concentration of approximately 120mmHg and CO₂ concentration of approximately 35mmHg in the bath. This approximates O₂ availability in vivo while the concentration of CO₂ contributes to the maintenance of an optimum buffer pH (MacLean et al., 1996).

Buffer temperature was maintained at 37°C. Krebs buffer was replaced every 15 minutes.

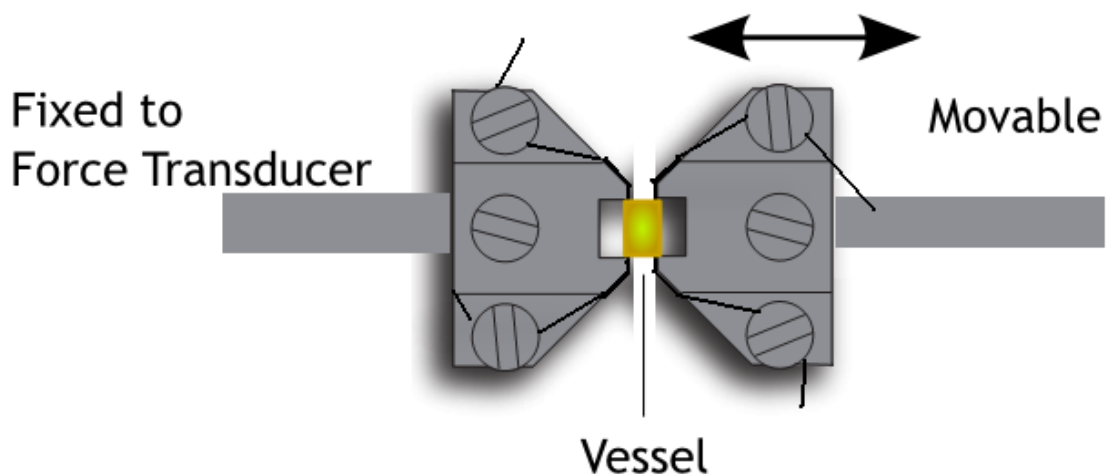


Figure 2.3 Schematic diagram of wire myograph. The wire myograph consists of two metal jaws: one of which is adjustable using a caliper which provides values of displacement to the nearest 10 μ m and one of which is fixed and provides input to the force transducer. A length of wire is threaded under the mounting screw of one side, through the vessel being mounted and under the second screw on the same side. When this is repeated on the other set of jaws, the two wires threaded through the myograph enable an experimenter to apply a known tension to the vessel by adjusting the movable jaw away from the fixed jaw.

The small size of these vessels necessitates the following normalisation protocol when setting them at a tension. This procedure was carried out such that the tension upon vessels was similar to that experienced *in vivo* at a pulmonary pressure of 12 - 16mmHg and was calculated using the following equation (*Equation 5*):

Pressure (P) = $2\pi \times \text{Wall Tension} / \text{Internal Circumference}$

$$P = 2\pi F / 2L(0.2056 + (2(X_n - X_0)))$$

Where: P = Equivalent pressure

F = Force

L = Vessel length

X_n = Position of the calliper at tension

X₀ = Position of the caliper at zero displacement

Equation 5: Formula for the normalisation of small vessels. The application of this formula in the process of setting tension on small pulmonary arteries allows the tension to be set to an equivalent intra-mural pressure *in vivo*.

When normalising vessels, decreasing the distance between the calipers until they were just in contact with one another produced a large negative reading of force which was observable on the trace (Figure 2.4). The reading on the calliper at this point was taken as X₀. The displacement of the calliper was then increased until a tensile force of 1.2mN was observed and the displacement of the calliper at this point was taken as X₁. Subtracting X₀ from X₁ provides the

diameter of the vessel at this tension and enables the calculation of the corresponding pressure which would be experienced by this vessel at this tension *in vivo*. The displacement of the callipers was then increased in a step-wise fashion so as to raise the tensile force observed by 0.3mN at a time (e.g. 1.5mN, 1.8mN, 2.1mN, etc.) and the displacement of the callipers noted (e.g. X₂, X₃, X₄, etc.). After each increase, the corresponding pressure *in vivo* was calculated until this value lay between 12mmHg and 16mmHg.

The calculated pressure values corresponding to each vessel diameter were noted. A graph of displacement against force was then generated to produce a graph which gave an indication as to the compliance of the vessel: that is to say, the amount of tensile force generated by increasing values of distension of the vessel. For example, a reduction in compliance would be manifest as the emergence of higher tensile forces at lower diameters of stretch.

Following normalisation, the tissue was left at resting tension for a further 15 minutes before 2 challenges with 50mM KCl to normalise the sensitivity of these vessels to Ca²⁺ and to ensure viability. Vessels producing a constriction of less than 0.1mN to 50mM KCl were discarded. Subsequent contractile responses to constricting agents were expressed as a percentage of the maximum observed constriction to 50mM KCl.

For studies involving contractile agents, ascending concentrations of drug were added to the water baths (5HT: 300pM- 30μM; U46619: 300pM-30μM) cumulatively and the responses recorded. In studies concerned with relaxation in response to SNP, vessels were pre-constricted with U46619 at a concentration representing ~70% of the maximum observed contraction to KCl. After 30 minutes pre-constriction (the time taken for the contraction to stabilise),

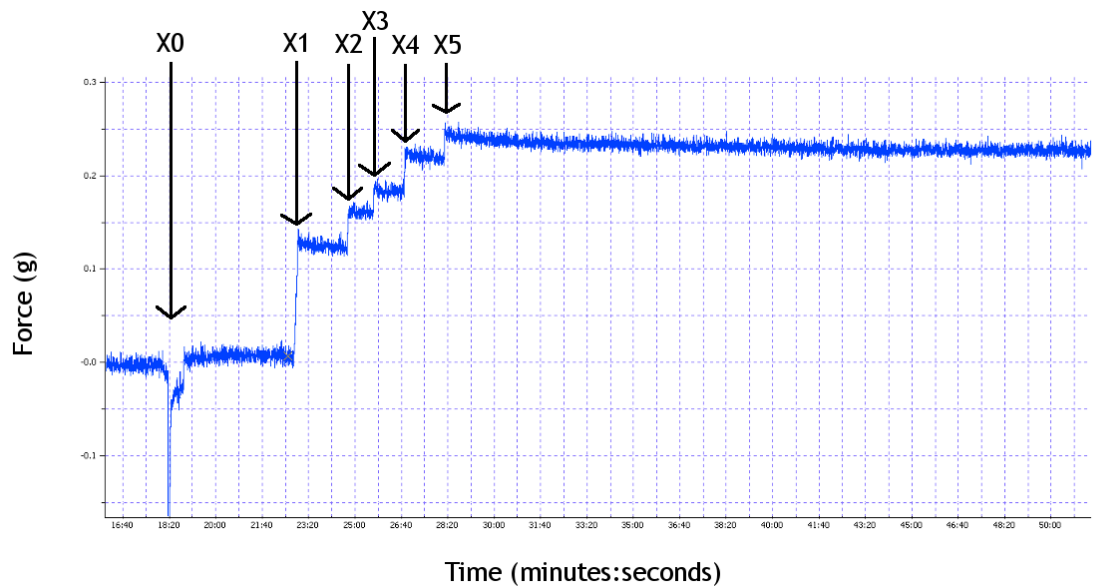


Figure 2.4 Representative trace depicting the normalisation of intrapulmonary vessels mounted on a wire myograph. The jaws of the myograph are moved apart until a given tensile force is observed. Subtracting the displacement (X_n) from the point where the jaws meeting (X_0) provides the vessel diameter and allows the calculation of the pressure which would produce this tension in a particular vessel. Displacement is increased such that tensile force is observed to increase by 0.3mN at a time and the equivalent pressure calculated at each point until it falls within the range encountered in vivo (12-16mmHg). X_0 = zero displacement; X_1 = displacement producing 1.2mN of tensile force; X_2 = displacement producing 1.5mN of tensile force; X_3 = displacement producing 1.8mN of tensile force; X_4 = displacement producing 2.1mN of tensile force; X_5 = displacement producing 2.4mN of tensile force.

ascending concentrations of SNP (300pm-300 μ M) were added to the bath and the responses calculated as a percentage of relaxation where a return to baseline tone would be considered 100%.

For concentration-response curves to U46619 and SNP, sigmoidal curves were fitted using QtiPlot by application of the following equation (*Equation 6*):

$$y = A_2 + (A_1 - A_2) / (1 + (-x/x_0)^p)$$

Where:
A₁ = left horizontal asymptote
A₂ = right horizontal asymptote
x₀ = point of inflection
p = power

Equation 6: Formula used for the fitting of sigmoidal curves to concentration-responses.

Each of these parameters are calculated by the software based upon the mean magnitude of contraction \pm SEM produced by each concentration. In a situation where the lowest studied concentration represented a supra-threshold stimulus, sigmoidal curves were manually constrained to zero by setting A₂=0, producing the following function (*Equation 7*).

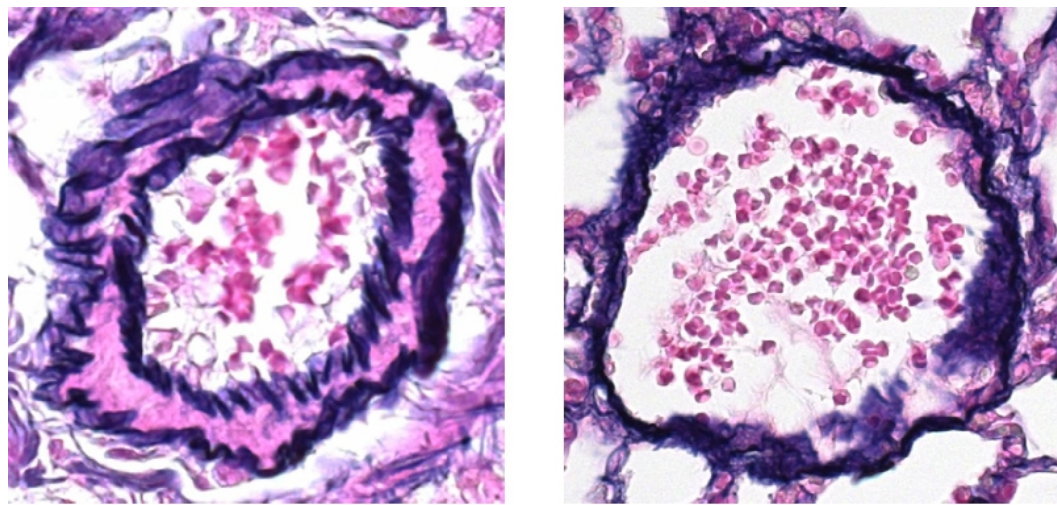
$$y = (A_1) / (1 + (-x/x_0)^p)$$

Equation 7: Simplified formula used for the fitting of sigmoidal curves to concentration-responses.

All curves were fitted using the scaled Levenberg-Marquardt algorithm.

2.2.7 Assessment of pulmonary vascular remodelling

Once fixed, the right lung was paraffin-embedded and cut into 5 μ m sagittal sections for mounting on salinized glass microscope slides. Sections from each lung were elastica Van Gieson stained and examined under an objective microscope by a blinded observer. Three sagittal sections per lung were examined and at least 100 vessels per lung assessed for vascular remodelling. The extent of pulmonary vascular remodelling was assessed by counting the number of vessels <80 μ m in diameter which possessed a distinctive double elastic lamina (the criterion for remodelling) (Figure 2.5). The extent of pulmonary vascular remodelling was assessed as the number of remodelled vessels divided by the total number of vessels multiplied by 100. This percentage was used as a comparative measure of pulmonary vascular remodelling between animals and treatment groups.



A

B

Figure 2.5: Assessment of vascular remodelling using sagittal sections of formalin-fixed murine lung. Representative images of small-diameter pulmonary vessels ($<80\mu\text{M}$) stained with elastica Van Gieson stain. Remodelled vessels (A) possess a distinct double elastic lamina which is used to distinguish them from unremodelled vessels (B). The extent of pulmonary vascular remodelling in each lung was assessed by considering the number of remodelled vessels divided by the total number of vessels multiplied by 100. Image kindly provided by Margaret Nielsen.

2.3 Cell culture

Chinese hamster lung fibroblasts (CCL39) from frozen stock were rapidly defrosted in a 37°C water bath and cultured in 75cm² flasks in DMEM containing 2mM L-Glutamine, 100U/ml penicillin, 100µg/ml streptomycin and 10% foetal calf serum. Cells were maintained in an incubator (37°C in a humidified 5% CO₂ atmosphere) until they approached confluence. At this point, cells were split using a 0.05% solution of trypsin containing 0.2mM EDTA. Trypsin is an enzyme which cleaves the molecules which are responsible for cell adhesion. A subset of these molecules, the cadherins, undergoes a conformational change and is protected from the actions of trypsin in the presence of calcium (Pokutta et al., 1994). Cells were therefore first washed with Ca²⁺/Mg²⁺ free PBS before the addition of 2ml 0.05% trypsin in 0.2mM EDTA solution. Once cells were visually confirmed via microscope as having detached from the flask, 6ml of media containing 10% FCS. Overexposure to trypsin can lead to damage of the cells. However, it is inactivated by the addition of media containing FCS due to the presence of enzymes which inhibit its activity, e.g. α-1-antitrypsin (Tarone et al., 1982). Cells were then split at a ratio of 1:4 or 1:8. Data from the literature suggests a doubling time of approximately or just less than 24 hours (Sadowski et al., 1988) in these cells and this is consistent with the observations of others in this laboratory. Cellular medium was changed every 48 hours and cells split upon reaching confluence, usually within 48 hours for a 1:4 split and 4 days for a 1:8 split. After thawing, cells were passaged at least once before any experiments were carried out.

For studies on proliferation, cells were grown to ~70% of confluence, washed with sterile PBS, trypsinised and transferred onto a 24 well plate. Each

well was seeded with 2×10^4 cells in medium containing 10% FCS and placed in the incubator. After 24 hours, cells were washed and incubated with medium containing 0% FCS. After 24 hours of quiescence, medium containing 0% FCS as well as MCP-1, sRAGE, 5HT, or combinations of these was added to each well. Each treatment was carried out in triplicate. For experiments examining the effect of sRAGE on proliferation to 5HT, sRAGE was preincubated for a period of 30 minutes before the 24 hour treatment period.

In studies assessing the effects of hypoxia upon proliferation, cells were quiesced for a period of 24 hours before pharmacological placement in an incubator maintaining a hypoxic gas mixture of 10% O₂, 5% CO₂. Soluble RAGE was preincubated in normoxia for 30 minutes before the onset of the hypoxic challenge in studies concerned with its effects on hypoxia-induced proliferation.

At the end of this period, cells were washed with sterile PBS and removed from cell culture wells with trypsin. Once the detachment of cells had been verified under the microscope, cells were pipetted into 1ml Eppendorf tubes and spun-down in a centrifuge at 10,000 rpm for 5 minutes, causing the deposition of a pellet of cells separate from the supernatent medium. Supernatent fluid was removed and cells re-suspended once again in cellular medium. After agitation to evenly disperse cells, 1μl of cell-containing fluid was pipetted onto a haemocytometer and the number of cells in four 1mm² sectors counted. This was repeated twice for each epindorph (*i.e.* 8 sectors counted per well).

Cellular proliferation was expressed as an elevation above the mean number of cells counted in control wells containing DMEM with 0% FCS only.

2.4 Statistical analysis

Statistical analyses were carried out using *RKWard v0.5.4*, an open source graphical front-end to the R statistical analysis environment, running *R v2.14.2*.

Differences between concentration response curves were assessed by a linear mixed-effects (LME) model. This method of analysis produces comparable output to that of a two-way ANOVA but accounts for the fact that multiple measurements (*i.e.* contractile responses to doses of drugs at a range of concentrations) are made within a single experiment and are therefore not independent. The statistical independence of observations is an assumption of analysis by two-way ANOVA. The LME model therefore provides a more rigorous means for the comparison of dose-response curves.

LME models are also useful in assessing cell counts in that they allow for the individual, triplicated cell counts to be included in the analysis as a blocking factor, thus increasing the robustness of the analysis.

Analysis of all haemodynamic parameters, RVH, extent of remodelling and comparisons between EC₅₀s and maximal responses to pharmacological agents were by linear model followed by *post-hoc* analysis with Fisher's least significant difference test for multiple comparisons. A *p*-value < 0.05 was considered significant after *p*-correction using the Bonferroni method to account for multiple comparisons. Student's one-way and paired t-tests were also used where appropriate.

Chapter 3.

Chronic hypoxia-induced pulmonary

hypertension in mice and the monocyte

chemoattractant protein-1 synthesis

inhibitor Bindarit

3.1 Introduction

RAGE has been strongly implicated in vascular inflammation due to its ability to sustain or amplify inflammatory responses by upregulating inflammatory molecules such as ICAM-1, VCAM-1, etc.. The extent to which downstream inflammatory molecules are upregulated and/or secreted after RAGE activation is therefore frequently examined in many models of disease as a means of assessing the importance of the receptor in these conditions.

One such molecule is the inflammatory chemotactic cytokine monocyte chemoattractant protein-1 (MCP-1). MCP-1 is released by vascular cells in response to other inflammatory mediators and is highly chemotactic for monocytes, lymphocytes and neutrophils. It produces these actions by interacting with a GPCR: chemokine receptor 2 (CCR2) (Zlotnik et al., 2006; Deshmane et al., 2009). In recruiting leukocytes to sites of inflammation, MCP-1 has been implicated in diseases such as rheumatoid arthritis (Hayashida et al., 2001) as well as vascular diseases such as atherosclerosis (Ni et al., 2001; Kusano et al., 2004).

MCP-1 is upregulated downstream of RAGE activation (Gu et al., 2006; Marsche et al., 2007; Isoda et al., 2008) and the upregulation and/or secretion of MCP-1 is frequently cited as a proxy for the induction of an inflammatory response downstream of RAGE activation. Indeed, one study in rat vascular smooth muscle cells found RAGE-induced MCP-1 expression to be the most robust of the responses measured as proxies for inflammation (others included interleukin-6 and ICAM-1 (Hayakawa et al., 2012)). Human umbilical vein endothelial cells, once stimulated with AGEs, show increased expression of RAGE, facilitating further inflammatory responses to subsequent exposure to

heterodimeric S1008/S1009; one of which is the upregulation of MCP-1 (Ehlermann et al., 2006). In a model of diabetic atherosclerosis, the aortae of rats showed elevated expression of both MCP-1 and RAGE and a significant correlation between levels of RAGE and MCP-1 expression (Feng et al., 2011). Similarly, reduced RAGE expression, reduced activation of pathways downstream of RAGE (including ROS, P38 MAPK, ERK1/2 and NF- κ B) and the reduced expression of inflammatory markers including MCP-1, VCAM-1 and ICAM-1 are cited in the literature as favourable outcomes when assessing the effects of potentially beneficial compounds or of RAGE deletion (Matsui et al., 2007, 2009; Soro-Paavonen et al., 2008; Ide et al., 2010; Feng et al., 2011; Ishibashi et al., 2011; Maeda et al., 2011; Dou et al., 2012).

MCP-1 has also been implicated in PH. Elevated circulating levels of MCP-1 in the plasma of patients with idiopathic PH and chronic thromboembolic PH are observed in comparison to control patients. Immunostaining for MCP-1 on sections of large pulmonary arteries from patients with idiopathic PH revealed an increased presence of MCP-1 in the endothelium and the smooth muscle of remodelled vessels as well as in macrophages which had migrated into the vessel wall (Kimura et al., 2001; Itoh et al., 2006). Pulmonary vascular remodelling is associated with a recruitment of circulating leukocytes into the vessel wall (Stenmark et al., 2006). MCP-1 is a chemotactic stimulus for T and B lymphocytes as well as monocytes (Carr et al., 1994; Taub et al., 1995; Frade et al., 1997). These cells have been observed in proximity to remodelled vessels in patients (Tuder et al., 1994; Tuder and Voelkel, 1998). *In vivo*, monocrotaline treatment in rats producing pulmonary hypertension induced expression of MCP-1 in serum and in bronchoalveolar lavage fluid, the magnitude of which correlated well with the severity of disease (Kasahara et al., 1998).

As discussed in the introduction, the proliferation and migration of adventitial fibroblasts are thought to play a key role in hypoxia-induced pulmonary vascular remodelling. Stimuli associated with pulmonary hypertension such as hypoxia and PDGF induce a pro-inflammatory phenotype including the upregulation of proinflammatory mediators, including MCP-1, in pulmonary arterial fibroblasts (Cochran et al., 1983; Li et al., 2011). Secretion of MCP-1 from these cells is implicated in contributing to adhesion and migration of monocytes and macrophages (Li et al., 2011). RAGE activation has been also shown to induce MCP-1 expression of adventitial fibroblasts, as well as migration of cultured adventitial fibroblasts obtained from the systemic vessels of rats (Liu et al., 2010). Pathways activated downstream of RAGE such as P38 MAPK are implicated in pulmonary arterial fibroblast proliferation in response to hypoxia (Welsh et al., 2001, 2006). Though both proliferation and the secretion of MCP-1 are documented responses of adventitial pulmonary fibroblasts to proliferative stimuli, we are unaware of any study in the literature examining any potential interplay between MCP-1 and fibroblast proliferation.

Bindarit is a small organic molecule of formula 2-methyl-2-[[1-(phenylmethyl)-1H-indazol-3yl]methoxy]propanoic acid which first drew interest due to an observed beneficial effect in mouse models of rheumatoid arthritis and chronic inflammation (Cioli et al., 1992; Guglielmotti et al., 1993). It has since been shown to selectively inhibit production of MCP-1 in monocytes in response to LPS *in vitro* (Sironi et al., 1999). Since, beneficial effects of treatment with bindarit have been observed in animal models of systemic lupus erythematosus (Guglielmotti et al., 1998; Zoja et al., 1998; Strand, 1999) and arthritis (Guglielmotti et al., 2002; Rulli et al., 2009, 2011). It has also proven effective in inhibiting in-stent stenosis and neo-intima formation in models of

systemic vascular disease (Grassia et al., 2009; Ialenti et al., 2011). Prevention of MCP-1/CCR2 interaction by a blocking antibody or gene transfer of the MCP-1 7ND has been shown to reduce medial thickness in the pulmonary arterioles of rats treated with monocrotaline. The mortality rate of these rats was also reduced by MCP-1 inhibition (Kimura et al., 1998; Ikeda et al., 2002). These data, in concert with observations showing that bindarit treatment has produced benefit via reduced MCP-1 expression in other models, led us to hypothesise that treatment with bindarit might produce a beneficial effect upon the increase in pulmonary pressure, pulmonary vascular remodelling and right ventricular hypertrophy observed in mice challenged with 2 weeks of hypoxia.

3.1.1 Aims

In the current study, our aim was to assess the ability of treatment with IP bindarit to inhibit chronic hypoxia-induced pulmonary hypertension in mice. Additionally, the ability of MCP-1 to induce proliferation in cultured CCL39 pulmonary fibroblasts was assessed.

3.2 Methods

3.2.1 Induction and assessment of chronic hypoxia-induced pulmonary hypertension

In the current study, female C57BL/6 mice approximately 2 months of age were randomly assigned to one of 4 groups: 1) 2 weeks of normoxia with vehicle; 2) 2 weeks of normoxia with 3mg/day IP bindarit; 3) 2 weeks hypoxia with

vehicle; 4) 2 weeks of hypoxia with 3mg/day IP bindarit. Mice assigned to the hypoxic group were challenged with 14 days of hypobaric hypoxia as described in Chapter 2. In this instance, the pressure in the chamber was normalised to atmospheric pressure once a day to facilitate dosing. Mice assigned to the normoxic group were housed in the same room as hypoxic mice and received doses at the same time.

All mice received a daily intraperitoneal injection of 300 μ l/day of either 10mg/ml bindarit suspended in 0.5% methylcellulose (Sigma-Aldrich) or methylcellulose vehicle only. The first dose was commenced 1 hour before the onset of hypoxia, and the final dose approximately 1 hour before the assessment of RVP *in vivo*.

Right ventricular haemodynamics were assessed in each mouse *in vivo* before removal of the heart and lungs *en bloc* for the purpose of assessing RVH, pulmonary vascular remodelling, vascular elastance and vascular reactivity.

3.2.2 Cell culture

CCL39 Chinese hamster lung fibroblasts were cultured in Dulbecco's modified Eagle medium (DMEM), supplemented with 10% FBS, 100 μ g/ml penicillin, 250 μ g/ml streptomycin and 2 mM L-glutamine. Cellular medium was changed every 2-3 days and cells passaged at a 1:4 ratio upon reaching confluence.

Cellular proliferation studies were carried out as described in Chapter 2. Cellular proliferation was expressed as an elevation above the mean number of cells counted in control wells containing DMEM with 0% FBS only. Wells containing 10% serum only were also included in each experiment to ensure the

viability of cells in each instance.

Bindarit powder was kindly supplied by Angelo Guglielmotti and Angelini Pharmaceuticals, Rome, Italy.

3.2.3 Statistical analysis

For the purpose of making statistical comparisons of the effects of various stimuli on cell proliferation, normalised cell counts were assessed by means of a linear model to identify treatments which induced a statistically significant increase above baseline. The effects of treatments were compared using Student's t-test or Fisher's LSD test where appropriate.

Analysis of all haemodynamic parameters, the extent of RVH and of remodelling, and comparisons between EC₅₀s and maximal responses to pharmacological agents were by one-way ANOVA followed by post-hoc analysis with Fisher's least significant difference test for multiple comparisons. *p*-values < 0.05 were considered significant after *p*-correction using the Bonferroni method to account for multiple comparisons.

3.3 Results

Systolic RVP was assessed in thirty female mice aged 2-3 months in this study. No mortality was observed during dosing. Ten experiments were terminated before the assessment of SAP. No significant differences in systemic arterial pressure (SAP) or HR were observed *in vivo* between any of the treatment groups.

3.3.1 In vivo effects of bindarit in normoxia and hypoxia

Systolic RVP in normoxic C57BL/6 mice treated with methylcellulose vehicle was 21.86 ± 0.56 mmHg (Figure 3.1). Treatment with bindarit produced no significant effect upon normoxic sRVP (20.92 ± 1.04 mmHg). After two weeks of chronic hypoxia, sRVP appeared mildly elevated in both mice receiving bindarit and mice receiving vehicle. Surprisingly, this elevation was not statistically significant in either instance (Vehicle: 24.70 ± 1.22 mmHg; bindarit: 23.29 ± 1.1 mmHg) (n=5-8).

The extent of vascular remodelling in normoxic vehicle-dosed mice was $9.54 \pm 4.56\%$. Similar to the case of sRVP, this was unaltered by treatment with bindarit ($8.77 \pm 3.51\%$). After chronic hypoxia, small intrapulmonary vessels exhibiting remodelling could be observed in sections from both vehicle-treated and bindarit-treated animals (Figure 3.2). While the extent of vascular remodelling in the lung appeared increased by hypoxia in both treatment groups, neither of these changes reached significance (Vehicle: $19.72 \pm 6.52\%$; bindarit: $16.99 \pm 4.29\%$), nor did they differ significantly from one another.

The ratio of RV:LV+S in normoxic, vehicle-treated animals was 0.24 ± 0.01 .

Though this value appeared mildly elevated, this was not statistically different to that observed in normoxic animals treated with bindarit (0.27 ± 0.01). In this instance, exposure of vehicle-treated animals to hypoxia produced a significant increase in RVH to 0.31 ± 0.01 . Such an increase was not observed in bindarit-dosed animals exposed to hypoxia (0.30 ± 0.01) when compared to normoxic animals receiving the same treatment. This increase was statistically different to that observed in normoxic, vehicle-treated animals however.

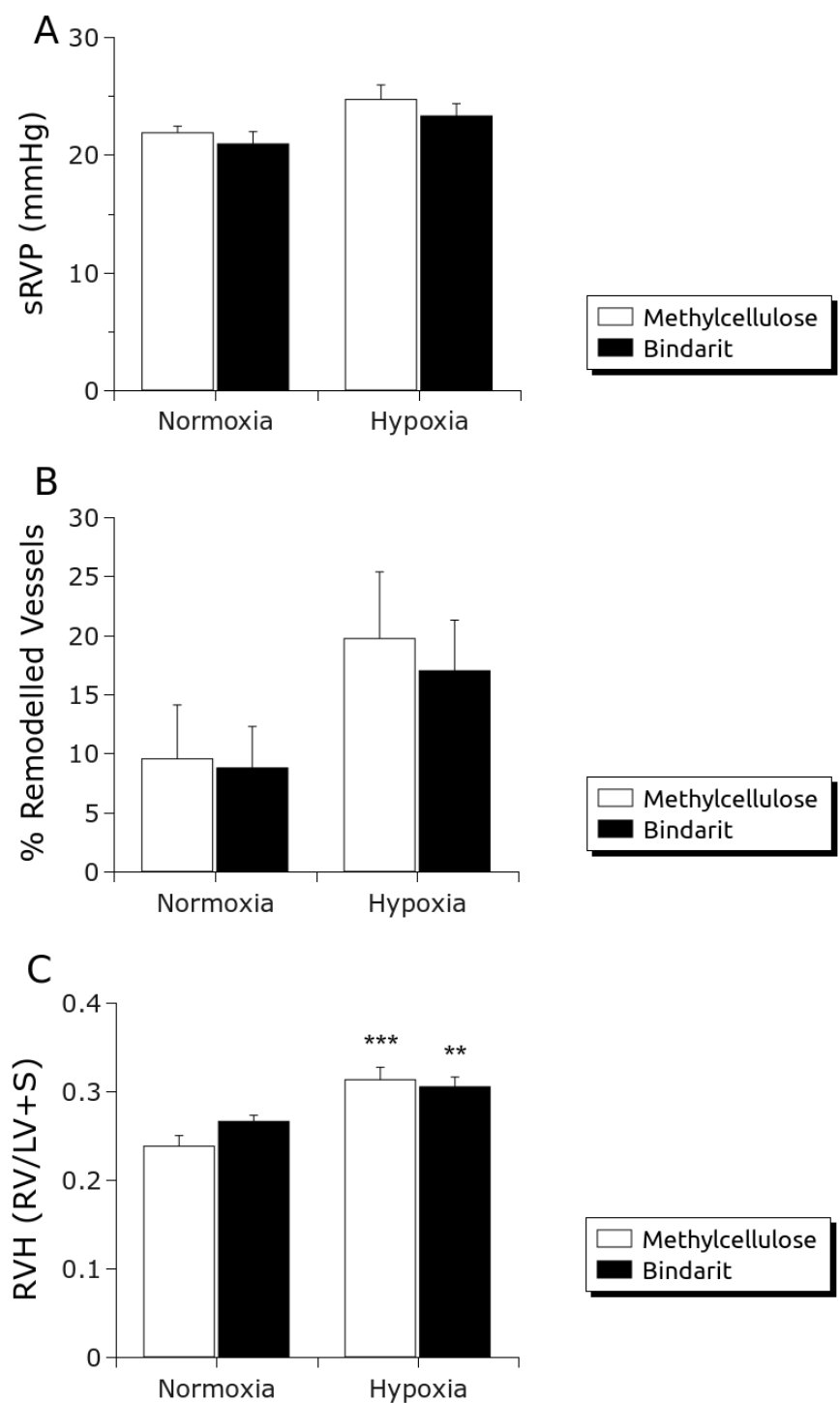


Figure 3.1 Effects on sRVP, vascular remodelling and RVH in mice exposed to hypoxia and treated with bindarit. Data are expressed as mean \pm SEM and analysed Fisher's LSD test (p-values corrected for multiple comparisons using the Bonferroni method). ** $p < 0.01$, *** $p < 0.001$ vs. normoxic methylcellulose-treated animals (Vehicle Normoxic: n=8; Bindarit Normoxic: n=7; Vehicle Hypoxic: n=6; Bindarit Hypoxic: n=9).

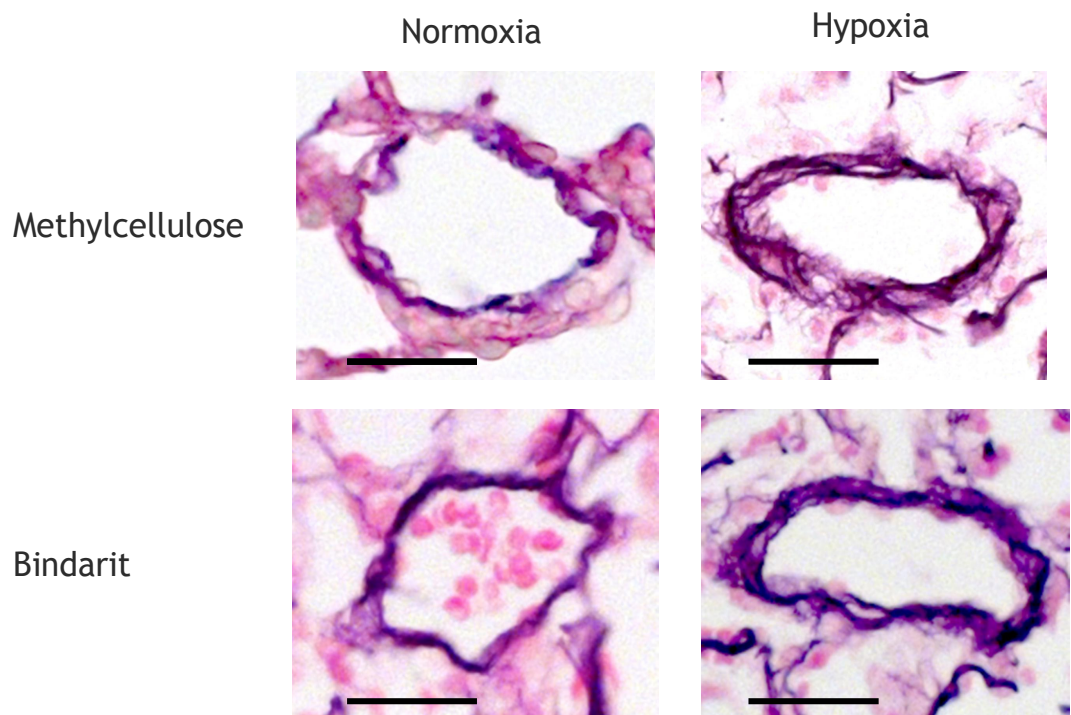


Figure 3.2 Images of representative small pulmonary arteries in C57Bl/6 mice treated with bindarit or methylcellulose vehicle in normoxia and after chronic hypoxia. Though total counts did not reach significant values, remodelled vessels could be observed after two weeks of hypoxia in sections of lung from both bindarit and vehicle-treated animals. Compared with vehicle, bindarit did not appear to produce any effects on remodelling in normoxia. Photographs taken under x40 objective magnification. Scale bar = 50 μ m.

3.3.2 MCP-1 and proliferation in fibroblasts

Cells were incubated with 0.1ng/ml, 1ng/ml, 10ng/ml and 100ng/ml MCP-1 (Figure 3.3). Analysis by linear model revealed no significant effect of MCP-1 treatment upon cell count ($p=0.1844$).

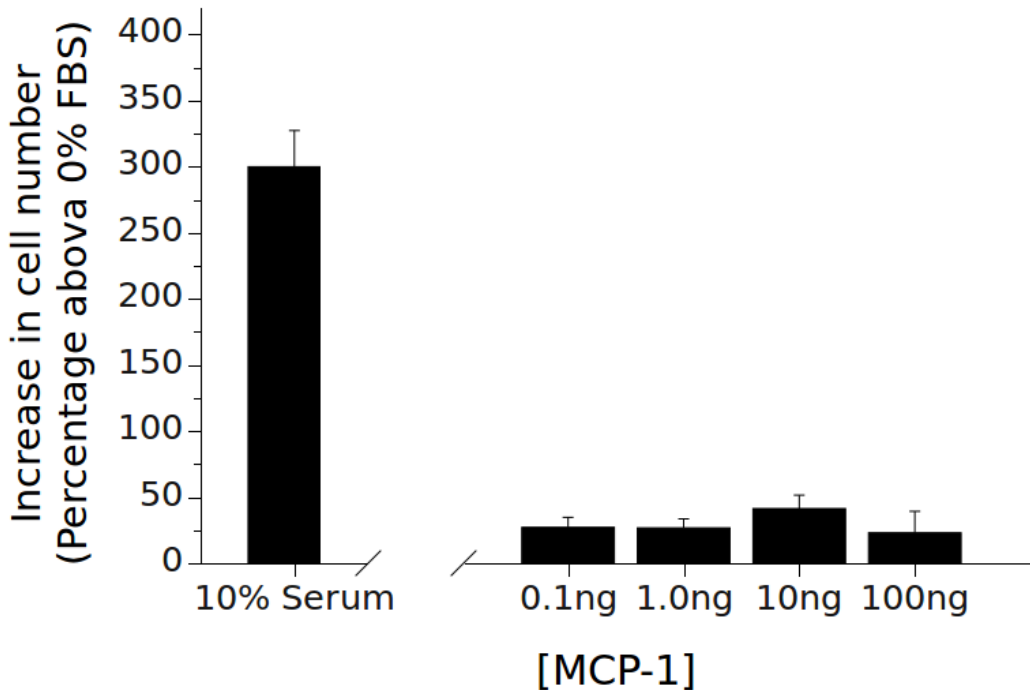


Figure 3.3 MCP-1 produces no significant effect on proliferation in response to MCP-1. No significant proliferation in response to MCP-1 was observed in CCL39 cells. Marked proliferation was observed in the presence of 10% FBS demonstrating the ability of these cells to proliferate in the presence of a mitogenic stimulus. Data are presented as mean increase above baseline \pm SEM. Statistical analyses were by one-sample t-test and Fisher's LSD test for multiple corrections with p-values corrected using the Bonferroni method. (n=4)

3.3.3 Effects of co-incubation of MCP-1 with 5HT

Since we observed no effect of MCP-1 alone upon proliferation, we next co-incubated with 5HT, a known mitogen in this cell line (Mair et al., 2008). Incubation of CCL39 fibroblasts with 10 μ M 5HT resulted in a statistically significant increase in proliferation to 73 \pm 11% ($p<0.001$) above baseline values. Co-incubation with 10 μ M 5HT and 25ng/ml MCP-1 also produced a significant increase in proliferation above baseline (78 \pm 10%; $p<0.001$) however, there was no observable enhancement of the proliferative response to 5HT. The number of cells in wells incubated with 25ng/ml of MCP-1 was neither enhanced nor diminished compared with baseline (Figure 3.4).

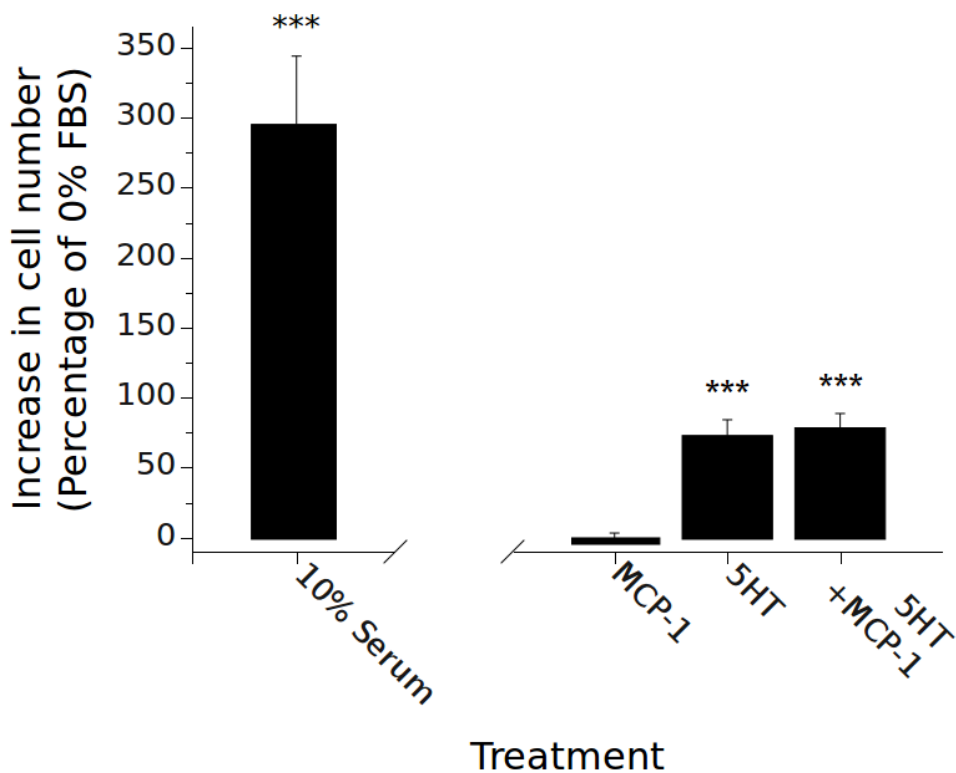


Figure 3.4 No co-operative effects upon proliferation in Fbs were observed in the presence of both MCP-1 and 5HT. Data are presented as mean increase above baseline \pm SEM. Statistical analysis was by one-sample t-test to test significant against baseline and two-sample t-test to test significance between treatment groups. *** $p<0.001$ versus baseline. (n=4)

3.4 Discussion

Our primary aim in the current study was to assess the effects of a small molecule inhibitor of MCP-1 in the chronic hypoxic model employed throughout this thesis. MCP-1 is implicated as one of the downstream mediators of the pro-inflammatory effects associated with RAGE activation (Ehlermann et al., 2006; Li et al., 2011). We aimed to test the hypothesis that daily dosing with bindarit would prove protective against the development of experimental pulmonary hypertension in mice as induced by chronic hypoxia.

In normoxic, vehicle-treated mice, we were surprised to observe no significant increase in sRVP induced by hypoxia in the current study. Hypoxia-induced increases in sRVP are typically smaller in magnitude in female rodents in comparison to males (Rabinovitch et al., 1981; White et al., 2011). The values observed for normoxic mice here were very similar (~20mmHg) to those described for female C57BL/6 mice by the literature (~20mmHg) (Hansmann et al., 2007; William et al., 2007) (and by others in this laboratory (White et al., 2011)). These sources report a response to chronic hypoxia in the region of 30mmHg but the response in this study was less impressive.

Given that our control values appear to reflect previous observations rather well, it seems less likely that the discrepancy observed in hypoxic mice is due to some inconsistency in the method of assessment of sRVP. This is particularly true given that the results are consistent with others produced using the very same apparatus by others in the laboratory. It is possible that since the pressure in the hypobaric chamber was being normalised daily, the overall magnitude of the hypoxic stimulus over the course of the two week challenge was lessened. However, other studies in this laboratory involving the daily dosing

of animals whilst in hypoxia produced a degree of pulmonary hypertension that was greater than that observed here and were comparable to studies in which no daily equalisation of pressure was carried out (Dempsie et al., 2008).

We next looked to other points of the experimental design which could explain this result. One candidate is a direct effect of the methylcellulose vehicle. In the current study, each mouse received 300 μ l/day of 0.5% methylcellulose solution: equivalent to 50mg/kg/day in a 30g mouse. There is some data in the literature of haematological effects which could contribute to observations made here. Chronic IP methylcellulose administration was previously used as a rat model for hypersplenism, based on the observation that chronic administration produced a large increase in the weight of the spleen (splenomegaly) as well as significant decreases in levels of serum haemoglobin, platelets, white blood cells and a reduced haematocrit (Palmer et al., 1953; Pérez-Tamayo et al., 1960; Alwmark et al., 1986). These effects were observed at a range of doses of methylcellulose (~32-115mg/kg/day) and after a period of dosing of the order of 12-15 weeks. No alteration in body weight of these rats was observed. One study assessed the effects of methylcellulose administration in rats after 2 weeks and while the number of red blood cells was unaltered at this time point, platelet counts were significantly reduced (Pérez-Tamayo et al., 1961). Additionally, a study in which mice receive an equivalent daily dose of ~5.37mg/kg/day for 2 weeks (lower than in the current study) demonstrated that they had possessed a decreased haematocrit after two weeks of treatment (Stang and Boggs, 1977). No change in body weight was observed in this study after 2 or 4 weeks of IP methylcellulose administration.

These observations may have relevance to the current study in that exposure to hypoxia results in increased secretion of erythropoietin: a hormone

that is secreted in response to hypoxia which erythropoiesis (Chateauvieux et al., 2011). An increase in the number of red blood cells can lead to increased haematocrit (the number of cells per unit volume of serum) and, as a consequence, the viscosity of the blood. This increase in haematocrit has been demonstrated to occur in a hypoxic rodent model of pulmonary hypertension (Weissmann et al., 2005). Since viscosity is a component in the Hagen-Poiseuille equation (Chapter 1, Equation 2), an increase in viscosity may contribute to an increased pulmonary vascular resistance.

It is conceivable that the haematocrit is being lowered by chronic treatment with methylcellulose in the current study. Though we note that the value of sRVP in normoxic mice is in line with what we might expect in noting previous observations in the literature, there are indications that methylcellulose does not effect a reduction of haematocrit by reducing erythropoietin but by increased clearance of RBCs by the spleen (Weissmann et al., 2005). Additionally, chronic methylcellulose treatment has been observed to increase erythropoietin secretion in response to acute hypoxia (Zuckerman et al., 1984). There are indications in the literature that increased erythropoietin may actually exert a beneficial reduction in pulmonary vascular remodelling (Petit et al., 1995; Weissmann et al., 2005).

In any case, this remains firmly within the realm of speculation without further additions to the current study. With that, it is clear that due to the complexity of the relationship between hypoxia, erythropoietin secretion, haematocrit and pulmonary vascular remodelling (to say nothing of any potential effects on pulmonary vascular tone, which are not considered here) it is very difficult to predict how these changes, if any are present, would ultimately manifest as an alteration of blood pressure in the pulmonary circulation. The

current study would therefore have benefited greatly from a control group of animals receiving a daily IP injection of physiological saline to assess whether the lack of production of a pulmonary hypertensive state by chronic hypoxia was indeed a product of treatment with the vehicle compound. This is true, both in that an effect of the relatively low dose of methylcellulose studied here upon the generation of pulmonary hypertension would represent a novel observation, and also in that any potential beneficial effect of bindarit treatment may be masked by the reduction of sRVP in both of the treatment groups challenged with hypoxia.

In experiments utilising CCL39 fibroblasts *in vitro*, we observed no evidence for a proliferative effect of MCP-1. While there is evidence that stimuli associated with pulmonary hypertension such as hypoxia and PDGF induces the upregulation of various proinflammatory mediators, including MCP-1, in pulmonary arterial fibroblasts (Cochran et al., 1983; Li et al., 2011), MCP-1 does not itself appear to be important in the regulation of fibroblast survival. Furthermore, treatment with MCP-1 in the presence of an additional mitogenic stimulus, 5HT, produced no additive effects.

3.5 Conclusions

In the current study, the effects of MCP-1 inhibition upon hypoxia-induced pulmonary hypertension were investigated, however any effects *in vivo* may have been masked by the apparent lack of a hypoxia-induced pulmonary hypertensive state here. This may be due to chronic methylcellulose administration but further clarification is needed to confirm this. Additionally, MCP-1 appears not to have a role in FB proliferation in normoxia. A future study

utilising Bindarit to inhibit MCP-1 production in response to hypoxia might reveal whether or not MCP-1 has any autocrine effects upon FB proliferation in addition to their previously described ability to stimulate migration and the onset of a pro-inflammatory phenotype in leukocytes.

Chapter 4.

*Effects of RAGE ligand overexpression
in a hypoxic mouse model of PAH*

4.1 Introduction

4.1.1 Mice overexpressing the RAGE ligand MTS1/S100A4

The MTS1/S100A4 mouse is fairly unique among rodent models of pulmonary vascular disease. There are many established rodent models which display proxies of PAH (e.g. elevated RVPs, right ventricular hypertrophy, muscularisation of distal pulmonary vessels, the formation of double elastic laminae, etc.), but the development of severe and/or occlusive PVD in rodent models often requires a fairly dramatic and often multi-modal intervention, e.g. chronic-hypoxia with unilateral pneumonectomy or vascular endothelial growth factor (VEGF) receptor blockade; the surgical establishment of an aortic-pulmonary shunt. Therefore, the observation of spontaneous generation of obliterative, plexiform-like pulmonary vascular lesions in ~5% of MTS1/S100A4 mice >1 year old is striking. Considered in combination with *in vitro* studies in PASMCs which demonstrate the association of the MTS1/S100A4-RAGE interaction with other pathways thought to be important in mediating the development of PAH and which are involved in PASMC proliferation (5HT_{1b} and SERT; bone morphogenetic protein receptor II (BMPRII)) (Lawrie et al., 2005; Spiekerkoetter et al., 2009), the MTS1/S100A4 mouse presents an attractive avenue for further investigation into the role of RAGE in the pathogenesis of PAH.

It has been reported in the literature that systolic right ventricular pressures (sRVP) in mice overexpressing the MTS1/S100A4 protein (MTS1/S100A4 mice) are mildly but spontaneously raised above those of their wildtype (WT) counterparts (Merklinger et al., 2005). On exposure to chronic hypoxia, MTS1/S100A4 mice also developed increased sRVP when compared to WT mice.

Despite these haemodynamic differences, the distal pulmonary vessels in the lungs of these mice did not undergo rarefaction or muscularisation greater than that observed in WT controls. The most notable difference between the MTS1/S100A4 mouse and its WT counterpart therefore seemed to lie in the extent to which these proxies of PAH were reversed when the animal was left to recover in a normoxic environment after a chronic hypoxic challenge. When WT mice are allowed to recover in a normoxic environment for a period of 1-3 months, the observed increases in sRVP, RVH and vascular remodelling were at least partially reversed and often normalised. MTS mice show an inhibition of this reversal when allowed to recover in normoxic conditions.

The induction of occlusive lesions and PAH in the MTS1/S100A4 mouse using a vasculotropic virus was recently described (Spiekerkoetter et al., 2008). In this model, it was demonstrated that infection with the murine γ -herpesvirus (γ HV68) generated PVD and PAH in the MTS1/S100A4 mouse associated with increased elastase activity. It had been previously shown that MTS1/S100A4 induces proliferation and migration of PASMCs in vitro (Lawrie et al., 2005). It was therefore surprising that when MTS1/S100A4 mice were challenged with a chronic hypoxic insult that, despite producing augmented pulmonary hypertension in comparison to WT mice, they demonstrated no additional increase in the amount of muscularisation of the distal pulmonary circulation. Microarray analysis revealed that MTS1/S100A4 overexpression in mice is associated with enhanced expression of the calcium binding protein Fibulin-5. Fibulin-5 binds to elastin and is essential for elastin fibre assembly (Nakamura et al., 2002; Yanagisawa et al., 2002). In line with this observation, elastin levels as assessed in the whole lung of MTS1/S100A4 mice were higher than in WT mice, accompanied by increased thickness of the internal and external elastic laminae

of small distal pulmonary arteries. *In vitro*, MTS1/S100A4 induced fibulin-5 expression in hPASMCs (Merklinger et al., 2005).

Since enhanced elastin deposition can impede SMC proliferation (Karnik et al., 2003), it was subsequently suggested that enhanced elastin deposition occurring as a result of increased fibulin-5 expression in MTS1/S100A4 mice might prevent the enhancement of SMC proliferation in the media of pulmonary arteries that might otherwise be expected when these animals are exposed to hypoxia. Similarly, it was proposed that enhanced elastin deposition might reinforce structural changes occurring in the MTS1/S100A4 mouse lung on exposure to hypoxia such that the reversion of these changes, when animals are returned to a normoxic environment and allowed to recover, is impaired.

The association of the development of occlusive vascular disease with increased elastase activity in MTS1/S100A4 mice infected with γ HV68 lends some weight to this hypothesis. The degradation of elastin of the pulmonary vasculature was associated with the formation of a neointima comprised largely of cells which were positively stained for α -smooth muscle actin. Additionally, the increased generation of elastin peptides generated through the action of elastase on elastin appears to be partially responsible for the proliferation and migration of SMCs in the neointima as well as the increased recruitment of circulating inflammatory cells into the vessel wall in these mice (Spiekerkoetter et al., 2008).

4.1.2 RAGE blockade in PAH

As yet, despite interest in the MTS1/S100A4 mouse and the MTS1/S100A4-RAGE pathway in a variety of *in vitro* and *in vivo* settings related to PAH, there

have been no studies examining the effect of RAGE blockade or the reduction of RAGE ligand bioavailability in a PAH model *in vivo*. In studies of other vascular diseases (e.g. atherosclerosis), the impairment of both the generation of disease as well as stabilisation of established disease has been described using a variety of means to impair RAGE-ligand interactions (Park et al., 1998; Bucciarelli et al., 2002; Hudson et al., 2003; Harja et al., 2008). These include the generation of RAGE^{-/-} mice, transfection with DN-RAGE (an isoform of the receptor which lacks the signal transducing cytoplasmic domain) and treatment with sRAGE (an isoform of RAGE which lacks both the cytoplasmic and transmembrane domains). Soluble RAGE is free in solution and will compete with the intact, membrane-bound RAGE molecule for ligand (Park et al., 1998).

The MTS1/S100A4 mouse presented an attractive opportunity for an intervention study in that the augmented manifestation of disease in these animals provides a contrast to the development of disease in the WT. Therefore, in intervening to reduce RAGE-ligand interactions, we can attempt to normalise or reverse the augmentation of PAH which is attributable to the overexpression of RAGE ligand.

Having said this, investigating a pathology which only emerges after 1 year and only in a small subset of animals presents a practical challenge, particularly in the absence of a means to assess the development of occlusive PVD which is not invasive or dependent on the assessment of histology carried out *post mortem*. Infection with γHV68 as described by (Spiekerkoetter et al., 2008) appears to be a reliable means for deliberately inducing severe PAH and occlusive PVD in the MTS1/S100A4 mouse, however they also reported that this technique was only effective in animals aged >1 year. Infection with γHV68 in animals aged 3 months produced neither PAH nor PVD. Furthermore, the length

of time from inoculation until the establishment of occlusive PVD was at least 6 weeks and often as long as 3 months. The use of this model in an intervention study would therefore prove prohibitive in terms of both overall timescale and the quantity of sRAGE necessary to undertake an intervention over the period from inoculation to the development of disease.

The most pronounced difference described in younger MTS1/S100A4 mice (~3 months) was the impaired reversion of sRVP, RVH and PVR to baseline values when animals were returned to normoxic conditions after a hypoxic challenge. Since this represents the most pronounced difference in the response to chronic hypoxia between transgenic and WT mice, it was an attractive point at which to attempt an intervention.

Intervening at this stage is also of interest since RAGE has been implicated as an agent which maintains inflammation, and hence disease, in atherosclerosis. Treatment with sRAGE prevented the advancement of established atherosclerosis in the ApoE-/- mouse (Bucciarelli et al., 2002).

Before undertaking such an intervention study in the MTS1/S100A4 mouse, it was first necessary to ensure the reproducibility of data as reported in the literature. This also presented an opportunity for the production of novel data through investigation of the functional characteristics of isolated pulmonary arteries in these mice. An enhanced increase in sRVP in response to acute hypoxia, an effect which may be attributed in part to enhanced vasoconstriction, was reported in the MTS1/S100A4 mouse. Additionally, the reversal of this increase was impaired in MTS1/S100A4 mice when returned to normoxia or when treated with the labile vasodilator NO. Despite these data, and despite the fact that elevated pressures in normoxia and after a chronic hypoxic challenge may be partially attributable to the contractile properties of

the pulmonary vasculature, no direct investigation into the functional characteristics of the pulmonary arteries of these mice has yet been carried out.

The response of these vessels to pharmacological agents which are present endogenously and which may modulate vascular tone represents a means of controlling pulmonary pressure which is distinct from the contractile response of these vessels to hypoxia or altered PVR due to structural remodelling. Based on the fact that elevations in sRVP greater than those in WT mice were reported in both normoxia and hypoxia in the MTS1/S100A4 mouse, and in the absence of an augmentation in the extent of pulmonary vascular remodelling (Merklinger et al., 2005), we hypothesised that pulmonary arteries isolated from the lungs of MTS1/S100A4 mice might display enhanced contraction to 5HT and to the thromboxane A2 analogue U46619. Similarly, we hypothesised that vessels from MTS1/S100A4 mice might display retarded relaxation to the NO donor SNP.

4.1.3 Aims

Our purpose in carrying out the current investigation was to characterise the haemodynamics of MTS/S100A4 mice as compared to WT mice under normoxic, hypoxic and recovery conditions with the addition of an investigation into the functional characteristics of intrapulmonary arteries (IPAs) in these mice.

4.2 Methods

In the current study, male MTS1/S100A4 and WT mice between 2 and 3 months of age were randomly assigned to one of three groups: 1) normoxia, 2)

chronic hypobaric hypoxia for 2 weeks and 3) chronic hypobaric hypoxia for 2 weeks followed by a 4 week period of recovery in normoxia. In addition to an assessment of haemodynamics, RVH and vascular remodelling, the response of isolated intrapulmonary arteries to contractile and relaxatory compounds was assessed using small artery wire myography.

Right ventricular haemodynamics were assessed in each mouse *in vivo* before removal of the heart and lungs *en bloc* for the purpose of assessing RVH, pulmonary vascular remodelling, vascular reactivity and vascular compliance.

Functional alterations in pulmonary arteries were assessed by small-wire myography as described in Chapter 2. Cumulative concentration response curves to 5HT, U46619 and SNP were constructed to assess the relative sensitivity of these vessels to contractile and relaxatory stimuli. In experiments involving SNP, vessels were preconstricted to a value corresponding to 70% of the maximal constriction to U46619 as determined by a prior concentration response curve to this agent.

For concentration-response curves to pharmacological agents, a mean E_{max} value was calculated as the mean maximum value of contraction observed from each experiment. An EC_{50} value was obtained from each experiment by estimating the concentration of agonist which produced a response which was half the magnitude of the E_{max} . Graphical representations of concentration-response curves were produced using QtiPlot software. By using the 'data reader' function of this software and selecting a point on the y-axis of the concentration-response corresponding to to half the value of E_{max} , the corresponding value on the x-axis is provided to the user and may be taken as estimation of the EC_{50} . Relationships between the diameter of intrapulmonary arteries and the amount of elastic tensile force were compared by LME model.

4.2.1 Statistical analysis

Statistical analyses were carried out as described in Chapter 2.

4.3 Results

Systolic RVP was assessed in fifty-nine male mice aged 2-3 months in this study. No mortality was observed during hypoxia or recovery. Sixteen experiments were terminated before the assessment of SAP. No significant differences in SAP or HR were observed *in vivo* (Figure 4.1A and 4.1B).

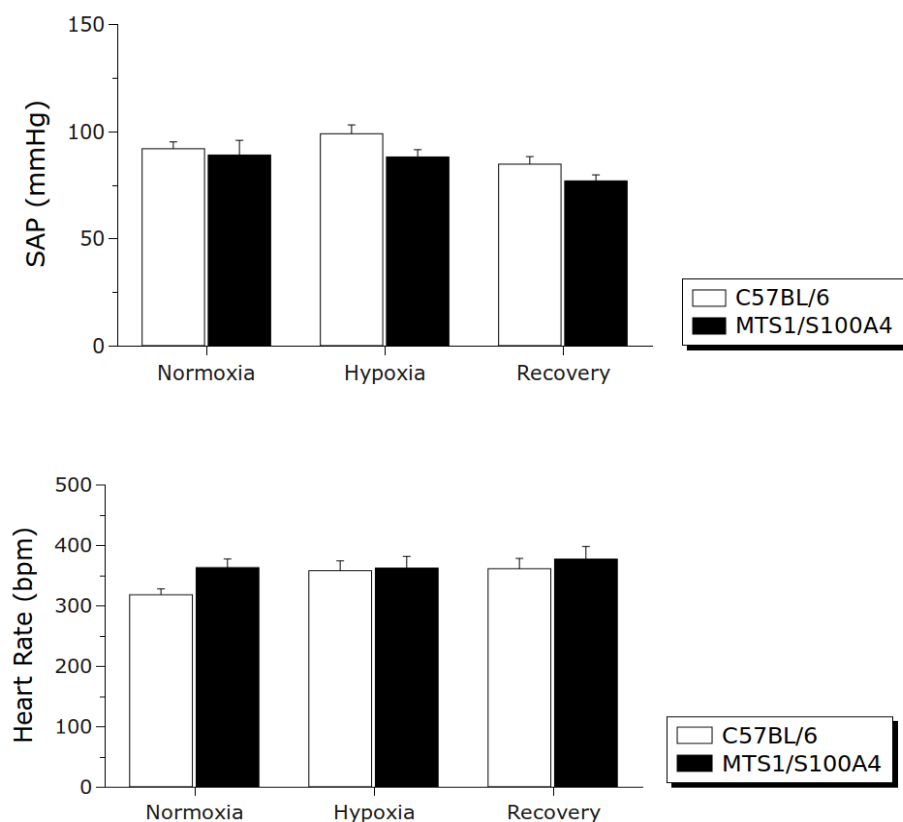


Figure 4.1 Systemic arterial pressure and HR remain unaltered in all treatment groups studied. Data are presented as mean \pm SEM (A) (WT Normoxic: n=12; WT Hypoxic: n=8; WT Recovery: n=10; MTS1/S100A4 Normoxic: n=11; MTS1/S100A4 Hypoxic: n=12; MTS1/S100A4 Recovery: n=6) (B) (WT Normoxic: n=6; WT Hypoxic: n=6; WT Recovery: n=9; MTS1/S100A4 Normoxic: n=9; MTS1/S100A4 Hypoxic: n=8; MTS1/S100A4 Recovery: n=5).

4.3.1 Effects of strain and hypoxia on haemodynamics and remodelling in C57BL/6 and MTS1/S100A4 mice

In comparison to their C57BL/6 WT counterparts, MTS1/S100A4 mice displayed no significant difference in mean sRVP (WT: 20.16 ± 0.76 mmHg; MTS1/S100A4: 21.30 ± 1.078 mmHg) under baseline normoxic conditions (Figure 4.2A).

In WT and MTS1/S100A4 mice, exposure to two weeks of hypobaric hypoxia induced a significant increase in mean sRVP (Figure 4.2A; WT: 29.84 ± 1.36 mmHg, $p < 0.001$; MTS1/S100A4: 33.62 ± 1.34 mmHg, $p < 0.001$). Mean mRVP in hypoxic MTS1/S100A4 mice was elevated above normoxic MTS1/S100A4 mice (Figure 4.3; hypoxic: 17.26 ± 1.54 mmHg; normoxic: 11.31 ± 0.54 mmHg; $p < 0.001$) and above hypoxic C57BL/6 mice (13.45 ± 0.94 mmHg; $p < 0.05$). Mean mRVP was not significantly elevated in hypoxic C57BL/6 mice in comparison to normoxic mice of the same strain (10.48 ± 0.26 mmHg). Under normoxic conditions, MTS1/S100A4 mice showed no increase in the extent of pulmonary vascular remodelling (WT: $11.94 \pm 3.30\%$; MTS1/S100A4: $10.94 \pm 4.04\%$) (Figure 4.2B) nor was there any evident structural difference in these vessels, when compared to their WT counterparts (Figure 4.4).

In WT mice, exposure to hypoxia produced a statistically significant increase in the percentage of small remodelled vessels possessing a double elastic lamina ($24.37 \pm 2.56\%$; $p < 0.05$) while, surprisingly, MTS1/S100A4 mice showed no such increase ($13.36 \pm 1.81\%$) (Figure 4.2A; Figure 4.4).

When WT mice were challenged with two weeks of hypobaric hypoxia and then allowed to recover for 4 weeks at normal atmospheric pressure, mean sRVP was observed to fall to a value significantly lower than that of mice exposed to hypoxia alone (23.86 ± 1.23 mmHg; $p<0.01$) (Figure 4.2A). Similar to WT mice, mean sRVP in MTS1/S100A4 mice allowed 4 weeks of recovery from hypoxia was significantly reduced in comparison to hypoxic MTS1/S100A4 mice ($p<0.01$). Mean mRVP in MTS1/S100A4 mice allowed to recover from hypoxia was significantly reduced compared to that of hypoxic mice (Figure 4.3; 11.89 ± 0.89 mmHg; $p<0.01$) and not statistically different to that observed in normoxic MTS1/S100A4 mice. Mean mRVP in C57Bl/6 mice remained unchanged after 4 weeks recovery from hypoxia (Figure 4.3; 12.09 ± 0.85 mmHg).

When allowed to recover for 4 weeks at atmospheric pressure after the hypoxic challenge, the percentage of remodelled vessels possessing a double elastic lamina in WT mice was significantly reduced when compared to hypoxic mice of the same strain ($14.44 \pm 2.82\%$; $p<0.05$) (Figure 4.2B; Figure 4.4), and not statistically different to normoxic WT mice. The extent of remodelling after 4 weeks recovery in MTS1/S100A4 mice remained unchanged when compared to normoxic and hypoxic MTS1/S100A4 mice ($12.47 \pm 2.61\%$) (Figure 4.2A; Figure 4.4).

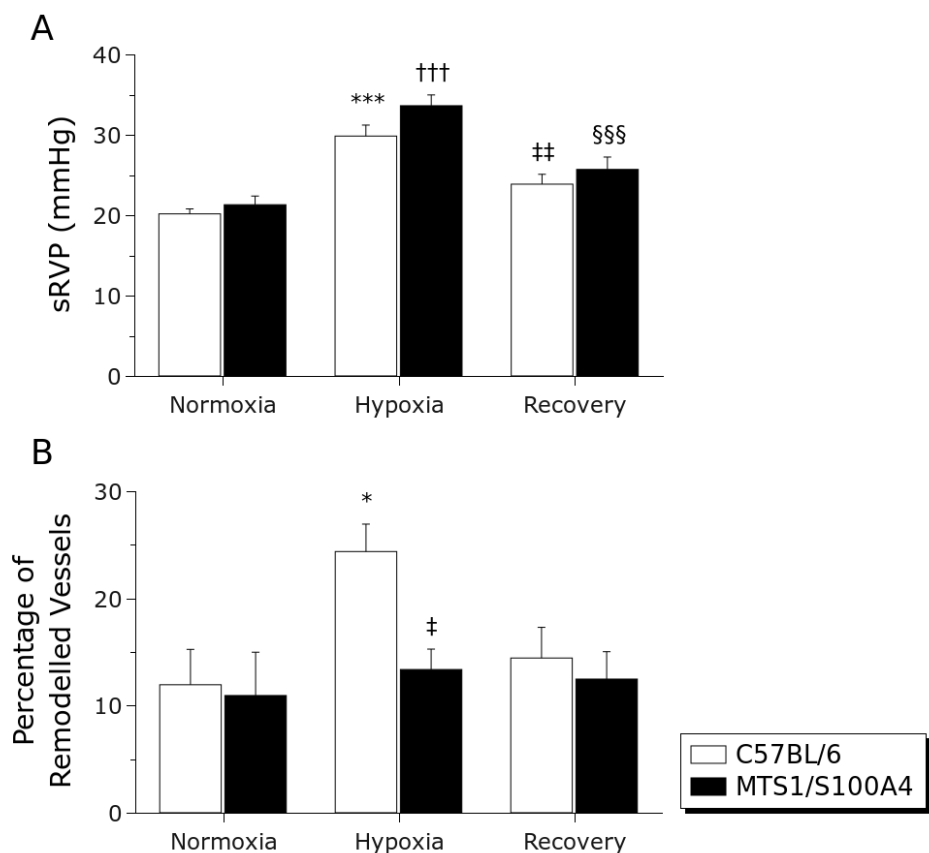


Figure 4.2 Pulmonary hypertension in C57BL/6 and MTS1/S100A4 mice in normoxic, hypoxia and after recovery. Systolic right ventricular pressure (sRVP; A) was unaltered in MTS1/S100A4 mice at baseline and after hypoxia. The percentage of remodelled vessels (B) is elevated by hypoxia in WT mice but not MTS1/S100A4 mice. Right ventricular hypertrophy (C) is elevated to a similar degree in both MTS1/S100A4 and WT mice. Data are expressed as mean \pm SEM and analysed by LME model followed by Fisher's LSD test (p-values corrected for multiple comparisons). * p<0.05, ** p<0.01, *** p<0.001 vs. normoxic C57BL/6; ††† p<0.001 vs. normoxic MTS1/S100A4; ‡ p<0.05, # p<0.01 vs. hypoxic C57BL/6; §§§ p<0.001 vs. hypoxic MTS1/S100A4 mice. (WT Normoxic: n=12; WT Hypoxic: n=8; WT Recovery: n=10; MTS1/S100A4 Normoxic: n=11; MTS1/S100A4 Hypoxic: n=12; MTS1/S100A4 Recovery: n=6).

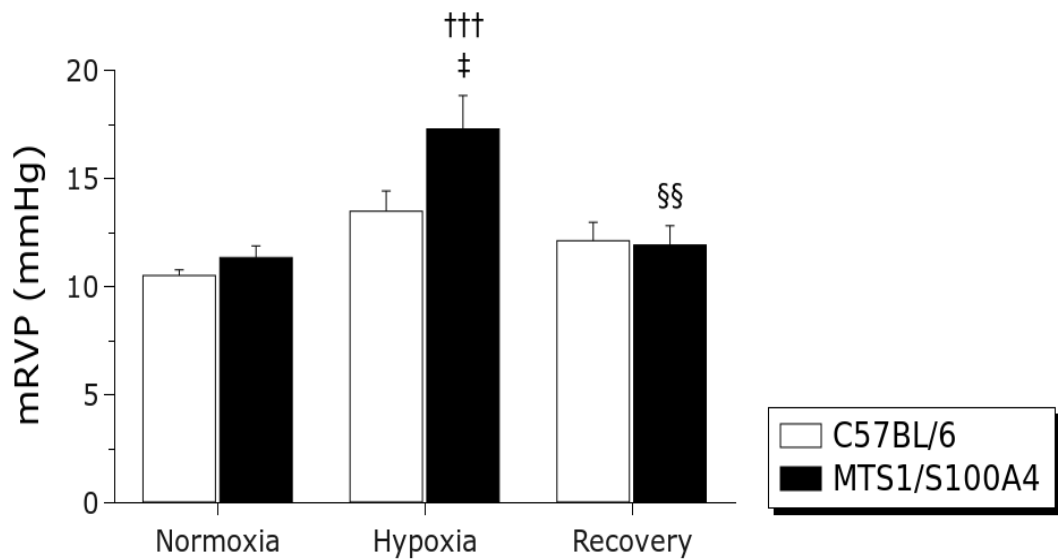


Figure 4.3 Mean RVP is significantly elevated after hypoxia in MTS1/S100A4 mice but not in C57BL/6 mice. ††† $p<0.001$ vs. normoxic MTS1/S100A4; ‡ $p<0.05$ vs. hypoxic C57BL/6; §§ $p<0.01$ vs. hypoxic MTS1/S100A4 mice. (WT Normoxic: n=12; WT Hypoxic: n=8; WT Recovery: n=10; MTS1/S100A4 Normoxic: n=11; MTS1/S100A4 Hypoxic: n=12; MTS1/S100A4 Recovery: n=6).

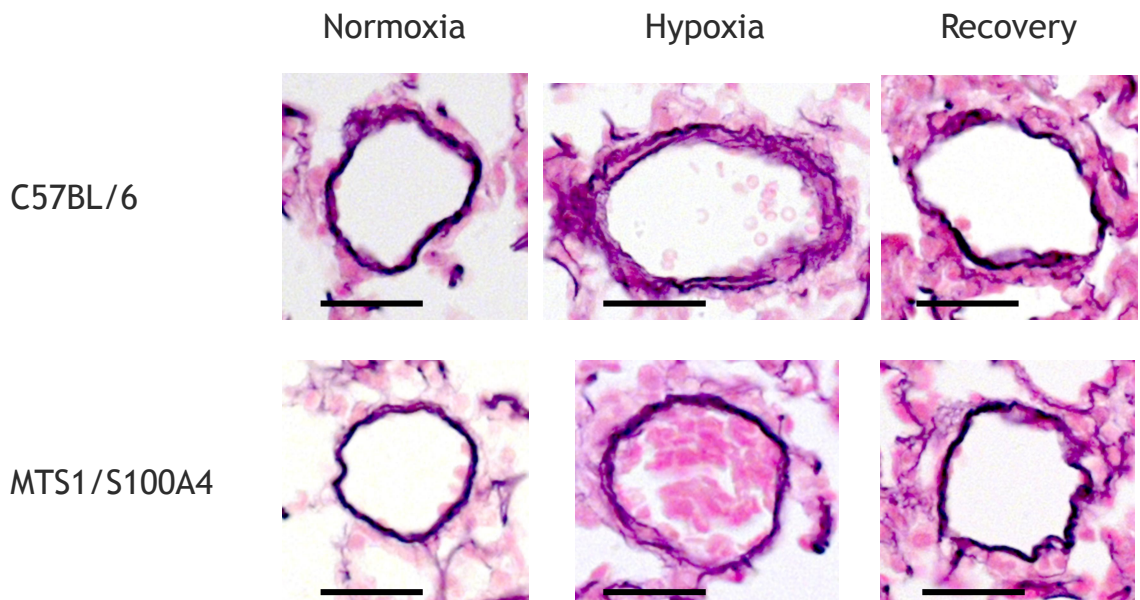


Figure 4.4 Images of representative small pulmonary arteries in C57Bl/6 and MTS1/S100A4 mice in normoxia, after chronic hypoxia and after recovery from hypoxia. Small intrapulmonary vessels did not exhibit remodelling in sections from WT or MTS1/S100A4 mice in normoxia. In WT mice, remodelled small intrapulmonary vessels possessing a double elastic lamina were observed in histological sections after two weeks of hypoxia resulted. This appeared to be reversed in mice allocated 4 weeks of recovery from chronic hypoxia. Small vessels in MTS1/S100A4 mice did not show any qualitative differences from those of WT mice in normoxia. The effects of hypoxia upon these vessels in MTS1/S100A4 mice was greatly reduced or abolished compared to WT vessels. No further changes were observed in MTS1/S100A4 mice allocated to 4 weeks recovery from chronic hypoxia. Photographs taken under x40 objective magnification. Scale bar = 50µm.

4.3.2 Effects of strain and hypoxia on right ventricular hypertrophy in C57BL/6 and MTS1/S100A4 mice

In order to assess right ventricular hypertrophy our aim was to assess alterations in the weight of the right ventricle between mouse strains or treatment groups. To do so, it is desirable to normalise the weight of the right ventricle to some other attribute of the mouse that may contribute to any changes observed. Two commonly used attributes are the body weight (BW) of the mouse and the weight of the left ventricle plus the ventricular septum (LV+S). In the current study it was desirable to assess the relative merits of these. We therefore examined variations in the BW, RV and LV+S of WT of the WT MTS1/S100A4 mice used in the current study.

Mean BW of mice in the normoxic group were not statistically different between strains (WT: $28.46 \pm 1.02\text{g}$; MTS1/S100A4: $27.34 \pm 0.56\text{g}$) (Figure 4.5A). However, MTS1/S100A4 mice possessed lower LV+S weight when compared to WT mice (WT: $0.113 \pm 0.004\text{g}$; MTS1/S100A4 mice: $0.095 \pm 0.003\text{g}$; $p<0.05$) (Figure 4.5B).

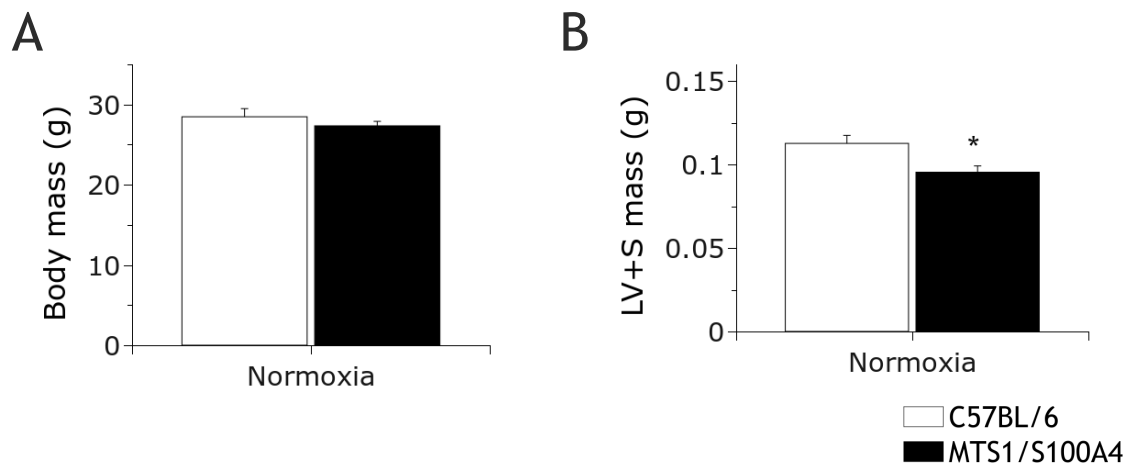


Figure 4.5 Mouse body mass and weight of left ventricle plus septum in normoxic C57BL/6 and MTS1/S100A4 mice. (A) Mean body weights of mice in the normoxic group were not statistically different between strains (WT: 28.46 ± 1.02 g; MTS1/S100A4: 27.34 ± 0.56 g). However, (B) MTS1/S100A4 mice appeared to possess a smaller total ventricle weight when compared to WT mice (WT: 0.113 ± 0.004 g; MTS1/S100A4 mice: 0.095 ± 0.003 g; $p<0.05$). Data are presented as mean \pm SEM. Statistical analyses were by Fisher's LSD test. * $p<0.05$ vs. normoxic WT mice (WT Normoxic: n=11; MTS1/S100A4 Normoxic: n=11).

Assessing mean mouse body weight and LV+S (the largest ventricle and therefore the primary determinant of total ventricle weight) across treatment groups, it was observed that while these remained very similar across treatment groups in the MTS1/S100A4 mouse. Two weeks of hypoxia reduced the BW of WT mice to $23.51 \pm 0.86\text{g}$ ($p<0.001$) (Figure 4.6A), significantly lower than that of hypoxic MTS1/S100A4 mice ($26.76 \pm 0.59\text{g}$; $p<0.01$). This was completely reversed after 4 weeks recovery in normoxia ($30.38 \pm 0.73\text{g}$; $p<0.001$ vs. hypoxic WT mice; not significant vs. normoxic WT mice) (Figure 4.6A). The weight of LV+S was reduced in WT mice exposed to hypoxia (Normoxic: $0.112 \pm 0.005\text{g}$; Hypoxic: $0.091 \pm 0.003\text{g}$; $p<0.01$) (Figure 4.6B), lower than that observed in hypoxic MTS1/S100A4 mice ($0.089 \pm 0.001\text{g}$; $p<0.01$). This was reversed in mice allowed to recover for 4 weeks ($0.113 \pm 0.004\text{g}$; $p<0.01$ vs. hypoxic WT mice; not significant vs. normoxic WT mice) (Figure 4.6B). This value was significantly larger than that of recovery MTS1/S100A4 mice ($0.087 \pm 0.002\text{g}$; $p<0.001$). In contrast to WT mice, MTS1/S100A4 mice showed no significant change in BW or weight of LV+S after 2 weeks of hypoxia (BW = $26.76 \pm 0.59\text{g}$; LV+S = $0.089 \pm 0.001\text{g}$) or 4 weeks of recovery (BW = $27.70 \pm 0.58\text{g}$; LV+S = $0.087 \pm 0.002\text{g}$).

Since values of LV+S weight across treatment groups appeared to vary in a very similar pattern to that of BW, the ratio of LV+S to BW was assessed in each treatment group to establish if these were varying proportionally. Normalisation of LV+S to BW removed the variation observed between treatment groups in WT mice observed in the un-normalised values (Normoxic WT: $3.97 \times 10^{-3} \pm 0.15 \times 10^{-3}$; Hypoxic WT: $3.86 \times 10^{-3} \pm 0.12 \times 10^{-3}$; Recovery WT: $3.71 \times 10^{-3} \pm 0.20 \times 10^{-3}$) (Figure 4.6C). No significant differences were observed between different treatment groups in WT mice. No variation in LV+S/BW between treatment groups were

observed in MTS1/S100A4 mice (Normoxic MTS1/S100A4: $3.49 \times 10^{-3} \pm 0.11 \times 10^{-3}$; Hypoxic MTS1/S100A4: $3.32 \times 10^{-3} \pm 0.07 \times 10^{-3}$; Recovery MTS1/S100A4: $3.14 \times 10^{-3} \pm 0.10 \times 10^{-3}$) (Figure 4.6C). However, values observed in hypoxia and recovery were significantly lower in MTS1/S100A4 mice than WT (Hypoxic: $p < 0.05$; Recovery: $p < 0.05$). Consistent with the observation that weight of LV+S was reduced in the MTS1/S100A4 mouse in normoxia (Figure 4.5B), the ratio of LV+S/BW in MTS1/S100A4 mice was observed to be lower on average across all treatment groups when compared to WT mice. This was verified through analysis by one-way ANOVA (WT: Mean LV+S/BW = $3.89 \times 10^{-3} \pm 0.08 \times 10^{-3}$; MTS1/S100A4: Mean LV+S/BW = $3.34 \times 10^{-3} \pm 0.10 \times 10^{-3}$; $p < 0.001$).

When normalised to BW, RVH was lower on average across all treatment groups in the MTS1/S100A4 mouse (WT: RV/BW = $1.01 \times 10^{-3} \pm 0.04 \times 10^{-3}$; MTS1/S100A4: RV/BW = $0.90 \times 10^{-3} \pm 0.05 \times 10^{-3}$; $p < 0.05$; one-) (Figure 4.7A). Both WT and MTS1/S100A4 mice displayed evidence of increased RVH by this measure. Values for RV/BW observed after hypoxia were increased against normoxic mice of the same strain in both WT and MTS1/S100A4 mice (Normoxic: $0.90 \times 10^{-3} \pm 0.04 \times 10^{-3}$; Hypoxic: $1.18 \times 10^{-3} \pm 0.036 \times 10^{-3}$; $p < 0.01$) and MTS1/S100A4 (Normoxic: $0.81 \times 10^{-3} \pm 0.04 \times 10^{-3}$; Hypoxic: $1.02 \times 10^{-3} \pm 0.04 \times 10^{-3}$; $p < 0.05$). No additional statistically significant changes were observed between other treatment groups.

MTS1/S100A4 mice appear to possess a smaller total ventricle weight than C57BL/6 mice across all treatment groups, including the normoxic control group. However, RV/LV+S is similar in both strains of mice in normoxia. Since the objective here was to detect relative changes in the weight of RV between strains and treatment groups, and since the weight of LV+S was recorded under much more strictly controlled conditions than was the weight of the whole animal, the assessment of RVH as RV/LV+S would appear to be the method which

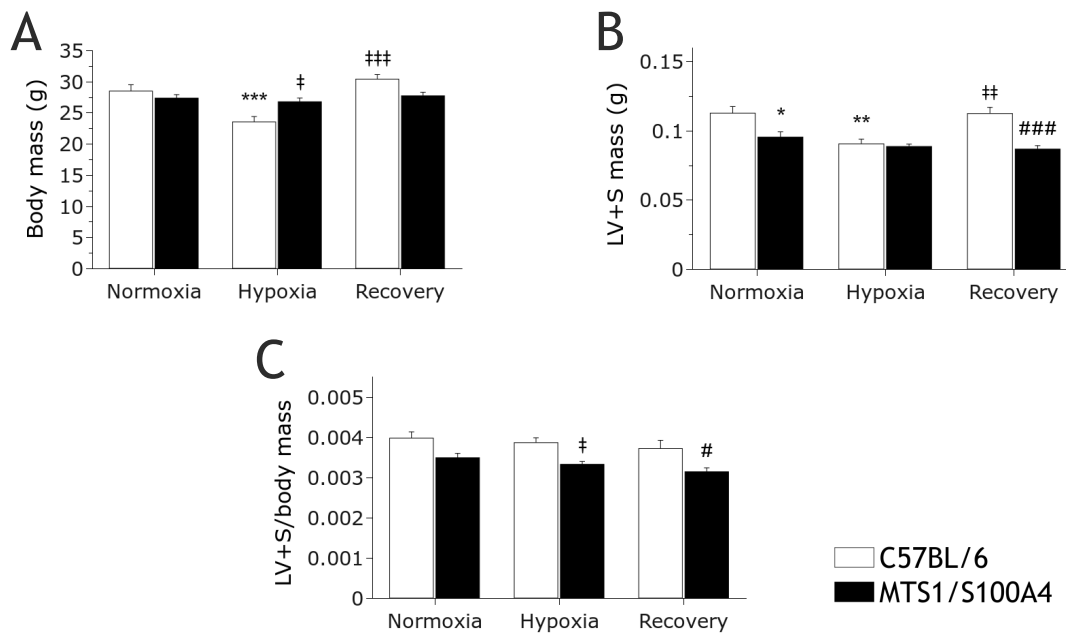


Figure 4.6 Weight of LV+S appears to vary closely with mouse body weight. (A) Bodyweight appeared to vary in C57BL/6 mice by treatment group, showing a decrease in body weight in hypoxia (Normoxic: $28.46 \pm 1.02\text{g}$; Hypoxic: $23.51 \pm 0.86\text{g}$; $p<0.001$). This was reversed after 4 weeks recovery ($30.38 \pm 0.73\text{g}$; $p<0.01$ vs. hypoxic WT mice; not significant vs. normoxic WT). No such fluctuations were observed in MTS1/S100A4 mice. (B) LV+S weight also differed across treatment groups and followed a similar pattern to that of mouse body weight. The weight of LV+S was reduced in WT mice exposed to hypoxia (Normoxic: $0.113 \pm 0.005\text{g}$; Hypoxic: $0.091 \pm 0.003\text{g}$; $p<0.01$). This was reversed in mice allowed to recover for 4 weeks ($0.112 \pm 0.004\text{g}$; $p<0.01$ vs. hypoxic WT mice; not significant vs. normoxic WT mice). (C) Normalisation of the weight of LV+S to mouse body weight eliminated the variation between treatment groups in C57BL/6 mice and also demonstrated that the ratio of LV+S/BW in MTS1/S100A4 mice is lower on average across all treatment groups. This was verified through analysis by one-way ANOVA (WT: Mean LV+S/BW = $3.89 \times 10^{-3} \pm 0.08 \times 10^{-3}$; MTS1/S100A4: Mean LV+S/BW = $3.34 \times 10^{-3} \pm 0.10 \times 10^{-3}$; $p<0.001$). Data are presented as mean \pm SEM. Statistical analyses were by one-way anova and Fisher's LSD test. * $p<0.05$, ** $p<0.01$, *** $p<0.001$ vs. normoxic C57BL/6; ‡ $p<0.05$, ## $p<0.001$ vs. hypoxic C57BL/6; # $p<0.05$, $p<0.001$ vs. recovery MTS1/S100A4 mice. (WT Normoxic: n=11; WT Hypoxic: n=8; WT Recovery: n=5; MTS1/S100A4 Normoxic: n=11; MTS1/S100A4 Hypoxic: n=12; MTS1/S100A4 Recovery: n=6).

provides the most precise measure. Furthermore, since LV+S appeared to vary in a way which is closely related to the weight of the animal, normalising RV to LV+S has the advantage of accounting for both the reduced ventricular weight in the MTS1/S100A4 mouse in general and the varying BW of mice across treatment groups in WT mice.

There was no evidence that the average ratio of RV:BW differed between WT and MTS1/S100A4 mice (WT: 0.269 ± 0.008 ; MTS1/S100A4: 0.272 ± 0.011 ; $p=0.777$; one-way ANOVA) (Figure 4.7B). When RV weight was normalised to the weight of LV+S, no difference in baseline values for mean RVH was observed between WT and MTS1/S100A4 mice (WT: 0.226 ± 0.008 ; MTS1/S100A4: 0.237 ± 0.008) (Figure 4.7B. Both WT and MTS1/S100A4 mice showed an increase in mean RVH when exposed to 2 weeks hypobaric hypoxia (WT: 0.301 ± 0.013 ; MTS1/S100A4: 0.303 ± 0.010) though there was no significant difference between strains. In both WT and MTS1/S100A4 mice, mean RVH appeared slightly decreased after recovery (Figure 4.7B; WT: 0.283 ± 0.013 ; MTS1: 0.282 ± 0.010) but did not differ statistically from those values observed in hypoxia. RVH after recovery remained significantly elevated above those observed in normoxia for both WT ($p<0.05$) and MTS1/S100A4 ($p<0.01$) mice.

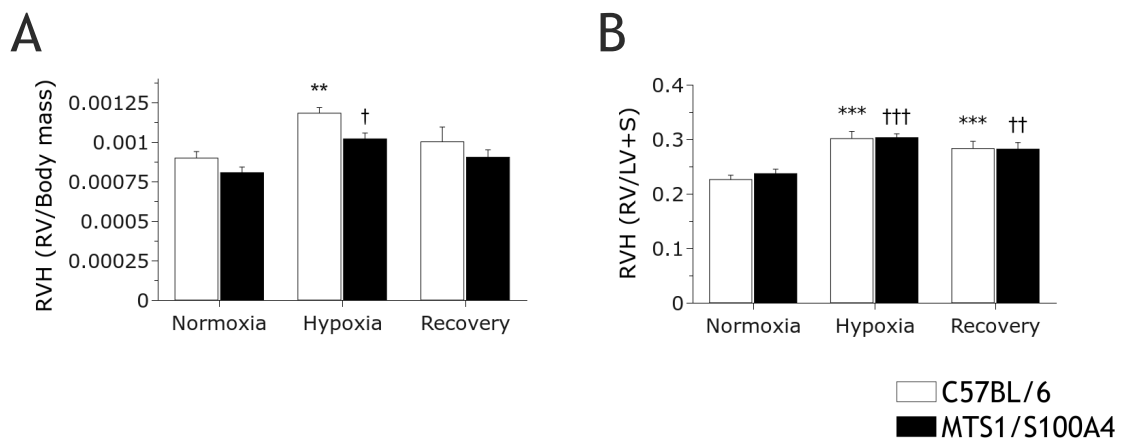


Figure 4.7 Normalisation of right ventricle weight to body weight and weight of left ventricle plus septum. (A) Hypoxia produced an increase in RVH in WT (Normoxic: $0.90 \times 10^{-3} \pm 0.04 \times 10^{-3}$; Hypoxic: $1.18 \times 10^{-3} \pm 0.036 \times 10^{-3}$; $p < 0.01$) and MTS1/S100A4 (Normoxic: $0.81 \times 10^{-3} \pm 0.04 \times 10^{-3}$; Hypoxic: $1.02 \times 10^{-3} \pm 0.04 \times 10^{-3}$; $p < 0.05$) mice when RV weight was normalised to mouse body weight. Consistent with results seen when LV+S weight was normalised to body weight, analysis by one-way ANOVA revealed that the ratio of RV:BW was reduced on average across treatment groups in the MTS1/S100A4 mouse (WT: $RV/BW = 1.01 \times 10^{-3} \pm 0.04 \times 10^{-3}$; MTS1/S100A4: $RV/BW = 0.90 \times 10^{-3} \pm 0.05 \times 10^{-3}$; $p < 0.05$). (B) There was no evidence that the average ratio of RV:BW differed between WT and MTS1/S100A4 mice (WT: 0.269 ± 0.008 ; MTS1/S100A4: 0.272 ± 0.011 ; $p = 0.777$; one-way ANOVA). Data are presented as mean \pm SEM. Statistical analyses were by one-way ANOVA and Fisher's LSD test. ** $p < 0.01$, *** $p < 0.001$ vs. normoxic C57BL/6; † $p < 0.05$, ††, $p < 0.01$, ††† $p < 0.001$ vs. normoxic MTS1/S100A4 mice. (WT Normoxic: $n = 11$; WT Hypoxic: $n = 8$; WT Recovery: $n = 5$; MTS1/S100A4 Normoxic: $n = 11$; MTS1/S100A4 Hypoxic: $n = 12$; MTS1/S100A4 Recovery: $n = 6$).

4.3.3 Vascular compliance

Vascular compliance in intrapulmonary vessels from C57BL/6 mice appeared to increase in a linear fashion with the application of increasing force (Figure 4.8). By comparison, vessels from MTS1/S100A4 mice appeared reduced to some degree at lower values of force. However, at forces of 1.8mN and above they appeared very similar. No statistically significant difference between these responses was detected ($p=0.114$; interaction $p=0.778$).

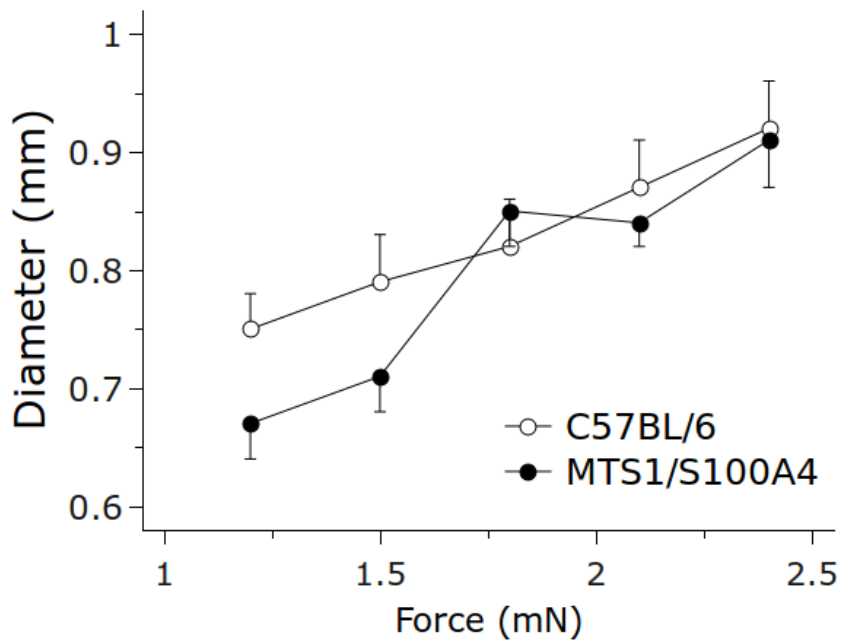
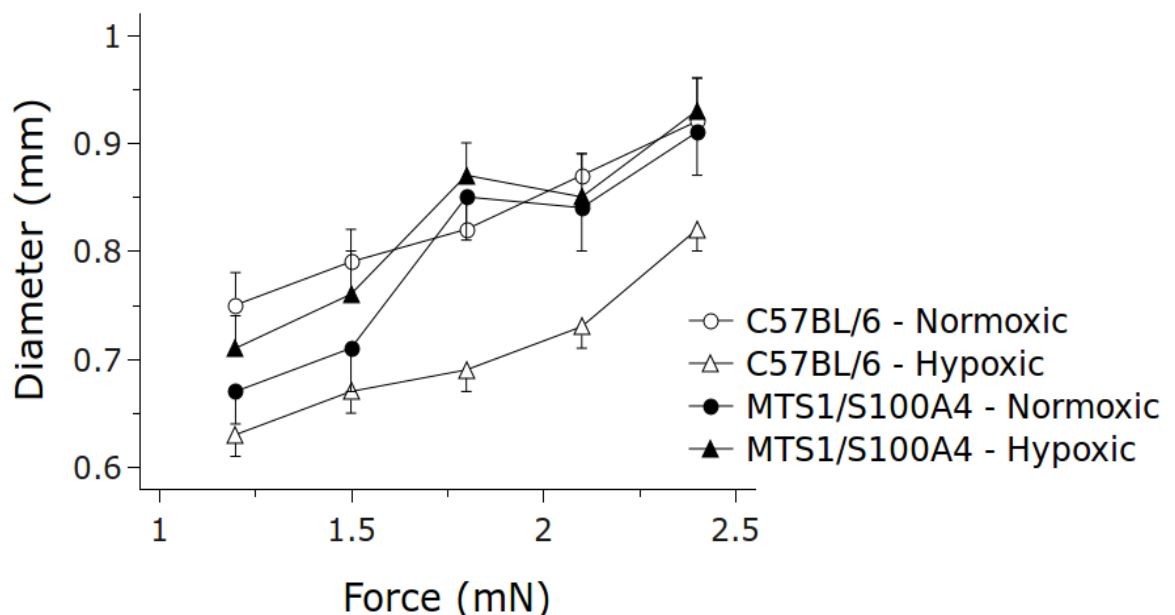


Figure 4.8 Overexpression of MTS1/S100A4 produces no alteration in the compliance of intrapulmonary mouse vessels. No significant differences in the relationship between force generation and stretch in MTS1/S100A4 and WT mice were observed ($p=0.114$), nor was any significant interaction between force and treatment observed ($p=0.778$). Statistical analysis was by LME model. For C57BL/6-Normoxic and MTS1/S100A4-Normoxic, n=11; n=7 at 1.2mN; n= 11; n= 11 at 1.5mN; n=10; n=11 at 1.8mN; n= 8; n=11 at 2.1mN; n= 6; n=7 at 2.4mN.

Exposure to 2 weeks of hypoxia produced a statistically significant reduction in the compliance of these vessels in WT mice (Figure 4.9; $p<0.05$; interaction $p<0.01$). By contrast, no such reduction was observed in hypoxic MTS1/S100A4 mice as compared to normoxic MTS1/S100A4 controls (Figure 4.9 $p=0.274$; interaction $p=0.266$). Direct comparison of vessels from hypoxic animals revealed a statistically significant reduction in the compliance in vessels from WT mice versus those of MTS1/S100A4 mice (interaction between force and strain $p<0.01$).

In vessels from WT mice allowed to recover from the chronic hypoxia stimulus, the relationship between force and diameter appeared much like that observed in normoxic mice. Comparison with vessels from WT mice exposed to hypoxia showed a statistically significant improvement in vascular compliance (Figure 4.10A; $p<0.05$). No difference between vessels from normoxic and recovery mice were detected ($p=0.303$; interaction $p=0.194$). Vessels from MTS1/S100A4 mice displayed no significant changes after recovery (Figure 4.10B; $p=0.405$; interaction $p=0.7120$ versus hypoxic; $p=0.808$; interaction $p=0.456$ versus normoxic). No differences in were detected between vessels from WT and MTS1/S100A4 mice after recovery ($p=0.177$; 0.407).

Figure 4.9 Compliance is reduced by hypoxia in vessels from WT but not MTS1/S100A4 mice. Exposure to 2 weeks of hypoxia produced a statistically significant reduction in the compliance of vessels from WT ($p<0.05$; interaction $p<0.01$) but not



MTS1/S100A4 ($p=0.274$; interaction $p=0.266$;) mice. Direct comparison of vessels from hypoxic animals revealed a statistically significant reduction in the compliance in vessels from WT mice versus those of MTS1/S100A4 mice (interaction $p<0.01$). Analysis was by LME model * $p<0.05$; ** $p<0.01$. For C57BL/6-Normoxic, C57BL/6-Hypoxic, MTS1/S100A4-Normoxic and MTS1/S100A4-Hypoxic n=11; 12; 7; 9 at 1.2mN; n= 11; 9; 11; 9 at 1.5mN; n=10; 12; 11; 9 at 1.8mN; n= 8; 8; 11; 7 at 2.1mN; n= 6; 5; 7; 2 at 2.4mN.

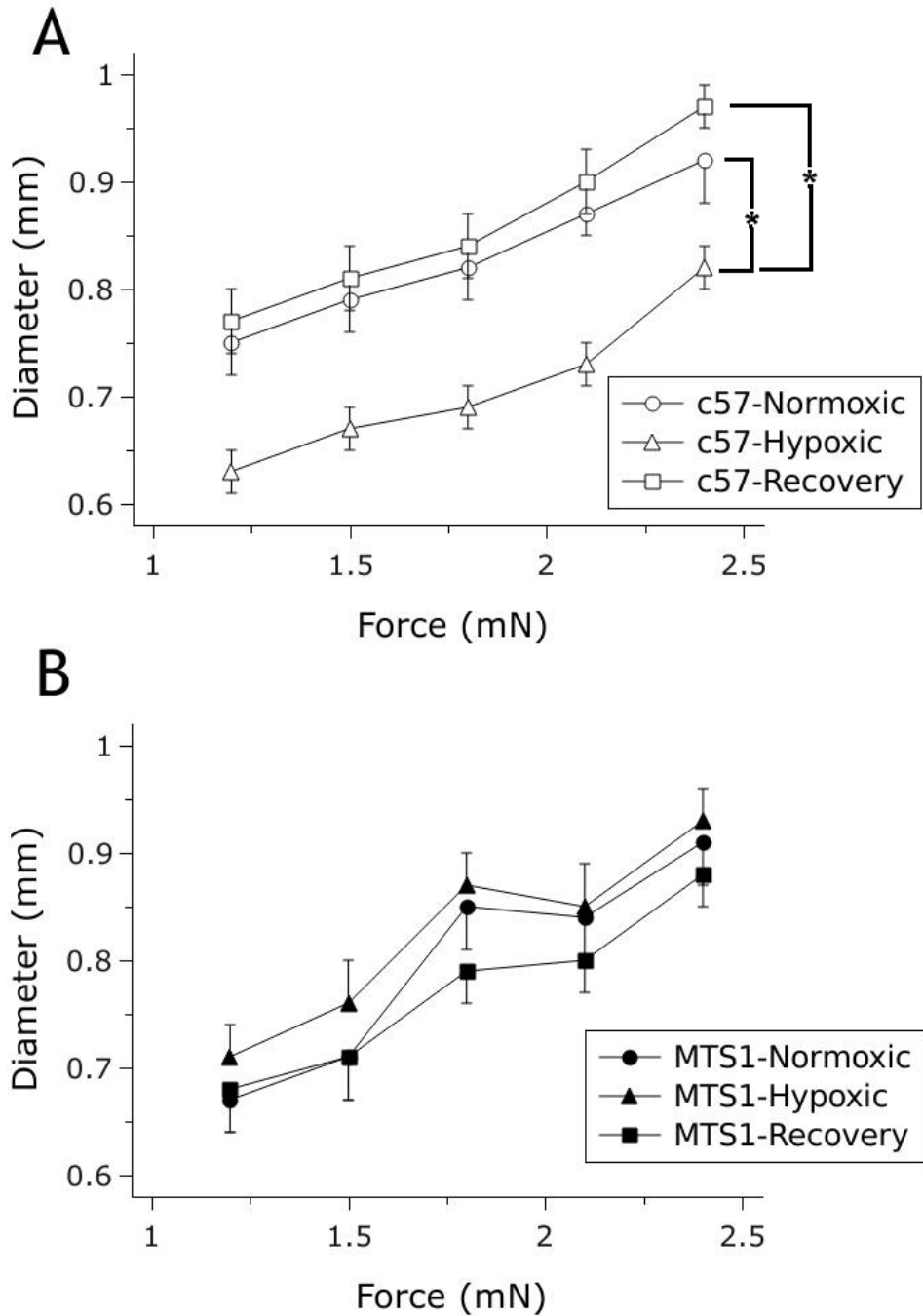


Figure 4.10 Compliance returns to baseline values in WT mice allowed to recover from chronic hypoxia. In C57BL/6 mice (A), compliance returned to values which were similar to baseline after 4 weeks recovery from chronic hypoxia. Recovery curves were significantly different from those obtained in vessels from hypoxic animals ($p<0.05$). (B) Conversely, no significant differences were observed in vessels from MTS1/S100A4 mice. Analysis was by LME model. * $p<0.05$. For C57BL/6-Normoxic, C57BL/6-Hypoxic, C57BL/6-Recovery, MTS1/S100A4-Normoxic, MTS1/S100A4-Hypoxic and MTS1/S100A4-Recovery, n=11; 12; 7; 11; 9; 9 at 1.2mN; n= 11; 9; 7; 11; 9; 9 at 1.5mN; n=10; 12; 6; 11; 9; 9 at 1.8mN; n= 8; 8; 5; 11; 7; 8 at 2.1mN; n= 6; 5; 3; 7; 2; 7 at 2.4mN.

4.3.4 Responses of isolated intrapulmonary arteries to pharmacological agents

Intrapulmonary arteries were isolated from WT and MTS1/S100A4 mice after the completion of *in vivo* measurements. Responses to contractile agonists are represented as a percentage of responses to 50mM KCl except where otherwise stated. No statistically significant differences in the average magnitude of contraction to 50mM KCl were detected for either strain or treatment group (Figure 4.11).

A summary of E_{max} and EC_{50} values for all pharmacological agents studied in the current chapter may be found in Table 4.1.

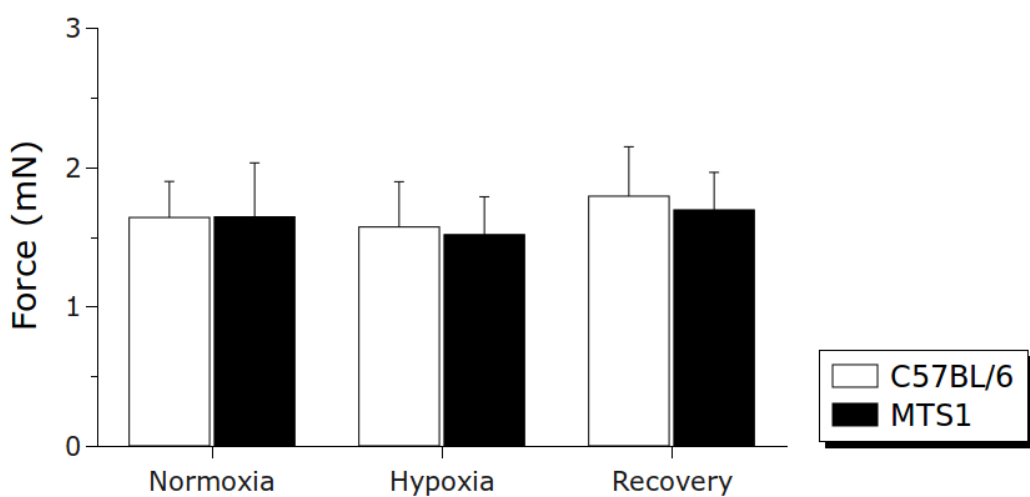


Figure 4.11 Responses to 50mM KCl were unaltered between normoxia, hypoxia and recovery in WT and MTS1/S100A4 mice. Data are presented as mean \pm SEM (WT Normoxic: n=7; WT Hypoxic: n=8; WT Recovery: n=9; MTS1/S100A4 Normoxic: n=7; MTS1/S100A4 Hypoxic: n=8; MTS1/S100A4 Recovery: n=7).

C57Bl/6 mice

Agonist		Normoxic	Hypoxic	Recovery
5HT	Emax (% KCl)	115 ± 12	156 ± 14 *	129 ± 4
	logEC50	-7.41 ± 0.22	-7.56 ± 0.16	-7.31 ± 0.14
	n	5	5	3
U19	Emax (% KCl)	146 ± 9	239 ± 29 **	137 ± 6 #
	logEC50	-7.29 ± 0.21	-7.40 ± 0.22	-7.30 ± 0.11
	n	5	4	6
SNP	Emax	96 ± 3	65 ± 12	59 ± 3
	logEC50	-6.91 ± 0.20	-7.17 ± 0.35	-7.09 ± 0.11
	n	6	4	4

MTS1/S100A4 mice

Agonist		Normoxic	Hypoxic	Recovery
5HT	Emax (% KCl)	133 ± 8	149 ± 10	122 ± 11
	logEC50	-7.51 ± 0.07	-7.58 ± 0.11	-7.37 ± 0.12
	n	4	5	7
U19	Emax (% KCl)	185 ± 37	237 ± 21 **	146 ± 8 §§
	logEC50	-7.78 ± 0.22	-7.41 ± 0.12	-7.30 ± 0.11
	n	4	4	5
SNP	Emax	94 ± 3	57 ± 9 †	82 ± 16
	logEC50	-8.00 ± 0.30 **	-7.11 ± 0.20 †††	-6.74 ± 0.04 †††
	n	3	5	5

Table 4.1 E_{max} and EC₅₀ values for responses to pharmacological agents in C57BL/6 and MTS1/S100A4 in normoxia, after hypoxia and after recovery from hypoxia.

* p<0.05, ** p<0.01 vs normoxic C57Bl/6; † p<0.05, ††† p<0.001 versus normoxic MTS1/S100A4 mice; §§ p<0.01 vs. hypoxic MTS1/S100A4 mice.

4.3.4.1 Responses to 5HT

The relationship between contractile force and concentration of 5-HT in intrapulmonary arteries isolated from normoxic WT mice was biphasic in nature; reaching a maximum before, at the highest concentrations, partially relaxing and stabilising at ~75% of the maximally observed contraction (Figure 4.12) The mean E_{max} for these vessels was $115 \pm 12\%$ and the $\log EC_{50}$ was -7.41 ± 0.21 .

Concentration response curves conducted in vessels isolated from MTS1/S100A4 mice were similar in form though the magnitude of contraction appeared to be mildly augmented at higher concentrations of 5-HT. Analysis of concentration-response of vessels isolated from normoxic MTS1/S100A4 and WT mice by LME model revealed both a global effect of strain as well as an interaction between concentration and strain which both approached, but did not achieve, significance ($p=0.059$; $p=0.066$ respectively) (Figure 4.12). No statistically significant difference in E_{max} ($115 \pm 12\%$ in WT vs. $133 \pm 8\%$ in MTS1/S100A4 mice) or $\log EC_{50}$ (-7.41 ± 0.22 vs. -7.51 ± 0.07) was observed between strains.

Concentration-response curves to 5-HT in vessels isolated from WT mice exposed to 2 weeks hypoxia were significantly different to those from normoxic controls ($p<0.05$; LME model), with a significant interaction between strain and concentration ($p<0.05$), and displayed a significant increase in the maximally observed contraction ($E_{max} = 156 \pm 14\%$; $p<0.05$) (Figure 4.13A). No such differences were observed in vessels isolated from hypoxic MTS1/S100A4 mice when compared to vessels from normoxic mice of the same strain ($p=0.183$; LME model) (Figure 4.13B). Though E_{max} appeared mildly increased in vessels from hypoxic MTS1/S100A4 mice in comparison to vessels from normoxic mice of the

same strain ($E_{max}=149 \pm 10\%$ in hypoxic vs. $133 \pm 8\%$ in normoxic MTS1/S100A4 mice) this did not achieve statistical significance ($p=0.211$). No significant changes in the $\log EC_{50}$ were detected between WT or MTS1/S100A4 mice in normoxia or hypoxia (WT normoxic: -7.41 ± 0.22 ; WT hypoxic: -7.56 ± 0.16 ; MTS1/S100A4 normoxic: -7.51 ± 0.07 ; MTS1/S100A4 hypoxic: -7.58 ± 0.11). Direct comparison of concentration-response curves to 5HT from hypoxic WT and MTS1/S100A4 mice revealed no significant differences ($p=0.9882$).

Dose-response curves in vessels isolated from WT mice allowed to recover from the hypoxic stimulus in normoxic conditions appeared to show a partial reversal of hypoxia-induced changes, but statistical analysis revealed strong evidence of a difference between concentration-response curves in vessels from these mice compared to those in the hypoxic group ($p=0.496$) (Figure 4.13A). Comparison of these curves with those obtained in normoxic approached but did not achieve significance ($p=0.072$). E_{max} in vessels from WT animals in the recovery group was $129 \pm 4\%$ and did not differ from values observed in normoxic or hypoxic mice. Concentration-response curves in vessels isolated from MTS1/S100A4 mice in the recovery group displayed no significant changes in comparison to vessels from normoxic ($p=0.942$) or hypoxic mice ($p=0.198$) (Figure 4.13B). The maximum observed contraction in vessels isolated from MTS1/S100A4 mice allowed 4 weeks recovery was $122 \pm 11\%$, however this was not significantly different from that of vessels from normoxic or hypoxic MTS1/S100A4 mice. $\log EC_{50}$ in vessels from animals in the recovery group were -7.31 ± 0.14 in WT mice and -7.37 ± 0.12 in MTS1/S100A4 mice. Neither of these values were significantly different from those observed in vessels from other treatment groups.

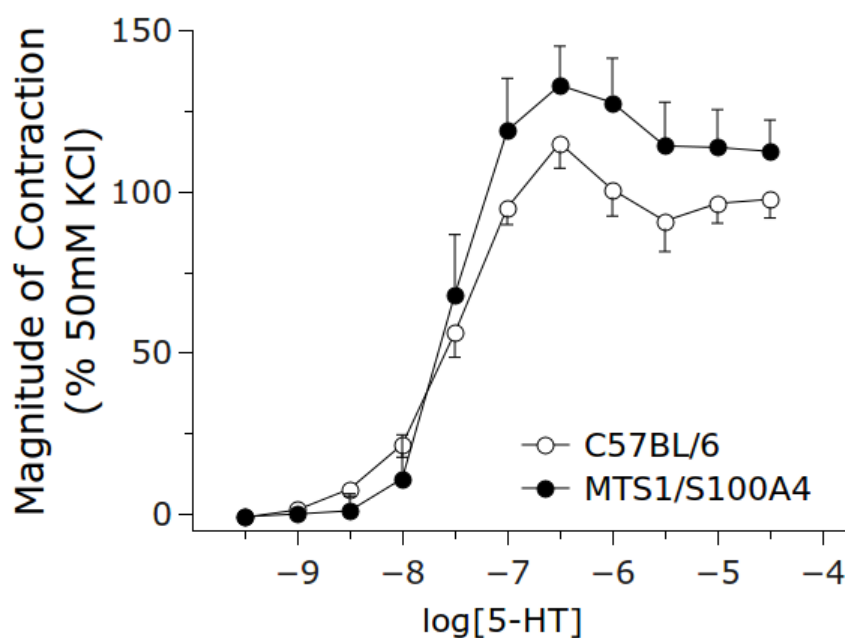


Figure 4.12 Contractile responses to 5HT in intrapulmonary arteries of C57BL/6 and MTS1/S100A4 mice. Responses to 5HT in vessels from normoxic MTS1/S100A4 and WT mice approached but did not achieve significant differences in due to MTS1/S100A4 expression and an interaction between MTS1/S100A4 overexpression and the concentration of 5HT ($p=0.059$; $p=0.066$, respectively) Data are presented as mean \pm SEM. (C57Bl/6: n=5; MTS1/S100A4: n=5)

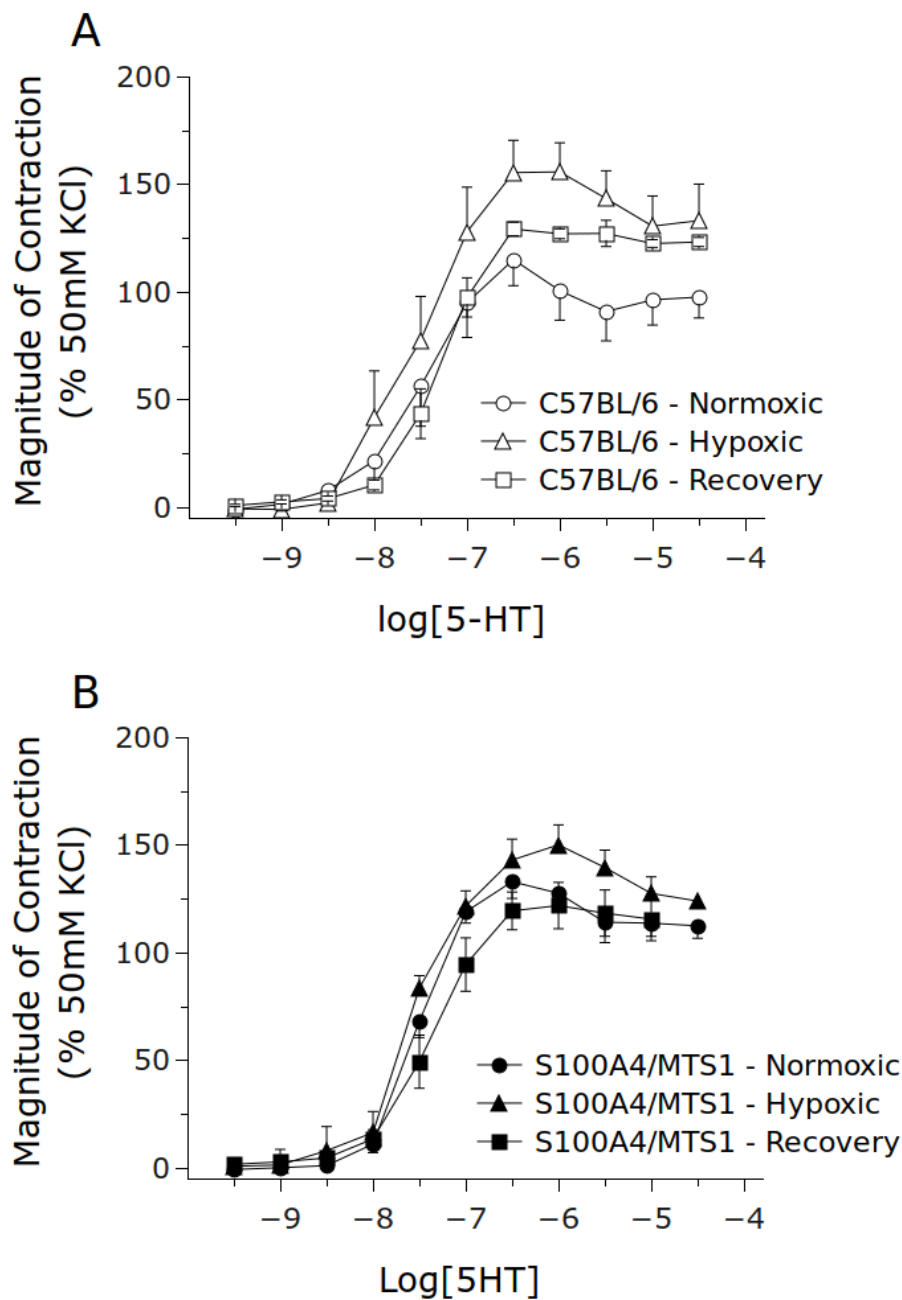


Figure 4.13 Effect of chronic hypoxia and recovery on contractile responses to 5-HT in intrapulmonary arteries. Contractile responses to 5-HT are augmented by chronic hypoxia in C57BL/6 (A; $p<0.05$) but not MTS1/S100A4 (B; $p=0.183$) mice. Similarly, the maximally observed contraction was significantly increased in hypoxic WT vessels ($E_{max} = 115 \pm 12\%$ vs. $E_{max} = 156 \pm 14\%$; $p<0.05$) but not MTS1/S100A4 mice ($133 \pm 8\%$ vs. $149 \pm 10\%$). No significant effects of recovery were detected in dose response curves to 5HT in either C57BL/6 or WT mouse strains. Data are expressed as mean \pm SEM for each concentration. Analyses were by LME model. (WT Normoxic: n=5; WT Hypoxic: n=5; WT Recovery: n=3; MTS1/S100A4 Normoxic: n=4; MTS1/S100A4 Hypoxic: n=5; MTS1/S100A4 Recovery: n=7)

4.3.4.2 Responses to U46619

Contractile responses to ascending concentrations of U46619 followed a sigmoidal distribution in normoxic WT with an E_{max} of $145.82 \pm 8.93\%$ and a $\log EC_{50}$ of -7.29 ± 0.21 (Figure 4.14). The maximal contraction in normoxic vessels from MTS1/S100A4 mice was $185 \pm 37\%$ and the $\log EC_{50}$ -7.78 ± 0.46 . The concentration response curve to U46619 in MTS1/S100A4 mice appeared to have a lower threshold concentration than WT mice and the relationship appeared to be shifted. Analysis by LME model revealed that the effect of strain was an overall increase which was statistically significant ($p<0.05$). No statistically significant differences in E_{max} or EC_{50} were detected.

In vessels from both WT and MTS1/S100A4 mice, concentration-response curves to U46619 were significantly augmented by hypoxia (WT: $p<0.001$; MTS1/S100A4: $p<0.05$) (Figure 4.15A and 4.15B) with a significant interaction between concentration and the hypoxic stimulus (WT: $p<0.05$; MTS1/S100A4: $p<0.05$). The maximal contraction to U46619 of vessels isolated from WT mice was significantly increased by 2 weeks exposure to hypoxia ($E_{max} = 239 \pm 29\%$; $p<0.01$). A mild increase in the mean value for E_{max} was observed in vessels isolated from MTS1/S100A4 after hypoxia ($E_{max} = 237 \pm 21\%$) and was not statistically significant when compared to that of vessels from normoxic MTS1/S100A4 mice. Log EC_{50} values were not significantly different to those observed in normoxic mice of either strain (WT: -7.40 ± 0.22 ; MTS1/S100A4: -7.41 ± 0.12). Direct comparison of concentration-response curves to U46619 in hypoxic WT and MTS1/S100A4 mice revealed no significant change ($p=0.3003$).

When allowed 4 weeks recovery in room air, contractile responses to U46619 in vessels isolated from WT mice were, on average, significantly reduced

in magnitude compared to those from hypoxic mice ($p<0.001$, LME model) (Figure 4.15A). A statistically significant interaction between the recovery stimulus and concentration was also observed ($p<0.001$). There was no evidence that concentration-response curves in vessels from recovery mice were statistically different from responses in vessels from normoxic mice ($p=0.465$). In line with these results, the E_{max} in vessels from WT mice in the recovery group ($137\pm 6\%$) was significantly decreased in comparison to the value in hypoxic mice ($p<0.005$) and not statistically different from the value obtained in normoxic mice.

Vessels from MTS1/S100A4 mice allowed 4 weeks recovery also showed a significantly altered response to U46619 when compared to vessels from hypoxic MTS1/S100A4 mice ($p<0.001$) (Figure 4.15B) with a statistically significant interaction between the recovery stimulus and concentration ($p<0.01$). Responses in vessels from animals in the recovery group were also significantly reduced in comparison to responses in normoxic vessels ($p<0.001$). The E_{max} in vessels from his group was $146 \pm 8\%$, significantly reduced in comparison to the value in vessels from hypoxic mice ($p<0.05$) and not statistically different to that observed in vessels from normoxic MTS1/S100A4 mice ($p>0.05$). No significant differences in the $\log EC_{50}$ for the response of these vessels to U46619 were detected between strain or treatment group (WT: -7.30 ± 0.11 ; MTS1/S100A4: -7.30 ± 0.11).

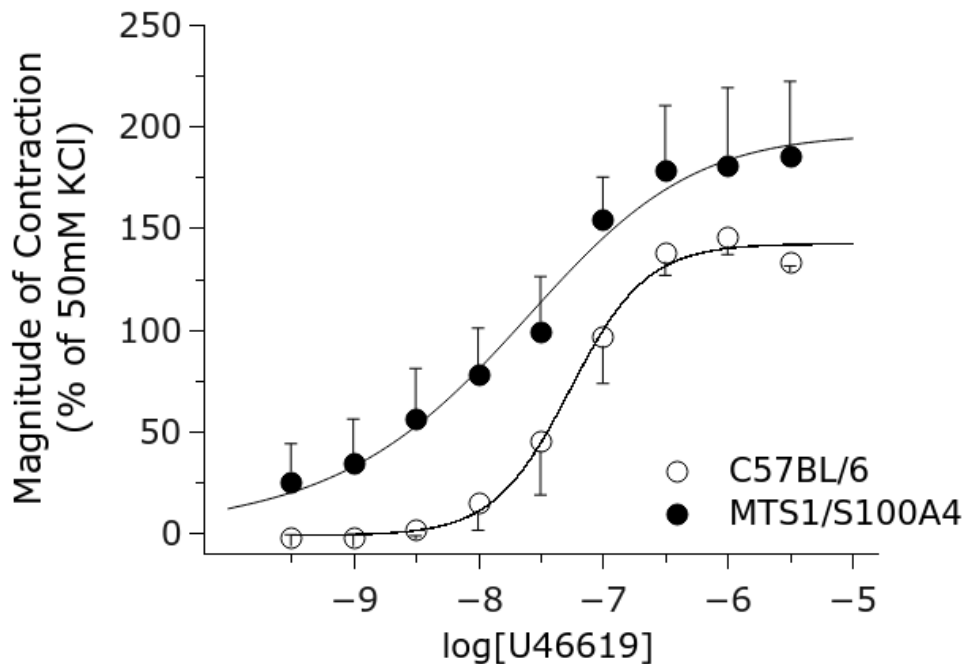


Figure 4.14 Contractile responses to U46619 in intrapulmonary arteries of C57BL/6 and MTS1/S100A4 mice. Intrapulmonary arteries from MTS1/S100A4 display an augmented response to U46619 ($p<0.05$). The maximally observed contraction was not significantly increased in MTS1/S100A4 mice ($185.19 \pm 36.90\%$) vs WT mice (145.80 ± 8.93). Data are expressed as mean \pm SEM for each concentration and relationships analysed by LME model. (C57BL/6: n=6; MTS1/S100A4: n=4).

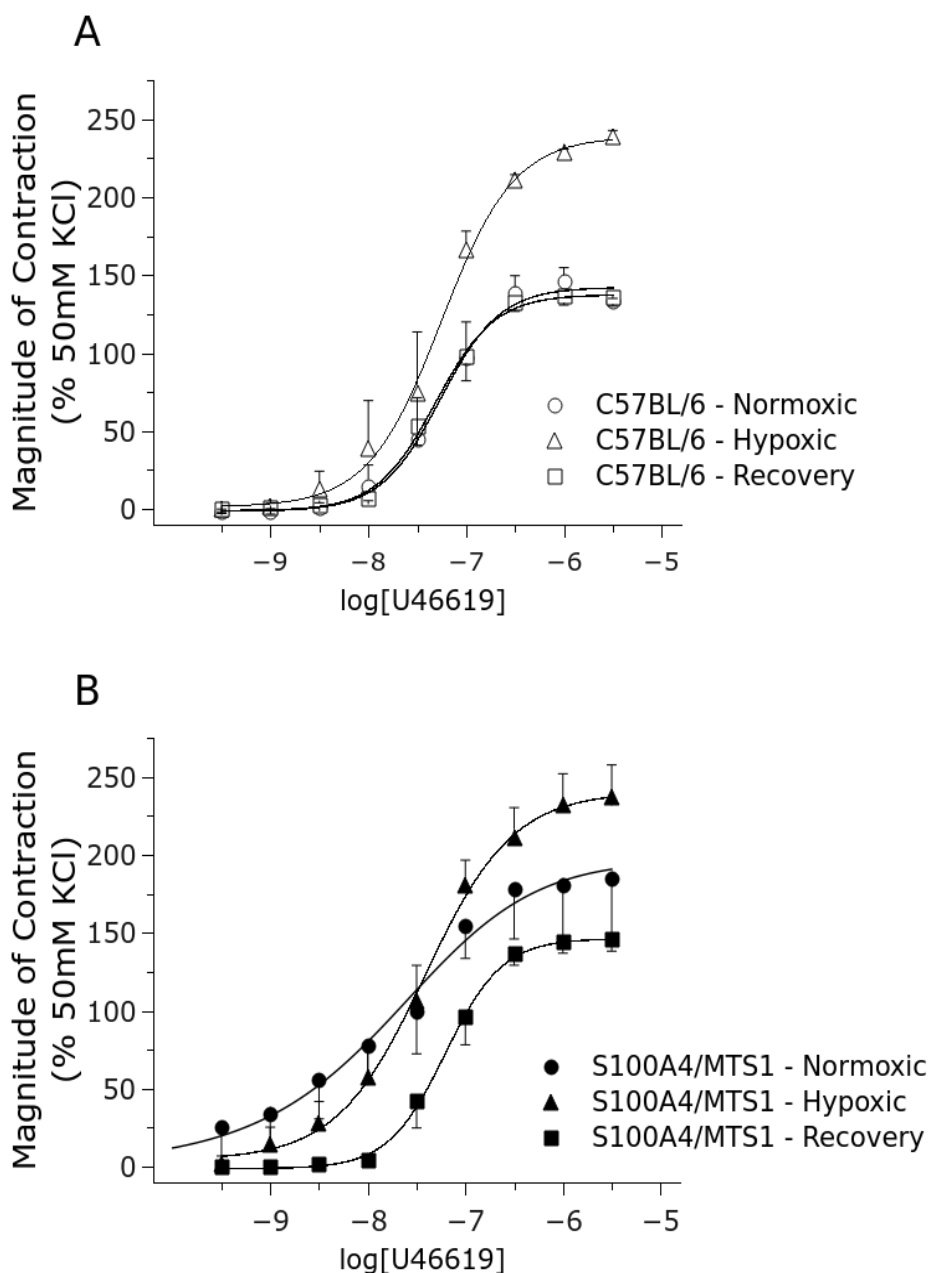


Figure 4.15 Effect of chronic hypoxia and recovery on contractile responses to U46619 in intrapulmonary arteries. Concentration-response curves to U46619 were significantly augmented by hypoxia in both WT ($p<0.001$; A) and MTS1/S100A4 (p<0.05; B) with significant interaction between $\log[\text{U46619}]$ and hypoxia (WT: $p<0.05$; MTS1/S100A4: $p<0.05$). Analysis revealed a significant change in the response of vessels isolated from both WT (A) and MTS1/S100A4 (B) mice allowed 4 weeks of recovery challenge compared to vessels from hypoxic animals ($p<0.001$ and $p<0.01$, respectively). Recovery responses were significantly reduced compared to those of normoxic vessels in MTS1 ($p<0.001$) but not WT mice. Data are presented as mean \pm SEM. Statistical analyses were by LME model. (WT Normoxic: n=6; WT Hypoxic: n=4; WT Recovery: n=6; MTS1/S100A4 Normoxic: n=4; MTS1/S100A4 Hypoxic: n=7; MTS1/S100A4 Recovery: n=6).

4.3.4.3 Responses to SNP

For the purposes of measuring the sensitivity of vessels to NO, vasodilatory responses to ascending concentrations of the NO donor SNP were observed in IPAs preconstricted with U46619 at a concentration producing ~70% of the maximal contraction observed in each vessel to stimulation with 50mM KCl.

Relaxatory responses to ascending concentrations of SNP in vessels from normoxic WT mice increased with concentration to an E_{max} of $96 \pm 3\%$ (Figure 4.16). The $\log EC_{50}$ was -6.91 ± 0.20 . Surprisingly, vessels from normoxic MTS1/S100A4 mice showed an increased sensitivity to SNP in comparison to WT mice. Analysis by LME model demonstrated a significant interaction between strain and concentration when comparing responses from WT and MTS1/S100A4 mice ($p<0.05$). The leftward shift observed in vessels from MTS1/S100A4 mice was verifiable statistically as a significant change in $\log EC_{50}$ ($\log EC_{50} = -8.00 \pm 0.30$; $p<0.01$) (Figure 4.16). E_{max} from these vessels was $94 \pm 3\%$ and was not statistically different to that of WT mice.

Concentration-response curves to SNP in vessels from WT mice exposed to hypoxia appeared blunted in comparison to normoxic controls (Figure 4.17A). Analysis by LME model revealed that responses in hypoxic WT mice were reduced ($p<0.01$) with a significant interaction between concentration and exposure to hypoxia ($p<0.001$). Although the maximum relaxation produced by SNP appeared reduced ($E_{max} = 65 \pm 11\%$), this was not significantly different from that observed in vessels from normoxic animals. $\log EC_{50}$ in hypoxic WT mice was unchanged in comparison in normoxic mice of the same strain ($\log EC_{50} = -7.17 \pm 0.35$). The alteration in the response to SNP in vessels from hypoxic MTS1/S100A4 mice in

comparison to normoxic mice of the same strain appeared more dramatic than in WT controls (Figure 4.17B). Analysis by LME model revealed a significant effect of hypoxic exposure alone ($p<0.01$), as well as a significant interaction between hypoxic treatment and the concentration of SNP ($p<0.01$). Both the potency and maximum efficacy of SNP in vessels from hypoxic MTS1/S100A4 mice were significantly reduced compared to normoxic mice of the same strain ($E_{max} = 57 \pm 9\%$; $p<0.05$; $\log EC_{50} = -7.11 \pm 0.20$; $p<0.05$). While sensitivity to SNP in vessels from normoxic MTS1/S100A4 mice was higher than in WT controls, analysis between strains revealed no statistically significant differences between hypoxic WT and hypoxic MTS1/S100A4 mice ($p=0.882$, LME model). Direct comparison of concentration-response curves from hypoxic WT and MTS1/S100A4 mice revealed no significant differences ($p=0.8974$).

Vessels isolated from WT mice allowed 4 weeks recovery from hypoxia displayed a response to SNP that was not statistically different from that observed in hypoxia ($p=0.566$, LME model) (Figure 4.17A) and still significantly reduced in comparison to that observed in normoxia ($p<0.001$) with a significant interaction between concentration and hypoxic exposure ($p<0.001$). The E_{max} for SNP in these vessels was $59 \pm 3\%$ which did not differ significantly from that observed in either normoxic or hypoxic mice. Similarly, no significant difference in the $\log EC_{50}$ (-7.09 ± 0.11) was detected.

Vessels taken from MTS1/S100A4, when allowed 4 weeks recovery, showed vasorelaxation in response to SNP that was significantly greater than that observed in vessels from hypoxic animals of the same strain ($p<0.05$) and with a significant interaction between concentration and the recovery stimulus ($p<0.001$) (Figure 4.17B). The response of vessels from animals in the recovery group was just significantly different to that of vessels from animals in the

hypoxic group ($p=0.04998$). The E_{max} for SNP in these vessels was $82 \pm 16\%$ and did not achieve significance when compared to either normoxic or hypoxic animals. LogEC_{50} in these vessels was -6.74 ± 0.043 : significantly altered in comparison to normoxic vessels ($p<0.001$) and similar to vessels from hypoxic animals.

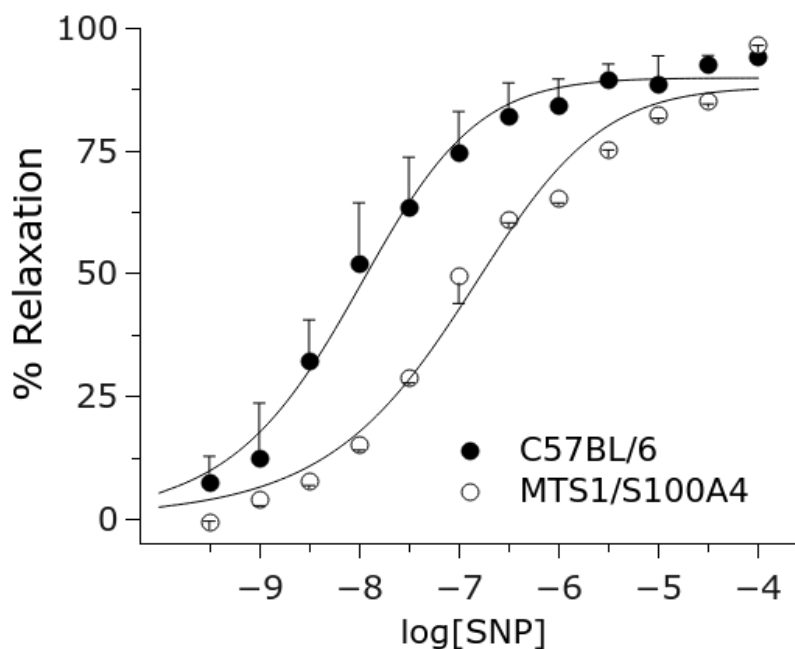


Figure 4.16 Effect of MTS1/S100A4 overexpression on the relaxatory response to sodium nitroprusside in intrapulmonary arteries. There was a significant effect of interaction between strain and concentration when comparing responses from WT and MTS1/S100A4 mice ($p<0.05$). (WT: n=3; MTS1/S100A4: n=3).

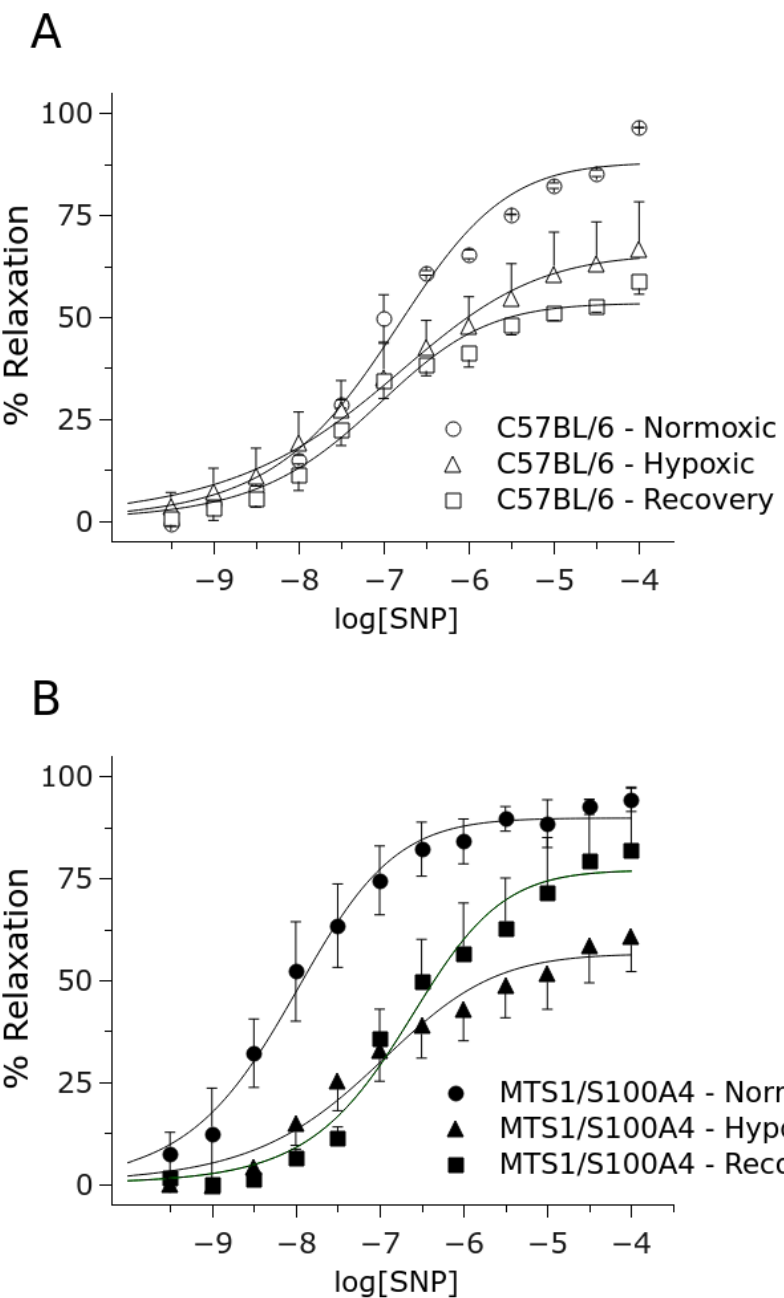


Figure 4.17 Effect of chronic hypoxia and recovery on relaxatory responses to U46619 in intrapulmonary arteries. Responses in vessels from both C57BL/6 (A) and MTS1/S100A (B) mice displayed statistically significant effects of hypoxia ($p<0.01$; $p<0.001$) and significant interactions between strain and hypoxia ($p<0.01$; $p<0.01$). Responses in vessels from C57BL/6 mice allowed to recover (A) were not statistically different from those of vessels from hypoxic mice ($p=0.882$). In MTS1/S100A4 mice, responses were significantly improved compared to those in hypoxic mice ($p<0.05$) though still altered in comparison to those in normoxic mice ($p<0.001$) with a significant interaction between concentration and baricity ($p<0.001$) (WT Normoxic: n=3; WT Hypoxic: n=4; WT Recovery: n=4; MTS1/S100A4 Normoxic: n=3; MTS1/S100A4 Hypoxic: n=5; MTS1/S100A4 Recovery: n=5).

4.4 Discussion

The aims of the study described in this chapter were two-fold: first, to ensure the repeatability of results in the literature regarding the development of PAH in the MTS1/S100A4 mouse with the aim of identifying a suitable point to commence a pharmacological intervention; and second, to obtain data regarding the function of pulmonary arteries to complement existing knowledge on alterations to the pulmonary circulation in the MTS1/S100A4 mouse when compared to WT controls.

In the current study, only very limited evidence for an enhancement of pulmonary hypertension by MTS1/S100A4 overexpression in either normoxia or hypoxia was observed as assessed through measurement of right ventricular haemodynamics in MTS1/S100A4 mice *in vivo*. This was manifest as a trend towards an increase in sRVP in hypoxic MTS1/S100A4 mice compared to WT mice, and as a statistically significant elevation in mRVP in hypoxic MTS1/S100A4 mice compared to WT mice. Additionally, we observed no significant enhancement of hypoxia-induced RVH in MTS1/S100A4 mice compared with WT counterparts. These results are not in agreement with observations by (Merklinger et al., 2005) which provided a basis for the current study: specifically, those showing that MTS1/S100A4 mice display mild but statistically significant elevations in sRVP and RVH above WT mice at baseline, and those showing that these quantities were increased to a greater degree by hypoxia in MTS1/S100A4 mice than in WT mice. Most surprisingly, MTS1/S100A4 mice appeared to be protected against the hypoxia-induced increase in pulmonary vascular remodelling observed in WT mice in the current study.

Data obtained from animals in the recovery group differed from that of

the literature in both the WT and MTS1/S100A4 groups. We found no evidence of sustained elevation of sRVP after 4 weeks normoxic recovery in MTS1/S100A4 mice. Conversely, it was observed that hypoxia-induced increases in RVH were sustained after 4 weeks normoxic recovery in WT and MTS1/S100A4 mice alike. Merklinger *et al.*, reported that 4 weeks of recovery in normoxia produced a complete reversal of hypoxia-induced increases in sRVP and RVH in WT mice which was not mirrored in MTS1/S100A4 mice.

One of the more striking and surprising observations in the current study was that MTS1/S100A4 overexpression appeared to be protective against hypoxia-induced pulmonary vascular remodelling, particularly given that this was not accompanied by a corresponding protection against hypoxia-induced sRVP elevation. Similarly, decreased compliance in intralobar pulmonary arteries was observed in WT mice after chronic hypoxia. Decreased compliance of conducting vessels can contribute to elevations in RVP (Zuckerman *et al.*, 1991). MTS1/S100A4 mice also appeared to be protected from this change. Remodelling is a key component of the pulmonary hypertensive state, and has been reported to be a good correlate of pulmonary vascular pressure in rodent models of disease (Rabinovitch *et al.*, 1983). Data from *in vitro* studies indicate that RAGE activation represents a mitogenic and proliferative stimulus in PASMCs (Lawrie *et al.*, 2005) as well as leading to increased elastin fibre assembly and deposition. These data provided a basis for the hypothesis that RAGE and its ligands may be involved in the remodelling associated with pulmonary hypertension.

With regards to the study conducted previously, there are some differences in the experimental design which may have affected the outcome. First, a hypobaric environment was used to administer a chronic hypoxic challenge in the current study whereas Merklinger *et al.* utilised a normobaric

preparation wherein the level of O₂ was continually maintained at 10% by replacement with nitrogen. These two techniques differ in that the hypobaric environment presents an additional physical stress on the lung as well as altering the nature of the gas being respired. For example, a subject breathing air of reduced barometric pressure will inspire a smaller mass of air for an equivalent volume of inspiration, leading to hyperventilation (Grover, 1965; Levine et al., 1988). Additionally, alterations in barometric pressure in alveoli appear to transmit directly to the interstitial fluid surrounding the pulmonary vasculature, possibly contributing to increased oedema observed in hypobaric versus normobaric hypoxia (Woolverton et al., 1978; Levine et al., 1988). Normobaric and hypobaric hypoxia have been shown to produce differing effects on pulmonary function and lung growth in growing rats (Sekhon et al., 1995; Sekhon and Thurlbeck, 1996).

There is little data in the literature specific to the comparative effects of normobaric and hypobaric hypoxia on pulmonary haemodynamics. Levine et al. (1988) reported a larger increase in pulmonary arterial pressure in sheep exposed to acute hypobaric hypoxia stimulus versus an equivalent normobaric stimulus. However, a study comparing the development of RVH and distal pulmonary vascular remodelling in rats exposed to either normobaric hypoxia (10% O₂) or hypobaric hypoxia (500mbar; equivalent of 10% O₂) found no difference between the two groups ((Sheedy et al., 1996)). Currently, it is very difficult to say how the addition of stresses associated with hypobaric hypoxia may have affected results in the current study. The physiological and physical differences introduced to an investigation by the choice of either normobaric or hypobaric hypoxia, as well as a lack of data on the relevance of these, suggest caution in ruling it out entirely.

It is of note that the differences in response between normoxia, hypoxia and recovery in the current study are not simply less dramatic examples of those described by Merklinger et al they are qualitatively different in several cases. This leads this investigator to speculate that a more likely element of the current study design in explaining this discrepancy is the gender of mice chosen for the study. Gender has been of interest in the study of PAH because there is a bias towards females in the development of PAH in human patients (Humbert et al., 2006; Peacock et al., 2007; Thenappan et al., 2007). In most models of PAH in mice and rodents, this bias tends to be reversed in that females seem protected against the development of PAH. However, recent work by others in this laboratory has demonstrated that there is a gender discrepancy in the manifestation of elevated pulmonary pressures in the MTS1/S100A4 mouse, with female MTS1/S100A4 mice displaying elevated pulmonary pressures in normoxia versus male MTS1/S100A4 mice. MTS1/S100A4 gene expression is elevated in the lungs of both male and female MTS1/S100A4. However, this expression is more pronounced in female mice. The female sex hormone 17 β -estradiol was observed to induce MTS1/S100A4 protein expression in human PASMCs in addition to stimulating proliferation in these cells. Interestingly, treatment with sRAGE inhibited proliferation of these cells in responses to 17 β -estradiol, implicating MTS1/S100A4 as a mediator of this proliferation (Dempsie et al., 2011). In another mouse model which replicates the female gender bias (mice overexpressing the SERT), ovariectomy in female mice abolished their predisposition to pulmonary hypertension while treatment of ovariectomised mice with exogenous 17 β -estradiol resulted in its re-establishment (White et al., 2011). The implication of these data is that there is an association between 17 β -estradiol (and by proxy the female gender), enhanced MTS1/S100A4 expression

and the development of pulmonary hypertension in these mouse models.

The mice used in the current study were male. Merklinger et al. refer to the gender-matching of MTS1/S100A4 mouse in their study suggesting that both male and female mice were used. However, it is not specific as to the comparative numbers of mice of either gender used. The proportion of males and females utilised could influence the outcome of such a study in the instance that male and female mice exhibit differing responses to MTS1/S100A4 overexpression and/or hypoxia.

Merklinger et al. observed altered haemodynamics and increased RVH in MTS1/S100A4 mice in the absence of enhanced vascular remodelling (a proxy for increased vascular resistance) which led them to speculate that some alteration in vascular tone might account for these changes. An augmented increase in sRVP in response to exposure to acute hypoxia *in vivo* and an impaired reversal of this increase in response to inhaled NO was also reported.

When examining the pharmacology of IPAs in the current study it was interesting to note that the responses that appeared most dramatically altered between strain were those in vessels isolated from normoxic animals. The consequence of this was that while the concentration-response curves to 5HT and U46619 in vessels from MTS1/S100A4 and WT mice after hypoxia appeared very similar in form and magnitude, the change in the response from normoxia to hypoxia was less dramatic in MTS1/S100A4 mice since responses in normoxic vessels appeared to be augmented. Evidence for this observation may be found in that responses to contractile stimuli in normoxic MTS1/S100A4 were augmented in comparison to those in WT mice, and to a degree which approached (5HT) or achieved (U46619) statistical significance. Furthermore, hypoxia produced a significant mean increase in the response to 5HT in WT, but

not MTS1/S100A4 mice.

In normoxic MTS1/S100A4 mice, the augmentation of contractile responses to contractile stimuli did not manifest as an increase in sRVP in MTS1/S100A4 mice *in vivo*. However, if an increase in response to contractile in the MTS1/mouse stimuli contributes to vascular resistance in the pulmonary circulation, then the surprising observation of an increase in sensitivity to SNP in vessels from MTS1/S100A4 mice may represent a compensatory mechanism which prevents this. This suggests that responses to endothelial NO might be similarly augmented. However, the study of endothelial-dependent relaxation in the vessels studied here is problematic because of the difficulty associated with isolating and mounting vessels of this size while maintaining the integrity of the endothelium for the purpose of constructing concentration-response curves to compounds such as ACh. On several preliminary attempts, vessels exposed to ascending concentrations of ACh displayed sub-maximal relaxation at low concentrations and constriction at higher concentrations (data not shown). How endogenous NO production by the endothelium is affected in the MTS1/S100A4 mouse is currently not known.

4.4.1 Further work

An *in vitro* study carried out in 2004 demonstrated that treatment of cells expressing the serotonin transporter with NO inhibited the transport of 5HT, possibly through nitrosation of the SERT protein (Bryan-Lluka et al., 2004). If vessel diameter in the MTS1/S100A4 mouse is reduced as demonstrated by Merklinger et al. then it is possible that NO synthesis might be increased as a result of increased flow and, consequently, shear on endothelial cells. (Rubanyi

et al., 1986; Kumar et al., 2010). 5HT transport through SERT has been implicated as required for upregulation and exocytosis of MTS1/S100A4 in hPASMCs. Subsequent RAGE activation by exocytozed MTS1/S100A4 is implicated in mediating the proliferative and migratory responses of PASMCs to 5HT (Lawrie et al., 2005); processes which are also implicated in the process of pulmonary vascular remodelling associated with PAH. It would therefore be of great interest to supplement *in vitro* studies on RAGE in PASMCs with studies in endothelial cells. In particular, it would be of interest to learn how activation of RAGE impacts upon the production of endogenous NO in these cells in response to pharmacological agents and to shear stress associated with flow. A variety of endothelial mediators are thought to be responsible for contributing to the vascular remodelling process and knowledge of how RAGE and its ligands may participate in this would prove valuable.

4.5 Conclusions

The aims of this study were to ensure repeatability of observations of enhanced PAH in the hypoxic MTS1/S100A4 mouse with the aim of producing preliminary data for the purpose of a future intervention study: namely an investigation of the effects of treatment with sRAGE in these mice. The purpose of such a study being to ascertain whether sRAGE treatment might normalise any changes observed in the proxies of PAH assessed here: namely PAP, RVH and the remodelling of distal vessels. While some interesting differences between WT and MTS1/S100A4 mice were observed in the current study, these were predominantly associated with the responses of IPAs to pharmacological agents. While these data provide interesting insight into vascular function in the

pulmonary circulation of MTS1/S100A4 mice, the fact that the observed changes in haemodynamic properties *in vivo* were not particularly dramatic made embarking on an intervention study in this mouse less appealing. This caution was brought by the value attached to the sRAGE molecule at the time this study was carried out, both in terms of monetary cost and uncertainty about the quantities which would ultimately be available for such an investigation.

Nevertheless, the current study highlights the complexity and subtlety of the contribution of MTS1/S100A4 to pulmonary vascular disease in this model.

Chapter 5.

*Treatment with recombinant soluble
receptor for advanced glycation end-
products in a hypoxic mouse model of
PAH*

5.1 Introduction

While transgenic mice are a valuable tool in modelling and understanding disease, intervention with small organic compounds or macromolecules such as sRAGE represents, with any number of caveats, a more direct analogue to the administration of therapeutics in the clinic.

In the previous chapter, we attempted to characterise the development of hypoxia-induced pulmonary hypertension in the MTS1/S100A4 mouse with the aim of identifying a suitable point for a pharmacological intervention. While some evidence of alterations in the functional characteristics of the pulmonary circulation in MTS1/S100A4 mice were observed, these were not as definitive as those observed and published in the literature. While the contractile responses of pulmonary arteries appeared augmented in MTS1/S100A4 mice in normoxia, this was not accompanied by an increase in right ventricular pressure; possibly due to a compensatory increase in the relaxatory responses to NO. Additionally, after hypoxia, these differences were not apparent.

Given that overexpression of MTS1/S100A4 did not result in a clear exacerbation of the pulmonary hypertensive state elicited by chronic hypoxia, and given that generation of pulmonary hypertension is reproducible and well characterised in the C57BL/6 mouse, examining the effect of sRAGE treatment upon hypoxia-induced PH in these mice seemed more likely to produce valuable insights into the role of RAGE in pulmonary hypertension.

As discussed in the introductory chapter, sRAGE has been successfully used as an intervention in mouse models of other diseases *in vivo* in which RAGE is thought to play a role including delayed-type hypersensitivity (Hofmann et al., 1999) and atherosclerosis (Harja et al., 2008). Results from the previous chapter

involving MTS1/S100A4 mice emphasise the need to attempt to gain as wide a perspective as possible of the impact of treatment upon the function of the lung. For this reason, we opted to once again examine the contractile properties of intrapulmonary arteries from the lungs of mice used in the current study. In the interests of further characterising the role of RAGE upon the cells constituting these vessels, we also resolved to examine the effects of sRAGE treatment upon cellular proliferation in CCL39 Chinese hamster lung fibroblasts. Proliferation due to RAGE activation has thus far been the most studied in PASMCs, as PASMC proliferation is thought key to the process of vascular remodelling *in vivo* (Rubin, 1997). However, in the hypoxic lung *in vivo*, adventitial fibroblasts demonstrate the most immediate and dramatic proliferation, before subsequently migrating to the media, transdifferentiating into myofibroblasts and secreting substances which are themselves mitogenic to PASMCs (Rose et al., 2002; Stenmark et al., 2006). Proliferation in PASMCs as described in the literature is inconsistent; with some studies showing proliferation to hypoxia only in the presence of other mitogens (Dempsey et al., 1991; Lannér et al., 2005) and others showing proliferation to hypoxia alone (Cooper and Beasley, 1999; Lu et al., 2005).

As was discussed in the introduction, varying cell types comprising the pulmonary arteries display heterogeneous behaviours and responses to inflammatory stimuli. This work therefore contributes to a more complete understanding of the roles of RAGE in the pulmonary circulation by building upon data in the literature examining the role of RAGE in the proliferation and migration of PASMCs.

5.2 Aims

Our aim in the current study was to observe the effect of sRAGE treatment on the generation of structural and functional changes associated with hypoxia-induced pulmonary hypertension in mice *in vivo*. Additionally, we aimed to characterise any potential role for RAGE in the proliferation of pulmonary fibroblasts *in vitro*.

5.3 Methods

Male C57BL/6 mice were randomly assigned to normoxia or to 2 weeks of hypobaric hypoxia, and to I.P. injection with either vehicle (PBS) or 20 μ g/day sRAGE. This dose was chosen based on the work of Harja et al. (2008) wherein it was demonstrated that daily dosing with sRAGE significantly impaired the worsening of disease in a mouse model of atherosclerosis. 40 μ g/day was observed to produce the maximal level of benefit with no further benefit derived from a dose of 100 μ g/day. However, the limited quantity of sRAGE available for the current investigation led us to choose the lower dose of 20 μ g/day. While the use of the higher dose would obviously be preferable, this compromise was deemed acceptable for two reasons: first, practically, it allowed for the dosing of a total of 13 mice while leaving a small quantity of sRAGE in excess for use in *in vitro* studies; and secondly, even though the maximal benefit of sRAGE treatment in the previous study was obtained at a higher dose, 20 μ g/day was still observed to produce a significant and convincing benefit.

Mice in the hypoxic group were returned to normoxia once a day to

facilitate dosing with either vehicle or sRAGE over the course of the intervention. At the end of this time, right ventricular haemodynamics and mean systemic arterial pressure were assessed in each mouse *in vivo* before removal of the heart and lungs *en bloc* for the purpose of assessing RVH, pulmonary vascular remodelling, vascular reactivity and vascular compliance. Normoxic mice were housed in the same room and were dosed at the same time as their hypoxic counterparts.

CCL39 cell culture and proliferation studies were carried out as described in Chapter 2. For studies on the effects of sRAGE upon another proliferative stimulus, cells were pre-incubated with sRAGE for a period of half an hour before the commencement of said stimulus.

Soluble RAGE was kindly provided by Dr. Anne Marie Schmidt at Columbia University Medical Center, New York, USA.

5.3.1 Statistical analysis

Statistical analyses were carried out as described in Chapter 2.

5.4 Results

Systolic RVP was assessed in 29 male mice aged 2-3 months in the current study. No mortality was observed during dosing. Six experiments were terminated before the assessment of SAP. The observed values for sRVP studied in vehicle-treated control mice in the current study were very similar to those observed in WT controls in the previous chapter under conditions of both normoxia and after exposure to chronic hypoxia. Mean SAP was not significantly

altered between treatment groups though heart rate was significantly lowered in hypoxic vehicle-treated animals versus normoxic controls in the current study (Figure 5.1). Heart rate was significantly reduced in hypoxic vehicle-treated mice ($HR = 276.31 \pm 2.28$ bpm; $p < 0.05$) and hypoxic sRAGE-treated mice ($HR = 269.26 \pm 10.21$ bpm; $p < 0.01$) when compared to normoxic vehicle-treated controls ($HR = 337.37 \pm 16.48$). Since pulmonary output is largely independent of pulmonary CO, this observation does not strongly affect subsequent interpretation of results relating to changes in sRVP.

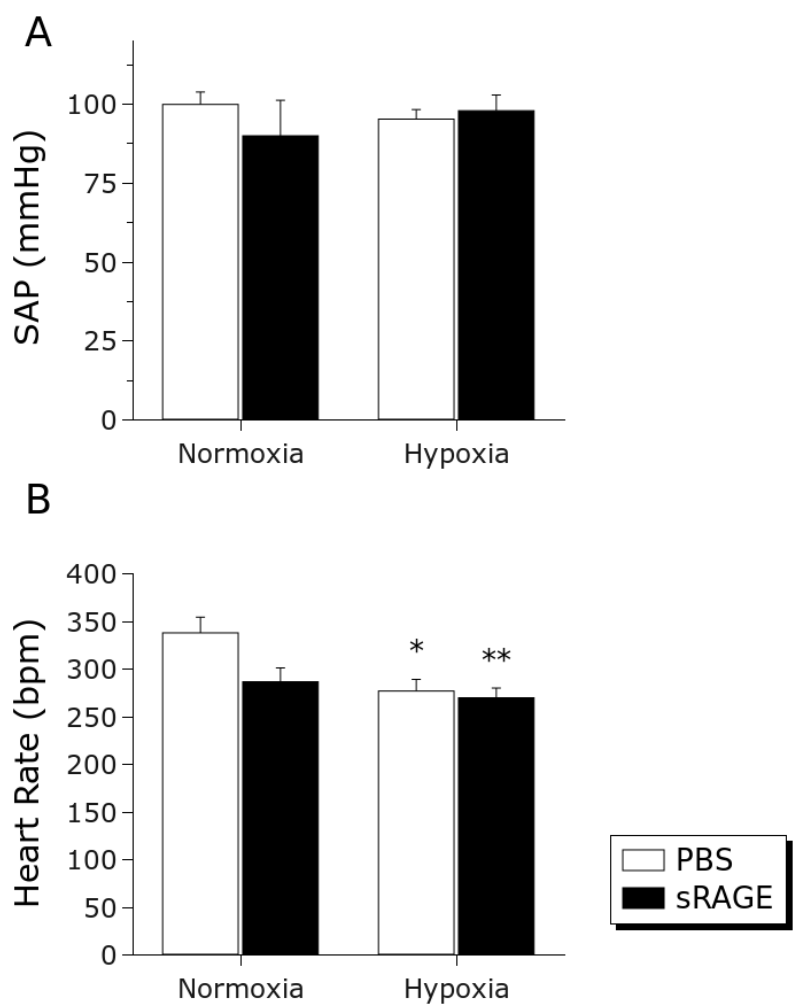


Figure 5.1 Mean systemic arterial pressure and heart rate - effects of sRAGE and hypoxia. No alterations in SAP were observed between treatment groups in normoxia or hypoxia (Vehicle Normoxic: n=7; Vehicle Hypoxic: n=6; sRAGE Normoxic: n=5 sRAGE hypoxic: n=5). HR appeared significantly reduced in hypoxic vehicle-treated mice and hypoxic sRAGE-treated mice compared to normoxic vehicle-treated mice (Vehicle Normoxic: n=7; Vehicle Hypoxic: n=9; sRAGE Normoxic: n=7; sRAGE hypoxic: n=6). Since pulmonary pressure is largely independent of CO it seems unlikely that this observation relates directly to the pulmonary arterial pressures observed. Data are expressed as mean \pm SEM. * $p<0.05$, ** $p<0.01$ versus normoxic vehicle-treated mice.

5.4.1 Effects of sRAGE dosing and hypoxia in C57BL/6 mice in vivo

In normoxic animals, treatment with 20 μ g/day sRAGE produced no significant changes in sRVP (Vehicle: 22.65 \pm 1.01 mmHg; sRAGE: 24.41 \pm 0.73 mmHg) (Figure 5.2A); proportion of remodelled vessels (Vehicle: 12.67 \pm 2.13%; sRAGE: 13.92 \pm 2.16%) (Figure 5.2B); or RVH (Vehicle: 0.27 \pm 0.013; sRAGE: 0.28 \pm 0.011) (Figure 5.2C) when compared to vehicle-treated controls. Small intrapulmonary vessels appeared structurally similar in vehicle-treated and sRAGE-treated mice in normoxia (Figure 5.3). In animals treated with PBS, 2 weeks of hypobaric hypoxia produced statistically significant increases in sRVP (31.02 \pm 1.51 mmHg; p <0.01). Animals treated with 20 μ g/day IP sRAGE displayed a mild increase in sRVP which was not significantly different from normoxic animals receiving the same treatment (26.92 \pm 1.53 mmHg) or from vehicle-treated animals. However, direct comparison of sRVP in hypoxic vehicle-treated and sRAGE-treated animals revealed no significant difference between these two groups.

No corresponding protection against hypoxia-induced increases in vascular remodelling was observed. Remodelled vessels possessing a double elastic lamina were evident in sections from hypoxic vehicle-treated mice (Figure 5.3) and the extent of this remodelling was significantly elevated above normoxic controls (Vehicle: 21.38 \pm 1.72; p <0.05) (Figure 5.2B). Remodelled vessels were also evident in sections from hypoxic sRAGE-treated animals. The character of this remodelling appeared similar to that observed in sections from hypoxic vehicle-treated mice (Figure 5.3). The extent of vascular remodelling in sRAGE-treated hypoxic mice was significantly elevated above both vehicle-treated and sRAGE-treated normoxic mice (25.97 \pm 2.15%; p <0.01 and p <0.001 respectively).

Indeed, the extent of hypoxia-induced remodelling appeared mildly increased above that observed in vehicle-treated mice exposed to hypoxia but analysis revealed no evidence of a difference between these groups. Right ventricular hypertrophy was significantly elevated in hypoxic vehicle-treated animals when compared to normoxic controls (0.34 ± 0.01 ; $p<0.01$). Right ventricular hypertrophy in hypoxic sRAGE-treated animals was significantly elevated above both vehicle-treated and sRAGE-treated normoxic mice (0.35 ± 0.01 ; $p<0.01$ and $p <0.001$ respectively).

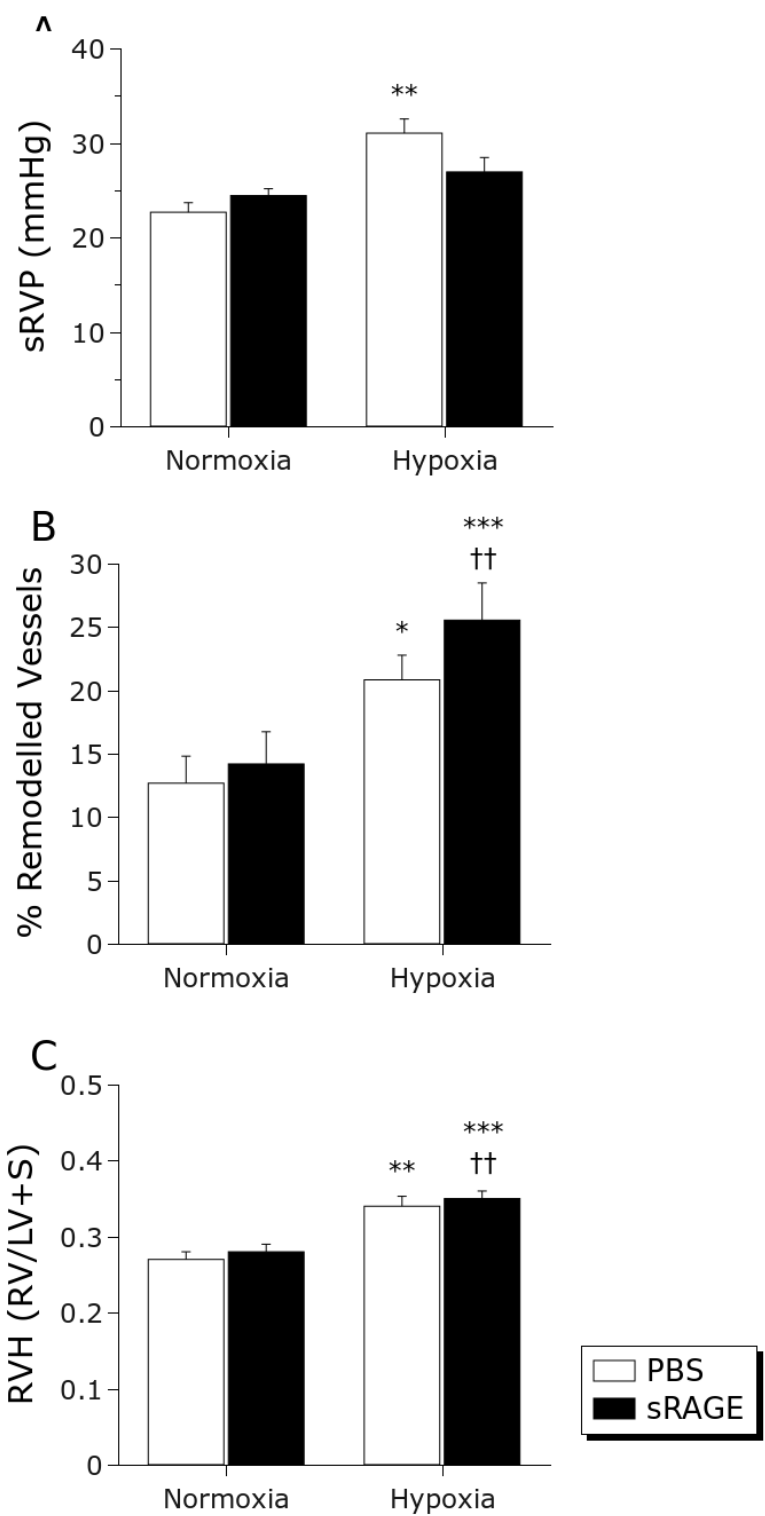


Figure 5.2 Treatment with sRAGE blunts a hypoxia-induced increase in sRVP but does not prevent increases in pulmonary vascular remodelling or RVH. Data are expressed as mean \pm SEM. Statistical analysis was by two-way ANOVA followed by Fisher's LSD test for multiple comparisons with p-values corrected using the Bonferroni method. * $p<0.05$, ** $p<0.01$, *** $p<0.001$ vs. normoxic, PBS-treated mice; †† $p<0.01$ vs normoxic, sRAGE treated mice. (Vehicle Normoxic: n=7; Vehicle Hypoxic: n=9; sRAGE Normoxic: n=7; sRAGE hypoxic: n=6).

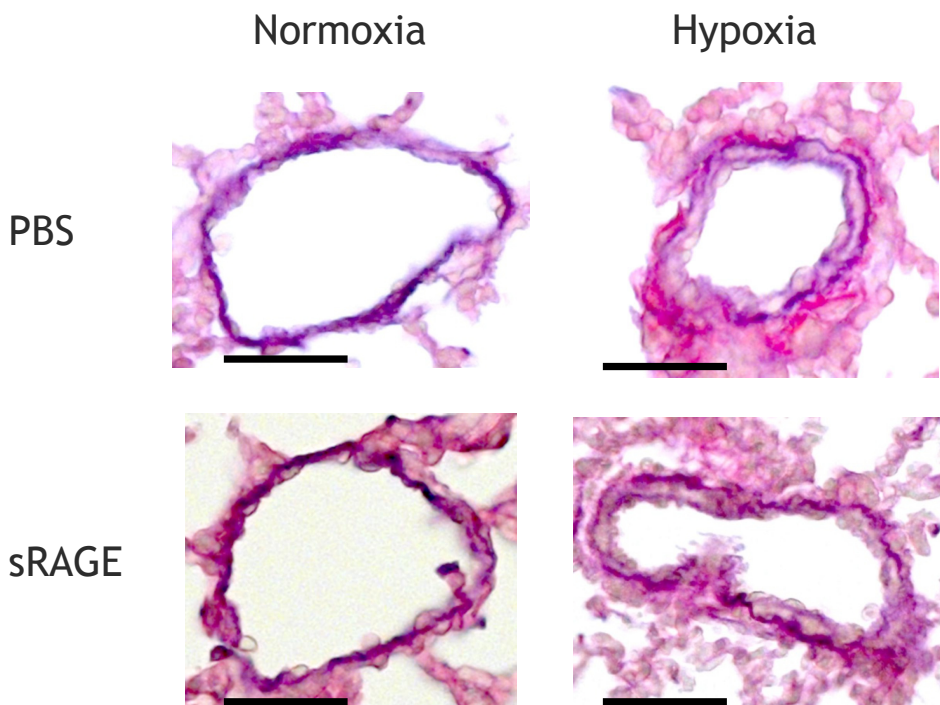


Figure 5.3 Images of representative small pulmonary arteries in C57Bl/6 mice treated with vehicle or sRAGE in normoxia and after 2 weeks hypoxia. Small intrapulmonary vessels possessing a double elastic lamina were evident in sections taken from vehicle-treated mice exposed to two weeks of hypoxia. Remodelled vessels were also evident after hypoxia in sections from sRAGE-treated mice. The remodelling did not appear characteristically different to that observed in vehicle-treated mice. No effect of treatment with vehicle or sRAGE was evident in sections from normoxic mice. Photographs taken under x40 objective magnification. Scale bar = 50 μ m.

5.4.2 Vascular compliance

The diameter of intrapulmonary vessels taken from vehicle-treated animals appeared to increase in a linear fashion with the application of increasing force (Figure 5.4). This relationship appeared very similar to that observed in vessels taken from animals treated with 20 μ g/day sRAGE. No statistically significant effect of sRAGE treatment ($p=0.143$) or interaction between sRAGE treatment and force was observed ($p=0.702$). As in the previous chapter, exposure to 2 weeks of hypoxia produced a statistically significant reduction in the compliance of these vessels in vehicle-treated mice (Figure 5.5A; $p<0.05$). In contrast, treatment with 20 μ g/day sRAGE showed no such decrease in comparison to either normoxic vehicle-treated mice ($p=0.909$; interaction $p=0.907$) or normoxic sRAGE-treated mice ($p=0.548$; interaction $p=0.708$; Figure 5.5B). Despite these results, a direct comparison of vehicle treated and sRAGE treated animals that had been exposed to hypoxia did not appear significant ($p=0.495$; interaction $p=0.620$).

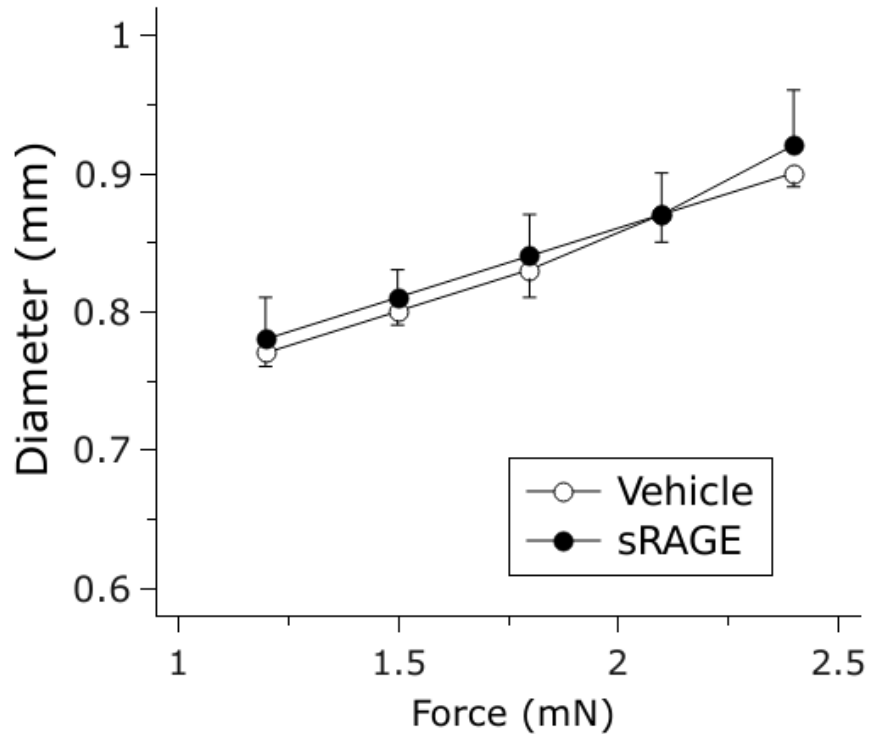


Figure 5.4 Treatment with sRAGE produces no alteration in compliance in intrapulmonary vessels. No significant differences in the relationship between force generation and stretch in vehicle-treated and sRAGE-treated animals were observed ($p=0.143$), nor was any significant interaction between force and treatment observed ($p=0.702$). Statistical analysis was by LME model. (For vehicle-treated and sRAGE-treated mice, $n=7$; $n=11$ at force=1.2, 1.5 and 1.8mN; $n= 7$; $n=11$ at force=2.1mN; $n= 6$; $n=9$ and at force = 2.4mN.)

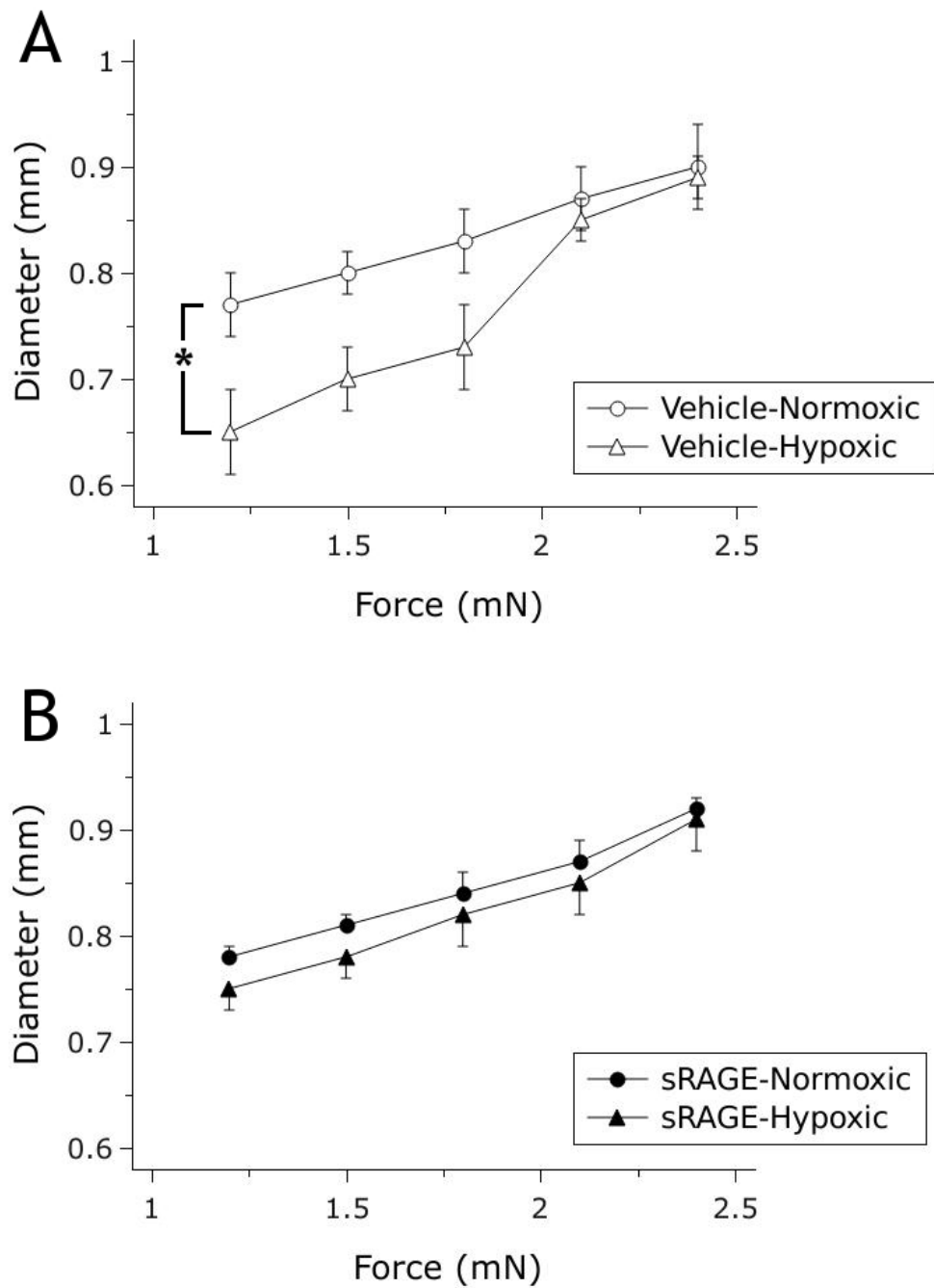


Figure 5.5 Vascular compliance is reduced by exposure to chronic hypoxia in vehicle-treated but not sRAGE-treated mice. (A) Compliance is significantly reduced in vehicle-treated mice exposed to 2 weeks hypoxia ($p<0.05$). (B) No such decrease was observed in hypoxic mice treated with sRAGE when compared to sRAGE-treated normoxic controls ($p=0.548$; interaction $p=0.708$). Despite these observations, comparison of vehicle and sRAGE treated animals exposed to hypoxia revealed no significant differences ($p=0.495$; interaction $p=0.620$). Statistical analysis was by LME model. * $p<0.05$; (For vehicle-normoxic, vehicle-hypoxia, sRAGE-normoxic and sRAGE hypoxic mice, n=7; 11; 11 and 7 at force=1.2, 1.5 and 1.8mN); n= 7; 7; 11 and 7 at force=2.1mN; n= 6; 6; 9 and 5 at force = 2.4mN.).

5.4.3 Responses to pharmacological agents

Intrapulmonary arteries were isolated from WT and MTS1 mice after the completion of *in vivo* measurements. Two rings were isolated from each lung. Experiments utilising 5HT were carried on one of these sections immediately while the other was kept in chilled buffer overnight for use in experiments involving U46619 and SNP. Responses to contractile agonists are represented as a percentage of responses to 50mM KCl except where otherwise stated.

A summary of E_{max} and EC_{50} values for all pharmacological agents studied in the current chapter may be found in Tables 5.1 and 5.2.

5.4.3.1 Responses to KCl

Exposure to 2 weeks of chronic hypoxia produced no significant alteration in the magnitude of contraction in response to 50mM KCl in vessels isolated from animals dosed with vehicle (Normoxic: 1.72 ± 0.22 mN; Hypoxic: 1.61 ± 0.10 mN) (Figure 5.6). While treatment with 20 μ g/day sRAGE alone did not produce any significant alteration in the magnitude of contraction in response to KCl (2.00 ± 0.29 mN) in these vessels, dosing with sRAGE and exposure to 2 weeks of hypoxia produced slightly less than a doubling of the magnitude of contraction. Analysis by Fisher's LSD test revealed that this increase was statistically significant in comparison to the response observed in vessels from normoxic, vehicle-treated mice ($p<0.01$), normoxic, sRAGE-treated mice ($p<0.05$) and hypoxic, vehicle-treated mice ($p<0.01$).

Agonist		Vehicle		sRAGE	
		Normoxic	Hypoxic	Normoxic	Hypoxic
5HT	E_{max} (% KCl)	126 ± 6	147 ± 6 *	114 ± 5	134 ± 5
	$\log EC_{50}$	-7.56 ± 0.21	-7.22 ± 0.14	-7.65 ± 0.11	-7.81 ± 0.09 §§
	n	4	4	5	4
U19	E_{max} (% KCl)	149 ± 16	177 ± 44	165 ± 19	148.72 ± 16
	$\log EC_{50}$	-7.22 ± 0.15	-8.29 ± 0.09 *	-7.30 ± 0.30	-8.23 ± 0.34 *
	n	3	2	2	2
SNP	E_{max} (% KCl)	N/A	80 ± 14	N/A	69 ± 14
	$\log EC_{50}$	-7.02 ± 0.4	-7.14 ± 0.40	-6.49 ± 0.43	-7.57 ± 0.37
	n	3	4	4	3

Table 5.1 Normalised E_{max} and EC_{50} values for responses to pharmacological agents in vehicle-treated and sRAGE-treated mice in normoxia and hypoxia. The maximum response to 5HT was augmented in hypoxic, vehicle-treated mice in comparison with normoxic controls when assessed as a percentage of previous contraction to KCl. This increase was not observed in sRAGE-treated animals. However, the concentration-response curve was shifted to the left in comparison to hypoxic vehicle-treated animals. When compared to normoxic, vehicle-treated mice, concentration-response curves to U46619 were significantly shifted to the left in hypoxic, vehicle-treated mice and sRAGE-treated mice. No other statistically significant changes were detected. Data are presented as mean ± SEM. * $p<0.05$ vs normoxic vehicle-treated animals; §§ $p<0.01$ vs. hypoxic vehicle-treated animals.

		Vehicle		sRAGE	
		Normoxic	Hypoxic	Normoxic	Hypoxic
5HT	E_{max} (mN)	2.37 ± 0.43	2.47 ± 0.24	2.28 ± 0.27	3.94 ± 0.57 †
	n	4	4	5	4
U19	E_{max} (mN)	3.55 ± 0.65	2.85 ± 0.80	3.86 ± 0.65	4.95 ± 1.13
	n	3	2	2	2

Table 5.2 Absolute E_{max} and EC_{50} values for responses to pharmacological agents in vehicle-treated and sRAGE-treated mice in normoxia and hypoxia. The maximal response to 5HT is increased in hypoxic, sRAGE-treated animals compared to normoxic animals receiving the same treatment when measured in terms of absolute force generated. No other statistically significant changes were observed. Data are presented as mean ± SEM. † $p<0.05$ vs normoxic sRAGE-treated animals.

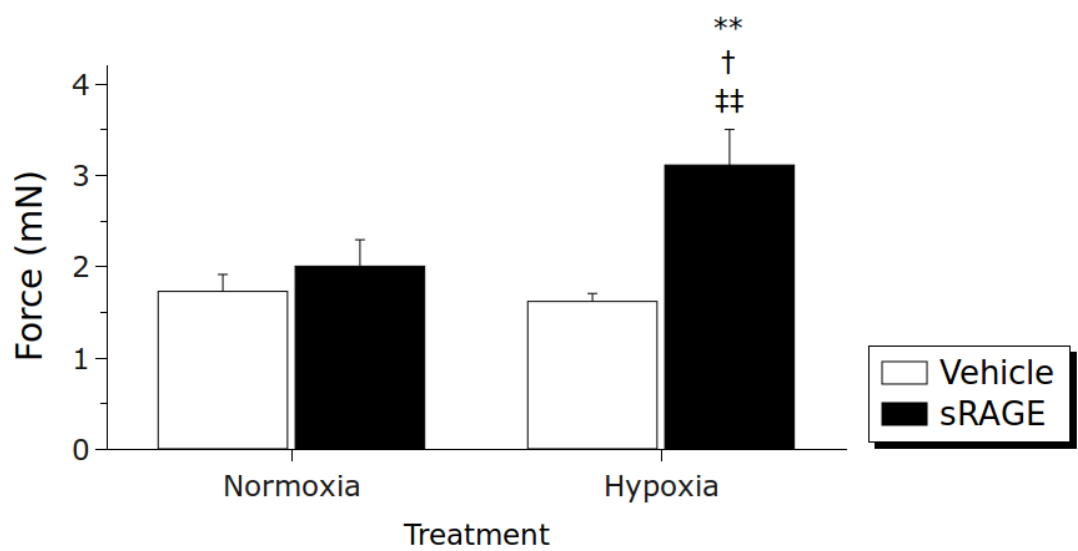


Figure 5.6 Treatment with sRAGE results in an increased force of contraction in response to 50mM KCl in intrapulmonary arteries isolated from animals exposed to hypoxia. ** $p < 0.01$ vs normoxic vehicle-treated mice; † $p < 0.05$ versus normoxic sRAGE-treated mice; ‡‡ $p < 0.01$ versus hypoxic vehicle-treated mice. Data are presented as mean \pm SEM. Statistical analyses were by one-way ANOVA followed by Fisher's LSD test. (Vehicle Normoxic: n=6; Vehicle Hypoxic: n=6; sRAGE Normoxic: n=7 sRAGE hypoxic: n=6).

5.4.3.2 Responses to 5HT

Responses of IPAs isolated from vehicle-treated normoxic animals were qualitatively and quantitatively similar to those observed in the previous chapter (Figure 5.7). Analysis by LME model revealed no significant difference between the responses of vessels in each study group ($p=0.561$) and no significant interaction between study group and the concentration of 5HT ($p=0.617$).

When examining the differences between normalised responses, analysis by LME model revealed no significant differences in the responses of vessels from vehicle and sRAGE treated animals to 5HT ($p=0.204$) and no significant interaction between treatment and the concentration of 5-HT ($p=0.189$). Similarly, no statistically significant differences in E_{max} (Vehicle: $126 \pm 6\%$; sRAGE: $114 \pm 5\%$) or EC_{50} (Vehicle: -7.56 ± 0.21 ; sRAGE: -7.65 ± 0.11) were detected. When concentration-responses curves to 5HT were examined in terms of the absolute force generated, the E_{max} was 2.37 ± 0.43 mN in vessels from normoxic vehicle-treated animals and 2.28 ± 0.27 in vessels from normoxic sRAGE-treated animals. These values were not significantly different. No significant effect of sRAGE treatment ($p=0.780$) and no significant interaction between sRAGE treatment and concentration ($p=0.747$) were observed on analysis by LME model.

Exposure to two weeks hypoxia produced concentration-response curves to 5HT which were augmented to a lesser degree than in the previous study, though the mean E_{max} value appeared augmented above those of vessels from normoxic animals. Analysis by LME model detected no significant difference in overall response ($p=0.854$) and no significant interaction between concentration and the hypoxic stimulus ($p=0.786$) (Figure 5.8A). The mean E_{max} was significantly increased to $147 \pm 6\%$ ($p<0.05$) by 2 weeks exposure to hypoxia. EC_{50} was not

significantly altered in vessels isolated from vehicle-treated mice exposed to 2 weeks hypoxia (-7.22 ± 0.14).

In contrast to normalised responses, responses considered in terms of absolute force of contraction appeared unaltered by exposure to 2 weeks hypoxia (Figure 5.9A). Analysis by LME model revealed no difference in these responses due to either hypoxia ($p=0.557$) or an interaction between hypoxia and concentration ($p=0.815$). Similarly, absolute E_{max} in vessels from hypoxic, vehicle-treated animals was unchanged from normoxic animals at 2.47 ± 0.24 mN ($p>0.05$).

The response to 5HT in vessels isolated from mice exposed to 2 weeks of hypoxia and treated with 20 μ g/day sRAGE appeared augmented in comparison to normoxic, sRAGE-treated mice, however this difference did not achieve significance (Figure 5.8B; $p=0.327$; LME model) and nor was there any significant interaction between sRAGE treatment and the concentration of 5HT ($p=0.565$). E_{max} and $\log EC_{50}$ values for responses in vessels isolated from mice in the hypoxic, sRAGE-treated group vessels did not differ significantly from vessels from normoxic, sRAGE-treated animals ($E_{max} = 134 \pm 5\%$; $EC_{50}: -7.81 \pm 0.09$). Responses in vessels from hypoxic, sRAGE treated animals were not significantly different from those of normoxic, vehicle-treated animals ($p=0.696$; interaction $p=0.940$). Direct comparison by LME model of concentration-response curves to 5HT in hypoxic sRAGE-treated and vehicle-treated animals revealed no significant difference ($p=0.858$; interaction $p=0.858$). However, $\log EC_{50}$ was significantly altered in vessels from hypoxic sRAGE-treated mice compared to those from hypoxic vehicle treated mice ($p<0.01$).

When responses in these vessels were considered in terms of absolute force, responses in vessels from normoxic animals treated with sRAGE were

significantly altered compared to vessels from sRAGE-treated animals exposed to hypoxia ($p<0.05$; Figure 5.9B) with a significant interaction between exposure to hypoxia and the concentration of 5HT ($p<0.05$). E_{max} values in vessels from hypoxic sRAGE-treated animals were significantly elevated above their normoxic counterparts ($E_{max} = 3.94 \pm 0.57\text{mN}$; $p<0.05$). Responses in vessels from hypoxic sRAGE-treated were also significantly different from those in normoxic, vehicle-treated mice ($p<0.01$; interaction $p<0.01$) and from those in hypoxic, vehicle-treated mice ($p<0.05$; interaction $p=0.1154$).

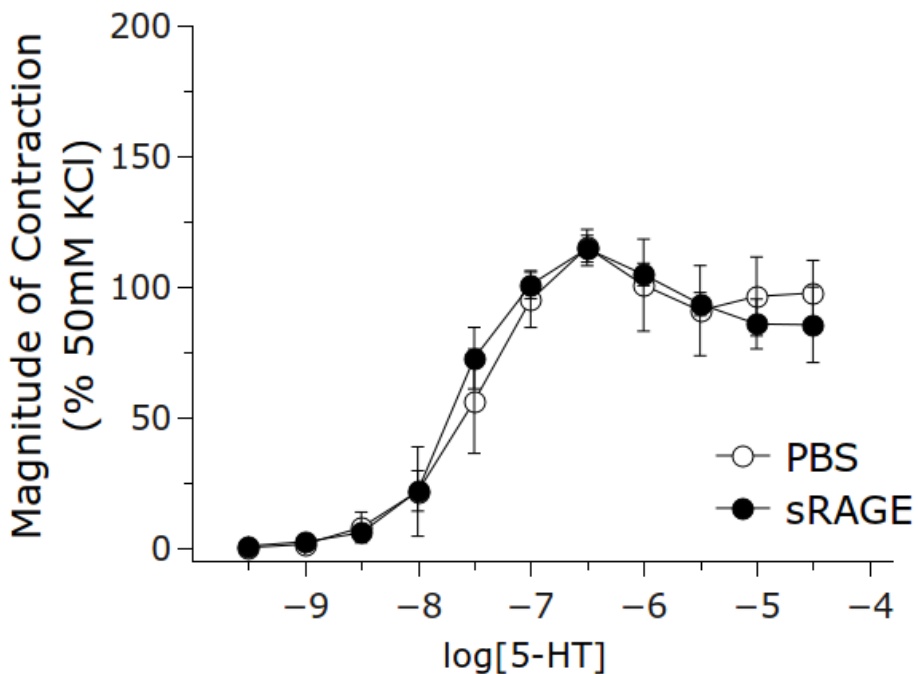


Figure 5.7 Treatment with soluble RAGE has no effect on the response to 5HT in vessels isolated from normoxic mice compared to vehicle-dosed controls. Analysis by LME model revealed no significant differences in the response of vessels from vehicle and sRAGE treated animals to 5HT ($p=0.204$) and no significant interaction between treatment and the concentration of 5-HT ($p=0.189$). Similarly, no statistically significant differences in E_{max} (Vehicle: $126 \pm 6\%$; sRAGE: $114 \pm 5\%$) or EC_{50} (Vehicle: -7.56 ± 0.21 ; sRAGE: -7.65 ± 0.11) were detected. Data are expressed as mean \pm SEM. (Vehicle: n=4; sRAGE: n=5).

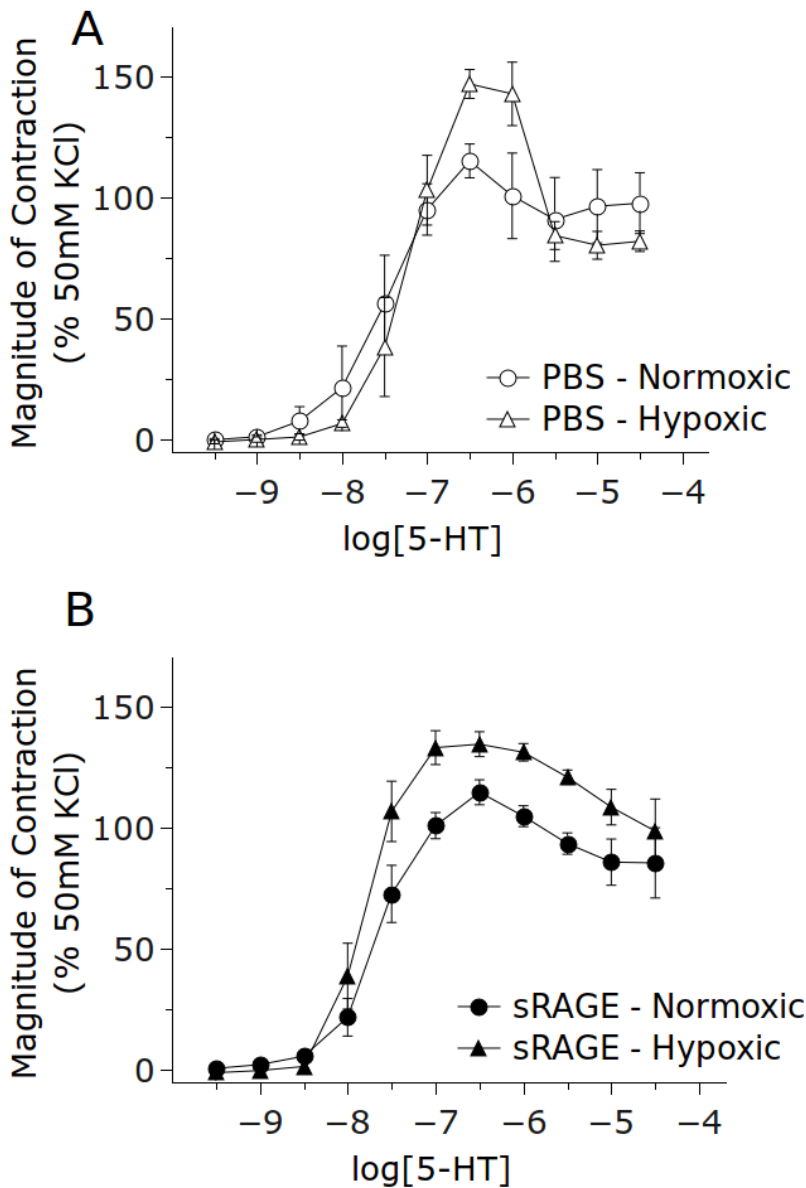


Figure 5.8 Effects of sRAGE treatment on 5HT-induced contraction in normoxia and hypoxia. (A) In vessels isolated from vehicle-treated mice, analysis by LME model detected no significant difference in overall response ($p=0.854$) and no significant interaction between concentration and the hypoxic stimulus ($p=0.786$). Mean E_{max} was significantly increased $146.63 \pm 5.93\%$ ($p<0.05$) by 2 weeks exposure to hypoxia and EC_{50} unaltered by hypoxia (-7.22 ± 0.14). (B) The response to 5HT in vessels isolated from hypoxic, sRAGE-treated mice appeared augmented in comparison to normoxic, sRAGE-treated mice but did not achieve significance ($p=0.327$; LME model) nor was there any significant interaction between sRAGE treatment and [5HT] ($p=0.565$). E_{max} and EC_{50} of responses in vessels from hypoxic, sRAGE-treated mice were unchanged from normoxic mice (E_{max} : $134.27 \pm 5.13\%$; EC_{50} : -7.81 ± 0.09) and there was no evidence of a difference in these concentration-response curves ($p=0.696$; interaction $p= 0.940$). (Vehicle Normoxic: n=4; Vehicle Hypoxic: n=4; sRAGE Normoxic: n=5 sRAGE hypoxic: n=4).

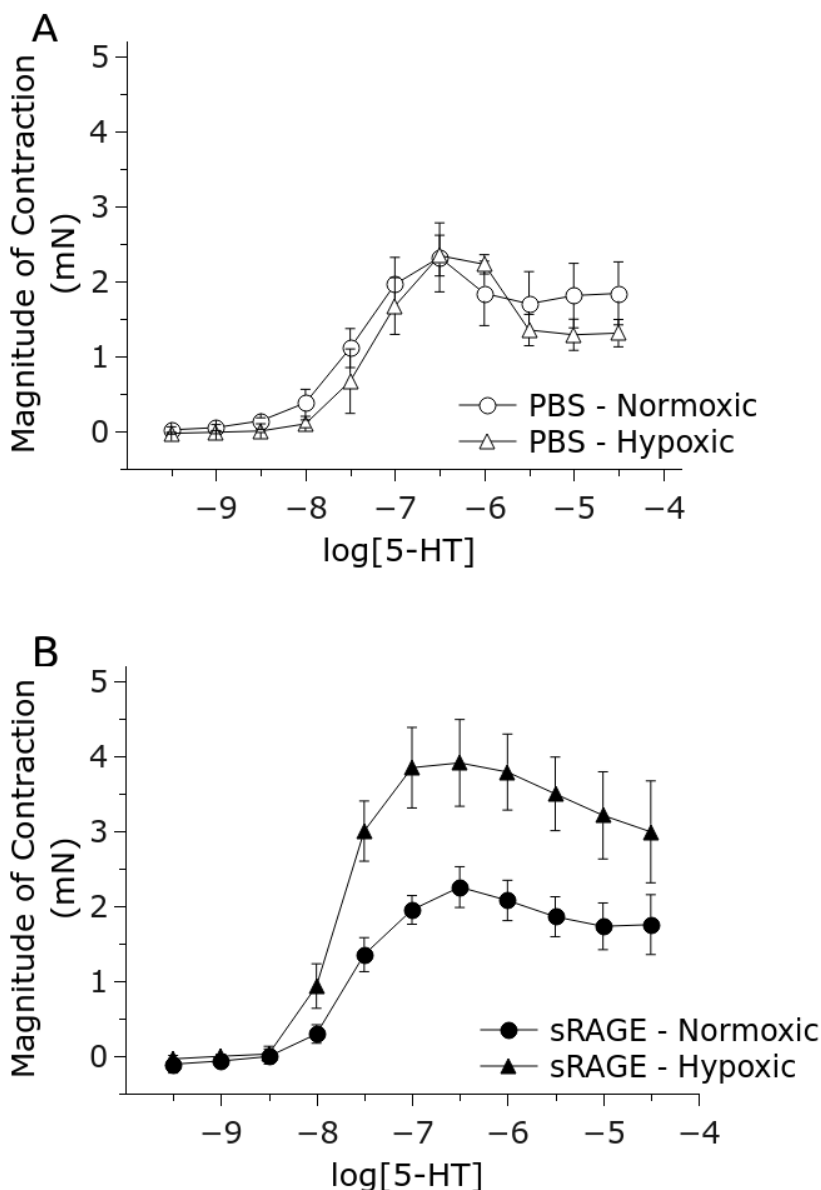


Figure 5.9 Effects of sRAGE treatment on the absolute force of contraction in response to 5HT in normoxia and hypoxia. (A) Hypoxia produced no alteration in the concentration-response curve to 5HT in vessels from vehicle-treated animals ($p=0.780$) nor was any interaction between concentration and sRAGE treatment detected ($p=0.747$). (B) Responses in vessels treated with sRAGE were significantly altered by hypoxia ($p<0.05$) with a significant interaction between exposure to hypoxia and the concentration of 5HT ($p<0.05$). Responses in vessels from hypoxic sRAGE-treated were also significantly different from those in normoxic, vehicle-treated mice ($p<0.01$; interaction $p<0.01$) and from those in hypoxic, vehicle-treated mice ($p<0.05$; interaction $p=0.1154$). E_{max} in hypoxic, sRAGE treated vessels was significantly increased in comparison to hypoxic, vehicle treated mice ($p<0.05$) but not normoxic, vehicle-treated or sRAGE-treated vessels. Data are expressed as mean \pm SEM. Analysis was by LME model. (Vehicle Normoxic: n=4; Vehicle Hypoxic: n=4; sRAGE Normoxic: n=5 sRAGE hypoxic: n=4).

5.4.3.3 Responses to U46619

Due to the limited number of available mice for the current study, n values for experiments involving U46619 were low (2-3) limiting the utility of statistical analyses and the data as a whole. However, the results are included here in the interests of completeness and discussion.

Dose responses to U46619 in vessels isolated from normoxic, vehicle-treated mice were sigmoidal in form (Figure 5.10) and did not differ from mice of the control group in the previous study ($p=0.646$; LME model). The mean E_{max} of these responses was $149 \pm 16\%$ and the mean EC_{50} was -7.22 ± 0.15 . Neither of these values was significantly altered in comparison to the previous study.

Treatment with 20 μ g/day sRAGE produced no significant overall alteration in the response to the normalised response to U46619 (Figure 5.11; $p=0.481$; LME model) and no significant interaction between concentration and sRAGE treatment ($p=0.468$; LME model). The mean E_{max} and EC_{50} values were similarly unchanged ($E_{max}: 165 \pm 19\%$; $EC_{50}: -7.30 \pm 0.30$) (Figure 5.11). When responses were considered in terms of absolute force, no difference in the absolute concentration-response curve to U46619 was detected in normoxic sRAGE-treated mice compared with vehicle-treated controls ($p=0.423$) nor was any significant interaction between sRAGE treatment and the concentration of U46619 observed ($p=0.414$) (Figure 5.12). Absolute E_{max} values were unchanged between vessels from normoxic vehicle-treated mice and normoxic sRAGE-treated mice (vehicle: $E_{max} = 3.55 \pm 0.65$; sRAGE: $E_{max} = 3.86 \pm 0.65$; $p>0.05$).

Concentration-response curves to U46619 obtained in vessels isolated from animals exposed to 2 weeks of hypoxia appeared shifted to the left in both vehicle-treated and sRAGE-treated animals (Figure 5.11). However, analysis by

LME model did not detect any significant effects of hypoxia (Vehicle: $p=0.433$; sRAGE: $p=0.863$) nor any significant interaction between hypoxia and the concentration of U46619 (Vehicle: $p=0.956$; sRAGE: $p=0.530$). Similarly, no increase in E_{max} was detected in the response of vessels of either treatment group after hypoxia (Vehicle: $177 \pm 44\%$; sRAGE: $149 \pm 16\%$). LogEC₅₀ of responses to U46619 in vessels isolated from hypoxic, vehicle-treated mice was significantly shifted in comparison to normoxic animals receiving the same treatment (-8.29 ± 0.09 ; $p<0.05$). Though the logEC₅₀ of responses in vessels from hypoxic, sRAGE-treated animals was not significantly different from normoxic, sRAGE treated animals (-8.23 ± 0.34), this was significantly different from normoxic, vehicle-treated animals ($p<0.05$). Analysis by LME model did not produce evidence of a difference between responses of hypoxic, sRAGE-treated animals and normoxic, vehicle-treated animals, however ($p=0.619$; interaction $p=0.9259$). Direct comparison of concentration-responses in vessels from hypoxic, vehicle-treated mice and hypoxic, sRAGE-treated mice revealed no significant differences ($p=0.813$; interaction $p=0.908$).

When responses were considered in terms of absolute force, responses to U46619 in vessels from vehicle-treated animals displayed no significant change associated with exposure to hypoxia (Figure 5.12A; $p=0.182$). However, a statistically significant interaction between hypoxia and concentration was found ($p=0.048$), consistent with a lateral shift in the concentration-response relationship. The absolute E_{max} of responses to U46619 in vessels from animals exposed to hypoxia appeared mildly reduced in comparison to that of normoxic mice, but this change was not significant ($E_{max} = 2.85 \pm 0.80\text{mN}$).

In vessels from sRAGE-treated mice exposed to hypoxia, the absolute E_{max} of the response to U46619 appeared increased but was not significantly altered

(Figure 5.12B; $E_{max} = 4.95 \pm 1.13\text{mN}$). The effect of hypoxia in vessels from mice treated with sRAGE approached but did not achieve significance in comparison to responses in vessels from normoxic sRAGE-treated mice ($p=0.073$) while a significant interaction between exposure to hypoxia and the concentration of U46619 was found ($p<0.05$). Similarly, concentration responses in vessels from hypoxic, sRAGE treated animals were significantly altered in comparison to those of normoxic, vehicle-treated animals ($p<0.05$; interaction $p<0.05$). A direct comparison of responses from vessels isolated from hypoxic, vehicle-treated and hypoxic, sRAGE-treated vehicles approached significance ($p=0.057$) with a significant interaction between [U46619] and hypoxia ($p<0.01$).

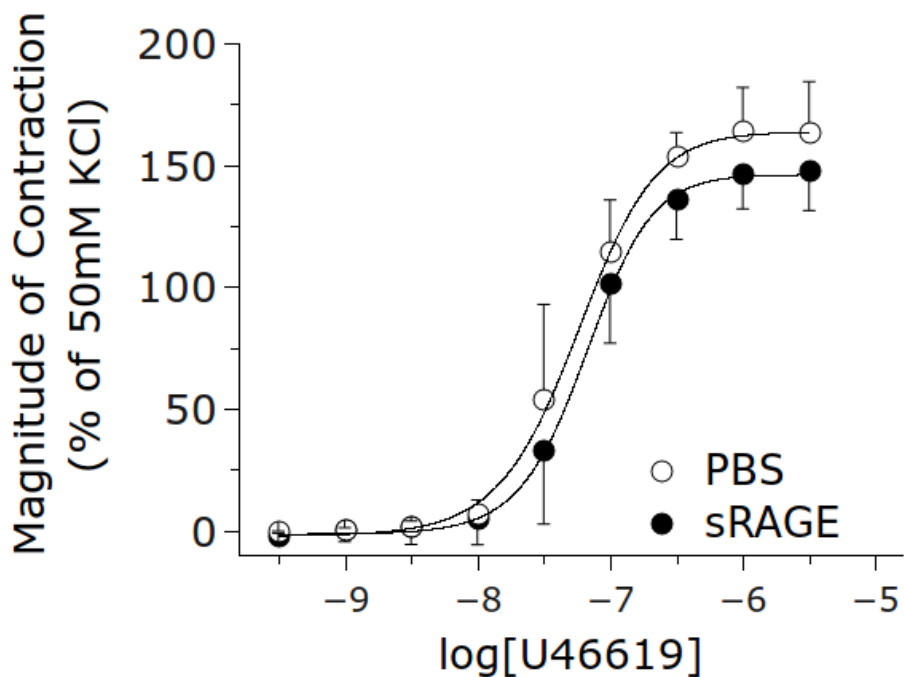


Figure 5.10 Concentration-response curves to U46619 are not altered by treatment with 20 μ g/day IP sRAGE. Treatment with 20 μ g/day sRAGE produced no significant overall alteration in the response to U46619 ($p=0.481$; LME model) and no significant interaction between concentration and sRAGE treatment ($p=0.468$; LME model). The mean E_{max} and EC_{50} values were similarly unchanged ($E_{max}: 165 \pm 20\%$; $EC_{50}: -7.30 \pm 0.30$). (n=2-3). Data are expressed as mean \pm SEM. (Vehicle n=3; sRAGE: n=2).

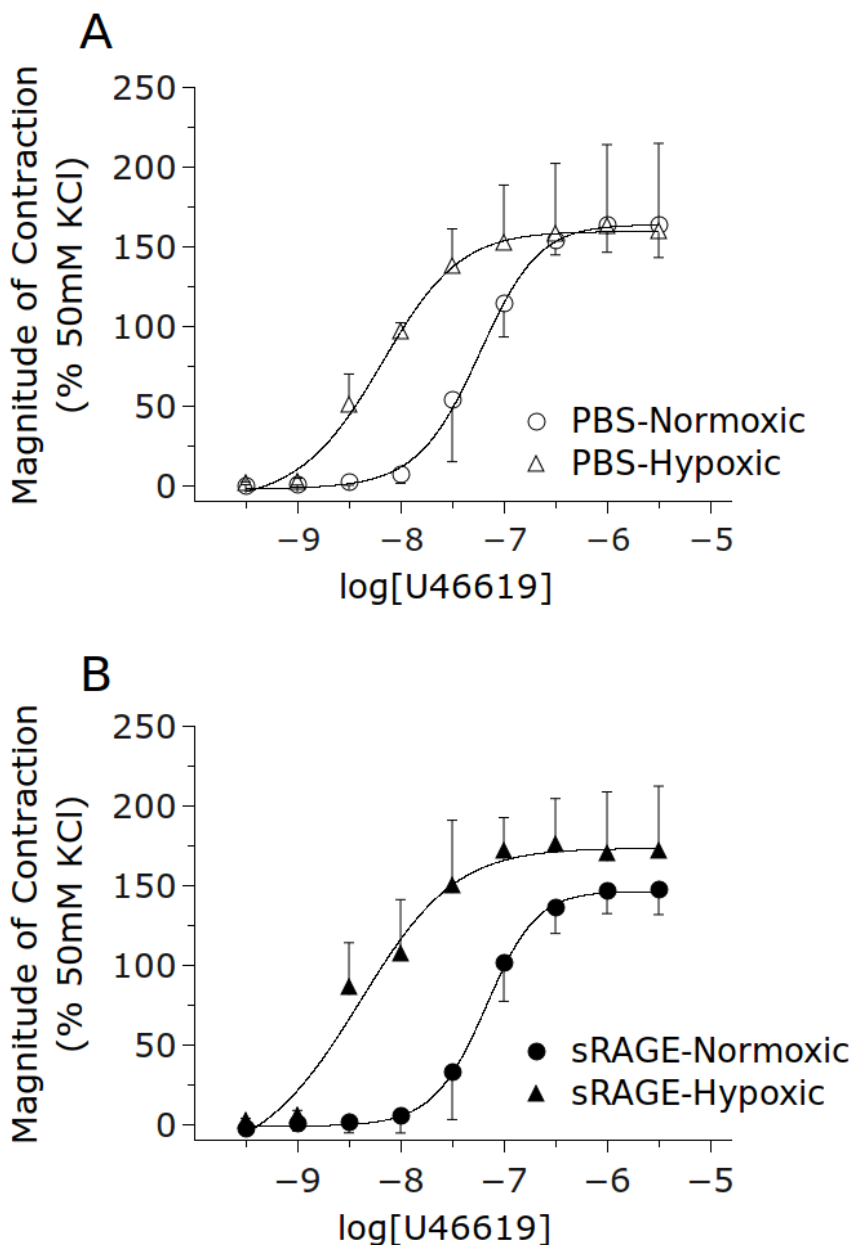


Figure 5.11 Chronic-hypoxia appears to increase sensitivity of intrapulmonary arteries to U46619 in vessels isolated from animals receiving 20 μ g/day sRAGE or vehicle. No significant effects of hypoxia ((A) Vehicle: $p=0.433$; (B) sRAGE: $p=0.863$) nor any significant interaction between hypoxia and the concentration of U46619 (Vehicle: $p=0.956$; sRAGE: $p=0.530$) were observed. Similarly, no increase in E_{max} was detected in the response of vessels of either treatment group after hypoxia (Vehicle: $176.93 \pm 43.83\%$; sRAGE: $148.72 \pm 15.95\%$). EC₅₀ of responses to U46619 in vessels isolated from hypoxic, vehicle-treated mice was significantly shifted in comparison to normoxic animals receiving the same treatment (-8.29 ± 0.09 ; $p<0.05$). This was not the case for hypoxic, sRAGE-treated animals (-8.23 ± 0.34). Data are expressed as mean \pm SEM. (Vehicle Normoxic: n=3; sRAGE normoxic: n=2; Vehicle Hypoxic: n=2 sRAGE hypoxic: n=2).

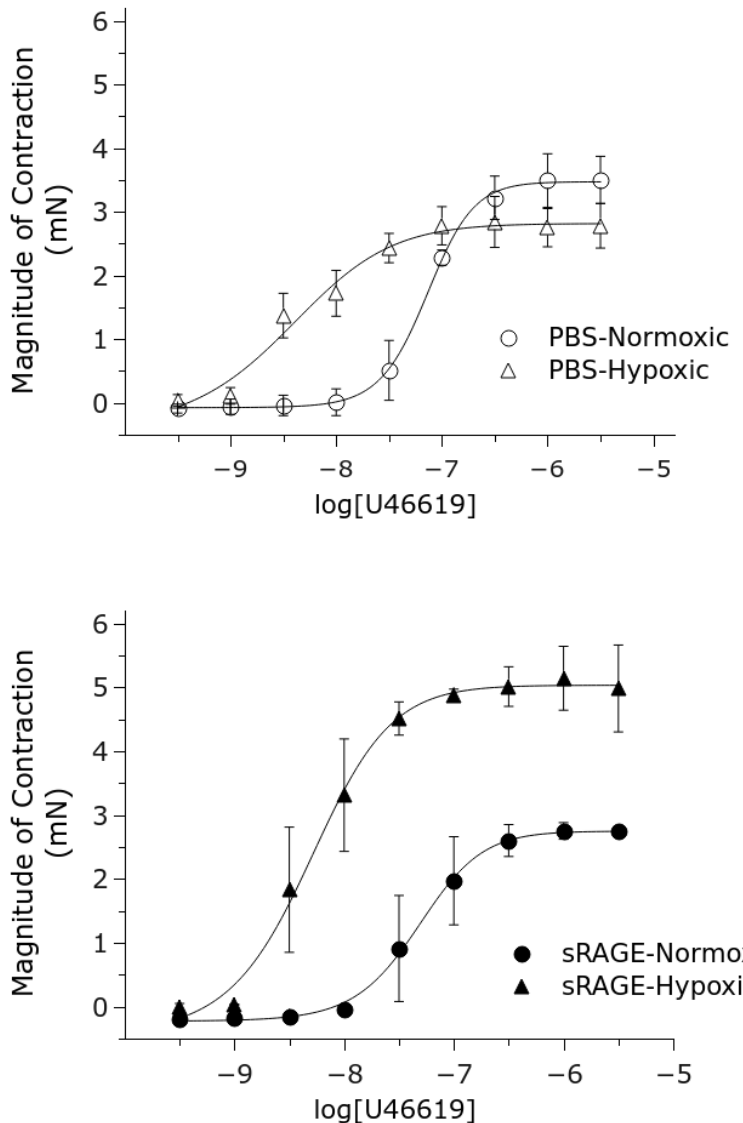


Figure 5.12 Effects of sRAGE treatment on the absolute force of contraction in response to U46619 in normoxia and hypoxia. (A) Responses to U46619 in vessels from vehicle-treated animals displayed no significant change associated with exposure to hypoxia ($p=0.182$). However, a statistically significant interaction between hypoxia and concentration was found ($p=0.048$), consistent with a lateral shift in the concentration-response relationship. (B) The effect of hypoxia on responses in vessels treated with sRAGE approached but did not achieve significance ($p=0.073$) while a significant interaction between exposure to hypoxia and the concentration of U46619 was found ($p<0.05$). Responses in vessels from hypoxic, sRAGE treated animals were significantly altered in comparison to those of normoxic, vehicle-treated animals ($p<0.05$; interaction $p<0.05$). Responses in vessels isolated from hypoxic, vehicle-treated and hypoxic, sRAGE-treated vehicles approached significance ($p=0.057$) with a significant interaction between [U46619] and hypoxia ($p<0.01$). Data are expressed as mean \pm SEM. Analysis was by LME model. (Vehicle Normoxic: n=3; Vehicle Hypoxic: n=2; sRAGE normoxic: n=2; sRAGE hypoxic: n=2).

5.4.3.4 Responses to SNP

Administration of ascending concentrations of SNP to vessels isolated from normoxic, vehicle-treated animals in the current study produced a less impressive relaxation than was observed in vessels from control mice in the previous study, possibly due to the necessity of storing vessels overnight before the construction of concentration-response curves. This was statistically verifiable in that a comparison of normoxic responses in the current study with those of the previous study by LME model revealed both a significant effect of study group ($p<0.001$) and a significant interaction between study group and the concentration of SNP ($p<0.001$).

In the current study, treatment with 20 μ g/day sRAGE produced no observable effect upon the relaxatory response of vessels to SNP (Figure 5.13). Statistical analysis by LME model revealed no significant effect of either sRAGE treatment ($p=0.5574$) and no significant interaction between sRAGE treatment and the concentration of SNP ($p=0.606$).

Furthermore, analysis by LME model revealed no significant effect of hypoxia and no significant interaction between hypoxia and the concentration of SNP in vessels isolated from either vehicle-treated ($p=0.830$; $p=0.889$) or sRAGE-treated animals ($p =0.516$; $p=0.118$) (Figure 5.14) in comparison to normoxic animals receiving the same treatments. A statistically significant interaction between [SNP] and the hypoxic stimulus was observed on comparison of responses in vessels from hypoxic, sRAGE-treated mice to those of normoxic, vehicle-treated mice ($p=0.294$; interaction $p<0.05$). A direct comparison of responses in vessels from hypoxic, vehicle-treated mice and those of hypoxic, sRAGE treated mice showed no significant differences though the interaction

term approached significance ($p=0.277$; interaction $p=0.081$). It is worth noting that responses in vessels from both vehicle-treated and sRAGE-treated hypoxic mice appeared to reach a maximum value within the range of concentrations of SNP studied here (Vehicle: $E_{max} = 80 \pm 14\%$; sRAGE: $E_{max} = 69 \pm 14\%$) (Figure 5.14). Conversely, responses in vessels isolated from normoxic animals appeared still to be increasing at the maximum concentration utilised. This suggests that hypoxia may have reduced the maximal relaxatory response of hypoxic vessels to SNP. However, in the absence of E_{max} values for normoxic responses, a quantitative comparison is not possible.

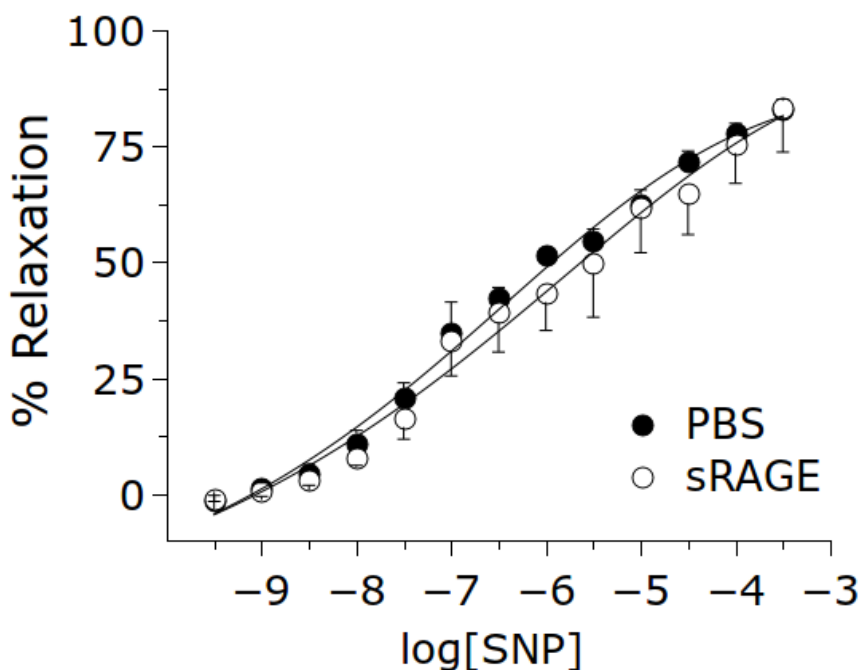


Figure 5.13 Administration of 20 μ g/day sRAGE produced no alteration in the concentration-response to SNP. Statistical analysis by LME model revealed no significant effect of sRAGE treatment ($p=0.557$) and no significant interaction between sRAGE treatment and the concentration sRAGE of SNP ($p=0.606$). Data are expressed as mean \pm SEM. (Vehicle: n=3; sRAGE: n=4).

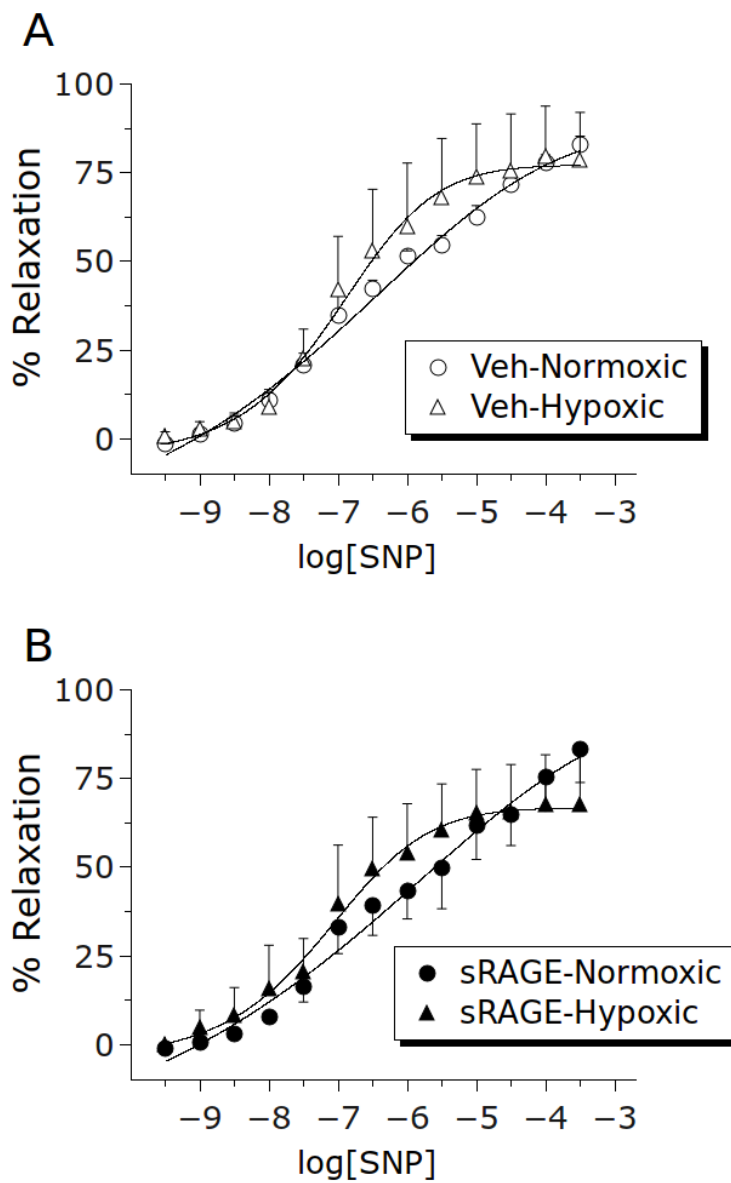


Figure 5.14 Responses to SNP in vessels isolated from mice treated with 20 μ g/day sRAGE or vehicle. Relaxatory responses to SNP did not reach a maximum in vessels from vehicle-treated nor sRAGE-treated animals in a normoxic environment, preventing the calculation of meaningful E_{max} or $\log EC_{50}$ values. Responses in vessels from animals exposed to chronic hypoxia appeared to plateau at a maximum value which was lesser in magnitude than the maximum observed value in normoxic animals. This appeared true for vessels for both vehicle-treated and sRAGE-treated animals, suggesting that the maximal relaxation to SNP is blunted in these vessels. However, with no data on the maximum responses in the other two treatment groups, a quantitative comparison to ascertain this is not possible. As the data stand, no statistically significant effect of hypoxia, or interaction between hypoxia and concentration, upon the concentration-response curve was detected in either treatment group (Vehicle: $p=0.830$; $p=0.889$; sRAGE: $p=0.516$; $p=0.118$). Data are expressed as mean \pm SEM and analysis was by LME model. (Vehicle Normoxic: $n=3$; Vehicle Hypoxic: $n=4$; sRAGE Normoxic: $n=4$; sRAGE Hypoxic: $n=3$).

5.4.3.5 Acute affects of sRAGE in isolated intrapulmonary arteries

Since treatment with 20 μ g/day sRAGE in conjunction with exposure to chronic hypoxia for two weeks produced an overall increase in the magnitude of contraction observed in response to several contractile stimuli, it was of interest to observe the acute effects of sRAGE upon the contractile response of intrapulmonary arteries in the myograph. The volume of fluid in the myograph was reduced to 3ml and the water level raised with the aid of some space-occupying K-nex \circledC bricks.

In intrapulmonary vessels isolated from C57BL/6 mice, treatment with 10 μ g/ml sRAGE produced a small, sustained contraction reaching a maximum at approximately 30 minutes (Figure 5.15). This contraction had a mean magnitude of 0.31 ± 0.07 mN: equal to $15 \pm 1\%$ as a percentage of the observed response to KCl (Figure 5.16). Analysis by two-sample t-test revealed that this elevation was statistically significant when compared to the mean response of vessels treated with vehicle. Responses in vessels treated with vehicle did not deviate significantly from zero (0.04 ± 0.045 mN; $2 \pm 2\%$; $p=0.389$; one-sample t-test).

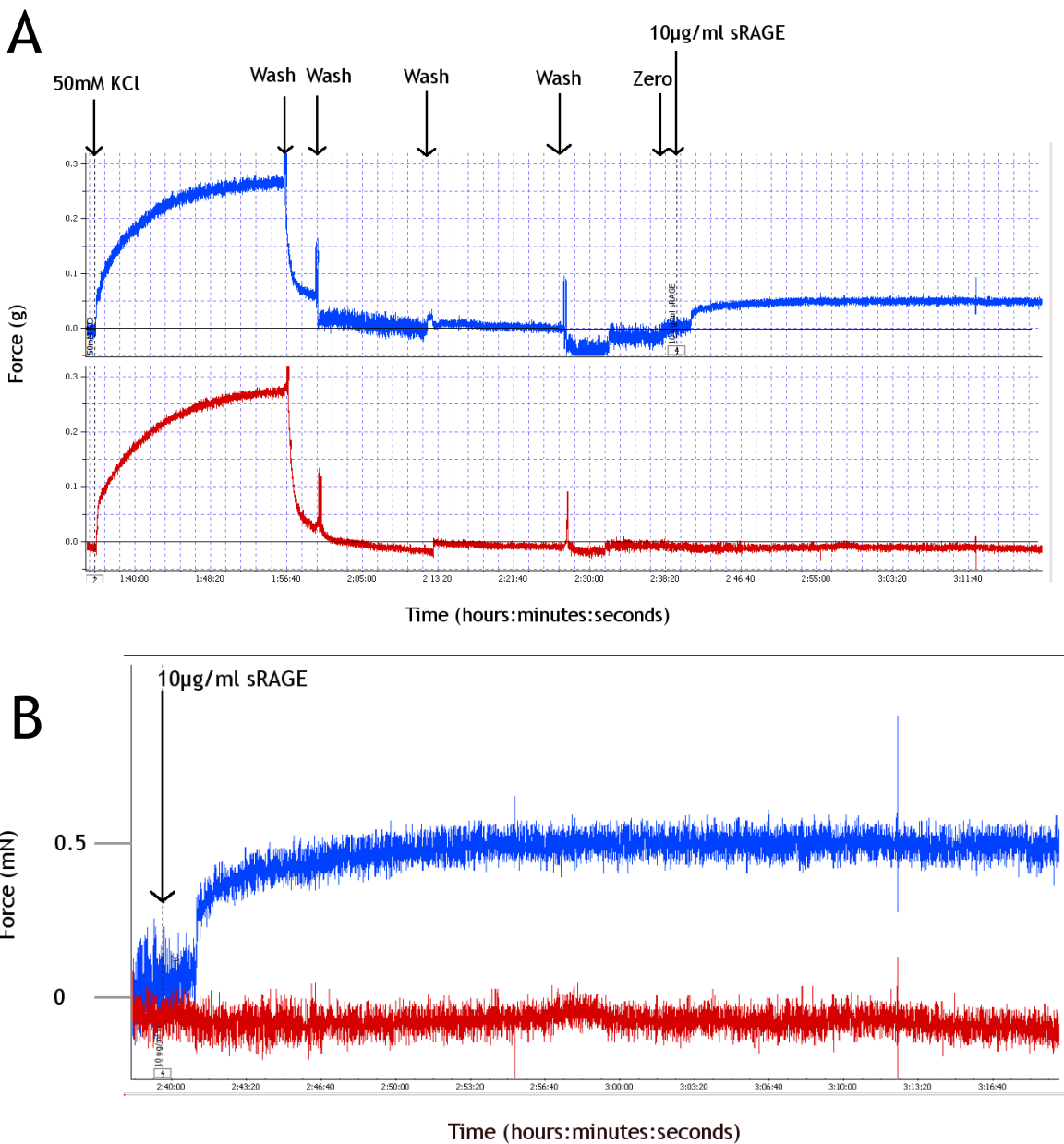


Figure 5.15 Representative myography traces displaying increased generation of force with time in response to sRAGE. (A) Screen capture of a single experiment showing traces from two vessel segments. The addition of 50mM KCl followed by multiple washes (*i.e.* replacement of buffer in the myograph) and a resetting of the baseline (Zero) are displayed followed by the addition of 10 μ g/ml sRAGE in the top trace only. (B) A trace from the same experiment showing the response to 10 μ g/ml sRAGE (upper trace) in more detail. Addition of 10 μ g/ml sRAGE to the myograph resulted in increased force generation in murine intrapulmonary vessels.

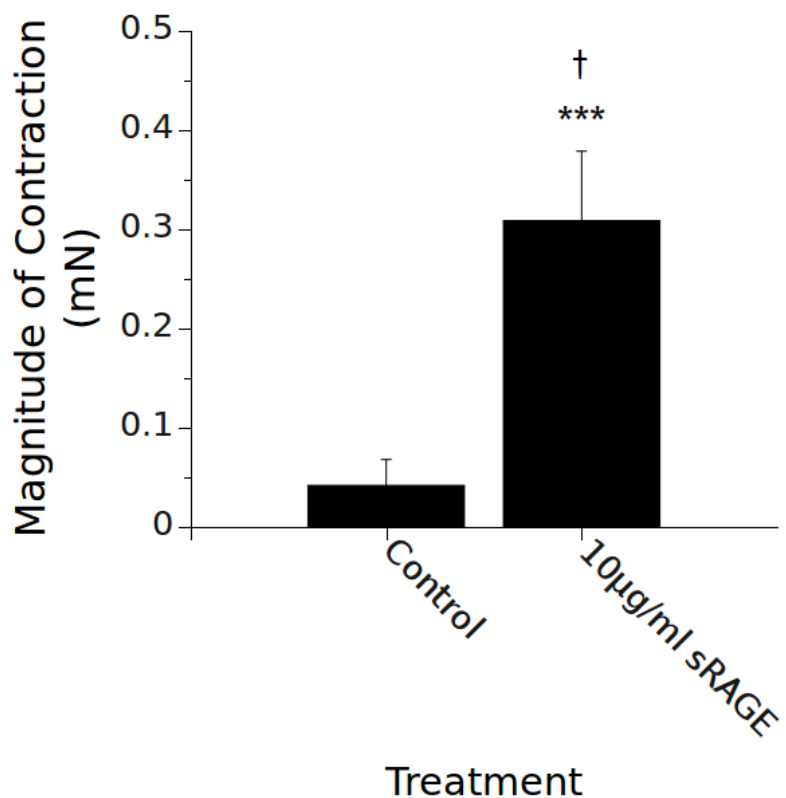


Figure 5.16 Treatment with sRAGE results in the generation of contractile force in isolated intrapulmonary arteries. * $p<0.001$ vs zero, † $p<0.05$ vs Control Data are expressed as mean \pm SEM. (Control: n=5; sRAGE: n=4).**

5.4.3.6 Responses to 5HT: effects of sRAGE treatment

Since sRAGE had previously been shown to modulate the proliferative response of PASMCs to 5HT by preventing the interaction of MTS1/S100A4 with RAGE (Lawrie et al., 2005), and since chronic hypoxia in conjunction with sRAGE treatment *in vivo* altered vascular contractility directly, it was of interest to see if the concentration-response curve to 5HT in pulmonary arteries was altered in the presence of sRAGE.

Preincubation with 10 μ g/ml sRAGE produced a concentration response curve to 5HT which appeared to reach a higher maximal contraction in comparison to vessels incubated with PBS vehicle (Figure 5.17). Analysis by LME model revealed a highly significant effect of sRAGE treatment ($p<0.001$) and an interaction between sRAGE treatment and the concentration of 5HT which approached significance ($p=0.054$). Despite this, the E_{max} was not significantly altered in these responses when compared to control (Vehicle: 0.250 ± 0.033 mN; sRAGE: 0.317 ± 0.037 , $p=0.223$). In sRAGE-treated vessels, EC_{50} also approached a significant change (Vehicle: -7.62 ± 0.16 ; sRAGE: -7.19 ± 0.09 ; $p=0.058$).

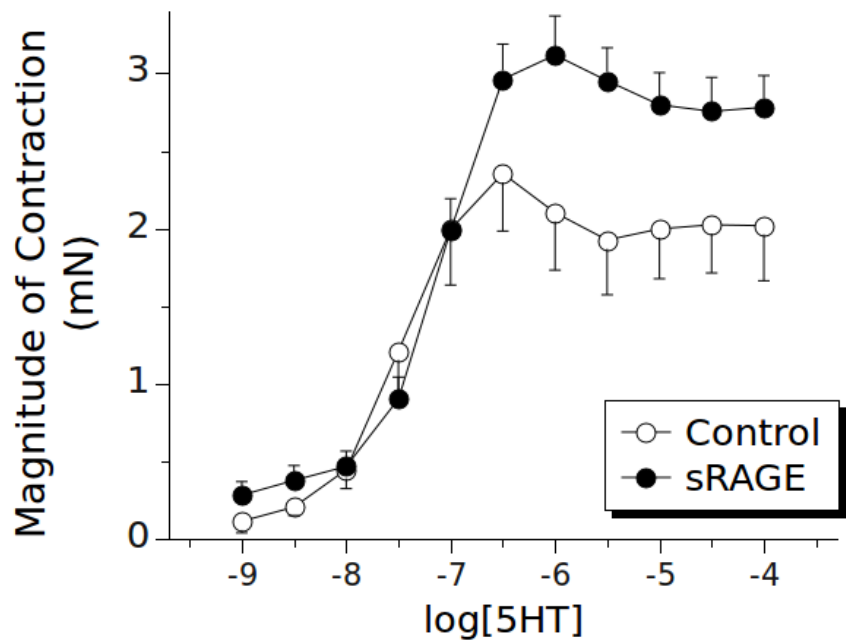


Figure 5.17 Preincubation with 10 μ g/ml sRAGE augments the contractile response to 5HT. Contractile responses to 5HT were significantly augmented by preincubation with 10 μ g/ml sRAGE. A significant effect of sRAGE treatment was detected ($p<0.001$). An interaction between the concentration of 5HT and sRAGE treatment tended towards significance ($p=0.054$). Data are presented as mean \pm SEM. Analyses were by LME model. (Control: n=5; sRAGE: n=4).

5.4.4 Cellular proliferation

5.4.4.1 5HT-induced increases in cell number

Incubation with 0.1 μ M 5HT for 24 hours produced a statistically significant increase in cell number of 57 \pm 23% ($p<0.01$; linear model). Ascending concentrations of 5HT appeared to produce a biphasic increase in cell number (Figure 5.18: with 1 μ M 5HT producing an increase of 77 \pm 18% above baseline ($p<0.001$; linear model) increasing with concentration to a mean maximum of 88 \pm 17% above baseline numbers ($p<0.001$; linear model) at 10 μ M before decreasing again at 100 μ M (32 \pm 8%; $p=0.104$; linear model)).

5.4.4.2 Effects of sRAGE upon 5HT-induced increases in cell number

As the dose producing the largest increase in cell number, 10 μ M 5HT was subsequently used to investigate the effects of sRAGE incubation upon 5HT-induced increases in cell number.

Treatment with 2.5 μ g/ml sRAGE did not inhibit the increase in cell number produced by treatment with 10 μ M 5HT (62.60 \pm 14.61%: 10 μ M 5HT; 50.83 \pm 19.41%: 10 μ M 5HT + 2.5 μ g/ml sRAGE) (Figure 5.19). Both treatments produced a statistically significant increase in cell number above that observed at baseline. Interestingly, 2.5 μ g/sRAGE alone produced a modest increase in cell number to 31.90 \pm 8.12% ($p<0.01$; linear model). Analysis by Fisher's LSD test detected no significant differences between the responses to 10 μ M 5HT, 2.5 μ g/ml sRAGE or 10 μ M 5HT + 2.5 μ g/ml sRAGE after correction of p -values to account for multiple comparisons.

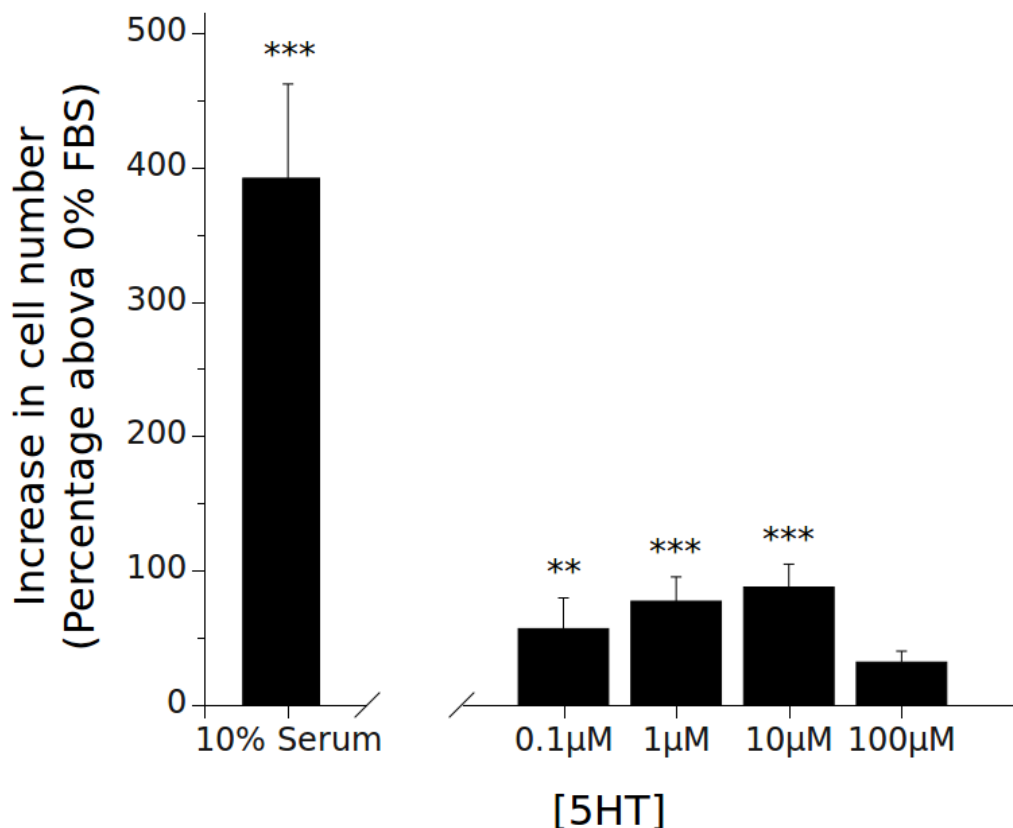


Figure 5.18 5HT produces an increase in cell number in CCL39 Chinese hamster lung fibroblasts. The proliferative response of these cells to increasing concentrations of 5-HT was biphasic in nature: increasing to a maximum of $88 \pm 17\%$ at $10\mu\text{M}$ before decreasing again at $100\mu\text{M}$. Data are expressed as mean percentage increase above baseline (0% FBS) \pm SEM. Analyses were by linear model. ** $p < 0.01$, *** < 0.001 vs. baseline. ($n=3$)

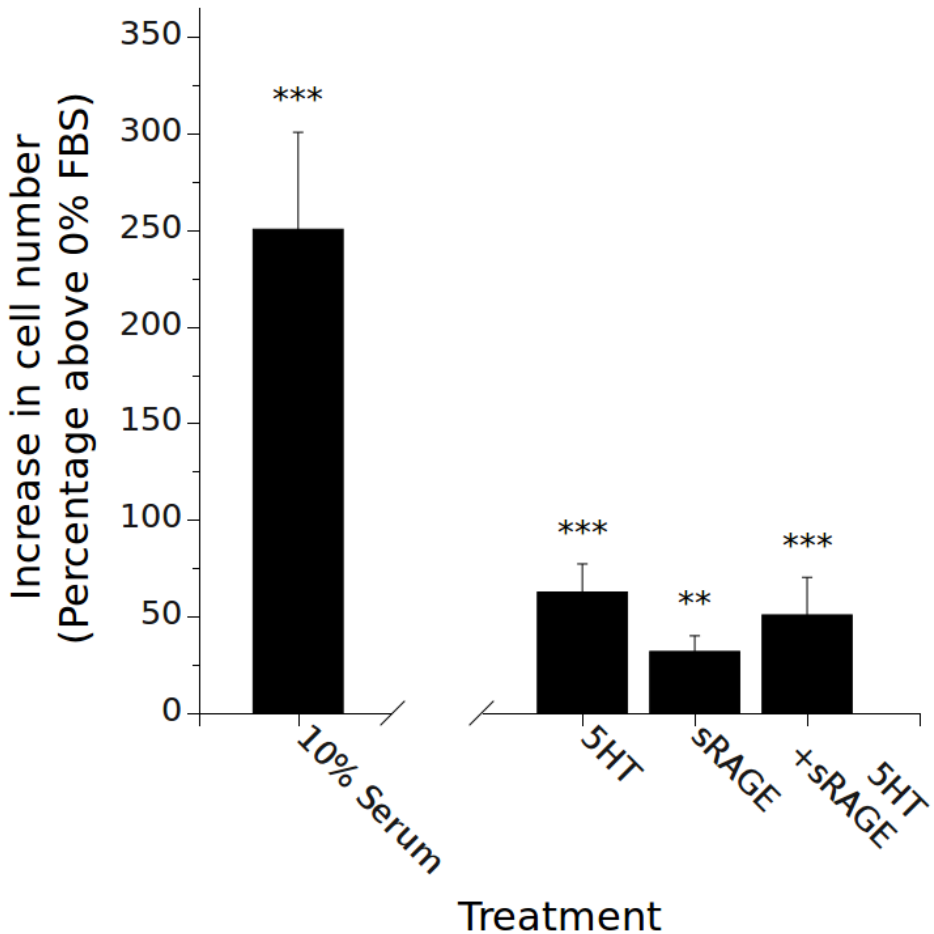


Figure 5.19 Incubation with 2.5 μ g/ml sRAGE produces an increase in cell number and does not inhibit the 5HT-induced increase in cell number in CCL39 Chinese hamster lung FBs. 10 μ M 5HT induced a statistically significant increase in cell number to $63 \pm 15\%$ above baseline. Preincubation with 2.5 μ g/ml sRAGE before treatment with 5HT resulted in a similar increase to $51 \pm 19\%$ above baseline. Surprisingly, treatment with sRAGE alone produced a significant increase in proliferation to $32 \pm 8\%$ above baseline. No statistically significant differences between treatment groups were observed. Data are presented as mean \pm SEM. Analyses were by linear model, one way-ANOVA and Fisher's LSD test. ** $p < 0.01$, *** $p < 0.001$ vs. baseline ($n=4$).`

5.4.4.3 Effects of sRAGE upon hypoxia-induced increases in cell number

Since the *in vivo* drug intervention with sRAGE described in the current study utilises a model of disease induced by hypoxia, it was of interest to observe how the presence of sRAGE would affect the proliferative response of pulmonary fibroblasts to hypoxia. After quiescence, cells were incubated with either 2.5 μ g/ml sRAGE or an equivalent concentration of PBS vehicle for a period of 30 minutes before being incubated under hypoxic conditions for 24 hours.

Incubation in hypoxia produced a statistically significant increase in cell number to 121 \pm 24% above baseline ($p<0.01$; linear model) (Figure 5.20). Preincubation with 2.5 μ g/ml sRAGE produced a significant increase in cell number to 210 \pm 113% above baseline ($p<0.001$; linear model). Surprisingly, this value was significantly larger than that observed for hypoxia alone ($p<0.05$; Fisher's LSD test). As before, 2.5 μ g/ml sRAGE was observed to produce a small but significant increase above baseline values to 30 \pm 13% in cells incubated in normoxia ($p<0.01$; linear model).

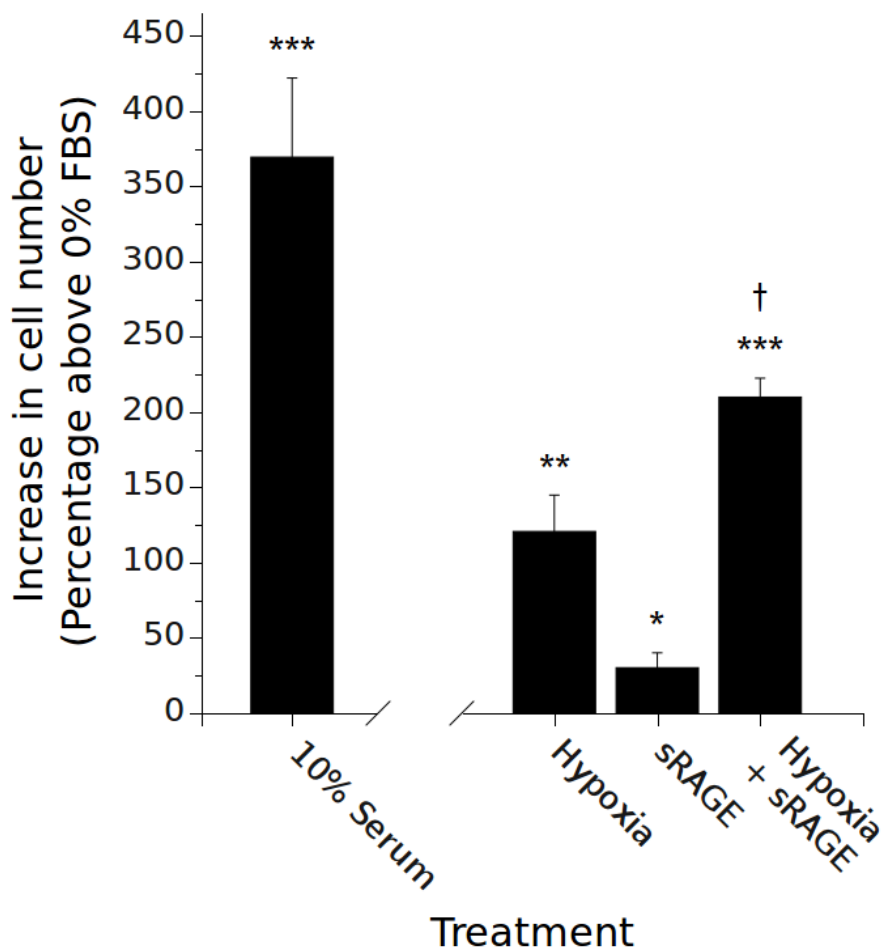


Figure 5.20 2.5 μ g/ml sRAGE enhances the hypoxia-induced increase in cell number in CCL39 Chinese hamster lung FBs. Incubation of CCL39 cells in a hypoxic environment for 24 hours produced a significant increase in the number of cells counted to $120.70 \pm 24.18\%$ above baseline. Surprisingly, preincubation with 2.5 μ g/ml sRAGE produced a statistically significant augmentation of the hypoxia-induced increase in cell number ($210 \pm 13\%$). Treatment with 2.5 μ g/ml sRAGE alone again produced a small but significant increase in cell number ($30 \pm 13\%$) * $p < 0.05$; ** $p < 0.01$, *** $p < 0.001$, † $p < 0.05$ vs Hypoxia. (n=3)

5.5 Discussion

The aim of the current study was to characterise the effects of sRAGE in two novel settings: as an intervention to hypoxia-induced pulmonary hypertension *in vivo*, and its influence upon proliferation to mitogenic stimuli in pulmonary fibroblasts. In a chronic hypoxia-induced model of pulmonary hypertension, sRAGE treatment was shown to reduce the magnitude of a hypoxia-induced elevation in sRVP. Interestingly, this was effected without an accompanying inhibition of remodelling or RVH. These findings were further confounded by the observation that the force of contraction in vessels isolated from sRAGE-treated animals exposed to hypoxia was increased.

In contrast to previous studies in PASMCs, sRAGE did not produce an inhibition of 5HT-induced proliferation in pulmonary fibroblasts. Since MTS1/S100A4 had been implicated as mediator of proliferation in PASMCs through an action at RAGE (Lawrie et al., 2005), we would initially have hypothesised that daily treatment with sRAGE might reduce the extent of pulmonary vascular remodelling and produce an accompanying decrease in the magnitude of any hypoxia-induced increase in sRVP. However, though there is some evidence that MTS1/S100A4 mice display altered pulmonary responses to a chronic hypoxic stimulus, we observed in the previous chapter that these responses were complex; differentially affecting the various parameters (PVR, vasoconstriction, etc.) which determine the pulmonary blood pressure.

Consistent with these previous observations, the increase in sRVP in response to hypoxia was indeed reduced or ablated by treatment with sRAGE, but without any corresponding reduction (and even a possible trend towards an increase) in the extent of vascular remodelling. These observations were further

confounded by the results of experiments related to the contractility of intrapulmonary arteries. The sensitivity of vessels to the contractile agonists studied here was unchanged between vehicle-treated and sRAGE-treated normoxic animals. This also appeared to be true of hypoxic animals of both treatment groups. However, a significant increase in the absolute force of contraction in response to 50mM KCl of the order of 75-100% was observed only in vessels from animals who received both sRAGE treatment and the chronic hypoxia stimulus. This was also true for concentration-response curves to U46619 and 5HT. While the sensitivity of vessels to pharmacological agents *per se* appeared unaltered, these stimuli produced an augmentation in the overall force of contraction. This suggests an increase in the contractility of the vascular smooth muscle. While an effect of sRAGE upon vascular contractility in mice exposed to chronic hypoxia is interesting and novel, it is counter-intuitive in combination with a lessening of the hypoxia-induced increase in sRVP and a lack of prevention of vascular remodelling.

In the scientific literature, instances in which the extent of pulmonary vascular remodelling does not correlate with alterations in pulmonary pressures *in vivo* have previously been described. Studies on chronic lung infection using *Pseudomonas aeruginosa* have demonstrated remodelling of intra-acinar pulmonary vessels which are not accompanied by increased PVR as assessed in both an isolated lung preparation (Cadogan et al., 1999) and *in vivo* (Graham et al., 1990). Similarly, the prostacyclin analogue treprostinil was observed to diminish monocrotaline-induced increases in pulmonary vascular pressures with no corresponding decrease in vascular remodelling (van Albada et al., 2006). Treprostanil had also previously been shown to inhibit SMC and FB proliferation *in vitro* (Clapp et al., 2002; Ali et al., 2006). In the current study, we quantified

the extent of remodelling as the number of vessels possessing a double elastic lamina. It is therefore possible that the increased diameter of the media is due to an outward expansion which does not result in lumen occlusion (Pak et al., 2007). Such a phenomenon has been characterised in diseases of the systemic vasculature (Glagov et al., 1987; Gibbons and Dzau, 1994). Therefore, rather than preventing the generation of vascular remodelling, the reduced bioavailability of RAGE ligands may have altered its nature.

While small distal vessels are implicated in raising vascular resistance through muscularisation, vasoconstriction and reduced lumen diameter, larger distal conducting vessels contribute to elevated pulmonary pressures through smooth muscle cell hyperplasia and hypertrophy resulting in a loss of elasticity or compliance. The lost ability of these vessels to 'buffer' the pulmonary pressure at right ventricular systole through stretch increases pressure in the pulmonary artery at systole and increases shear stress on more distal vessels (Zuckerman et al., 1991; Hopkins and McLoughlin, 2002). Returning to the current study, in vessels from sRAGE-treated mice exposed to hypoxia (the same vessels in which we observed increased contractility) we observed that sRAGE treatment was protective against a hypoxia-induced fall in compliance compared to vessels from control animals. In the absence of a beneficial effect upon the remodelling of the distal circulation, this may have contributed to the ability of sRAGE treatment to reduce sRVP. However, it is difficult to speculate how large a contribution this constitutes in the absence of more specific information on the haemodynamics of the pulmonary circulation. That is to say, it is difficult to assess the importance of proximal artery compliance in the absence of a quantitative measure of distal pulmonary vascular resistance.

In addition to our observations *in vivo* we described some novel effects of

sRAGE on proliferation of CCL39 Chinese hamster lung fibroblasts. Since sRAGE is capable of preventing the proliferation of PASMCs *in vitro* to 5HT, we examined whether a similar inhibition could be accomplished in FBs. In fact, we observed no significant inhibition of 5HT-induced proliferation by sRAGE. A more interesting observation was that sRAGE alone appeared to induce a small amount of proliferation. This presents several possibilities. First, sRAGE may interact directly with some structure on the cellular membrane which is tied to downstream pathways associated with either proliferative or anti-apoptotic processes within the cell. Second, if MTS1/S100A4 or some other RAGE ligand mediates proliferative responses in these cells, as has been described in PASMCs (Lawrie et al., 2005), and if this mediator were constitutively released, then sRAGE may interfere with its binding at cytoplasmic RAGE (or other receptor), thereby altering basal levels of activation. Lastly, it was recently demonstrated that cytoplasmic RAGE forms homodimers on the cell surface, and that this process is important in both ligand recognition and signal transduction (Xie et al., 2008; Zong et al., 2010). Moreover, it was demonstrated that free sRAGE is capable of binding to and forming a heterodimer with cytoplasmic RAGE: preventing the cytoplasmic sRAGE homodimerisation and downstream signalling typically associated with RAGE signalling (*e.g.* NF- κ B activation). The sRAGE molecule may therefore act as a direct antagonist at RAGE as well as a scavenging molecule for RAGE ligands.

This raises a third possibility with regards to the proliferation of FBs induced by sRAGE which is that cytoplasmic RAGE may display some low degree of constitutive anti-proliferative or pro-apoptotic activity which is reduced or ablated by the formation of sRAGE-RAGE heterodimers.

In the current study, 24 hours of hypoxia was observed to produce a

doubling in the total cell count of FBs *in vitro* compared to baseline. This is in line with other *in vitro* studies on pulmonary FBs in the literature (Welsh et al., 1998, 2001, 2006; Stenmark et al., 2002). Interestingly, and in contrast to studies in PASMCs, the presence of sRAGE was observed to markedly enhance the proliferation produced by 24 hours of hypoxia.

In vitro data on the proliferative effects of MTS1/S100A4-mediated proliferation in PASMCs in response correlated poorly with observations related to vascular remodelling *in vivo* in both the previous and current chapters. The addition of data on the effect of sRAGE upon hypoxia-induced proliferation in FBs here is valuable as it is more directly relevant to the current hypoxia-induced model of PAH. However, data in the literature on the proliferative effect of hypoxia in PASMCs is contradictory: with some studies showing proliferation to hypoxia only in the presence of other mitogens (Dempsey et al., 1991; Lannér et al., 2005) and others showing proliferation to hypoxia alone (Cooper and Beasley, 1999; Lu et al., 2005). Rose et al. (2002) demonstrated that while hypoxia produced proliferation in a combined culture of FBs and PASMCs, it did not do so in PASMCs alone. Furthermore, incubation of PASMCs with media collected from a culture of FBs previously exposed to hypoxia also produced proliferation in PASMCs. The implication of this is that pulmonary FBs regulate the proliferative response of PASMCs in hypoxia which is observed *in vivo*.

In the current study, we observed some evidence of an action upon SMCs in that vascular contractility was greatly enhanced by a combination of chronic-hypoxia and sRAGE treatment. If the proliferation of adventitial FBs also occurred *in vivo*, then it is conceivable that PASMC proliferation and/or remodelling is actually encouraged by sRAGE. However, we had no direct means of accounting for FB or SMC proliferation *in vivo* in the current study. It would

also be of interest to attempt to elucidate whether the release of mediators of PASMC proliferation by FBs in response to sRAGE and/or hypoxia is altered. Furthermore, it is unclear whether PAMSC proliferation, in the presence of sRAGE, would be encouraged due to increased numbers of FBs and the resulting increased in concentration of PASMC mitogens, or discouraged due to a direct inhibition of PASMC proliferation by sRAGE. To complicate matters further, proliferative mediators can produce their effects differentially throughout the pulmonary circulation. For example, prostacyclin has been shown to inhibit the growth of cultured hPASMCs from distal but not proximal arteries (Wharton et al., 2000) As highlighted by our divergent findings on the effects of sRAGE treatment and hypoxia on structural changes in the proximal and distal circulation (*i.e.* protection against reduced compliance in proximal vessels with no effect upon distal vascular remodelling), it would be of value to expand this and other studies of the role of RAGE in cellular proliferation with studies on cells isolated from different locales in the pulmonary circulation.

Since, a combination of hypoxia and sRAGE treatment *in vivo* produced an increase in vascular contractility; we also elected to examine the acute effects of sRAGE administration in isolated vessels under tension. Additionally, since treatment with sRAGE and anti-RAGE had previously been shown to inhibit the proliferative response of PASMCs to 5HT, it was of interest to see if RAGE antagonism might modulate the contractile response of vessels to 5HT. To our surprise, a small, slowly-developing contraction was observed in response to 10 μ g/ml sRAGE alone. Additionally, sRAGE augmented the maximum contraction observed in concentration-response curves to 5HT. It is noteworthy that the magnitude of the difference between the E_{max} values in response to 5HT appeared far greater than those observed in the presence of sRAGE alone. This is

suggestive of an increased sensitivity of the contractile apparatus of PASMCs to Ca^{2+} , or possibly an action on the vascular endothelium producing either an increase in the basal release of contractile mediators (ET-1, TxA_2 , etc.) or decreased release of relaxatory mediators (NO, prostaglandin I_2 , etc.). Further work is required to elucidate the mechanism at work.

5.5.1 Further work

Though novel and interesting data were generated in the current study, it would greatly benefit from augmentation in several areas. First, it would be of great interest to attempt to link the observed enhancement of FB proliferation by hypoxia *in vitro* with any possible parallel increase in hypoxia-induced proliferation *in vivo*. This could be accomplished using immunohistochemistry to attempt to identify areas of FB infiltration and/or proliferation.

With regards to the assessment of FB proliferation *in vitro*, it is worth noting that cell counting is not an assay of proliferation *per se*. It is, rather, an assay for the total number of cells, which enforces certain limitations on the inferences that can be drawn using data obtained by this method. In culture, the total number of counted cells in the population will be the product of ongoing and simultaneous proliferative and apoptotic processes. It is therefore not possible to determine by counting cells whether, for example, a treatment producing an increase in cell number is bringing this effect about by stimulating proliferation or inhibiting apoptosis. In a future study, it would therefore be valuable to assess the means by which hypoxia is inducing an increase in the number of CCL39 FBs and how this is altered by treatment with sRAGE. Such an enhancement would be of interest since RAGE ligands have been shown to cause

both proliferation (Lawrie et al., 2005; Spiekerkoetter et al., 2005; Shubbar et al., 2012; Tsoporis et al., 2012) and apoptosis (Huttunen et al., 1999; Jin et al., 2011) in various cell types; occasionally displaying the ability to produce either effect depending on the concentration of ligand.

Proliferation can be assessed by means of radiolabelled, immunoreactive or fluorescent molecules which are incorporated into DNA during replication in proliferating cells. Exposing cells in culture to radioactive tritiated thymidine, a constituent of DNA, results in its incorporation into the DNA of proliferating cells (Reichard and Estborn, 1951; Taylor et al., 1957; Hughes et al., 1958; Baserga and Kisielecki, 1962). The extent to which proliferation has occurred can then be assessed by scintillation counting in treated cell populations. Alternatives to tritiated thymidine include the thymidine analogue 5-bromo-2'-deoxyuridine (BrdU) or the more recent 5-ethynyl-2'-deoxyuridine (EdU) (Gratzner, 1982; Cavanagh et al., 2011). After incorporation, the extent of BrdU incorporation may be assessed by colorimetric immunoassay or ELISA. Assessment of proliferation by this method is less labour intensive than that involving tritiated thymidine and does not require the use of radioactive materials (Muir et al., 1990; Vega-Avila and Pugsley, 2011). EdU incorporation provides a further refinement in that the fluorescent probe which targets EdU-incorporated DNA is a small molecule which readily permeates into cells (Cavanagh et al., 2011; Hua and Kearsey, 2011).

Methods for the assessment of apoptosis also exist and include terminal deoxynucleotidyl transferase-mediated dUTP nick end-labeling (TUNEL) assay for detecting fragmented DNA and propidium iodide staining with flow cytometry (Nicoletti et al., 1991; Negoescu et al., 1996).

In the current study, changes effected by challenge with a hypoxic insult

were assessed in terms of alterations to the circulation which persevere even when the animal is returned to a normoxic environment. Previously, (Merklinger et al., 2005) showed that MTS1/S100A4 mice possessed elevated pulmonary pressures in the absence of enhanced remodelling. Aware that MTS1/S100A4 had been shown to induce PASMC proliferation, they demonstrated that the deposition of elastin in the pulmonary vessels of these mice was also elevated. They suggested that the increased matrix protein deposition had inhibited PASMC migration in response to hypoxia to some degree, but that this same phenomenon contributed to the impaired reversibility of the pulmonary hypertensive state when the animals were allowed to recover in normoxia for 4-12 weeks. In the current study, though the need for further clarification is clear, we would speculate that an sRAGE-driven inhibition of elastin deposition, possibly in concert with an enhanced proliferative response in pulmonary fibroblasts might produce precisely the opposite effect. If deposition of elastin in response to hypoxia is inhibited by sRAGE, then this may have permitted or possibly even facilitated the proliferation and migration of PASMCs in the vascular media, particularly if FB proliferation has been enhanced.

While this would appear to be a negative outcome of the sRAGE intervention (an apparent generation of pulmonary vascular disease), a decrease in the deposition of elastic matrix proteins during hypoxia might result in pulmonary arteries retaining greater distensibility and prevent the alterations in pulmonary vascular resistance which endure on the animal's return to normoxia.

More generally, given the disconnect observed between PASMC proliferation *in vitro* as described in the literature with the development of vascular remodelling in the current study, as well as the apparent disconnect observed between the extent of vascular remodelling and the alteration of sRVP,

it would be of benefit to attempt a more comprehensive assessment of pulmonary vascular remodelling; taking into account parameters such as lumen diameters, muscularisation, the comparative densities of vessels in each lung and the relative elasticity of the vessels contained there.

The functional data obtained in IPAs by wire-myography in the current study provide an interesting supplement to the haemodynamic and structural data obtained and offer some insight into the contribution of vasoreactivity to pulmonary vascular resistance and PAH in the MTS1/S100A4 mouse. An assessment of modulations in vascular tone is important to any model of PAH though the overall importance of vasoconstriction to the human PAH condition is disputed, with many advocating the remodelling process as the primary pathological concern. Whether this is true or not, an assessment of the functional characteristics of vessels from the lungs of an animal used to model disease provides additional information as to the relative contributions of vasoconstriction and pulmonary vascular remodelling to the increase in pulmonary vascular resistance which leads to sustained PAH. Also, the extent of apparent remodelling does not always correlate well with pulmonary vascular resistances and/or pulmonary vascular pressures.

Having said this, while wire myography in addition to a histological assessment of structural remodelling is easily defensible as being superior to histological assessment of remodelling alone, the limitation of this technique becomes apparent upon attempting to elucidate causal relationships between functional changes in IPAs in terms of haemodynamic observations made *in vivo*, whether evidence of vascular remodelling is present or not. The pulmonary vessels which can be successfully isolated and mounted on the myograph are conducting arteries, which will contribute little to the pulmonary vascular

resistance. Furthermore, the alteration of the smooth muscle which occurs in response to hypoxia is qualitatively different in the proximal and distal pulmonary arteries (Pak et al., 2007). It would, in future, be far preferable to establish pulmonary vascular remodelling in terms of how it contributes to pulmonary vascular resistance through the utilisation of an isolated, perfused lung preparation. This would allow a determination of the ease with which fluid may flow through the pulmonary circulation in the absence of any active tone generation through usage of vasodilatory compounds such as NO donors or RhoK inhibitors. An even more in depth assessment of the properties of the pulmonary circulation may be obtained using a pulsatile perfusion pump at a range of pulse frequencies to obtain information on the pulmonary vascular impedance as described by (Vanderpool et al., 2010). This provides a more comprehensive assessment of the characteristics of the pulmonary vasculature in that by examining pulse frequencies which are either very similar or dissimilar to the native heart rate, the contribution of the compliance and elasticity of the proximal vasculature, and the constriction of the small, distal vasculature may be differentially elucidated.

Such an isolated lung preparation might provide a more complete insight into exactly how the functional changes in the proximal intrapulmonary vessels isolated in the current study and the structural changes observed in histological sections for the assessment of small, distal vessels coalesce to produce the changes in haemodynamics observed *in vivo*.

5.6 Conclusions

The current study was, to our knowledge, the first study examining the

effects of sRAGE upon pulmonary hypertension in any model. Additionally, this work is the first to show a modulation of pulmonary vascular tone by sRAGE and the enhancement of FB proliferation in both normoxia and hypoxia by sRAGE. It was notable that, in the studies described in both this chapter and the last, apparently contradictory changes in sRVP, vascular remodelling and vascular tone were observed. Therefore, these data provide more than enough justification for the continued study of RAGE and its ligands in the function of the pulmonary circulation in both health and disease; however, they also highlight the need for a more comprehensive approach in the assessment of functional and structural changes in the pulmonary circulation when attempting to draw causal relationships between these and the production of a pulmonary hypertensive state.

Chapter 6.

General discussion

6.1 General Discussion

Since its initial description, the receptor for advanced glycation end-products has been implicated as a mediator of both acute and chronic vascular inflammation. Interest in the potential role of RAGE in the development of PAH was incited by the following observations: first, high basal expression of RAGE in the lung; second, immunohistological evidence for an increased presence of the RAGE ligand MTS1/S100A4 in occlusive vascular lesions in PAH patients; third, the spontaneous development of advanced occlusive pulmonary vascular disease, including the development of plexiform-like lesions in the pulmonary circulation of transgenic mice overexpressing the MTS1/S100A4 protein (Neeper et al., 1992; Brett et al., 1993; Greenway et al., 2004; Lawrie et al., 2005). These initial data were bolstered by *in vitro* studies demonstrating the direct mitogenic and migratory consequences of RAGE activation in PASMCs. It was observed that MTS1/S100A4 is upregulated in PASMCs by treatment with 5HT by a mechanism that is dependent on the activation of both the 5HT_{1b} receptor and SERT. Additionally, MTS1/S100A4 is subsequently removed into the extracellular space where it may act at plasmalemmal RAGE. Most interestingly, the upregulation and extrusion of MTS1/S100A4, through its action at RAGE, appears to mediate the mitogenic actions of 5HT in PASMCs *in vitro* (Spiekerkoetter et al., 2005). 5HT is a well defined vasoconstrictor and mitogen in the pulmonary circulation and is frequently implicated in the genesis of PAH (MacLean et al., 2000; Dempsie et al., 2008). It has also since been demonstrated that PASMC migratory processes mediated by pERK1/2 are co-dependently induced by RAGE and BMPRII, a molecule whose mutation in patients is a well-defined risk factor in the development of PAH (Deng et al., 2000; Lane et al., 2000; Spiekerkoetter

et al., 2009).

Transgenic mice overexpressing MTS1/S100A4 were also reported to show elevated RVPs in the absence of increased vascular remodelling at baseline, as well as showing an increase in RVP in response to chronic hypoxia that is enhanced in comparison to that observed in WT mice; this was also observed in the absence of enhanced remodelling of the pulmonary circulation.

MTS1/S100A4 mice possess increased systolic right ventricular pressures and right ventricular hypertrophy at baseline in comparison to WT mice, and show an enhanced increase in these parameters after chronic hypoxia. Interestingly, while these increases are indicative of increased pulmonary vascular resistance, they are observed in the absence of an increase in pulmonary vascular remodelling. This suggests that some other structural or functional parameter of the pulmonary circulation had been altered in association with the overexpression of MTS1/S100A4 (Merklinger et al., 2005).

Pulmonary hypertension is a complex disease with a multifactorial pathology. The generation of increased pulmonary arterial pressure is due to a persistent increase in pulmonary vascular resistance: the product of a combination between phenotypical, structural changes in the vasculature due to remodelling processes and reversible, functional changes in vascular tone. In the current study, we sought to obtain a greater understanding of the role of RAGE in the pulmonary circulation: first, by further characterising the role of MTS1/S100A4 overexpression *in vivo* and second, by examining the effects of reduced bioavailability of RAGE ligands *in vivo*, an intervention which has proven beneficial in models of other inflammatory vascular diseases. In both cases, these *in vivo* studies were supplemented with studies in isolated vessels to examine how MTS1/S100A4 and RAGE may impact vascular reactivity with a view

to better understanding if and how alterations in vascular reactivity may contribute to the disease state induced by chronic hypoxia. We also took the opportunity to examine how treatment with a small molecule inhibitor of MCP-1, a molecule upregulated downstream of RAGE activation, may impact upon the development of PAH in a mouse model of the disease.

In the current work, we were surprised to find that our observations in the MTS1/S100A4 mouse did not correspond with those described in the literature and this leads us to suspect that an unaccounted for experimental parameter, possibly gender, is responsible. This discrepancy was observed in mice treated with normoxia, chronic hypoxia and those allowed to recover after chronic hypoxia. While dramatic differences between WT and MTS1/S100A4 mice were not observed in RVP measurements from *in vivo* studies, we did observe significant effects upon vascular contractility suggesting that pulmonary arteries of normoxic MTS1/S100A4 undergo greater contraction in the presence of contractile stimuli, but that this may be mitigated to some degree by an increased sensitivity to the relaxatory effects of NO. The mechanisms by which these changes are effected remains unknown and this is an attractive avenue for further study.

The current study was also limited to the functional assessment of vessels which were large enough for dissection and mounting on a wire myograph. In the mouse, this restricts us to the study of intralobar conductance vessels. The assessment of vascular reactivity in resistance arterioles, perhaps in a larger animal, or using a pulsatile perfusion isolated lung preparation to infer alterations in the impedance of both proximal and distal branches of the pulmonary circulation (Vanderpool et al., 2010, 2011) would provide data on the vasculature that is more directly relevant to the RVP observed *in vivo*. Even still,

the data obtained in the current study argue strongly that RAGE is involved in the modulation of pulmonary vascular reactivity.

This assertion is reinforced by data obtained in mice treated with sRAGE. Treatment with sRAGE in mice exposed to chronic hypoxia produced two seemingly contradictory results: first, a reduction in sRVP when the animals were returned to normoxia that was not accompanied by a decrease in the extent of vascular remodelling or RVH; and second, a marked increase in the force of contraction generated by depolarising contractile stimuli. These observations were made no more clear by the observation that sRAGE produces a small but significant acute constriction in isolated vessels when added to the myograph, and appears to synergistically enhance the maximal contraction of these vessels to 5HT.

While this is an interesting and novel result, the first to show a direct vasoconstrictive effect of sRAGE, the relevance of this to our previous intervention study is unclear since chronic treatment of normoxic mice with sRAGE produced no effect on either sRVP or on the vasoreactivity of vessels isolated from these mice. Additionally, the mechanism by which sRAGE exerts its acute vasoconstrictive effects remains unclear. It would be of particular interest in future studies to determine if sRAGE is producing these effects through reduced bioavailability of RAGE ligand which may regulate vascular tone through constitutive release. Another possibility is that sRAGE, in forming heterodimers with cytoplasmic RAGE, may inhibit some constitutive activity of the receptor itself which persists in the absence of any ligand.

In the current study, we observed a direct proliferative effect of sRAGE upon CCL39 Chinese hamster lung fibroblasts. Furthermore, while we observed hypoxia to be a potent proliferative stimulus in these cells, proliferation due to

hypoxia was enhanced still further by incubation with sRAGE. We also observed no inhibition of 5HT-induced proliferation by sRAGE in these cells. These results are in contrast with observations in PASMCs showing that their proliferation in response to 5HT is dependent upon the action of RAGE (Spiekerkoetter et al., 2005). The inhibition of PASMC proliferation, considered an important component of pulmonary vascular remodelling associated with PAH, by inhibition of RAGE was key to the hypothesis in the current study that inhibition of RAGE might prove protective in an *in vivo* model of PAH. However, in the hypoxic lung *in vivo*, adventitial fibroblasts demonstrate an immediate and dramatic proliferation, before subsequently migrating to the media, transdifferentiating into myofibroblasts and secreting substances which are themselves mitogenic to PASMCs. (Rose et al., 2002; Stenmark et al., 2006)

These results, taken together, emphasise the importance of considering the behaviour of different cell types to differing stimuli while investigating pulmonary hypertension in that, *in vivo*, sRAGE may be working to produce seemingly contradictory effects: the enhanced proliferation of fibroblasts, which are thought to produce mitogens for PASMCs, and the impaired proliferation of SMCs in response to MTS1/S100A4 and/or 5HT. Similarly, this example of complexity provides a compelling argument for the carrying out of *in vivo* experiments in the current study.

6.2 Conclusions

In the course of this thesis, the chronic-hypoxia model of pulmonary hypertension was examined in 3 circumstances: a transgenic mouse, during treatment with a macromolecule for the inhibition of RAGE, and during

treatment with a small molecule inhibitor of one of the downstream inflammatory effectors of RAGE.

Reconciling some of the seemingly contradictory results generated here will require a focus on bridging the gaps in knowledge and data on the spectrum ranging from more reductionist molecular techniques up to a systems-level understanding of physiology. Some of the seemingly anomalous data on vascular contractility produced here would be bolstered by functional studies of the whole lung *ex vivo*, further studies of vascular properties in resistance arteries and perhaps by a more rigorous approach to characterising and quantifying functional and structural changes in the vasculature. The current study highlights the complexities associated with the study of pulmonary hypertension and has shed light on some avenues for future investigation.

Reference List

- Adami, C., Bianchi, R., Pula, G., Donato, R., 2004. S100B-stimulated NO production by BV-2 microglia is independent of RAGE transducing activity but dependent on RAGE extracellular domain. *Biochim. Biophys. Acta* 1742, 169-177.
- Alexander, S., Mathie, A., Peters, J., 2011. Guide to Receptors and Channels (GRAC), 5th edition. *British Journal of Pharmacology* 164, S1-S2.
- Alwmark, A., Bengmark, S., Gullstrand, P., Zoucas, E., 1986. Hypersplenism--effect on haemostasis. An experimental study in the rat. *Res Exp Med (Berl)* 186, 21-27.
- Ambartsumian, N., Grigorian, M., Lukyanidin, E., 2005. Genetically modified mouse models to study the role of metastasis-promoting S100A4(mts1) protein in metastatic mammary cancer. *J. Dairy Res.* 72 Spec No, 27-33.
- Anderson, M.M., Heinecke, J.W., 2003. Production of N(epsilon)-(carboxymethyl)lysine is impaired in mice deficient in NADPH oxidase: a role for phagocyte-derived oxidants in the formation of advanced glycation end products during inflammation. *Diabetes* 52, 2137-2143.
- Barman, S.A., 1998. Potassium channels modulate hypoxic pulmonary vasoconstriction. *Am. J. Physiol.* 275, L64-70.
- Barman, S.A., 2005. Effect of nitric oxide on mitogen-activated protein kinases in neonatal pulmonary vascular smooth muscle. *Lung* 183, 325-335.
- Barst, R.J., Rubin, L.J., Long, W.A., McGoon, M.D., Rich, S., Badesch, D.B., Groves, B.M., Tapson, V.F., Bourge, R.C., Brundage, B.H., Koerner, S.K., Langleben, D., Keller, C.A., Murali, S., Uretsky, B.F., Clayton, L.M., Jöbsis, M.M., Blackburn, S.D., Shortino, D., Crow, J.W., 1996. A Comparison of

- Continuous Intravenous Epoprostenol (Prostacyclin) with Conventional Therapy for Primary Pulmonary Hypertension. *New England Journal of Medicine* 334, 296-301.
- Baserga, R., Kisielecki, W., 1962. Comparative study of the kinetics of cellular proliferation of normal and tumorous tissues with the use of tritiated thymidine. I. Dilution of the label and migration of labeled cells. *J. Natl. Cancer Inst.* 28, 331-339.
- Basta, G., 2008. Receptor for advanced glycation endproducts and atherosclerosis: From basic mechanisms to clinical implications. *Atherosclerosis* 196, 9-21.
- Basta, G., Lazzerini, G., Del Turco, S., Ratto, G.M., Schmidt, A.M., De Caterina, R., 2005. At least 2 distinct pathways generating reactive oxygen species mediate vascular cell adhesion molecule-1 induction by advanced glycation end products. *Arterioscler. Thromb. Vasc. Biol.* 25, 1401-1407.
- Basta, G., Lazzerini, G., Massaro, M., Simoncini, T., Tanganelli, P., Fu, C., Kislinger, T., Stern, D.M., Schmidt, A.M., De Caterina, R., 2002. Advanced glycation end products activate endothelium through signal-transduction receptor RAGE: a mechanism for amplification of inflammatory responses. *Circulation* 105, 816-822.
- Berne, R.M., Levy, M.N., Koeppen, B.M., Stanton, B.A., 2008. Berne & Levy physiology. Mosby/Elsevier, Philadelphia, PA.
- Berridge, M.J., 1993. Inositol trisphosphate and calcium signalling. *Nature* 361, 315-325.
- Bierhaus, A., Hofmann, M.A., Ziegler, R., Nawroth, P.P., 1998. AGEs and their interaction with AGE-receptors in vascular disease and diabetes mellitus. I. The AGE concept. *Cardiovascular Research* 37, 586 -600.

- Brett, J., Schmidt, A.M., Yan, S.D., Zou, Y.S., Weidman, E., Pinsky, D., Nowygorod, R., Neeper, M., Przysiecki, C., Shaw, A., 1993. Survey of the distribution of a newly characterized receptor for advanced glycation end products in tissues. *Am. J. Pathol.* 143, 1699-1712.
- Brownlee, M., Vlassara, H., Cerami, A., 1984. Nonenzymatic glycosylation and the pathogenesis of diabetic complications. *Ann. Intern. Med.* 101, 527-537.
- Bryan-Lluka, L.J., Papacostas, M.H., Paczkowski, F.A., Wanstall, J.C., 2004. Nitric oxide donors inhibit 5-hydroxytryptamine (5-HT) uptake by the human 5-HT transporter (SERT). *British Journal of Pharmacology* 143, 63-70.
- Bucciarelli, L.G., Wendt, T., Qu, W., Lu, Y., Lalla, E., Rong, L.L., Goova, M.T., Moser, B., Kislinger, T., Lee, D.C., Kashyap, Y., Stern, D.M., Schmidt, A.M., 2002. RAGE blockade stabilizes established atherosclerosis in diabetic apolipoprotein E-null mice. *Circulation* 106, 2827-2835.
- Burke, A.P., Kolodgie, F.D., Zieske, A., Fowler, D.R., Weber, D.K., Varghese, P.J., Farb, A., Virmani, R., 2004. Morphologic findings of coronary atherosclerotic plaques in diabetics: A postmortem study. *Arteriosclerosis, Thrombosis, and Vascular Biology* 24, 1266-1271.
- Calfee, C.S., Ware, L.B., Eisner, M.D., Parsons, P.E., Thompson, B.T., Wickersham, N., Matthay, M.A., 2008. Plasma receptor for advanced glycation end products and clinical outcomes in acute lung injury. *Thorax* 63, 1083-1089.
- Carlos, T.M., Harlan, J.M., 1994. Leukocyte-endothelial adhesion molecules. *Blood* 84, 2068-2101.
- Carr, M.W., Roth, S.J., Luther, E., Rose, S.S., Springer, T.A., 1994. Monocyte

- chemoattractant protein 1 acts as a T-lymphocyte chemoattractant. Proc. Natl. Acad. Sci. U.S.A. 91, 3652-3656.
- Cavanagh, B.L., Walker, T., Norazit, A., Meedeniya, A.C.B., 2011. Thymidine analogues for tracking DNA synthesis. Molecules 16, 7980-7993.
- Chateauvieux, S., Grigorakaki, C., Morceau, F., Dicato, M., Diederich, M., 2011. Erythropoietin, erythropoiesis and beyond. Biochem. Pharmacol. 82, 1291-1303.
- Chavakis, T., Bierhaus, A., Al-Fakhri, N., Schneider, D., Witte, S., Linn, T., Nagashima, M., Morser, J., Arnold, B., Preissner, K.T., Nawroth, P.P., 2003. The Pattern Recognition Receptor (RAGE) Is a Counterreceptor for Leukocyte Integrins A Novel Pathway for Inflammatory Cell Recruitment. J Exp Med 198, 1507-1515.
- Cioli, V., Ciarniello, M.G., Guglielmotti, A., Luparini, M.R., Durando, L., Martinelli, B., Catanese, B., Fava, L., Silvestrini, B., 1992. A new protein antidenaturant agent, bindarit, reduces secondary phase of adjuvant arthritis in rats. J. Rheumatol. 19, 1735-1742.
- Clapp, L.H., Finney, P., Turcato, S., Tran, S., Rubin, L.J., Tinker, A., 2002. Differential Effects of Stable Prostacyclin Analogs on Smooth Muscle Proliferation and Cyclic AMP Generation in Human Pulmonary Artery. American Journal of Respiratory Cell and Molecular Biology 26, 194 -201.
- Cochran, B.H., Reffel, A.C., Stiles, C.D., 1983. Molecular cloning of gene sequences regulated by platelet-derived growth factor. Cell 33, 939-947.
- Comroe, J.H., Jr, 1966. The main functions of the pulmonary circulation. Circulation 33, 146-158.
- Cool, C.D., Kennedy, D., Voelkel, N.F., Tuder, R.M., 1997. Pathogenesis and evolution of plexiform lesions in pulmonary hypertension associated with

- scleroderma and human immunodeficiency virus infection. *Hum. Pathol.* 28, 434-442.
- Cooper, A.L., Beasley, D., 1999. Hypoxia stimulates proliferation and interleukin-1 α production in human vascular smooth muscle cells. *American Journal of Physiology - Heart and Circulatory Physiology* 277, H1326 -H1337.
- Daub, B., Schroeter, M., Pfitzer, G., Ganitkevich, V., 2003. Expression of members of the S100 Ca2+-binding protein family in guinea-pig smooth muscle. *Cell Calcium* 33, 1-10.
- Dempsey, E.C., McMurtry, I.F., O'Brien, R.F., 1991. Protein kinase C activation allows pulmonary artery smooth muscle cells to proliferate to hypoxia. *American Journal of Physiology - Lung Cellular and Molecular Physiology* 260, L136 -L145.
- Dempsie, Y., MacLean, M.R., 2008. Pulmonary hypertension: therapeutic targets within the serotonin system. *Br. J. Pharmacol.* 155, 455-462.
- Dempsie, Y., Morecroft, I., Welsh, D.J., MacRitchie, N.A., Herold, N., Loughlin, L., Nilsen, M., Peacock, A.J., Harmar, A., Bader, M., MacLean, M.R., 2008. Converging Evidence in Support of the Serotonin Hypothesis of Dexfenfluramine-Induced Pulmonary Hypertension With Novel Transgenic Mice. *Circulation* 117, 2928 -2937.
- Dempsie, Y., Nilsen, M., White, K., Mair, K.M., Loughlin, L., Ambartsumian, N., Rabinovitch, M., Maclean, M.R., 2011. Development of pulmonary arterial hypertension in mice over-expressing S100A4/Mts1 is specific to females. *Respir. Res.* 12, 159.
- Deng, Z., Morse, J.H., Slager, S.L., Cuervo, N., Moore, K.J., Venetos, G., Kalachikov, S., Cayanis, E., Fischer, S.G., Barst, R.J., Hodge, S.E., Knowles, J.A., 2000. Familial primary pulmonary hypertension (gene

- PPH1) is caused by mutations in the bone morphogenetic protein receptor-II gene. Am. J. Hum. Genet. 67, 737-744.
- Deshmane, S.L., Kremlev, S., Amini, S., Sawaya, B.E., 2009. Monocyte chemoattractant protein-1 (MCP-1): an overview. J. Interferon Cytokine Res. 29, 313-326.
- Dipp, M., Nye, P.C., Evans, A.M., 2001. Hypoxic release of calcium from the sarcoplasmic reticulum of pulmonary artery smooth muscle. Am. J. Physiol. Lung Cell Mol. Physiol. 281, L318-325.
- Donato, R., 1999. Functional roles of S100 proteins, calcium-binding proteins of the EF-hand type. Biochim. Biophys. Acta 1450, 191-231.
- Donato, R., 2001. S100: a multigenic family of calcium-modulated proteins of the EF-hand type with intracellular and extracellular functional roles. Int. J. Biochem. Cell Biol. 33, 637-668.
- Donato, R., 2003. Intracellular and extracellular roles of S100 proteins. Microsc. Res. Tech. 60, 540-551.
- Dou, L., Lu, Y., Shen, T., Huang, X., Man, Y., Wang, S., Li, J., 2012. Panax notoginseng saponins suppress RAGE/MAPK signaling and NF-kappaB activation in apolipoprotein-E-deficient atherosclerosis-prone mice. Cell. Physiol. Biochem. 29, 875-882.
- Ehlermann, P., Eggers, K., Bierhaus, A., Most, P., Weichenhan, D., Greten, J., Nawroth, P.P., Katus, H.A., Remppis, A., 2006. Increased proinflammatory endothelial response to S100A8/A9 after preactivation through advanced glycation end products. Cardiovasc Diabetol 5, 6.
- Esposito, C., Gerlach, H., Brett, J., Stern, D., Vlassara, H., 1989. Endothelial Receptor-Mediated Binding of Glucose-Modified Albumin Is Associated with Increased Monolayer Permeability and Modulation of Cell Surface

- Coagulant Properties. *J Exp Med* 170, 1387-1407.
- Euler, U.S. v., Liljestrand, G., 1946. Observations on the Pulmonary Arterial Blood Pressure in the Cat. *Acta Physiologica Scandinavica* 12, 301-320.
- Feng, B., Xu, L., Wang, H., Yan, X., Xue, J., Liu, F., Hu, J.-F., 2011. Atorvastatin exerts its anti-atherosclerotic effects by targeting the receptor for advanced glycation end products. *Biochim. Biophys. Acta* 1812, 1130-1137.
- Trade, J.M., Mellado, M., del Real, G., Gutierrez-Ramos, J.C., Lind, P., Martinez-A, C., 1997. Characterization of the CCR2 chemokine receptor: functional CCR2 receptor expression in B cells. *J. Immunol.* 159, 5576-5584.
- Galichet, A., Weibel, M., Heizmann, C.W., 2008. Calcium-regulated intramembrane proteolysis of the RAGE receptor. *Biochem. Biophys. Res. Commun.* 370, 1-5.
- Galiè, N., Brundage, B.H., Ghofrani, H.A., Oudiz, R.J., Simonneau, G., Safdar, Z., Shapiro, S., White, R.J., Chan, M., Beardsworth, A., Frumkin, L., Barst, R.J., 2009. Tadalafil therapy for pulmonary arterial hypertension. *Circulation* 119, 2894-2903.
- Galiè, N., Ghofrani, H.A., Torbicki, A., Barst, R.J., Rubin, L.J., Badesch, D., Fleming, T., Parpia, T., Burgess, G., Branzi, A., Grimminger, F., Kurzyna, M., Simonneau, G., 2005. Sildenafil citrate therapy for pulmonary arterial hypertension. *N. Engl. J. Med.* 353, 2148-2157.
- Giaid, A., Saleh, D., 1995. Reduced expression of endothelial nitric oxide synthase in the lungs of patients with pulmonary hypertension. *N. Engl. J. Med.* 333, 214-221.
- Giaid, A., Yanagisawa, M., Langleben, D., Michel, R.P., Levy, R., Shennib, H., Kimura, S., Masaki, T., Duguid, W.P., Stewart, D.J., 1993. Expression of

- Endothelin-1 in the Lungs of Patients with Pulmonary Hypertension. New England Journal of Medicine 328, 1732-1739.
- Giardino, I., Edelstein, D., Brownlee, M., 1996. BCL-2 expression or antioxidants prevent hyperglycemia-induced formation of intracellular advanced glycation endproducts in bovine endothelial cells. J Clin Invest 97, 1422-1428.
- Gifford, J.L., Walsh, M.P., Vogel, H.J., 2007. Structures and metal-ion-binding properties of the Ca²⁺-binding helix-loop-helix EF-hand motifs. Biochemical Journal 405, 199.
- Golovina, V.A., Platoshyn, O., Bailey, C.L., Wang, J., Limsuwan, A., Sweeney, M., Rubin, L.J., Yuan, J.X., 2001. Upregulated TRP and enhanced capacitative Ca(2+) entry in human pulmonary artery myocytes during proliferation. Am. J. Physiol. Heart Circ. Physiol. 280, H746-755.
- Grassia, G., Maddaluno, M., Guglielmotti, A., Mangano, G., Biondi, G., Maffia, P., Ialenti, A., 2009. The anti-inflammatory agent bindarit inhibits neointima formation in both rats and hyperlipidaemic mice. Cardiovasc. Res. 84, 485-493.
- Gratzner, H.G., 1982. Monoclonal antibody to 5-bromo- and 5-iododeoxyuridine: A new reagent for detection of DNA replication. Science 218, 474-475.
- Greenway, S., van Suylen, R.J., Du Marchie Sarvaas, G., Kwan, E., Ambartsumian, N., Lukanidin, E., Rabinovitch, M., 2004. S100A4/Mts1 produces murine pulmonary artery changes resembling plexogenic arteriopathy and is increased in human plexogenic arteriopathy. Am. J. Pathol. 164, 253-262.
- Grover, R.F., 1965. EFFECTS OF HYPOXIA ON VENTILATION AND CARDIAC OUTPUT*. Annals of the New York Academy of Sciences 121, 662-673.

- Guglielmotti, A., Aquilini, L., D'Onofrio, E., Rosignoli, M.T., Milanese, C., Pinza, M., 1998. Bindarit prolongs survival and reduces renal damage in NZB/W lupus mice. *Clin. Exp. Rheumatol.* 16, 149-154.
- Guglielmotti, A., D'Onofrio, E., Coletta, I., Aquilini, L., Milanese, C., Pinza, M., 2002. Amelioration of rat adjuvant arthritis by therapeutic treatment with bindarit, an inhibitor of MCP-1 and TNF-alpha production. *Inflamm. Res.* 51, 252-258.
- Guglielmotti, A., Silvestrini, B., Saso, L., Zwain, I., Cheng, C.Y., 1993. Chronic inflammatory response in the rat can be blocked by bindarit. *Biochem. Mol. Biol. Int.* 29, 747-756.
- Gu, L., Hagiwara, S., Fan, Q., Tanimoto, M., Kobata, M., Yamashita, M., Nishitani, T., Gohda, T., Ni, Z., Qian, J., Horikoshi, S., Tomino, Y., 2006. Role of receptor for advanced glycation end-products and signalling events in advanced glycation end-product-induced monocyte chemoattractant protein-1 expression in differentiated mouse podocytes. *Nephrol. Dial. Transplant.* 21, 299-313.
- Hansmann, G., Wagner, R.A., Schellong, S., de Jesus Perez, V.A., Urashima, T., Wang, L., Sheikh, A.Y., Suen, R.S., Stewart, D.J., Rabinovitch, M., 2007. Pulmonary Arterial Hypertension Is Linked to Insulin Resistance and Reversed by Peroxisome Proliferator-Activated Receptor- γ Activation. *Circulation* 115, 1275 -1284.
- Hardingham, G.E., Chawla, S., Johnson, C.M., Bading, H., 1997. Distinct functions of nuclear and cytoplasmic calcium in the control of gene expression. *Nature* 385, 260-265.
- Harja, E., Bu, D.-X., Hudson, B.I., Jong, S.C., Shen, X., Hallam, K., Kalea, A.Z., Lu, Y., Rosario, R.H., Oruganti, S., Nikolla, Z., Belov, D., Lalla, E.,

- Ramasamy, R., Shi, F.Y., Schmidt, A.M., 2008. Vascular and inflammatory stresses mediate atherosclerosis via RAGE and its ligands in apoE^{-/-} mice. *Journal of Clinical Investigation* 118, 183-194.
- Hayakawa, E., Yoshimoto, T., Sekizawa, N., Sugiyama, T., Hirata, Y., 2012. Overexpression of receptor for advanced glycation end products induces monocyte chemoattractant protein-1 expression in rat vascular smooth muscle cell line. *J. Atheroscler. Thromb.* 19, 13-22.
- Hayashida, K., Nanki, T., Girschick, H., Yavuz, S., Ochi, T., Lipsky, P.E., 2001. Synovial stromal cells from rheumatoid arthritis patients attract monocytes by producing MCP-1 and IL-8. *Arthritis Res.* 3, 118-126.
- Heizmann, C.W., Ackermann, G.E., Galichet, A., 2007. Pathologies involving the S100 proteins and RAGE. *Subcell. Biochem.* 45, 93-138.
- Hishikawa, K., Nakaki, T., Marumo, T., Hayashi, M., Suzuki, H., Kato, R., Saruta, T., 1994. Pressure promotes DNA synthesis in rat cultured vascular smooth muscle cells. *J. Clin. Invest.* 93, 1975-1980.
- Hofmann, M.A., Drury, S., Fu, C., Qu, W., Taguchi, A., Lu, Y., Avila, C., Kambham, N., Bierhaus, A., Nawroth, P., Neurath, M.F., Slattery, T., Beach, D., McClary, J., Nagashima, M., Morser, J., Stern, D., Schmidt, A.M., 1999. RAGE Mediates a Novel Proinflammatory Axis: A Central Cell Surface Receptor for S100/Calgranulin Polypeptides. *Cell* 97, 889-901.
- Hopkins, N., McLoughlin, P., 2002. The structural basis of pulmonary hypertension in chronic lung disease: remodelling, rarefaction or angiogenesis? *J Anat* 201, 335-348.
- Hori, O., Brett, J., Slattery, T., Cao, R., Zhang, J., Chen, J.X., Nagashima, M., Lundh, E.R., Vijay, S., Nitecki, D., 1995. The receptor for advanced glycation end products (RAGE) is a cellular binding site for amphotericin.

- Mediation of neurite outgrowth and co-expression of rage and amphoterin in the developing nervous system. *J. Biol. Chem.* 270, 25752-25761.
- Hoshikawa, Y., Ono, S., Suzuki, S., Tanita, T., Chida, M., Song, C., Noda, M., Tabata, T., Voelkel, N.F., Fujimura, S., 2001. Generation of oxidative stress contributes to the development of pulmonary hypertension induced by hypoxia. *J. Appl. Physiol.* 90, 1299-1306.
- Hua, H., Kearsey, S.E., 2011. Monitoring DNA replication in fission yeast by incorporation of 5-ethynyl-2'-deoxyuridine. *Nucleic Acids Res.* 39, e60.
- Huang, W., Yen, R.T., McLaurine, M., Bledsoe, G., 1996. Morphometry of the human pulmonary vasculature. *J Appl Physiol* 81, 2123-2133.
- Hudson, B.I., Bucciarelli, L.G., Wendt, T., Sakaguchi, T., Lalla, E., Qu, W., Lu, Y., Lee, L., Stern, D.M., Naka, Y., Ramasamy, R., Yan, S.D., Yan, S.F., D'Agati, V., Schmidt, A.M., 2003. Blockade of receptor for advanced glycation endproducts: a new target for therapeutic intervention in diabetic complications and inflammatory disorders. *Archives of Biochemistry and Biophysics* 419, 80-88.
- Hughes, W.L., Bond, V.P., Brecher, G., Cronkite, E.P., Painter, R.B., Quastler, H., Sherman, F.G., 1958. CELLULAR PROLIFERATION IN THE MOUSE AS REVEALED BY AUTORADIOGRAPHY WITH TRITIATED THYMIDINE*. *Proc Natl Acad Sci U S A* 44, 476-483.
- Humbert, M., Morrell, N.W., Archer, S.L., Stenmark, K.R., MacLean, M.R., Lang, I.M., Christman, B.W., Weir, E.K., Eickelberg, O., Voelkel, N.F., Rabinovitch, M., 2004. Cellular and molecular pathobiology of pulmonary arterial hypertension. *J. Am. Coll. Cardiol.* 43, 13S-24S.
- Humbert, M., Sitbon, O., Chaouat, A., Bertocchi, M., Habib, G., Gressin, V., Yaici, A., Weitzenblum, E., Cordier, J.-F., Chabot, F., Dromer, C., Pison,

C., Reynaud-Gaubert, M., Haloun, A., Laurent, M., Hachulla, E.,
Simonneau, G., 2006. Pulmonary arterial hypertension in France: results
from a national registry. Am. J. Respir. Crit. Care Med. 173, 1023-1030.

Humbert, M., Sitbon, O., Simonneau, G., 2004. Treatment of Pulmonary Arterial
Hypertension. New England Journal of Medicine 351, 1425-1436.

Huttunen, H.J., Fages, C., Rauvala, H., 1999. Receptor for advanced glycation
end products (RAGE)-mediated neurite outgrowth and activation of NF-
kappaB require the cytoplasmic domain of the receptor but different
downstream signaling pathways. J. Biol. Chem. 274, 19919-19924.

Huttunen, H.J., Kuja-Panula, J., Sorci, G., Agnelli, A.L., Donato, R., Rauvala,
H., 2000. Coregulation of neurite outgrowth and cell survival by
amphoterin and S100 proteins through receptor for advanced glycation
end products (RAGE) activation. J. Biol. Chem. 275, 40096-40105.

Ialenti, A., Grassia, G., Gordon, P., Maddaluno, M., Di Lauro, M.V., Baker, A.H.,
Guglielmotti, A., Colombo, A., Biondi, G., Kennedy, S., Maffia, P., 2011.
Inhibition of in-stent stenosis by oral administration of bindarit in porcine
coronary arteries. Arterioscler. Thromb. Vasc. Biol. 31, 2448-2454.

Ide, Y., Matsui, T., Ishibashi, Y., Takeuchi, M., Yamagishi, S., 2010. Pigment
epithelium-derived factor inhibits advanced glycation end product-elicited
mesangial cell damage by blocking NF-kappaB activation. Microvasc. Res.
80, 227-232.

Ikeda, Y., Yonemitsu, Y., Kataoka, C., Kitamoto, S., Yamaoka, T., Nishida, K.-I.,
Takeshita, A., Egashira, K., Sueishi, K., 2002. Anti-monocyte
chemoattractant protein-1 gene therapy attenuates pulmonary
hypertension in rats. Am. J. Physiol. Heart Circ. Physiol. 283, H2021-2028.

Imanaga, Y., Sakata, N., Takebayashi, S., Matsunaga, A., Sasaki, J., Arakawa, K.,

- Nagai, R., Horiuchi, S., Itabe, H., Takano, T., 2000. In vivo and in vitro evidence for the glycoxidation of low density lipoprotein in human atherosclerotic plaques. *Atherosclerosis* 150, 343-355.
- Ishibashi, Y., Matsui, T., Takeuchi, M., Yamagishi, S., 2011. Vardenafil, an inhibitor of phosphodiesterase-5, blocks advanced glycation end product (AGE)-induced up-regulation of monocyte chemoattractant protein-1 mRNA levels in endothelial cells by suppressing AGE receptor (RAGE) expression via elevation of cGMP. *Clin. Exp. Med.* 11, 131-135.
- Isoda, K., Folco, E., Marwali, M.R., Ohsuzu, F., Libby, P., 2008. Glycated LDL increases monocyte CC chemokine receptor 2 expression and monocyte chemoattractant protein-1-mediated chemotaxis. *Atherosclerosis* 198, 307-312.
- Itoh, T., Nagaya, N., Ishibashi-Ueda, H., Kyotani, S., Oya, H., Sakamaki, F., Kimura, H., Nakanishi, N., 2006. Increased plasma monocyte chemoattractant protein-1 level in idiopathic pulmonary arterial hypertension. *Respirology* 11, 158-163.
- Jaulmes, A., Thierry, S., Janvier, B., Raymondjean, M., Maréchal, V., 2006. Activation of sPLA2-IIA and PGE2 production by high mobility group protein B1 in vascular smooth muscle cells sensitized by IL-1beta. *FASEB J.* 20, 1727-1729.
- Jeffery, T.K., Morrell, N.W., 2002. Molecular and cellular basis of pulmonary vascular remodeling in pulmonary hypertension. *Prog Cardiovasc Dis* 45, 173-202.
- Jeffery, T.K., Wanstall, J.C., 2001. Pulmonary vascular remodeling: a target for therapeutic intervention in pulmonary hypertension. *Pharmacol. Ther.* 92, 1-20.

- Jin, Q., Chen, H., Luo, A., Ding, F., Liu, Z., 2011. S100A14 Stimulates Cell Proliferation and Induces Cell Apoptosis at Different Concentrations via Receptor for Advanced Glycation End Products (RAGE). *PLoS One* 6.
- Jones, R., 1992. Ultrastructural analysis of contractile cell development in lung microvessels in hyperoxic pulmonary hypertension. Fibroblasts and intermediate cells selectively reorganize nonmuscular segments. *Am. J. Pathol.* 141, 1491-1505.
- Kalinina, N., Agrotis, A., Antropova, Y., DiVitto, G., Kanellakis, P., Kostolias, G., Illyinskaya, O., Tararak, E., Bobik, A., 2004. Increased expression of the DNA-binding cytokine HMGB1 in human atherosclerotic lesions: role of activated macrophages and cytokines. *Arterioscler. Thromb. Vasc. Biol.* 24, 2320-2325.
- Karnik, S.K., Brooke, B.S., Bayes-Genis, A., Sorensen, L., Wythe, J.D., Schwartz, R.S., Keating, M.T., Li, D.Y., 2003. A critical role for elastin signaling in vascular morphogenesis and disease. *Development* 130, 411-423.
- Kasahara, Y., Kimura, H., Kurosu, K., Sugito, K., Mukaida, N., Matsushima, K., Kuriyama, T., 1998. MCAF/MCP-1 protein expression in a rat model for pulmonary hypertension induced by monocrotaline. *Chest* 114, 67S.
- Kay, J.M., Harris, P., Heath, D., 1967. Pulmonary hypertension produced in rats by ingestion of *Crotalaria spectabilis* seeds. *Thorax* 22, 176-179.
- Kimura, H., Kasahara, Y., Kurosu, K., Sugito, K., Takiguchi, Y., Terai, M., Mikata, A., Natsume, M., Mukaida, N., Matsushima, K., Kuriyama, T., 1998. Alleviation of monocrotaline-induced pulmonary hypertension by antibodies to monocyte chemotactic and activating factor/monocyte chemoattractant protein-1. *Lab. Invest.* 78, 571-581.
- Kimura, H., Okada, O., Tanabe, N., Tanaka, Y., Terai, M., Takiguchi, Y., Masuda,

- M., Nakajima, N., Hiroshima, K., Inadera, H., Matsushima, K., Kuriyama, T., 2001. Plasma monocyte chemoattractant protein-1 and pulmonary vascular resistance in chronic thromboembolic pulmonary hypertension. Am. J. Respir. Crit. Care Med. 164, 319-324.
- Kislanger, T., Tanji, N., Wendt, T., Qu, W., Lu, Y., Ferran, L.J., Taguchi, A., Olson, K., Bucciarelli, L., Goova, M., Hofmann, M.A., Cataldegirmen, G., D'Agati, V., Pischetsrieder, M., Stern, D.M., Schmidt, A.M., 2001. Receptor for Advanced Glycation End Products Mediates Inflammation and Enhanced Expression of Tissue Factor in Vasculature of Diabetic Apolipoprotein E-Null Mice. Arterioscler Thromb Vasc Biol 21, 905-910.
- Kol, A., Libby, P., 1998. The Mechanisms by Which Infectious Agents May Contribute to Atherosclerosis and Its Clinical Manifestations. Trends in Cardiovascular Medicine 8, 191-199.
- Krakauer, T., 2008. Nuclear Factor- κ B: Fine-Tuning a Central Integrator of Diverse Biologic Stimuli. International Reviews of Immunology 27, 286-292.
- Kumar, S., Sud, N., Fonseca, F.V., Hou, Y., Black, S.M., 2010. Shear stress stimulates nitric oxide signaling in pulmonary arterial endothelial cells via a reduction in catalase activity: role of protein kinase C delta. Am. J. Physiol. Lung Cell Mol. Physiol. 298, L105-116.
- Kusano, K.F., Nakamura, K., Kusano, H., Nishii, N., Banba, K., Ikeda, T., Hashimoto, K., Yamamoto, M., Fujio, H., Miura, A., Ohta, K., Morita, H., Saito, H., Emori, T., Nakamura, Y., Kusano, I., Ohe, T., 2004. Significance of the level of monocyte chemoattractant protein-1 in human atherosclerosis. Circ. J. 68, 671-676.
- Lander, H.M., Tauras, J.M., Ogiste, J.S., Hori, O., Moss, R.A., Schmidt, A.M.,

1997. Activation of the receptor for advanced glycation end products triggers a p21(ras)-dependent mitogen-activated protein kinase pathway regulated by oxidant stress. *J. Biol. Chem.* 272, 17810-17814.
- Lane, K.B., Machado, R.D., Pauciulo, M.W., Thomson, J.R., Phillips, J.A., 3rd, Loyd, J.E., Nichols, W.C., Trembath, R.C., 2000. Heterozygous germline mutations in BMPR2, encoding a TGF-beta receptor, cause familial primary pulmonary hypertension. *Nat. Genet.* 26, 81-84.
- Lannér, M.C., Raper, M., Pratt, W.M., Rhoades, R.A., 2005. Heterotrimeric G Proteins and the Platelet-Derived Growth Factor Receptor- β Contribute to Hypoxic Proliferation of Smooth Muscle Cells. *American Journal of Respiratory Cell and Molecular Biology* 33, 412 -419.
- Lan, Q., Mercurius, K.O., Davies, P.F., 1994. Stimulation of transcription factors NF kappa B and AP1 in endothelial cells subjected to shear stress. *Biochem. Biophys. Res. Commun.* 201, 950-956.
- Lawrie, A., Spiekerkoetter, E., Martinez, E.C., Ambartsumian, N., Sheward, W.J., MacLean, M.R., Harmar, A.J., Schmidt, A.-M., Lukanidin, E., Rabinovitch, M., 2005. Interdependent Serotonin Transporter and Receptor Pathways Regulate S100A4/Mts1, a Gene Associated With Pulmonary Vascular Disease. *Circulation Research* 97, 227 -235.
- Leclerc, E., Fritz, G., Weibel, M., Heizmann, C.W., Galichet, A., 2007. S100B and S100A6 differentially modulate cell survival by interacting with distinct RAGE (receptor for advanced glycation end products) immunoglobulin domains. *J. Biol. Chem.* 282, 31317-31331.
- Levine, B.D., Kubo, K., Kobayashi, T., Fukushima, M., Shibamoto, T., Ueda, G., 1988. Role of barometric pressure in pulmonary fluid balance and oxygen transport. *Journal of Applied Physiology* 64, 419 -428.

- Li, J., Li, W., Altura, B.T., Altura, B.M., 2005. Peroxynitrite-induced relaxation in isolated rat aortic rings and mechanisms of action. *Toxicol. Appl. Pharmacol.* 209, 269-276.
- Li, M., Riddle, S.R., Frid, M.G., El Kasmi, K.C., McKinsey, T.A., Sokol, R.J., Strassheim, D., Meyrick, B., Yeager, M.E., Flockton, A.R., McKeon, B.A., Lemon, D.D., Horn, T.R., Anwar, A., Barajas, C., Stenmark, K.R., 2011. Emergence of Fibroblasts with a Proinflammatory Epigenetically Altered Phenotype in Severe Hypoxic Pulmonary Hypertension. *The Journal of Immunology* 187, 2711 -2722.
- Lin, L., Park, S., Lakatta, E.G., 2009. RAGE signaling in inflammation and arterial aging. *Front Biosci* 14, 1403-1413.
- Liu, Y., Liang, C., Liu, X., Liao, B., Pan, X., Ren, Y., Fan, M., Li, M., He, Z., Wu, J., Wu, Z., 2010. AGEs increased migration and inflammatory responses of adventitial fibroblasts via RAGE, MAPK and NF-kappaB pathways. *Atherosclerosis* 208, 34-42.
- Li, W., Sama, A.E., Wang, H., 2006. Role of HMGB1 in cardiovascular diseases. *Curr Opin Pharmacol* 6, 130-135.
- Lupi-Herrera, E., Bialostozky, D., Sobrino, A., 1981. The role of isoproterenol in pulmonary artery hypertension of unknown etiology (primary): short- and long-term evaluation. *Chest* 79, 292-296.
- Lu, S.-Y., Wang, D.-S., Zhu, M.-Z., Zhang, Q.-H., Hu, Y.-Z., Pei, J.-M., 2005. Inhibition of hypoxia-induced proliferation and collagen synthesis by vasonatrin peptide in cultured rat pulmonary artery smooth muscle cells. *Life Sciences* 77, 28-38.
- Maclean, M.R., Dempsie, Y., 2010. The serotonin hypothesis of pulmonary hypertension revisited. *Adv. Exp. Med. Biol.* 661, 309-322.

- MacLean, M.R., Deuchar, G.A., Hicks, M.N., Morecroft, I., Shen, S., Sheward, J., Colston, J., Loughlin, L., Nilsen, M., Dempsie, Y., Harmar, A., 2004. Overexpression of the 5-hydroxytryptamine transporter gene: effect on pulmonary hemodynamics and hypoxia-induced pulmonary hypertension. *Circulation* 109, 2150-2155.
- MacLean, M.R., Herve, P., Eddahibi, S., Adnot, S., 2000. 5-hydroxytryptamine and the pulmonary circulation: receptors, transporters and relevance to pulmonary arterial hypertension. *Br. J. Pharmacol.* 131, 161-168.
- MacLean, M.R., Sweeney, G., Baird, M., McCulloch, K.M., Houslay, M., Morecroft, I., 1996. 5-Hydroxytryptamine receptors mediating vasoconstriction in pulmonary arteries from control and pulmonary hypertensive rats. *Br. J. Pharmacol.* 119, 917-930.
- Madden, J., Vadula, M., Kurup, V., 1992. Effects of hypoxia and other vasoactive agents on pulmonary and cerebral artery smooth muscle cells.
- Maeda, S., Matsui, T., Takeuchi, M., Yoshida, Y., Yamakawa, R., Fukami, K., Yamagishi, S., 2011. Pigment epithelium-derived factor (PEDF) inhibits proximal tubular cell injury in early diabetic nephropathy by suppressing advanced glycation end products (AGEs)-receptor (RAGE) axis. *Pharmacol. Res.* 63, 241-248.
- Mandegar, M., Fung, Y.-C.B., Huang, W., Remillard, C.V., Rubin, L.J., Yuan, J.X.-J., 2004. Cellular and molecular mechanisms of pulmonary vascular remodeling: role in the development of pulmonary hypertension. *Microvascular Research* 68, 75-103.
- Mandinova, A., Atar, D., Schäfer, B.W., Spiess, M., Aebi, U., Heizmann, C.W., 1998. Distinct subcellular localization of calcium binding S100 proteins in human smooth muscle cells and their relocation in response to rises in

- intracellular calcium. *J. Cell. Sci.* 111 (Pt 14), 2043-2054.
- Mark Evans, A., Ward, J.P.T., 2009. Hypoxic pulmonary vasoconstriction--invited article. *Adv. Exp. Med. Biol.* 648, 351-360.
- Marsche, G., Semlitsch, M., Hammer, A., Frank, S., Weigle, B., Demling, N., Schmidt, K., Windischhofer, W., Waeg, G., Sattler, W., Malle, E., 2007. Hypochlorite-modified albumin colocalizes with RAGE in the artery wall and promotes MCP-1 expression via the RAGE-Erk1/2 MAP-kinase pathway. *FASEB J* 21, 1145-1152.
- Matsui, T., Yamagishi, S., Takeuchi, M., Ueda, S., Fukami, K., Okuda, S., 2009. Nifedipine, a calcium channel blocker, inhibits advanced glycation end product (AGE)-elicited mesangial cell damage by suppressing AGE receptor (RAGE) expression via peroxisome proliferator-activated receptor-gamma activation. *Biochem. Biophys. Res. Commun.* 385, 269-272.
- Matsui, T., Yamagishi, S., Ueda, S., Nakamura, K., Imaizumi, T., Takeuchi, M., Inoue, H., 2007. Telmisartan, an angiotensin II type 1 receptor blocker, inhibits advanced glycation end-product (AGE)-induced monocyte chemoattractant protein-1 expression in mesangial cells through downregulation of receptor for AGEs via peroxisome proliferator-activated receptor-gamma activation. *J. Int. Med.* 262, 482-489.
- Matsunaga, T., Hokari, S., Koyama, I., Harada, T., Komoda, T., 2003. NF-kappa B activation in endothelial cells treated with oxidized high-density lipoprotein. *Biochem. Biophys. Res. Commun.* 303, 313-319.
- McCulloch, K.M., Docherty, C., MacLean, M.R., 1998. Endothelin receptors mediating contraction of rat and human pulmonary resistance arteries: effect of chronic hypoxia in the rat. *Br. J. Pharmacol.* 123, 1621-1630.
- McLaughlin, V.V., Shillington, A., Rich, S., 2002. Survival in primary pulmonary

- hypertension: the impact of epoprostenol therapy. Circulation 106, 1477-1482.
- McMurtry, I.F., Abe, K., Ota, H., Fagan, K.A., Oka, M., 2010. Rho kinase-mediated vasoconstriction in pulmonary hypertension. Adv. Exp. Med. Biol. 661, 299-308.
- McMurtry, I.F., Davidson, A.B., Reeves, J.T., Grover, R.F., 1976. Inhibition of hypoxic pulmonary vasoconstriction by calcium antagonists in isolated rat lungs. Circ. Res. 38, 99-104.
- Medzhitov, R., Janeway, C.A., Jr, 1997. Innate immunity: the virtues of a nonclonal system of recognition. Cell 91, 295-298.
- Merklinger, S.L., Wagner, R.A., Spiekerkoetter, E., Hinek, A., Knutsen, R.H., Kabir, M.G., Desai, K., Hacker, S., Wang, L., Cann, G.M., Ambartsumian, N.S., Lukanidin, E., Bernstein, D., Husain, M., Mecham, R.P., Starcher, B., Yanagisawa, H., Rabinovitch, M., 2005. Increased fibulin-5 and elastin in S100A4/Mts1 mice with pulmonary hypertension. Circ. Res. 97, 596-604.
- Meyrick, B., Reid, L., 1979. Hypoxia and incorporation of 3H-thymidine by cells of the rat pulmonary arteries and alveolar wall. Am. J. Pathol. 96, 51-70.
- Mohan, S., Hamuro, M., Koyoma, K., Sorescu, G.P., Jo, H., Natarajan, M., 2003. High glucose induced NF-kappaB DNA-binding activity in HAEC is maintained under low shear stress but inhibited under high shear stress: role of nitric oxide. Atherosclerosis 171, 225-234.
- Mohan, S., Hamuro, M., Sorescu, G.P., Koyoma, K., Sprague, E.A., Jo, H., Valente, A.J., Prihoda, T.J., Natarajan, M., 2003. IkappaBalphal-dependent regulation of low-shear flow-induced NF-kappa B activity: role of nitric oxide. Am. J. Physiol., Cell Physiol. 284, C1039-1047.
- Morrell, N.W., Morris, K.G., Stenmark, K.R., 1995. Role of angiotensin-converting

- enzyme and angiotensin II in development of hypoxic pulmonary hypertension. Am. J. Physiol. 269, H1186-1194.
- Muir, D., Varon, S., Manthorpe, M., 1990. An enzyme-linked immunosorbent assay for bromodeoxyuridine incorporation using fixed microcultures. Anal. Biochem. 185, 377-382.
- Mullarkey, C.J., Edelstein, D., Brownlee, M., 1990. Free radical generation by early glycation products: a mechanism for accelerated atherogenesis in diabetes. Biochem. Biophys. Res. Commun. 173, 932-939.
- Murphy, R.A., Rembold, C.M., 2005. The latch-bridge hypothesis of smooth muscle contraction. Can. J. Physiol. Pharmacol. 83, 857-864.
- Murray, T.R., Chen, L., Marshall, B.E., Macarak, E.J., 1990. Hypoxic contraction of cultured pulmonary vascular smooth muscle cells. Am. J. Respir. Cell Mol. Biol. 3, 457-465.
- Nakamura, T., Lozano, P.R., Ikeda, Y., Iwanaga, Y., Hinek, A., Minamisawa, S., Cheng, C.-F., Kobuke, K., Dalton, N., Takada, Y., Tashiro, K., Ross Jr, J., Honjo, T., Chien, K.R., 2002. Fibulin-5/DANCE is essential for elastogenesis in vivo. Nature 415, 171-175.
- Nakamura, Y., Horii, Y., Nishino, T., Shiiki, H., Sakaguchi, Y., Kagoshima, T., Dohi, K., Makita, Z., Vlassara, H., Bucala, R., 1993. Immunohistochemical localization of advanced glycosylation end products in coronary atherosclerosis and cardiac tissue in diabetes mellitus. Am. J. Pathol. 143, 1649-1656.
- Nepper, M., Schmidt, A.M., Brett, J., Yan, S.D., Wang, F., Pan, Y.C., Elliston, K., Stern, D., Shaw, A., 1992. Cloning and expression of a cell surface receptor for advanced glycosylation end products of proteins. Journal of Biological Chemistry 267, 14998 -15004.
- Negoescu, A., Lorimier, P., Labat-Moleur, F., Drouet, C., Robert, C., Guillermot,

- C., Brambilla, C., Brambilla, E., 1996. In situ apoptotic cell labeling by the TUNEL method: improvement and evaluation on cell preparations. *J Histochem Cytochem* 44, 959-968.
- Neish, A.S., Williams, A.J., Palmer, H.J., Whitley, M.Z., Collins, T., 1992. Functional analysis of the human vascular cell adhesion molecule 1 promoter. *J. Exp. Med.* 176, 1583-1593.
- Nelson, M.T., Patlak, J.B., Worley, J.F., Standen, N.B., 1990. Calcium channels, potassium channels, and voltage dependence of arterial smooth muscle tone. *American Journal of Physiology - Cell Physiology* 259, C3 -C18.
- Ng, L.C., McCormack, M.D., Airey, J.A., Singer, C.A., Keller, P.S., Shen, X.-M., Hume, J.R., 2009. TRPC1 and STIM1 mediate capacitative Ca²⁺ entry in mouse pulmonary arterial smooth muscle cells. *J. Physiol. (Lond.)* 587, 2429-2442.
- Nicoletti, I., Migliorati, G., Pagliacci, M.C., Grignani, F., Riccardi, C., 1991. A rapid and simple method for measuring thymocyte apoptosis by propidium iodide staining and flow cytometry. *J. Immunol. Methods* 139, 271-279.
- Ni, W., Egashira, K., Kitamoto, S., Kataoka, C., Koyanagi, M., Inoue, S., Imaizumi, K., Akiyama, C., Nishida, K.I., Takeshita, A., 2001. New anti-monocyte chemoattractant protein-1 gene therapy attenuates atherosclerosis in apolipoprotein E-knockout mice. *Circulation* 103, 2096-2101.
- Nobe, K., Sakai, Y., Nobe, H., Takashima, J., Paul, R.J., Momose, K., 2003. Enhancement effect under high-glucose conditions on U46619-induced spontaneous phasic contraction in mouse portal vein. *J. Pharmacol. Exp. Ther.* 304, 1129-1142.
- O'Callaghan, D.S., Savale, L., Montani, D., Jaïs, X., Sitbon, O., Simonneau, G., 203

- Humbert, M., 2011. Treatment of pulmonary arterial hypertension with targeted therapies. *Nat Rev Cardiol* 8, 526-538.
- Okada, K., Tanaka, Y., Bernstein, M., Zhang, W., Patterson, G.A., Botney, M.D., 1997. Pulmonary hemodynamics modify the rat pulmonary artery response to injury. A neointimal model of pulmonary hypertension. *Am J Pathol* 151, 1019-1025.
- Oka, M., Fagan, K.A., Jones, P.L., McMurtry, I.F., 2008. Therapeutic potential of RhoA/Rho kinase inhibitors in pulmonary hypertension. *Br. J. Pharmacol.* 155, 444-454.
- Oka, M., Homma, N., McMurtry, I.F., 2008. Rho kinase-mediated vasoconstriction in rat models of pulmonary hypertension. *Meth. Enzymol.* 439, 191-204.
- Orlova, V.V., Choi, E.Y., Xie, C., Chavakis, E., Bierhaus, A., Iharus, E., Ballantyne, C.M., Gahmberg, C.G., Bianchi, M.E., Nawroth, P.P., Chavakis, T., 2007. A novel pathway of HMGB1-mediated inflammatory cell recruitment that requires Mac-1-integrin. *EMBO J* 26, 1129-1139.
- Pak, O., Aldashev, A., Welsh, D., Peacock, A., 2007. The effects of hypoxia on the cells of the pulmonary vasculature. *European Respiratory Journal* 30, 364 -372.
- Palevsky, H.I., Schloo, B.L., Pietra, G.G., Weber, K.T., Janicki, J.S., Rubin, E., Fishman, A.P., 1989. Primary pulmonary hypertension. Vascular structure, morphometry, and responsiveness to vasodilator agents. *Circulation* 80, 1207-1221.
- Palinski, W., Koschinsky, T., Butler, S.W., Miller, E., Vlassara, H., Cerami, A., Witztum, J.L., 1995. Immunological evidence for the presence of advanced glycosylation end products in atherosclerotic lesions of euglycemic rabbits. *Arterioscler. Thromb. Vasc. Biol.* 15, 571-582.

- Palmer, J.G., Eichwald, E.J., Cartwright, G.E., Wintrobe, M.M., 1953. The Experimental Production of Splenomegaly, Anemia and Leukopenia in Albino Rats. *Blood* 8, 72 -80.
- Park, J.S., Svetkauskaite, D., He, Q., Kim, J.-Y., Strassheim, D., Ishizaka, A., Abraham, E., 2004. Involvement of Toll-Like Receptors 2 and 4 in Cellular Activation by High Mobility Group Box 1 Protein. *J. Biol. Chem.* 279, 7370-7377.
- Park, L., Raman, K.G., Lee, K.J., Lu, Y., Ferran Jr., L.J., Choe, W.S., Stern, D., Schmidt, A.M., 1998. Suppression of accelerated diabetic atherosclerosis by the soluble receptor for advanced glycation endproducts. *Nature Medicine* 4, 1025-1031.
- Peacock, A.J., Murphy, N.F., McMurray, J.J.V., Caballero, L., Stewart, S., 2007. An epidemiological study of pulmonary arterial hypertension. *Eur. Respir. J.* 30, 104-109.
- Pepkezaba, J., 1991. Inhaled nitric oxide as a cause of selective pulmonary vasodilatation in pulmonary hypertension. *The Lancet* 338, 1173-1174.
- Pérez-Tamayo, R., Mejia, S., Montfort, I., 1961. Influence of Spleen on Thrombocytopenia Induced by Humoral Factor(s) of Experimental Hypersplenism. *Blood* 18, 364 -369.
- Pérez-Tamayo, R., Mora, J., Montfort, I., 1960. Humoral Factor(s) in Experimental Hypersplenism. *Blood* 16, 1145 -1154.
- Person, B., Proctor, R.J., 1979. Primary pulmonary hypertension. Responses to indomethacin, terbutaline, and isoproterenol. *Chest* 76, 601-603.
- Petit, R.D., Warburton, R.R., Ou, L.C., Hill, N.S., 1995. Pulmonary vascular adaptations to augmented polycythemia during chronic hypoxia. *J. Appl. Physiol.* 79, 229-235.

- Pokutta, S., Herrenknecht, K., Kemler, R., Engel, J., 1994. Conformational changes of the recombinant extracellular domain of E-cadherin upon calcium binding. European Journal of Biochemistry 223, 1019-1026.
- Post, J.M., Hume, J.R., Archer, S.L., Weir, E.K., 1992. Direct role for potassium channel inhibition in hypoxic pulmonary vasoconstriction. Am. J. Physiol. 262, C882-890.
- Rabinovitch, M., Gamble, W.J., Miettinen, O.S., Reid, L., 1981. Age and sex influence on pulmonary hypertension of chronic hypoxia and on recovery. American Journal of Physiology - Heart and Circulatory Physiology 240, H62 -H72.
- Rabinovitch, M., Konstam, M.A., Gamble, W.J., Papanicolaou, N., Aronovitz, M.J., Treves, S., Reid, L., 1983. Changes in pulmonary blood flow affect vascular response to chronic hypoxia in rats. Circ. Res. 52, 432-441.
- Ramasamy, R., Yan, S.F., Schmidt, A.M., 2005. The RAGE Axis and Endothelial Dysfunction: Maladaptive Roles in the Diabetic Vasculature and Beyond. Trends in Cardiovascular Medicine 15, 237 - 243.
- Rammes, A., Roth, J., Goebeler, M., Klempt, M., Hartmann, M., Sorg, C., 1997. Myeloid-related protein (MRP) 8 and MRP14, calcium-binding proteins of the S100 family, are secreted by activated monocytes via a novel, tubulin-dependent pathway. J. Biol. Chem. 272, 9496-9502.
- Reichard, P., Estborn, B., 1951. Utilization of desoxyribosides in the synthesis of polynucleotides. J. Biol. Chem. 188, 839-846.
- Ritthaler, U., Deng, Y., Zhang, Y., Greten, J., Abel, M., Sido, B., Allenberg, J., Otto, G., Roth, H., Bierhaus, A., Ziegler, R., Schmidt, A.-M., Waldherr, R., Wahl, P., Stern, D.M., Nawroth, P.P., 1995. Expression of receptors for advanced glycation end products in peripheral occlusive vascular disease.

- American Journal of Pathology 146, 688-694.
- Robertson, T.P., Hague, D., Aaronson, P.I., Ward, J.P., 2000. Voltage-independent calcium entry in hypoxic pulmonary vasoconstriction of intrapulmonary arteries of the rat. *J. Physiol. (Lond.)* 525 Pt 3, 669-680.
- Rose, F., Grimminger, F., Appel, J., Heller, M., Pies, V., Weissmann, N., Fink, L., Schmidt, S., Krick, S., Camenisch, G., Gassmann, M., Seeger, W., Hänze, J., 2002. Hypoxic pulmonary artery fibroblasts trigger proliferation of vascular smooth muscle cells-role of hypoxia-inducible transcription factors. *The FASEB Journal*.
- Rubanyi, G.M., 1988. Vascular effects of oxygen-derived free radicals. *Free Radical Biology and Medicine* 4, 107-120.
- Rubanyi, G.M., Romero, J.C., Vanhoutte, P.M., 1986. Flow-induced release of endothelium-derived relaxing factor. *American Journal of Physiology - Heart and Circulatory Physiology* 250, H1145 -H1149.
- Rubin, L.J., 1997. Primary pulmonary hypertension. *N. Engl. J. Med.* 336, 111-117.
- Rubin, L.J., 2002. Therapy of Pulmonary Hypertension The Evolution from Vasodilators to Antiproliferative Agents. *Am. J. Respir. Crit. Care Med.* 166, 1308-1309.
- Rulli, N.E., Guglielmotti, A., Mangano, G., Rolph, M.S., Apicella, C., Zaid, A., Suhrbier, A., Mahalingam, S., 2009. Amelioration of alphavirus-induced arthritis and myositis in a mouse model by treatment with bindarit, an inhibitor of monocyte chemotactic proteins. *Arthritis Rheum.* 60, 2513-2523.
- Rulli, N.E., Rolph, M.S., Srikiatkachorn, A., Anantapreecha, S., Guglielmotti, A., Mahalingam, S., 2011. Protection from arthritis and myositis in a mouse

- model of acute chikungunya virus disease by bindarit, an inhibitor of monocyte chemotactic protein-1 synthesis. *J. Infect. Dis.* 204, 1026-1030.
- Sadowski, I., Pawson, T., Lagarde, A., 1988. v-fps protein-tyrosine kinase coordinately enhances the malignancy and growth factor responsiveness of pre-neoplastic lung fibroblasts. *Oncogene* 2, 241-247.
- Sandelin, M., Zabihi, S., Liu, L., Wicher, G., Kozlova, E.N., 2004. Metastasis-associated S100A4 (Mts1) protein is expressed in subpopulations of sensory and autonomic neurons and in Schwann cells of the adult rat. *J. Comp. Neurol.* 473, 233-243.
- Schmidt, A., Hori, O., Brett, J., Yan, S., Wautier, J., Stern, D., 1994. Cellular receptors for advanced glycation end products. Implications for induction of oxidant stress and cellular dysfunction in the pathogenesis of vascular lesions. *Arteriosclerosis, Thrombosis, and Vascular Biology* 14, 1521 -1528.
- Schmidt, A.M., Hori, O., Chen, J.X., Li, J.F., Crandall, J., Zhang, J., Cao, R., Yan, S.D., Brett, J., Stern, D., 1995. Advanced glycation endproducts interacting with their endothelial receptor induce expression of vascular cell adhesion molecule-1 (VCAM-1) in cultured human endothelial cells and in mice. A potential mechanism for the accelerated vasculopathy of diabetes. *J Clin Invest* 96, 1395-1403.
- Sekhon, H.S., Thurlbeck, W.M., 1996. Time course of lung growth following exposure to hypobaria and/or hypoxia in rats. *Respir Physiol* 105, 241-252.
- Sekhon, H.S., Wright, J.L., Thurlbeck, W.M., 1995. Pulmonary function alterations after 3 wk of exposure to hypobaria and/or hypoxia in growing rats. *J. Appl. Physiol.* 78, 1787-1792.
- Sheedy, W., Thompson, J.S., Morice, A.H., 1996. A comparison of pathophysiological changes during hypobaric and normobaric hypoxia in

- rats. *Respiration* 63, 217-222.
- Shubbar, E., Vegfors, J., Carlström, M., Petersson, S., Enerbäck, C., 2012. Psoriasin (S100A7) increases the expression of ROS and VEGF and acts through RAGE to promote endothelial cell proliferation. *Breast Cancer Res. Treat.* 134, 71-80.
- Singhal, S., Henderson, R., Horsfield, K., Harding, K., Cumming, G., 1973. Morphometry of the human pulmonary arterial tree. *Circ. Res.* 33, 190-197.
- Sironi, M., Guglielmotti, A., Polentarutti, N., Fioretti, F., Milanese, C., Romano, M., Vigini, C., Coletta, I., Sozzani, S., Bernasconi, S., Vecchi, A., Pinza, M., Mantovani, A., 1999. A small synthetic molecule capable of preferentially inhibiting the production of the CC chemokine monocyte chemotactic protein-1. *Eur. Cytokine Netw.* 10, 437-442.
- Sitbon, O., Humbert, M., Jagot, J.-L., Taravella, O., Fartoukh, M., Parent, F., Hervé, P., Simonneau, G., 1998. Inhaled nitric oxide as a screening agent for safely identifying responders to oral calcium-channel blockers in primary pulmonary hypertension. *European Respiratory Journal* 12, 265-270.
- Sitbon, O., Humbert, M., Jaïs, X., Loos, V., Hamid, A.M., Provencher, S., Garcia, G., Parent, F., Hervé, P., Simonneau, G., 2005. Long-term response to calcium channel blockers in idiopathic pulmonary arterial hypertension. *Circulation* 111, 3105-3111.
- Somlyo, A.P., Somlyo, A.V., 2003. Ca²⁺ sensitivity of smooth muscle and nonmuscle myosin II: modulated by G proteins, kinases, and myosin phosphatase. *Physiol. Rev.* 83, 1325-1358.
- Song, Y., Jones, J.E., Beppu, H., Keaney, J.F., Loscalzo, J., Zhang, Y.-Y., 2005.

Increased Susceptibility to Pulmonary Hypertension in Heterozygous BMPR2-Mutant Mice. *Circulation* 112, 553-562.

Soro-Paavonen, A., Watson, A.M.D., Li, J., Paavonen, K., Koitka, A., Calkin, A.C., Barit, D., Coughlan, M.T., Drew, B.G., Lancaster, G.I., Thomas, M., Forbes, J.M., Nawroth, P.P., Bierhaus, A., Cooper, M.E., Jandeleit-Dahm, K.A., 2008. Receptor for advanced glycation end products (RAGE) deficiency attenuates the development of atherosclerosis in diabetes. *Diabetes* 57, 2461-2469.

Spiekerkoetter, E., Alvira, C.M., Kim, Y.-M., Bruneau, A., Pricola, K.L., Wang, L., Ambartsumian, N., Rabinovitch, M., 2008. Reactivation of gammaHV68 induces neointimal lesions in pulmonary arteries of S100A4/Mts1-overexpressing mice in association with degradation of elastin. *Am. J. Physiol. Lung Cell Mol. Physiol.* 294, L276-289.

Spiekerkoetter, E., Guignabert, C., de Jesus Perez, V., Alastalo, T.-P., Powers, J.M., Wang, L., Lawrie, A., Ambartsumian, N., Schmidt, A.-M., Berryman, M., Ashley, R.H., Rabinovitch, M., 2009. S100A4 and bone morphogenetic protein-2 codependently induce vascular smooth muscle cell migration via phospho-extracellular signal-regulated kinase and chloride intracellular channel 4. *Circ. Res.* 105, 639-647, 13 p following 647.

Spiekerkoetter, E., Lawrie, A., Merklinger, S., Ambartsumian, N., Lukanidin, E., Schmidt, A.-M., Rabinovitch, M., 2005. Mts1/S100A4 Stimulates Human Pulmonary Artery Smooth Muscle Cell Migration Through Multiple Signaling Pathways*. *Chest* 128, 577S.

Stang, H.D., Boggs, D.R., 1977. Effect of methylcellulose injection on murine hematopoiesis. *American Journal of Physiology - Heart and Circulatory Physiology* 233, H234 -H239.

- Stenmark, K.R., Fagan, K.A., Frid, M.G., 2006. Hypoxia-Induced Pulmonary Vascular Remodeling. *Circulation Research* 99, 675 -691.
- Stenmark, K.R., Fasules, J., Hyde, D.M., Voelkel, N.F., Henson, J., Tucker, A., Wilson, H., Reeves, J.T., 1987. Severe pulmonary hypertension and arterial adventitial changes in newborn calves at 4,300 m. *J Appl Physiol* 62, 821-830.
- Stenmark, K.R., Meyrick, B., Galie, N., Mooi, W.J., McMurtry, I.F., 2009. Animal models of pulmonary arterial hypertension: the hope for etiological discovery and pharmacological cure. *Am J Physiol Lung Cell Mol Physiol* 297, L1013-L1032.
- Strand, V., 1999. Biologic agents and innovative interventional approaches in the management of systemic lupus erythematosus. *Curr Opin Rheumatol* 11, 330-340.
- Sun, L., Ishida, T., Yasuda, T., Kojima, Y., Honjo, T., Yamamoto, Y., Yamamoto, H., Ishibashi, S., Hirata, K., Hayashi, Y., 2009. RAGE mediates oxidized LDL-induced pro-inflammatory effects and atherosclerosis in non-diabetic LDL receptor-deficient mice. *Cardiovasc. Res.* 82, 371-381.
- Suzuki, Y.J., Day, R.M., Tan, C.C., Sandven, T.H., Liang, Q., Molkentin, J.D., Fanburg, B.L., 2003. Activation of GATA-4 by serotonin in pulmonary artery smooth muscle cells. *J. Biol. Chem.* 278, 17525-17531.
- Szasz, T., Thakali, K., Fink, G.D., Watts, S.W., 2007. A comparison of arteries and veins in oxidative stress: producers, destroyers, function, and disease. *Exp. Biol. Med. (Maywood)* 232, 27-37.
- Taraseviciene-Stewart, L., Kasahara, Y., Alger, L., Hirth, P., Mahon, G.M., Waltenberger, J., Voelkel, N.F., Tuder, R.M., 2001. Inhibition of the VEGF receptor 2 combined with chronic hypoxia causes cell death-dependent

- pulmonary endothelial cell proliferation and severe pulmonary hypertension. FASEB J 15, 427-438.
- Tarone, G., Galetto, G., Prat, M., Comoglio, P.M., 1982. Cell surface molecules and fibronectin-mediated cell adhesion: effect of proteolytic digestion of membrane proteins. J. Cell Biol. 94, 179-186.
- Taub, D.D., Proost, P., Murphy, W.J., Anver, M., Longo, D.L., van Damme, J., Oppenheim, J.J., 1995. Monocyte chemotactic protein-1 (MCP-1), -2, and -3 are chemotactic for human T lymphocytes. J. Clin. Invest. 95, 1370-1376.
- Taylor, J.H., Woods, P.S., Hughes, W.L., 1957. THE ORGANIZATION AND DUPLICATION OF CHROMOSOMES AS REVEALED BY AUTORADIOGRAPHIC STUDIES USING TRITIUM-LABELED THYMIDINE. Proc. Natl. Acad. Sci. U.S.A. 43, 122-128.
- Thenappan, T., Shah, S.J., Rich, S., Gomberg-Maitland, M., 2007. A USA-based registry for pulmonary arterial hypertension: 1982-2006. Eur. Respir. J. 30, 1103-1110.
- Treutiger, C.J., Mullins, G.E., Johansson, A.-S.M., Rouhiainen, A., Rauvala, H.M.E., Erlandsson-Harris, H., Andersson, U., Yang, H., Tracey, K.J., Andersson, J., Palmblad, J.E.W., 2003. High mobility group 1 B-box mediates activation of human endothelium. J. Intern. Med. 254, 375-385.
- Tsoporis, J.N., Izhar, S., Proteau, G., Slaughter, G., Parker, T.G., 2012. S100B-RAGE dependent VEGF secretion by cardiac myocytes induces myofibroblast proliferation. J. Mol. Cell. Cardiol. 52, 464-473.
- Tuder, R.M., Cool, C.D., Geraci, M.W., Wang, J., Abman, S.H., Wright, L., Badesch, D., Voelkel, N.F., 1999. Prostacyclin Synthase Expression Is Decreased in Lungs from Patients with Severe Pulmonary Hypertension.

- Am. J. Respir. Crit. Care Med. 159, 1925-1932.
- Tuder, R.M., Groves, B., Badesch, D.B., Voelkel, N.F., 1994. Exuberant endothelial cell growth and elements of inflammation are present in plexiform lesions of pulmonary hypertension. Am. J. Pathol. 144, 275-285.
- Tuder, R.M., Voelkel, N.F., 1998. Pulmonary hypertension and inflammation. J. Lab. Clin. Med. 132, 16-24.
- van Beijnum, J.R., Buurman, W.A., Griffioen, A.W., 2008. Convergence and amplification of toll-like receptor (TLR) and receptor for advanced glycation end products (RAGE) signaling pathways via high mobility group B1 (HMGB1). Angiogenesis 11, 91-99.
- Vanderpool, R.R., Kim, A.R., Molthen, R., Chesler, N.C., 2011. Effects of acute Rho kinase inhibition on chronic hypoxia-induced changes in proximal and distal pulmonary arterial structure and function. J. Appl. Physiol. 110, 188-198.
- Vanderpool, R.R., Naeije, R., Chesler, N.C., 2010. Impedance in isolated mouse lungs for the determination of site of action of vasoactive agents and disease. Ann Biomed Eng 38, 1854-1861.
- Vega-Avila, E., Pugsley, M.K., 2011. An overview of colorimetric assay methods used to assess survival or proliferation of mammalian cells. Proc. West. Pharmacol. Soc. 54, 10-14.
- Vincent, A.M., Perrone, L., Sullivan, K.A., Backus, C., Sastry, A.M., Lastoskie, C., Feldman, E.L., 2007. Receptor for Advanced Glycation End Products Activation Injures Primary Sensory Neurons Via Oxidative Stress. Endocrinology 148, 548-558.
- Voraberger, G., Schäfer, R., Stratowa, C., 1991. Cloning of the Human Gene for Intercellular Adhesion Molecule 1 and Analysis of Its 5'-Regulatory Region.

- Induction by Cytokines and Phorbol Ester. *J Immunol* 147, 2777-2786.
- Wagenvoort, C.A., 1960. Vasoconstriction and medial hypertrophy in pulmonary hypertension. *Circulation* 22, 535-546.
- Ward, J.P.T., 2007. Curiouser and curioser: the perplexing conundrum of reactive oxygen species and hypoxic pulmonary vasoconstriction. *Exp. Physiol.* 92, 819-820.
- Wedgwood, S., Black, S.M., 2003. Molecular mechanisms of nitric oxide-induced growth arrest and apoptosis in fetal pulmonary arterial smooth muscle cells. *Nitric Oxide* 9, 201-210.
- Weissmann, N., Manz, D., Buchspies, D., Keller, S., Mehling, T., Voswinckel, R., Quanz, K., Ghofrani, H.A., Schermuly, R.T., Fink, L., Seeger, W., Gassmann, M., Grimminger, F., 2005. Congenital erythropoietin over-expression causes “anti-pulmonary hypertensive” structural and functional changes in mice, both in normoxia and hypoxia. *Thromb. Haemost.* 94, 630-638.
- Welsh, D.J., PEACOCK, A.J., MacLEAN, M., HARNETT, M., 2001. Chronic Hypoxia Induces Constitutive p38 Mitogen-activated Protein Kinase Activity That Correlates with Enhanced Cellular Proliferation in Fibroblasts from Rat Pulmonary But Not Systemic Arteries. *American Journal of Respiratory and Critical Care Medicine* 164, 282 -289.
- Welsh, D.J., Scott, P.H., Peacock, A.J., 2006. p38 MAP kinase isoform activity and cell cycle regulators in the proliferative response of pulmonary and systemic artery fibroblasts to acute hypoxia. *Pulmonary Pharmacology & Therapeutics* 19, 128-138.
- Wharton, J., Davie, N., Upton, P.D., Yacoub, M.H., Polak, J.M., Morrell, N.W., 2000. Prostacyclin analogues differentially inhibit growth of distal and

proximal human pulmonary artery smooth muscle cells. Circulation 102, 3130-3136.

White, K., Dempsey, Y., Nilsen, M., Wright, A.F., Loughlin, L., MacLean, M.R., 2011. The serotonin transporter, gender, and 17 β oestradiol in the development of pulmonary arterial hypertension. Cardiovascular Research 90, 373 -382.

William, R., Wagner-Ballon Orianne, Saber Guitanouch, Hulin Anne, Marcos Elisabeth, Giraudier Stéphane, Vainchenker William, Adnot Serge, Eddahibi Saadia, Maitre Bernard, 2007. Effects of bone marrow-derived cells on monocrotaline- and hypoxia-induced pulmonary hypertension in mice.

Woolverton, W.C., Brigham, K.L., Staub, N.C., 1978. Effect of positive pressure breathing on lung lymph flow and water content in sheep. Circ. Res. 42, 550-557.

Yamamoto, Y., Harashima, A., Saito, H., Tsuneyama, K., Munesue, S., Motoyoshi, S., Han, D., Watanabe, T., Asano, M., Takasawa, S., Okamoto, H., Shimura, S., Karasawa, T., Yonekura, H., Yamamoto, H., 2011. Septic shock is associated with receptor for advanced glycation end products ligation of LPS. J. Immunol. 186, 3248-3257.

Yanagisawa, H., Davis, E.C., Starcher, B.C., Ouchi, T., Yanagisawa, M., Richardson, J.A., Olson, E.N., 2002. Fibulin-5 is an elastin-binding protein essential for elastic fibre development in vivo. Nature 415, 168-171.

Yang, Q.-W., Mou, L., Lv, F.-L., Wang, J.-Z., Wang, L., Zhou, H.-J., Gao, D., 2005. Role of Toll-like receptor 4/NF-kappaB pathway in monocyte-endothelial adhesion induced by low shear stress and ox-LDL. Biorheology 42, 225-236.

- Yang, Z., Tao, T., Raftery, M.J., Youssef, P., Di Girolamo, N., Geczy, C.L., 2001. Proinflammatory properties of the human S100 protein S100A12. *J. Leukoc. Biol.* 69, 986-994.
- Yan, S.D., Schmidt, A.M., Anderson, G.M., Zhang, J., Brett, J., Zou, Y.S., Pinsky, D., Stern, D., 1994. Enhanced cellular oxidant stress by the interaction of advanced glycation end products with their receptors/binding proteins. *J. Biol. Chem.* 269, 9889-9897.
- Yuan, X.J., Tod, M.L., Rubin, L.J., Blaustein, M.P., 1990. Contrasting effects of hypoxia on tension in rat pulmonary and mesenteric arteries. *Am. J. Physiol.* 259, H281-289.
- Zhang, H., Tasaka, S., Shiraishi, Y., Fukunaga, K., Yamada, W., Seki, H., Ogawa, Y., Miyamoto, K., Nakano, Y., Hasegawa, N., Miyasho, T., Maruyama, I., Ishizaka, A., 2008. Role of soluble receptor for advanced glycation end products on endotoxin-induced lung injury. *Am. J. Respir. Crit. Care Med.* 178, 356-362.
- Zlotnik, A., Yoshie, O., Nomiyama, H., 2006. The chemokine and chemokine receptor superfamilies and their molecular evolution. *Genome Biol.* 7, 243.
- Zoja, C., Corna, D., Benedetti, G., Morigi, M., Donadelli, R., Guglielmotti, A., Pinza, M., Bertani, T., Remuzzi, G., 1998. Bindarit retards renal disease and prolongs survival in murine lupus autoimmune disease. *Kidney Int.* 53, 726-734.
- Zuckerman, B.D., Orton, E.C., Stenmark, K.R., Trapp, J.A., Murphy, J.R., Coffeen, P.R., Reeves, J.T., 1991. Alteration of the pulsatile load in the high-altitude calf model of pulmonary hypertension. *J. Appl. Physiol.* 70, 859-868.

Zuckerman, G.B., Naughton, B.A., Gaito, A., Preti, R.A., Gordon, A.S., 1984. The
Effect of Methylcellulose on Extrarenal Erythropoietin Production.
Proceedings of the Society for Experimental Biology and Medicine. Society
for Experimental Biology and Medicine (New York, N.Y.) 176, 197 -202.